An mRNA-reprogramming method with improved kinetics and efficiency

and the successful transdifferentiation of human fibroblasts

using modified mRNA

David Alexander Preskey

Submitted in fulfilment for the degree of doctor of philosophy

Department of Biomedical Sciences

July 2017

Acknowledgements

Firstly, I would like to thank Professor Peter Andrews for offering me the opportunity to undertake a Ph.D. within his laboratory. I never knew why myself, a technician at the time, was offered such a fantastic opportunity, perhaps it was when Peter asked me if I wanted to do a Ph.D. and I said yes, but I'd like to think he saw something different in me. They called me 'Green-fingers' (in my head), I could make anything work which to this day is 100% accurate, sixty percent of the time. My favourite phrase of Peter's was, "have you got any exciting results?" It was like an instant laxative, he should probably patent that. Joking aside, I am very proud to have been working under Peter and I have nothing but praise and admiration for someone that has dedicated their life to their passion, something we should all strive to accomplish. The ginger wine is on me Peter!

I would also like to thank my co-supervisor Christian Unger. A Ph.D. can be stressful. Christian bore the brunt of my day-to-day stresses but it did not stop us working together as a unit, even if he is a German, coffee-drinking, environmentalist and I drive a car with a cheat device. I could not have done my Ph.D. without him. Despite being busy, I could still interrupt what he was doing and he would spend the time to deliberate my results or offer experimental advice. A good guy with an efficient German exterior. I will never forget experiment #105: The Optimisation of Trypsin-EDTA. This still gives me nightmares.

Further thanks to other senior academics, Paul Gokhale the fountain of knowledge, Mark Jones our political correspondent in charge of FACS analysis and Ivana Barbaric for being simply wonderful.

Now then, this is where things get serious. I would like to thank my Worms Armageddon compatriots Dylan Stavish, Adam Hirst and Tom Frith for co-creating Dropbox (not the £ billion file storage service, the game where you chip a ball in to a box). We were easily pleased… distracted. I would like to extend these thanks to Jim Hackland, Tom Allison and James Mason for joining in our summer activities: BBQ's in the park, the FIFA World Cup and a host of other painful ball-based games.

Finally, I would like to thank my wife, Mrs Clare Preskey. She is my absolute world. When I lose focus or motivation to do anything in life she kicks me up the butt and I keep going and my god did my motivation waver at times. Nevertheless, here we are, we got through it in the end just as we always do. I would like to dedicate my thesis to Clare. With her in my life, I can accomplish anything.

Abstract

Induced pluripotent stem (iPS) cells have the potential to generate a wide array of cell types from multiple lineages that enable us to explore the mechanisms that are involved in the conversion of cell states. The reprogramming process that generates iPS cells is complex, but since its discovery, technical advancements and improvements in the methodology have improved the speed and efficiency of generating integration-free, clinically relevant iPS cells. However, despite improvements, the mechanisms of reprogramming are not fully understood and so the process remains largely inefficient and slow. It has been reported that reprogramming mediated through the delivery of exogenous mRNAs encoding *OCT4*, *SOX2, KLF4* and *cMYC* is a fast and efficient method for generating integration-free iPS cells. Here we show that mRNA reprogramming can be enhanced further by employing an mRNA dose-ramping approach that provides greater control of the dose of mRNA that is introduced into the target cells. This improvement upon existing methods promotes the viability of the target cells during reprogramming which in turn improves the efficiency, speed and success of generating iPS cells. We also show that an optimisation to the reprogramming factor cocktail, replacing *OCT4* with a fusion between *OCT4* and the transcriptional activation domain of *MYOD1* – called M_3O, further improves the kinetics of reprogramming.

Reprogramming disease cells is also possible in that several iPS cell-disease models have been established that have successfully modelled aspects of disease development *in vitro*. Here we show the applicability of using the mRNA approach we have developed, on neuroblastoma cells and the characterisation of iPS cells reprogrammed from neuroblastoma cells using *OCT4*, *SOX2, KLF4* and *cMYC* delivered using Sendai viral vectors. Finally, we demonstrate how human fibroblasts introduced to a vector encoding *MYOD1* causes them to transdifferentiate in to myoblast-like cells without a genomic footprint.

Together this data demonstrates how integration-free mRNA can be used to control gene expression to direct cell fate through reprogramming and transdifferentiation. This mRNA approach provides proof of concept that warrants the testing of other genes to explore their function in reprogramming and other pathways that govern cell fate.

Publications

1) Preskey, D., et al., Synthetically modified mRNA for efficient and fast human iPS cell generation and direct transdifferentiation to myoblasts. Biochemical and Biophysical Research Communications, 2016. 473(3): p. 743-751.

2) Unger, C., et al., Isolation and Characterization of Human Embryonic Stem Cells and Future Applications in Tissue Engineering Therapies, in Principles of Stem Cell Biology and Cancer. 2015, John Wiley & Sons, Ltd. p. 1-25.

List of Abbreviations

Abbreviation	Meaning
5M-CTP	5-methylcytidine triphosphate
6WP	6-well plate
AF488	Alexa Fluor 488
AF647	Alexa Fluor 647
AB	Allele Biotech
ALK	Anaplastic Lymphoma Kinase
BMPs	Bone Morphogenetic Proteins
ChIP	Chromatin Immunoprecipitation
CDKs	Cyclin-Dependent Kinases
CT	Cycle Threshold
DMH1	Dorsomorphin homologue 1
EB	Embryoid Body
FBS	Fetal Bovine Serum
FGF	Fibroblast Growth Factor
FACS	Fluorescence Activated Cell Sorting
GFP	Green Fluorescent Protein
hESCs	Human Embryonic Stem Cells
HFFs	Human Foreskin Fibroblasts
ICC	Immunocytochemistry
iPS cells	Induced Pluripotent Stem Cells
IVT	In-Vitro Transcription
LIF	Leukaemia Inhibitory Factor
M_3	Transcriptional activation domain of *MYOD1*
M_3O	Fusion between the transcriptional activation domain of *MYOD1* & *OCT4*
MEFs	Mouse Embryonic Fibroblasts
mESCs	Mouse Embryonic Stem Cells
MyHC	Myosin Heavy Chain
MOPS	3-(N-Morpholino)propanesulfonic acid
NGF	Neural Growth Factor
NUFFs	Newborn Foreskin Fibroblasts
PFA	Paraformaldehyde
PCR	Polymerase Chain Reaction
pUTP	pseudouridine triphosphate
qPCR	Quantitative Polymerase Chain Reaction
RA	Retinoic Acid
ROCKi	Rho Kinase Inhibitor
SMA	Spinal Muscular Atrophy
SMAD	SMA protein & Mothers Against Decapentaplegic
SSEA	Stage Specific Embryonic Antigen
SG	Stemgent
TAD	Transcriptional Activation Domain
TGFβ	Transforming-growth factor βeta
UTRs	Untranslated Regions
WNT	Wingless-related integration site

Table of Figures

Table of Tables

Table of Contents

Chapter 1.

General Introduction.

1.1. Human embryonic stem cells

Human embryonic stem cells (hESCs) were first derived in 1998 by Thomson and colleagues and represent a unique cell type that can give rise to every cell type in the body as well as possessing the capacity for indefinite self-renewal [1]. This pluripotent state is achieved predominantly through increasing transforming-growth factor βeta (TGFβ)/Activin/Nodal and FGF signalling while repressing BMP signalling that causes hESCs to differentiate [2] (Figure. 1.1). The TGFβ/Activin/Nodal pathway signals through SMAD2/3/4 proteins [2] that help to induce the transcription of three key transcription factors, *OCT4*, *SOX2* and *NANOG,* by regulating the accessibility of the surrounding chromatin [3]. As chromatin binding sites become accessible, the SMAD2/3/4 proteins recruit epigenetic modifiers that modify the binding affinity between histones and DNA to allow or restrict transcription of target loci [4]. In addition, the FGF pathway uses MEK/ERK signalling to activate gene expression of *OCT4, SOX2* and *NANOG* [4]. These genes support the maintenance of hESCs in a pluripotent state by promoting the transcription of genes typically expressed in undifferentiated hESCs, by regulating their own expression through an auto regulatory feedback loop and by repressing differentiation-inducing genes activated through the BMP pathway [5-7]. The BMP pathway signals through SMAD1/5/8 proteins that repress pluripotency by inducing the transcription of differentiation-inducing genes [4]. However, the activity of SMAD1/5 is repressed via SMAD2/3 from the TGFβ/Activin/Nodal pathway and through self-renewal signals from the FGF signalling pathway [8]. This combination of signalling, gene repression and activation is tightly regulated and provides the core basis that enables hESCs to continuously divide in an undifferentiated state.

Figure 1.1. Signalling pathways that support pluripotency and self-renewal in hESCs

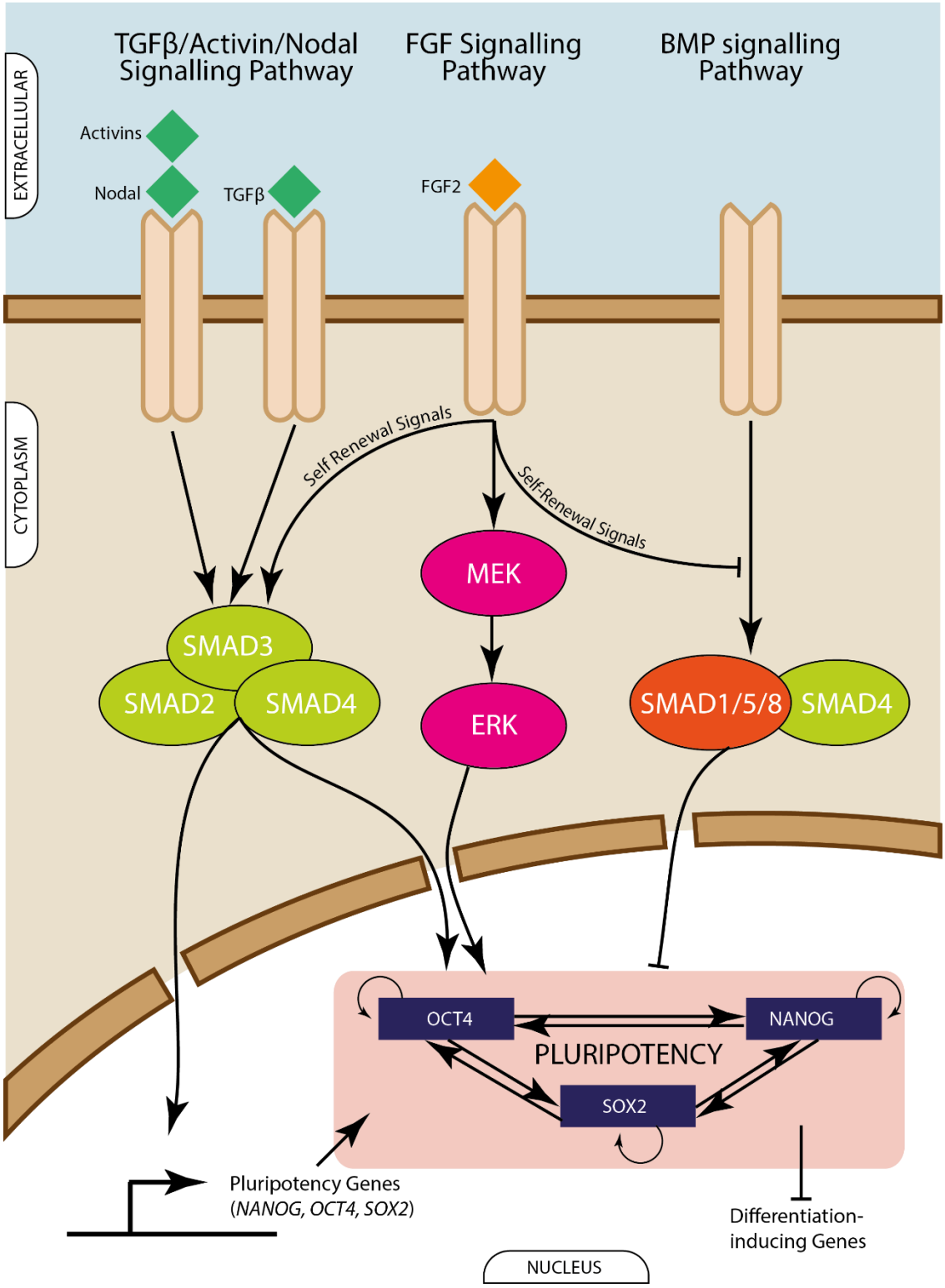

Figure 1.1: TGFβ/Activin/Nodal signalling utilises SMAD2/3/4 proteins to promote the transcription of *OCT4, SOX2* and *NANOG* that support the maintenance of hESCs in an undifferentiated state. FGF signalling supports pluripotency through MEK and ERK signalling while repressing BMP signalling that uses SMAD1/5/8 with SMAD4 to induce hESCs to differentiate. The pluripotency factors *OCT4, NANOG* and *SOX2* regulate themselves and one another in a coordinated way that enables the cells to remain in an undifferentiated state and self-renew.

HESCs are derived from the inner cell mass of pre-implantation blastocysts (Figure. 1.2) and once explanted can be induced to undergo tri-lineage differentiation i.e. differentiation to the three germ layers; endoderm, mesoderm and ectoderm, *in vitro* or *in vivo* after injection into severe combined immunodeficient mice [1]. Mice injected with hESC lines produce teratomas that contain multiple cell types derived from more than one germ layer [1]. Histological analysis of teratomas is used to determine the presence of each of the three germ layers to confirm the pluripotency status of the injected cells. Alternatively, pluripotency can be assessed *in vitro* by differentiating hESCs in non-adherent cultures to form hESC aggregates called embryoid bodies (EBs) [9]. These EBs can be dissociated and analysed by qPCR to detect gene expression levels that are characteristic of all three developmental germ layers.

The derivation procedure for hESCs was based on Thomson's previous work on primate ES cells [10]. ES cells derived from rhesus monkey provided a valuable and relevant tool for studying primate development being more closely related to humans than ES cells derived from other mammals such as rabbits [11], sheep [12], pigs [13] and mice [14]. Primate ES cells and hESCs are similar in many aspects including: morphology, cell surface marker expression, differentiation capacity and culture conditions required for long-term maintenance of established ES cell lines.

Figure 1.2. Derivation of human Embryonic Stem cells

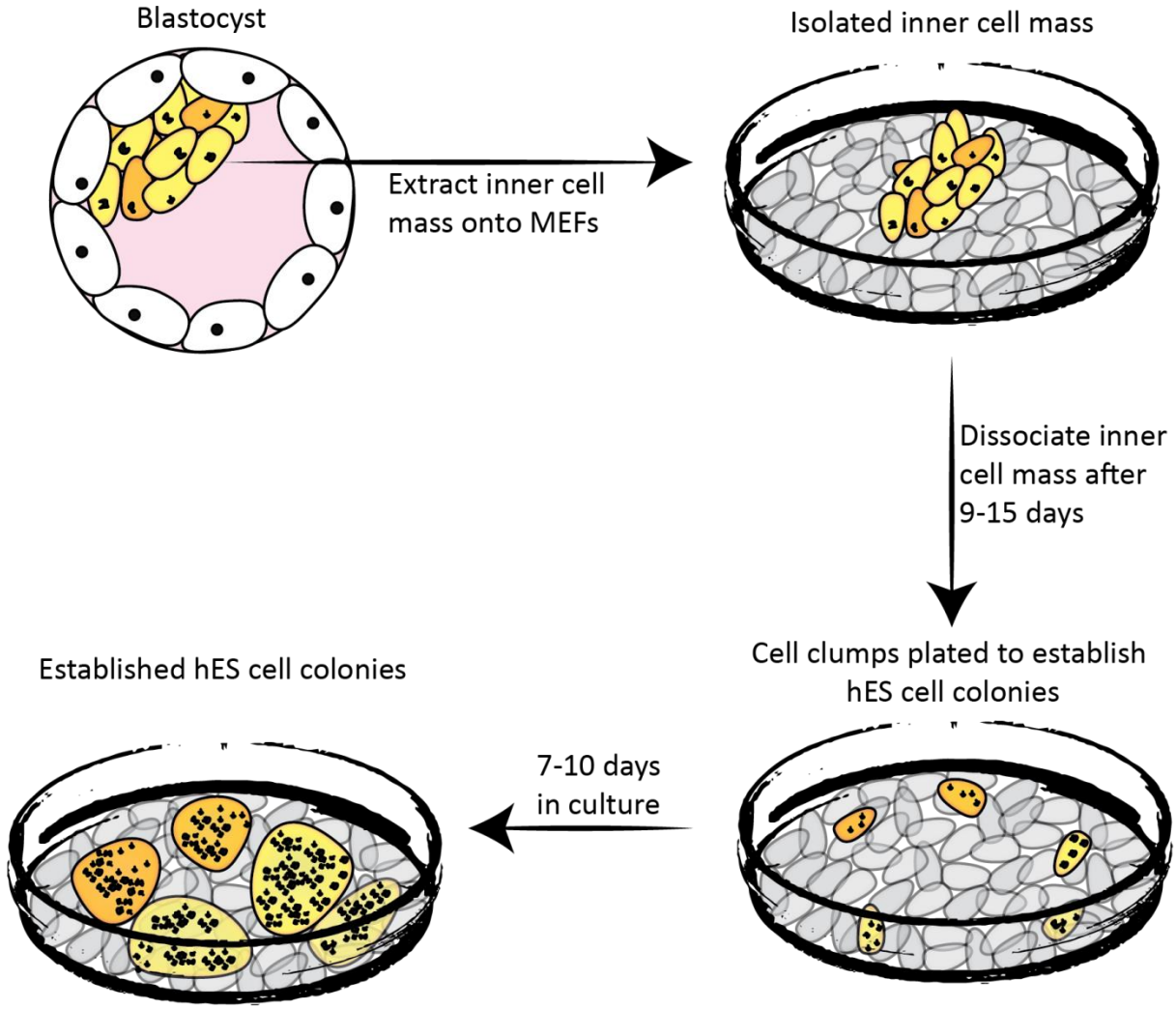

Figure 1.2: Schematic of hESC derivation. The inner cell mass is isolated from the blastocyst and plated on to an inactivated mouse embryonic fibroblast (MEF) feeder layer. After 9-15 days the inner cell mass is dissociated and re-plated on MEFs as cell clumps for a further 7-10 days to establish hESC colonies.

Undifferentiated hESCs, like primate ES cells, morphologically resemble flat, epithelial colonies with defined colony borders. Both cell types also express Stage Specific Embryonic Antigen (SSEA)-3 [15] and SSEA-4 [16] as well as high molecular glycoproteins TRA-1-60 and TRA-1-81 [17] in an undifferentiated state and SSEA-1 in response to differentiation [18]. HESCs are routinely passaged in clumps of cells as they have poor survival when dissociated as single cells [19] and like primate ES cells cannot be maintained in culture as undifferentiated cells without additional attachment factors such as a mouse embryonic feeder layer [1]. These characteristics are dissimilar to undifferentiated mouse embryonic stem cells (mESCs) and it is possible that hESCs correspond to a state later in embryonic development similar to mouse-derived epiblast stem cells [20]. Brons and colleagues demonstrated that deriving cells from the epiblast layer of mouse embryos possessed the morphological characteristics, capacity to differentiate and cell surface expression profile similarly displayed in undifferentiated hESCs [21]. As a result, it is considered that hESCs correspond to a primed pluripotent state while mESCs correspond to a 'naïve' pluripotent state. In contrast to mouse epiblast stem cells mESCs are characteristically different in that they form tightly-packed dome-shaped colonies and express SSEA-1 in an undifferentiated state [22]. Self-renewal is regulated in mESCs via LIF and bone morphogenetic proteins (BMPs) [23] while hESCs require fibroblast growth factors and transforming-growth factor βeta (TGFβ) signalling [2].

There are, however, similarities with respect to key genes required for self-renewal of pluripotent ES cells. The pluripotent status of both hESCs and mESCs is facilitated by the upregulation of key genes *OCT4, SOX2* and *NANOG* which work in synergy to regulate one another [7, 24]. When these genes are not expressed in the cells of the inner cell mass during embryo development, pluripotency cannot be established and instead the cells are trapped in a non-viable, intermediate state [25]. These genes, *OCT4, NANOG* and *SOX2*, are therefore critical for establishing and maintaining pluripotency in ES cells and are equally important in the establishment of iPS cells from somatic cells through reprogramming [26].

1.2. Reprogramming to induce pluripotency

Cellular reprogramming refers to the process whereby a somatic cell, such as a fibroblast, is artificially induced to become a different cell type through the erasure and remodelling of epigenetic marks, such as histones, that result in a shift in the cells gene expression profile [26, 27]. Yamanaka found that overexpressing four exogenous transcription factors: *OCT4*, *SOX2*, *KLF4* and *cMYC* in fibroblasts (Figure. 1.3), is sufficient to reprogramme their epigenetic status to that of a pluripotent stem cell [26]. Cells generated in this way are called induced pluripotent stem cells (iPS cells).

The identity of a cell is stabilised through epigenetic marks that act like switches turning genes on or off without affecting the underlying DNA code [28]. These epigenetic marks prevent aberrant cell fate changes by maintaining an epigenetic state appropriate to the cell type [29]. For example, a fibroblast cell will naturally promote the transcription of sections of DNA that can be translated into fibroblast proteins to keep the cell a fibroblast while repressing the transcription of non-fibroblast genes by configuring the chromatin structure in a way that makes transcription factor binding sites inaccessible. The accessibility of DNA is regulated by the chromatin structure which comprises multiple nucleosomes that form when DNA wraps around protein molecules called histones [30]. Chromosomes are made up of thousands of nucleosomes that are joined together by linker DNA to form chains [31]. The chains of nucleosomes are subsequently folded through higher order structures to compact the DNA so that it can fit inside the nucleus of a cell [31]. When chromatin becomes loosely packaged, genes can be actively transcribed. Conversely when the chromatin structure is tightly packaged, transcription is repressed [30]. The opening and closing of chromatin can be facilitated by epigenetic modifications such as DNA and histone methylation, acetylation and deacetylation [32]. These processes involve the recruitment of transcription activators and repressors such as histone

acetyltransferases and histone deacetylases respectively [32]. The accessibility of chromatin represents one of several limiting factors to reprogramming [33]. Other limiting factors to reprogramming include:

Limiting factor: The epigenetic status of the starting population

Reprogramming is predominantly an epigenetic process, and epigenetic modifiers have fundamental roles in remodelling chromatin in somatic cells so that repressed genes can be actively transcribed [33], which facilitates the conversion of cell states. Efficiencies of reprogramming in to distinct cell types, for example neurons (~20%)[34] and cardiomyocytes (20%)[35] are reportedly higher than reprograming to iPS cells (~0.1%)[36]. Variance in reprogramming efficiencies may be attributable to epigenetic barriers, for example transcribing genes in areas of inaccessible chromatin, that need to be overcome in order to execute reprogramming.

Limiting factor: The NuRD complex

During somatic cell reprogramming, the gene Zfp281 functions to repress Nanog expression in mice by directly recruiting the NuRD repressor complex to the Nanog promoter to inhibit its reactivation [37]. In addition, the depletion of *ZFN281*, the human orthologue to Zfp281, was shown in human cells to improve the reprogramming of pre-induced pluripotent stem cells to iPS cells [38]. Overexpressing *NANOG* during somatic cell reprogramming has been shown to improve the efficiency of generating iPS cells [39]. However, the NuRD complex represses the expression of *NANOG* and thus represents a barrier to reprogramming.

Limiting factor: p53 signalling pathway

In mouse embryonic fibroblasts (MEFs), p53 can cause apoptosis, promote differentiation and induce cell cycle arrest [40]. The p53 pathway is activated in MEFs following the individual and collective introduction of the reprogramming factors *Oct4*, *Sox2*, *Klf4* and *cMyc*. Activation of the p53 pathway has also been shown to inhibit the reprogramming of human somatic cells [41]. Several studies have demonstrated that the p53 pathway acts as a barrier to both human and mouse cell reprogramming and that reprogramming kinetics and efficiencies can be improved 10<100-fold following its suppression [42-44].

Reprogramming of somatic cells *in vitro* was first demonstrated in 2006 by Yamanaka and colleagues in mouse [36] and in 2007 in human [26, 45]. In addition to fibroblasts several other human cell types have been shown to be amenable to reprogramming to an ES cell-like state including retinal-pigmented epithelial cells [46] pancreatic islet β cells [47] and human neural stem cells [48].

The first evidence of reprogramming, however, dates back to the 1960's [49]. In this study by Gurdon [49], differentiated somatic cell nuclei in *Xenopus* were shown to contain genetic information that had an unrestricted capacity for multi-lineage differentiation. This was demonstrated by transplanting differentiated intestinal epithelium cell nuclei into enucleated frog eggs [49] that gave rise to feeding-tadpoles. While Gurdon demonstrated that a somatic cell nucleus can be reprogrammed in a host egg cell via somatic cell nuclear transfer, Yamanaka demonstrated that somatic cell reprogramming can be achieved by resetting the epigenetic status of a somatic cell through the overexpression of exogenous transcription factors.

Originally, a combination of 24 genes that are highly expressed in mouse ES cells were constitutively expressed using a retrovirus to generate iPS cells. It was eventually found that just

four factors, *Oct4*, *Sox2*, *Klf4* and *cMyc,* were sufficient to reprogramme mouse embryonic fibroblasts to iPS cells [36]. Generating iPS cells from human somatic cells is achievable using the same four factors [45]. Using lentiviral vectors, Yu et al. showed that a combination of *OCT4, SOX2, LIN28* and *NANOG*, substituting *KLF4* and *cMYC* with *LIN28* and *NANOG*, was similarly able to reprogramme human fibroblasts to iPS cells [45]. The addition of *LIN28* was shown to have a modest effect on reprogramming and has been demonstrated to inhibit the *let-7* micro-RNA (miRNA) that promotes differentiation [50]. The inclusion of *NANOG* as a reprogramming factor was shown to increase the survivability of emerging iPS cells as well as increase the efficiency of reprogramming [39, 45]. Generating iPS cells without using *cMYC* and *KLF4* has clinical relevance as it may prevent the risk of tumour formation as a result of oncogene reactivation [51]. However, the creation of iPS cells involves inducing somatic cells to transition from a mesenchymal to an epithelial phenotype, which *KLF4* facilitates [52] and is thus important for reprogramming. A study by Papapetrou identified that reprogramming MEFs using a three-fold relative increase of Oct4 compared to the other reprogramming factors: Sox2, Klf4 and cMyc significantly improved the speed and efficiency of reprogramming [53].

IPS cells are characteristically very similar to human embryonic stem cells, possessing the ability to undergo tri-lineage differentiation *in vitro* and by *in vivo* teratoma forming assays [1]. Morphologically iPS cells resemble flat, epithelial colonies much like hESCs and express similar cell surface markers SSEA-3, SSEA-4, TRA-1-60 and TRA-1-81 that characterise an undifferentiated cellular state [1, 26]. There are, however, two benefits to using human iPS cells over hESCs. Firstly the ethical dilemma associated with using cells derived from human embryos is circumvented. Secondly iPS cells are patient specific therefore issues with donor availability and immunological rejection are alleviated, which facilitates their use in autologous therapies.

Reprogramming mechanisms and roles of the reprogramming factors

In general, the efficiency of reprogramming is low in that <1% of somatic cells become fully reprogrammed iPS cells whether using lentiviral, episomal, Sendai-viral or RNA methods [54]. Initially the perception was that only a small fraction of cells within the starting cell population possessed stem or progenitor characteristics that made them amenable to reprogramming, and that these cells solely contributed to the generation of iPS cells [55]. However, it has been shown through clonal reprogramming assays that cells at different differentiation stages can all give rise to daughter cells that form iPS cells [56]. The reason for low reprogramming efficiencies is more likely due to the complexity of the process, involving many events and states that cells must go through in order to become iPS cells. Reprogramming can either be a stochastic or deterministic process in that following the commencement of reprogramming, all somatic cells proceed through various cell states at different times or at the same time respectively [56-58]. The stages that a fibroblast cell passes through in order to become an iPS cell is summarised below.

Initial sustained overexpression of the four reprogramming factors: *OCT4, SOX2,KLF4* and *cMYC* induces local epigenetic changes [28]. The first change that occurs is the repression of mesenchymal genes induced by the overexpression of *OCT4*, *SOX2* and *cMYC* [59]. The generation of iPS cells requires somatic cells to undergo a mesenchymal-to-epithelial transition (MET), therefore the suppression of genes that support an epithelial-to-mesenchymal transition (EMT) is required [28]. To achieve this, *OCT4* and *SOX2* repress the transcriptional regulator *SNAIL* that represses the promoter region of epithelial genes such as E-cadherin (*CDH1*) [60] while *cMYC* represses TGFβ1 and TGFβ receptor 2 that also support the EMT [52].

This is followed by the acceleration of the cell cycle mediated by *cMYC* through enhancing the production of elongating forms of RNA polymerase II to facilitate the transcription of cell cycle associated genes [61]. The cell cycle can also be accelerated by overexpressing *LIN28*, a non-

essential reprogramming factor that has been shown to improve reprogramming kinetics through enhanced translation of cell cycle associated proteins [62]. A further role of *cMYC* is to cooperatively work with the *OCT4*, *SOX2* and *KLF4* reprogramming factors to improve overall chromatin accessibility [58]. Initially *cMYC* engages accessible chromatin which opens up transcription factor binding sites on target loci for *OCT4*, *SOX2* and *KLF4* to bind which in turn permit *cMYC* to bind to target loci in previously inaccessible chromatin [63]. Improving chromatin accessibility permits the binding of exogenous transcription factors that facilitate the establishment of an endogenous pluripotency network [59].

The suppression of the EMT alleviates the repression of epithelial genes which allows *KLF4* to directly induce expression of epithelial genes such as E-cadherin (*CDH1*) to support the MET [52]. At this point, iPS cell intermediates begin to emerge that are dependent on sustained overexpression of the reprogramming factors [64]. In the later stages of reprogramming the cells become less reliant on the reprogramming factors to induce pluripotency as they begin to establish their own endogenous pluripotency network [65]. Finally, epigenetic modifications associated with pluripotency are re-established while DNA methylation patterns associated with somatic cells are erased [59]. The resultant iPS cells display characteristics and morphology specific to pluripotent stem cells including the capacity to differentiate to derivatives of all three germ layers.

As a result of the complex reprogramming process, most cells do not become fully reprogrammed iPS cells and the resultant reprogramming efficiency is low [54]. It has been shown that overexpression of *NANOG* can enhance the efficiency of reprogramming [39, 45], potentially by improving the ability for iPS colonies to form at very low cell densities [66]. The role of *NANOG* may also be important during the late stages of reprogramming in supporting iPS

cells to maintain a pluripotent state through signalling mechanisms previously described and illustrated in Figure 1.1.

1.2.1 Improving the methodology and efficiency of reprogramming

The process of reprogramming is very inefficient. In original protocols only 0.01% of fibroblasts were reprogrammed [45]. Considering iPS cells can be aberrantly, partially or fully reprogrammed with fully reprogrammed cells being the only type capable of multi-lineage differentiation [64], low efficiencies reduce the chance of generating high quality, fully reprogrammed iPS cells. This impacts their use in clinical applications hence, researchers have tried to enhance reprogramming through for example, using non-integrating methods, reducing the number of factors, use of cell permeable proteins and by using small molecules [67].

Relaxing the chromatin structure in somatic cells has also been shown to increase reprogramming efficiency [68]. There are two forms of chromatin, heterochromatin and euchromatin that function to silence or enable gene transcription respectively and can be remodelled by chromatin modifying proteins [69]. It has been shown that a fusion protein between *OCT4* and *MYOD* (called M_3O) more effectively recruits chromatin modifying proteins, than *OCT4* alone, to pluripotent loci during reprogramming [68]. This allows for genes such as *OCT4*, *NANOG* and *SOX2* that are not endogenously expressed in somatic cells to be more actively transcribed.

In addition to making reprogramming more efficient, researchers have also tried to simplify the process and reduce the number of transcription factors to less than the original four. For example, human neural stem cells have been reprogrammed using *OCT4* alone that is made

possible as human neural stem cells endogenously express *SOX2* and *cMYC* [48]. The study demonstrated that less than the original four reprogramming factors (*OCT4, SOX2, KLF4* and *cMYC*) could efficiently reprogramme cells that already endogenously express one or more of the reprogramming factors.

Coupled with broadening the range of reprogrammable cell types and factor combinations, advances in the development of integration-free reprogramming methods [70-72] have been the focus of intense research with the aim of generating integration-free iPS cells that can be used in therapeutic applications. Initially, reprogramming methods relied on highly efficient gene transfer using genome-integrating retroviral and lentiviral vectors [1, 26]. These integrating vectors randomly integrate into the host genome and can cause insertional mutagenesis, potentially activating proto-oncogenes which can lead to the formation of tumours [73]. As a result, the risk of insertional mutagenesis and oncogene activation in iPS cells derived using viral delivery methods renders the method unsuitable for generating clinically relevant cell types.

Non-integrating viruses such as the Sendai virus [70] or DNA-based methods such as episomal vectors [72] plasmids [74] or protein transfection [75] and also mRNA transfection [76] have been successfully used for reprogramming. DNA-based episomal vectors are virus free and operate extra-chromosomally avoiding the possibility of genomic integration. The reported reprogramming efficiencies, however, are extremely low, ~0.0003% [28], possibly due to the low establishment efficiency of colonies containing stably introduced episomes (~1% of transfected cells) [77]. With respect to plasmids and other DNA-based strategies to reprogramming, the risk of integration is ever-present [78-81] and these methods suffer from low efficiencies. Sendai virus and mRNA based integration-free reprogramming are the most efficient ways of reprogramming [54], both devoid of any DNA and hence removing the

risk of genomic integration. The Sendai virus contains a sequence-sensitive RNA replicase [81, 82] that catalyses the replication of RNA in the cytoplasm of transduced cells. However, mutations within this sequence can occur, conferring temperature sensitivity to the virus resulting in defective transcription and viral replication [70, 82, 83]. It is also very difficult to remove Sendai viral vectors from iPS cells derived using the Sendai virus [81], making informative analyses on such cells difficult without performing extensive genetic screening. While the use of Sendai virus vectors requires a P2 safety laboratory that may not be available in all facilities, Sendai virus reprogramming is now a standard method in many reprogramming laboratories, due to its commercial availability, high efficiency and reproducibility.

Besides the Sendai virus method, a further advanced mRNA-based approach reported by Warren et al [34] provides a virus-free, integration-free, faster and highly efficient way of generating human iPS cells. This mRNA reprogramming method involves introducing exogenous mRNAs encoding pluripotency factors in to somatic cells to induce pluripotency with high efficiency and speed [76]. One of the previous barriers to using *in vitro* transcribed mRNAs for reprogramming was the inability to sustain high levels of ectopic expression over time. This was partially attributable to the fact that single stranded mRNAs elicit an intracellular interferon immune response [76, 84] that involves the active transcription of over 300 immunosuppressant genes [85] which have been reviewed to cause widespread cell death via RNA cleavage [86]. In order to overcome this, Warren et al [34] modified mRNAs by substituting conventional triphosphates CTP and UTP for 5-methylcytidine (5M-CTP) and pseudouridine (pUTP) respectively (Figure. 1.4) during *in vitro* transcription reactions. Modified nucleotides have altered chemical structures compared to their normal counterparts to confer resistance against nucleases that rapidly degrade mRNAs [87]. To further prevent the intracellular interferon response the transfection medium was

supplemented with B18R (Figure. 1.4), a recombinant protein that binds interferon [88]. Warren found that by incorporating modified nucleotides in mRNAs and supplementing reprogramming medium with B18R sufficiently mitigates cell death, induced by the repeated addition of mRNAs, to enable levels of exogenous mRNA to be sustained for a length of time required to generate iPS cells. In this study, the reprogramming efficiency of mRNA-mediated reprogramming was ~ 1% and offers a quick and efficient, integration-free method for generating iPS cells [39].

Warren et al further showed through hierarchical clustering analysis that mRNA-reprogrammed iPS cells more closely relate to the transcriptional profile of hESCs than virally-mediated iPS cells [76], potentially owing to the absence of transgenes. Sendai-derived transgenes can be diluted from the reprogrammed cells over multiple cell divisions offering an advantage over retroviral and lentiviral methods [89]. Both the mRNA-based reprogramming method and the Sendai virus method negate the risk of genomic integration as post-transcriptionally modified mRNAs operate in the cytoplasm outside of the nucleus. Furthermore mRNAs are rapidly degraded owing to deadenylation [90] and endonuclease-mediated mRNA decay [91] which is advantageous over other methods that require excision of viral vectors and extensive genetic screening to purge the cells after reprogramming. In summary, mRNA-mediated reprogramming offers an efficient and safe way for generating iPS cells, however the methodology is technically demanding and requires optimisation compared to Sendai virus reprogramming.

Figure 1.3. A simplified process for creating iPS cells through mRNA-mediated reprogramming

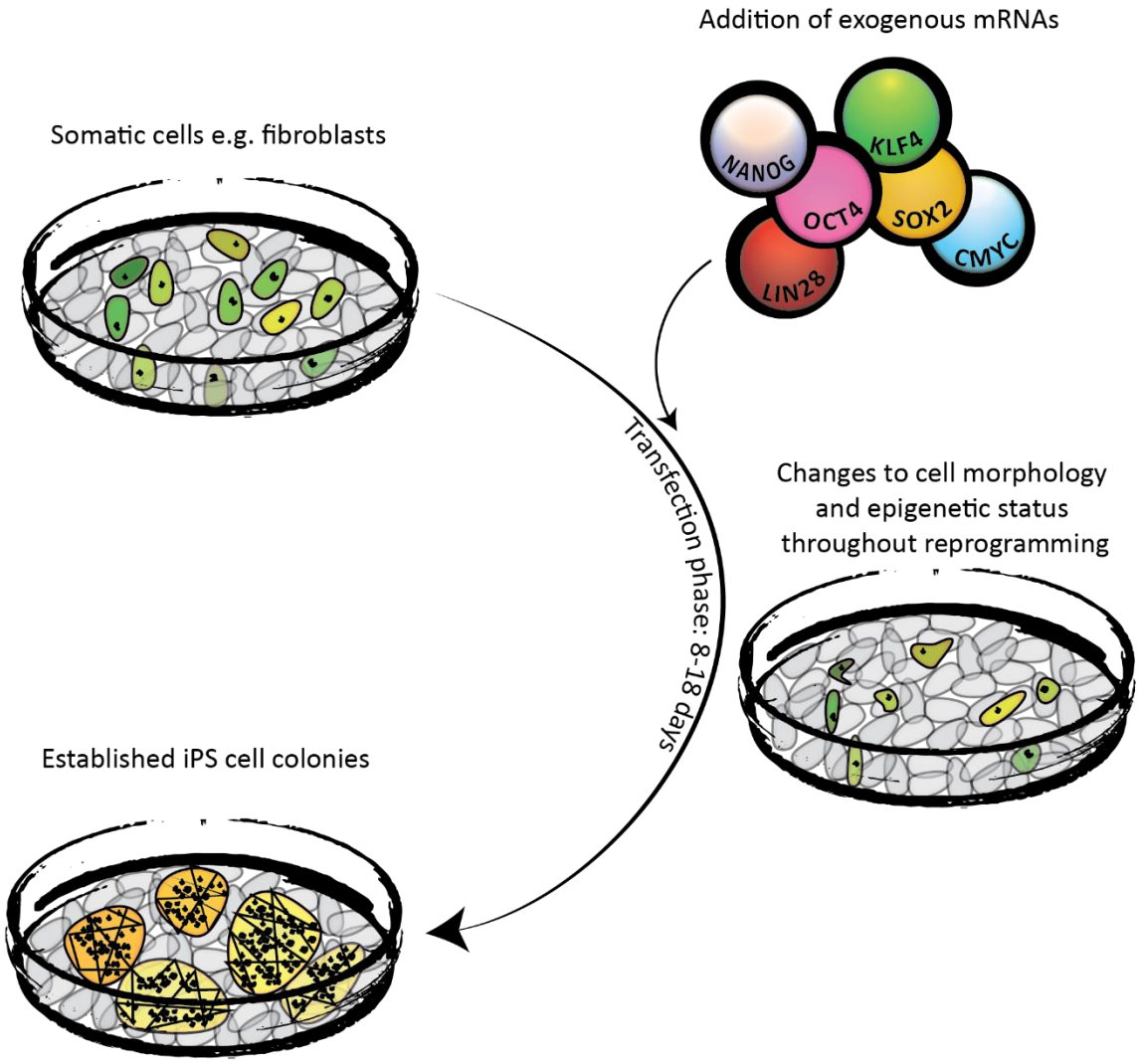

Figure 1.3: Schematic of iPS cell derivation using mRNA. Reprogramming is typically performed by introducing exogenous mRNAs encoding *OCT4, SOX2, KLF4, cMYC, LIN28* and *NANOG* into somatic cells. The entry of mRNA into somatic cells is facilitated by a lipofectamine-based transfection reagent, Stemfect (Stemgent, 00-0069). Repeated delivery and sustained overexpression of mRNAs in somatic cells induces epigenetic changes that lead to the establishment of an endogenous pluripotency network, resulting in the generation of iPS cells.

Figure 1.4. Preventing mRNA degradation via transcriptional modifications and B18R

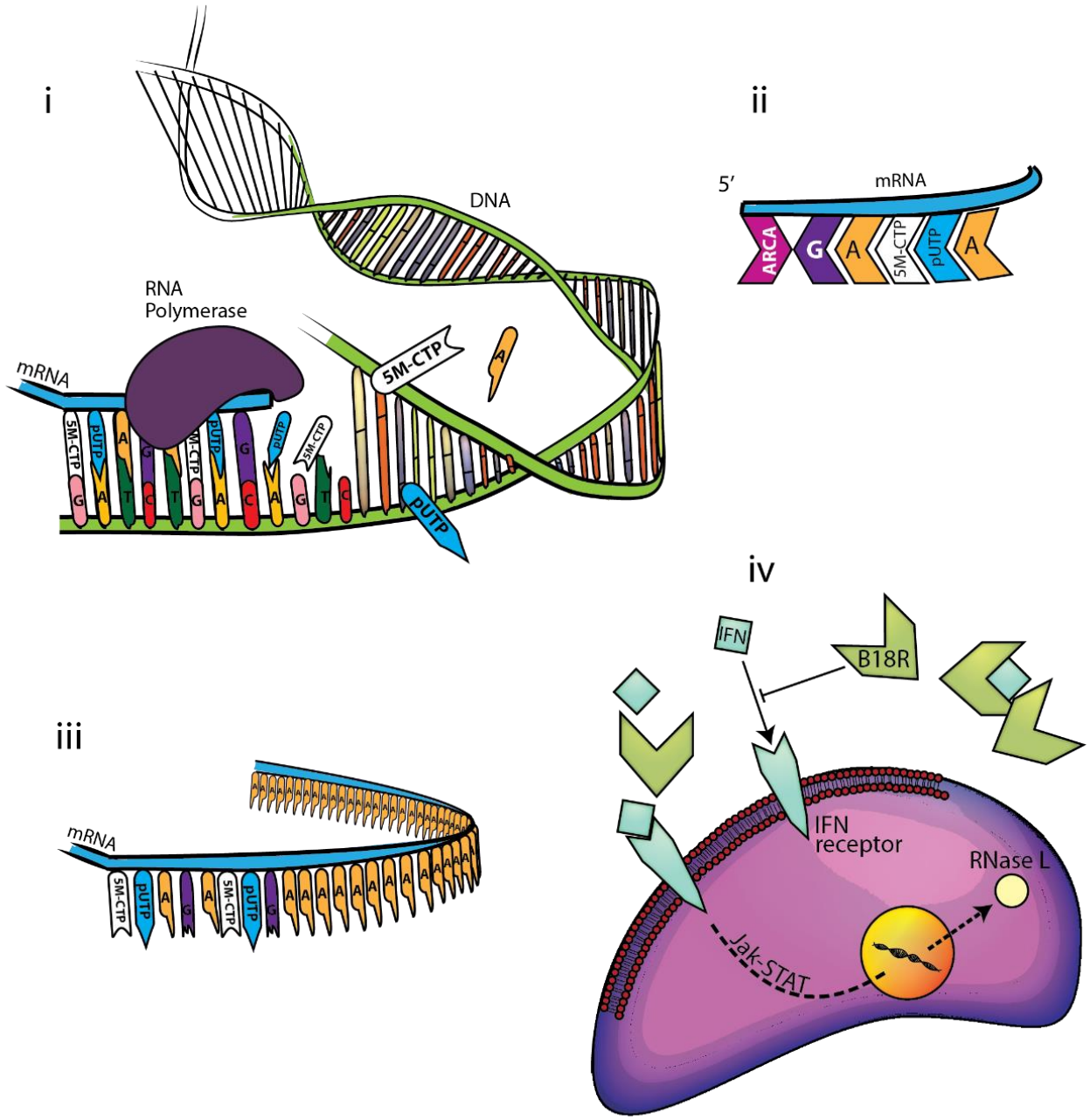

Figure 1.4: mRNA modifications and proteins that prevent mRNA degradation. mRNA can be modified to prevent premature degradation through (i) the incorporation of modified nucleotides, (ii) mRNA capping at the 5' end and (iii) the addition of a PolyA tail. (iv) B18R, a protein that contains a mimic IFN-1 receptor, can be added with mRNAs to repress the induction of an intra-cellular interferon immune response by specifically binding to IFN-1 molecules.

1.3. Disease modelling

Disease models provide a platform that allows for the initiation and development of diseases to be assessed both *in vivo* and *in vitro*. Disease models created in animals are often used to recapitulate aspects of human diseases as *Homo sapiens* share interspecies genomic similarities with animals such as mice [92], zebrafish [93] and *Drosophila* [94]. Such disease models provide a platform for both drug screening and research into the pathogenesis of a disease so that a greater understanding of how the disease develops can lead to the generation of therapies and cures. Disease models are often used for screening drugs as their effect on disease-affected cell types can be assessed, as reviewed by Hackam and Redelmeier [95] and Perel et al [96], with the intention of translating successful results into human clinical trials. The hope is that positive results obtained from *in vivo* studies will similarly induce a desirable effect in humans and thus generate novel therapeutic agents. However, on the majority of occasions clinical trials that were based on results translated from successful *in vivo* studies have proved unsuccessful [97, 98]. A recent review summarises that less than 8% of animal models have translated successfully into phase I clinical trials [99]. The failure rate may be attributable to physiological and molecular differences that exist between animals and humans, which ultimately limit the number of aspects of human biology that can be modelled through *in vivo* studies. While animal models without question remain an essential pre-clinical assessor of drug safety, the differences in pharmacokinetics, drug metabolism and excretion, mean that caution should be exercised when extrapolating data from animal models to understand human disease.

The discovery of hESCs and the generation of patient-specific pluripotent stem cells [26, 45] has improved our ability to model aspects of human disease development *in vitro*. Disease models can be created by reprogramming the somatic cells of a diseased patient to a cellular state that precedes that associated with the disease [100-102]. The subsequent differentiation of these

cells to the cell of origin from which a disease develops provides an *in vitro* system that allows for the assessment of the consequences of forcing the genome to operate in the context of a distinct lineage. Disease models also provide a drug-screening platform that facilitates the identification of novel therapeutic targets [103]. IPS cells lend themselves well to disease modelling for a few reasons. Firstly, the creation of iPS cells is not limited by the availability of donors and *in vitro* disease models can be created from a patients fibroblasts [26], retinal-pigmented epithelial cells [46] pancreatic islet β cells [47] or neural stem cells [48]. Secondly, iPS cells can generate an abundance of cellular material unlike somatic cells that have a reduced capacity to proliferate because of low telomerase activity [104]. Thirdly, genetic mutations harboured in the somatic cells of a patient with a genetic disease carry over in to iPS cells following reprogramming [100], which allows for drug screening and the pathophysiology of diseases to be studied.

Currently disease models for several diseases have successfully been established including those for spinal muscular atrophy (SMA) [100], Down's syndrome [101], several gastrointestinal cancers [105], schizophrenia [106] and long QT syndrome [107]. While SMA and long QT syndrome are associated with single mutations in the *SMN1* and *KCNQ1* genes respectively, some diseases such as schizophrenia and cancer involve a more complex interplay between genetic and epigenetic events [102]. When this is the case, disease models can help elucidate the effect of inducing and inhibiting disease related genes to gain insights into the mechanisms that govern disease development. Importantly it has been demonstrated that key genes involved in schizophrenia such as *NRG1* are not ubiquitously expressed in all host-derived cell types [106] stressing the importance of analysing phenotypic changes on the cell type relevant to the disease and not necessarily the iPS cells from which they were derived. This can often be a problem when the method to differentiate an iPS cell to the relevant cell type is unknown.

An additional problem with *in vitro* disease models is that diseases often affect multiple cell types and tissues that interact with one another to contribute to the pathogenesis and effects of a disease [108, 109]. Recapitulating these interactions *in vitro* is complex and therefore iPS cell disease models tend to focus on modelling a small aspect of a disease, such as modelling in the context of a distinct lineage, rather than the disease as a whole [52]. Epigenetic and aberrant genetic changes may also contribute to the pathogenesis of a disease. While it is difficult to transfer the epigenetic status of a disease cell to an iPS cell, owing to the erasure of the epigenetic landscape following reprogramming, there is evidence to suggest that transcription-factor derived iPS cells can harbour an epigenetic memory that is characteristic of their somatic cell of origin [110]. The inheritance of an epigenetic memory may influence an iPS cell's ability to differentiate because, for example, DNA methylation signatures drive the iPS cells to differentiate along pathways related to the parental cells [110].

Many of the currently established disease models including those aforementioned (SMA, Down's syndrome, several gastrointestinal cancers, schizophrenia and long QT syndrome) were generated through the use of integrating viruses. Whilst disease models do provide a valuable platform to study disease development, informative disease models rely on accurately analysing the functional effect that disease specific mutations have on normal development, a feature which is compromised by the presence of transgenes created by genomic integrations [111]. Transgenes undesirably affect the developmental potential and differentiation capacity of iPS cells, demonstrated by injecting transgene-containing iPS cells into murine blastocysts that formed embryos that displayed severe morphological abnormalities attributable to an inhibited ability to undergo tri-lineage differentiation [111]. A further undesirable effect of integrating methods is the possibility for oncogenic transgene reactivation which can occur if viral particles integrate downstream of nearby gene promoters [73]. As mRNA-derived iPS cell lines are advantageously footprint free and circumvent issues relating to insertional mutagenesis, it

suggests that disease models can be made more informative when generated using techniques that maintain genomic integrity, such as mRNAs.

1.4. Neural Crest

In normal development, neural crest cells are derived during neurulation (Figure. 1.5) following the formation of the three germ layers. Inductive signals, specifically the inhibition of bone-morphogenetic protein, specify a portion of the ectoderm to thicken to become neuroectoderm [112]. The neuroectoderm is separated from the non-neural ectoderm by neural plate borders which exhibit intermediate levels of BMP signalling [113]. This is in contrast to the devoid and elevated levels of BMP found in the neural plate and non-neural ectoderm respectively [113]. Ultimately, a BMP gradient is established across the neural plate that specifies different neural fates dependent on the dose of BMP [114]. The neural plate border is further distinguishable via elevated levels of fibroblast growth factors (FGFs) [115] and activation of canonical WNT signalling [116, 117] induced by the adjacent epidermis and paraxial mesoderm. After ectoderm specification the neural plate converges as a result of inductive signals from the notochord [118] and via apical constriction which is regulated by the expression of *SHROOM* [119]. The neural plate borders subsequently fuse together forming the neural tube that separates from the overlying ectoderm. The neural plate borders now reside as a population of neural crest cells on the most dorsal part of the neural tube. As the neural tube fuses, the neural crest cells delaminate and migrate along specific pathways to peripheral targets. A study on focal labelling of migrating neural crest cells showed that delamination tends to be directed in streams along rostrolateral and caudolateral trajectories [120]. Within this study and one follow up study [121] migration to and from the dorsal midline, wandering between rhombomere boundaries and attractions to neighbouring cells suggests that neural crest cell migratory pathways are at least partially controlled by cell-to-cell contacts. Differences in migration pathways between

populations of neural crest cells from different regions along the anteroposterior axis and from the same region suggest a level of heterogeneity with regard to guidance cues [120, 121]. Neural crest cells that populate the anterior end of this axis differentiate into derivatives different from those positioned more posteriorly. As the geographical location correlates with the type of neural crest derivatives formed, subcategories of neural crest populations; cranial, trunk, vagal or sacral are used to identify the various phenotypes [122]. During migration the neural crest cells develop integrin receptors that interact with extracellular matrices and trophic factors such as neural growth factor (NGF) to permit continued proliferation and migration [123, 124]. Upon reaching the final migratory destination, the neural crest cells differentiate into derivatives appropriate to the target site. A surplus of neural crest cells are available for differentiation into target cell types to ensure that sufficient physiological development can occur [125]. Excess neural crest cells that are surplus to requirement for differentiation into target cell types are then targeted for apoptosis via the withdrawal of NGF [125, 126].

Figure 1.5. Neurulation and the formation of the neural crest

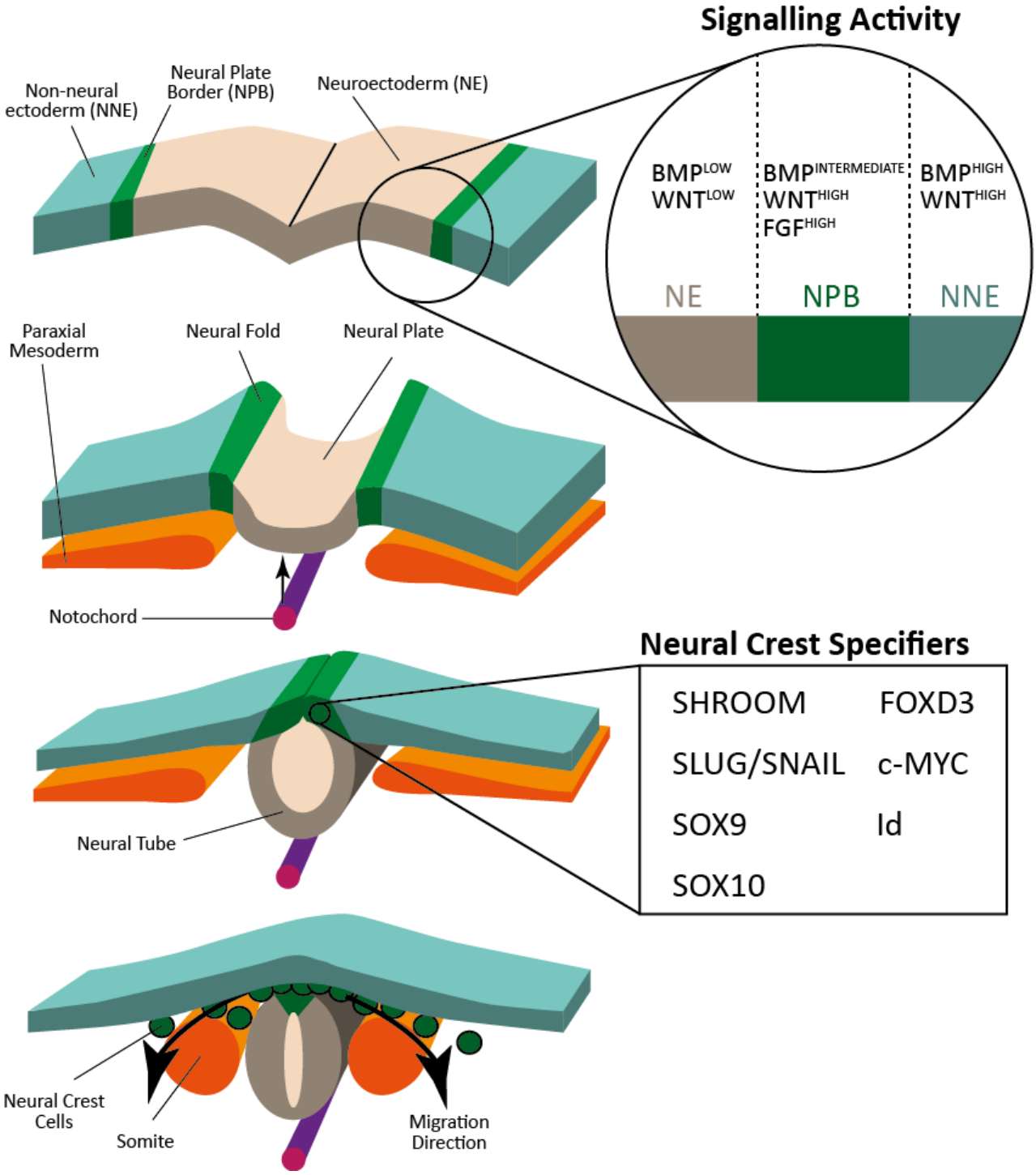

Figure 1.5: Neural crest cells reside in the neural plate border (NPB) that sits between the neuroectoderm (NE) and the non-neural ectoderm (NNE). These tissues are separated by a BMP gradient: NE = BMP^{low}, NPB = BMP^{med} and NNE = BMP^{high}. Inductive signals from the notochord induce the neuroectoderm layer to thicken and form the neural plate. As the neural plate is drawn downwards, neural folds converge and pinch together to form the neural tube. Neural crest cells reside at the uppermost part of the neural tube and are specified by numerous genes: *SHROOM, FOXD3, SLUG/SNAIL, cMYC, SOX9, Id* and *SOX10*. Closure of the neural tube causes the neural crest cells to detach from the overlying epidermis allowing them to migrate and differentiate into specialised cells.

1.5. Neuroblastoma

Recently we have generated a set of iPS cells from a neuroblastoma cell line called SK-N-SH, using lentivirus and Sendai virus reprogramming methods (unpublished work by Christian Unger). Neuroblastoma is the most common, extracranial, solid childhood tumour that can arise anywhere along the sympathetic nervous system chain although most commonly in the adrenal medulla [127]. While the underlying mechanisms for neuroblastoma initiation and progression are largely unknown, *in vivo* mouse models have begun to identify genes and factors that predispose neuroblastoma tumorigenesis [128]. In humans, genetic mutations in genes that regulate neural crest development including *MYCN* [129], *PHOX2B* [130] and *ALK* [131] contribute to an array of neurocristopathies including Hirschsprung disease [130, 132], congenital central hypoventilation syndrome [133] and neuroblastoma [134-137]. Modelling the effects of these mutations on neural crest cells within *in vitro* models may provide further insights into the development of neuroblastoma. These models could provide a platform for drug discovery and further insight into the aetiology and possible prevention of this malignant disease.

Neuroblastomas arise from cells that originate from the neural crest, a population of multipotent cells that can differentiate into a wide array of derivatives including craniofacial bones, melanocytes, chromaffin cells of the adrenal medulla and neurons and glia of the sensory, sympathetic and parasympathetic nervous system [138]. Normal development of neural crest cells is perturbed following the acquisition of mutations, for example in the mouse, somatic mutations in *Myc-n* [134] and germline mutations in *Phox2b* [135, 136] have been found to contribute to the abnormal development of cells derived from the neural crest, such as sympathetic ganglion cells, as has *ALK* mutations in humans [137]. *Phox2b* is functionally associated with regulating sympathetic neuronal differentiation [130]. Knockdown of

endogenous *Phox2b* has been functionally demonstrated in mouse, chick [135] and zebrafish models [136] to impair neuronal differentiation while neuroblastoma Phox2b variants have been shown to enhance sympathetic neuron proliferation and dedifferentiation [135]. Overexpression of *Myc-n* under the control of a tyrosine hydroxylase promoter in transgenic mice has been shown to initiate neuroblastoma pathogenesis [134] and is considered a primary oncogenic abnormality. In this study, the transgenic mice formed tumours after a period of latency indicating the involvement of other contributing factors in neuroblastoma development. One contributing factor is the resistance of neuroblastoma precursor cells to NGF withdrawal [139]. In SW-13 epithelial cells this is mediated through pleiotrophin-binding to *ALK* receptors [140]. Resistance to NGF withdrawal within the latent period after *MYCN* overexpression [141] indicates the role of *ALK* in tumour progression rather than tumour initiation. The overexpression and missense mutations of *ALK* have also been demonstrated to enhance the proliferation of cells that harbour these abnormalities [137, 142]. The survival of neuroblastoma cells in the absence of NGF is aided by further oncogenic changes such as the overexpression of *BCL-2* [143].

1.6. mRNAs as a tool for directing cell fate

Creating differentiated cell types that can be used to model aspects of disease development can be achieved by differentiating iPS cells that have been reprogrammed from a diseased somatic cell. An alternative way of obtaining differentiated cell types directly is through transdifferentiation. Transdifferentiation is the process whereby a somatic cell directly converts to a cell of a different lineage without passing through an intermediate pluripotent state. Transdifferentiation of fibroblasts has been extensively reported to lineages including neurons [144, 145], cardiomyocytes [35] and striated muscle cells [146] highlighting the amenability of fibroblasts to be reprogrammed to an altered cell fate. While iPS cells are beneficial for creating

endless supplies of cellular material, transdifferentiation offers a quicker more high-throughput alternative for isolating differentiated cell types. Transdifferentiation was first discovered in the 1970's whereby 5-azacytidine or Decitabine (5-aza-2'-deoxycytidine)-treated C3H10T1/2 mouse embryonic fibroblasts directly converted to adipocytes, chondrocytes and contractile striated muscle cells [146]. Decitabine is a drug that acts as an epigenetic modifier by remodelling chromatin through the inhibition of DNA methyltransferase, an enzyme that methylates gene promoters to repress gene expression [147]. Typically, exposing cells to Decitabine induces hypomethylation that causes repressed genes to become active. It has been shown that mouse embryonic fibroblasts exposed to Decitabine causes them to transdifferentiate to a myoblast phenotype at a conversion frequency of around 25% attributable to either a single or a select few demethylation events [148]. Weintraub went on to show that transfecting the DNA of transdifferentiated myoblasts into normal mouse embryonic fibroblasts mediated myogenic conversion [149]. Weintraub and colleagues compared myocyte-related gene expression between proliferating mouse embryonic fibroblasts and myoblasts revealing three candidate genes responsible for myogenic conversion. Upon cDNA transfection of the three candidate genes into normal mouse embryonic fibroblasts they identified demethylation at the *MYOD1* locus as a master regulator for myogenic conversion [150].

Transdifferentiation of mouse embryonic fibroblasts to myoblasts has been achieved using a single defined factor, MyoD1, by cDNA transfection [150], lentivirus [151] and retrovirus [152]. In these studies, adding exogenous MyoD1 to mouse embryonic fibroblasts activated endogenous *MyoD1* gene expression resulting in the formation of myoblasts. This is attributable to MyoD1 being a transcription factor that regulates the transcription of other muscle related genes, for example, *Myogenin* and *Cx43*, that are required for myoblast conversion from non-muscle cells [151]. Transdifferentiating fibroblasts to myoblasts has been established in several systems with high conversion frequencies compared to the low efficiencies when converting

fibroblasts to, for example, cardiomyocytes (16% conversion frequency) [35] or neural crest (3% conversion frequency) [93]. The reported myoblast conversion frequencies from mouse embryonic fibroblasts when delivering *MyoD1* by lentivirus was ~50% [111], by retrovirus ~5% [112] and following transfection of MyoD1 cDNA, ~50% [87]. To date there is no report of transdifferentiation of specifically human fibroblasts to myoblasts using mRNA encoding *MYOD1*. However, very recently a study demonstrated an mRNA method that successfully transdifferentiated C3H10T1/2 mouse embryonic fibroblasts to myoblasts through the repeated addition of murine MyoD1 mRNA [153]. In that study, the conversion of fibroblasts to myoblasts occurred within eight days, comprising a three-day transfection phase and a five-day transdifferentiation phase. However, the conversion frequency and the capacity of the myoblasts to form multinucleated myotubes was not reported.

Warren et al [76] demonstrated that iPS cells, but not fibroblasts, could be differentiated to an intermediate cell type that would transdifferentiate to myoblasts following the repeated introduction of human *MYOD1* mRNA. In that study, a validated mRNA-reprogrammed iPS cell line was differentiated for 28 days under conditions whereby fibroblast growth factor (FGF) had been removed, serum added and the cells were plated directly onto gelatine-coated dishes. After 28 days, mRNA encoding *MYOD1* was introduced into the cells daily for three days followed by three days culture in a low serum medium. At the end of the 34-day process, cells expressed myoblast-associated markers, myosin heavy-chain (MyHC) and Myogenin.

In addition to the transdifferentiation study performed by Warren et al involving *MYOD1*, several other experiments have utilised alternative factors, all delivered via lentiviral vectors, to convert somatic cells into alternative cell types. These experiments include using combinations of *Brn2, Ascl1* and *Myt1l* together to convert mouse fibroblasts into functional mouse neurons [144, 145], *Gata4, Mef2c*, and *Tbx5* together to convert mouse post-natal cardiac and dermal

fibroblasts into mouse cardiomyocytes [35] and *OCT4* in combination with a specific cytokine treatment to convert human dermal fibroblasts into human hematopoietic cells [154].

Recently, the overexpression of *SOX10* in human fibroblasts in the presence of epigenetic modifiers and growth factors was found to be sufficient to induce a neural crest phenotype [155]. Initially, the fibroblasts were differentiated from a hESC line containing a doxycycline regulated inducible system for *SOX10-eGFP*. After 14 days of *SOX10* induction in the presence of growth factors, laminin / fibronectin and/or the addition of 5-azacytidine, the culture was sorted for green fluorescing cells with varying frequencies of neural crest conversion. Utilising combinations of the aforementioned parameters resulted in conversion frequencies to putative neural crest cells ranging from 0.01% to 0.5%. These induced neural crest cells showed immunoreactivity to neural crest markers P75, HNK1 and AP2α, exhibited a morphology characteristic of neural crest cells and could be further differentiated to peripheral neurons, Schwann cells and melanocytes. This study highlights that the introduction of a single gene can convert fibroblasts to neural crest cells and postulates that other lineages may be derived following the introduction of lineage-specific master regulatory genes.

The vast majority of transdifferentiation experiments have utilised viruses as a means of delivering transdifferentiation factors into cells. These factors are often combined with epigenetic modifiers such as 5-azacytidine, Decitabine or enhancers of virus-mediated gene transfer such as polybrene, which incorporate into the DNA of the host cells. However due to the risk of viral-based methods introducing undesirable mutations it is more beneficial to generate differentiated cell types using non-integrating techniques, such as the use of transient transfections with mRNA, that maintain genomic integrity.

1.7. Aims and Objectives

AIM 1

To develop a reproducible mRNA-based reprogramming method with improved efficiency and kinetics that generates fully reprogrammed iPS cells from fibroblasts.

Reprogramming methods for producing human iPS cells, using mRNA to introduce the reprogramming factors in a transient manner, are currently inefficient and slow. We sought to establish a gold standard for reprogramming by using the commercially sourced Stemgent mRNA reprogramming kit (00-0071) to reprogramme human BJ fibroblasts, a cell line that has been reported by Stemgent to generate iPS cells efficiently using their system. We confirmed that the Stemgent system is effective as claimed, and established a benchmark from which to improve the technique. We tested technical and methodological improvements, such as mRNA dose-ramping, as well as alternative reagents such as the 6-factor reprogramming premix (ABP-SC-6FMRNA), Allele Biotech's *in vitro* transcription templates (ABP-SC-SEIPSET) and modified nucleotides, to increase our control over variables that affect the efficiency and speed of the reprogramming process.

AIM 2

To test whether the mRNA integration free approach can be used to reprogramme an established neuroblastoma cancer cell line to a pluripotent stem cell state despite its disrupted, cancer-associated genome, in order to establish a model in which to study the mechanisms by which that cancer genome leads to the formation of malignant neuroblastomas from neural crest precursors.

A neuroblastoma cell line, SK-N-SH, had been previously reprogrammed in our group to an iPS cell state using a lentivirus vector system. However, these cells continued to retain the integrated reprogramming genes with significant expression that could compromise their use to investigate neural crest differentiation and the ways in which this may be perturbed by the genetic changes that characterise the neuroblastoma genome. Successful reprogramming of SK-N-SH cells using the non-integrating mRNA approach would obviate this difficulty. As a contingency to the SK-N-SH cell line proving to be refractory to reprogramming using mRNAs, we used the Sendai virus system to reprogramme the SK-N-SH cell line. We then characterised and sought to differentiate these iPS cell lines to the neural crest, to see if this provides insights into the factors underlying the development of neuroblastoma.

AIM 3

To demonstrate that mRNA can be used to provide a transient signal that can direct cell fate by transdifferentiating somatic cells via the repeated addition of lineage-specific mRNA.

Modulating gene activity by transient expression of specific transcription factors is an attractive approach both for analysing mechanisms of cell fate determination during differentiation as well as providing practical tools for generating specific cell types. The technique of transfecting mRNAs encoding specific transcription factors that we are using to reprogramme somatic cells to iPS cells could equally be used to modulate other phenotypic conversions. The observation that overexpression of *MYOD1* in fibroblasts will convert them into myoblasts is well documented and provides a convenient test system for demonstrating that mRNAs can be used to effect transdifferentiation. In this case myoblast conversion typically requires the overexpression of a single factor, *MYOD1* and the conversion of somatic cells to myoblasts occurs at a high frequency compared to transdifferentiation studies on other cell types such as the neural crest.

Although *MYOD1*-mediatedtransdifferentiation of mouse fibroblasts using non-integrating techniques has been reported, this methodology has not yet been shown in the context of human somatic cell conversion.

Chapter 2.

Materials and Methods.

2.1. Gelatinisation of Cell Culture Vessels

T25 tissue-culture treated vessels (ThermoFisher, 156367) were coated with a solution containing 500mg of gelatine type-A (Sigma, G2500) which had been diluted in 500ml of sterile water (0.1% vol/vol) for 30 minutes. When the culture vessels were required for cell culture, the gelatine was removed and replaced with the appropriate cell culture medium.

2.2. Mouse Embryonic Fibroblast preparation

2.2.1. Generating p0 Mouse Embryonic Fibroblasts

Mouse embryonic fibroblast were obtained from MF1 outbred mice, killed using approved Schedule 1 procedures. The processes used abide by the criteria and guidelines set out in The Humane Killing of Animals under Schedule 1 to the Animals (Scientific Procedures) Act 1986 [156]. Pregnant females (10.5-12.5 days post coitum) were killed by cervical dislocation and the foetuses by decapitation. After evisceration in a petri dish, the foetuses were minced and then further dissociated using 0.25% trypsin-EDTA (Sigma, T4049) into single cells, which were seeded into tissue culture flasks at a ratio of one foetus per T75, in DMEM with 10% FCS. The cells were cultured until the resulting fibroblasts formed a confluent layer, when they were harvested and frozen at -80°C in a Nalgene Mr. Frosty freezing container (ThermoFisher, 5100-0001). The aliquots were transferred to liquid nitrogen for long-term storage.

2.2.2. Mouse Embryonic Fibroblast Inactivation

Two aliquots of primary MEFs (passage zero) were defrosted into three T75 cell culture vessels (ThermoFisher, 156472). These were passaged in DMEM (Sigma, D5546) containing 10% HyClone™ FBS (GE Healthcare Life Sciences, SH30071.03) and 1% bFGF (R&D Systems, AFL233) at a 1:3 ratio into three T175 cell culture vessels (ThermoFisher, 159920). The MEFs were continually passaged every two days or when confluency was reached until they reached p5. The fibroblasts were mitotically inactivated by a 2 hour incubation with 1mg/ml Mitomycin-C (Sigma, M4287) in batches of six T175's. The Mitomycin-C was then removed and the inactivated MEFs were washed two or three times with 1X Dulbeccos PBS (Sigma, D8537). They were then trypsinised with 0.25% trypsin-EDTA for 1-2 minutes at 37°C and then neutralised with DMEM containing 10% FBS. The inactivated MEFs were pelleted by centrifugation at 1200rpm for 5 minutes and then re-suspended in FBS containing 10% DMSO (Sigma, D2650). The inactivated MEFs were aliquoted into cryovials containing $2x10^6$ cells / 0.5ml FBS 10% DMSO and then frozen at -80°C.

2.2.3. Mouse Embryonic Fibroblasts Seeding

T25 tissue-culture treated vessels were gelatinised for 30 minutes and then the gelatine replaced with 3ml /$25cm^2$ DMEM 10% FBS. An aliquot of inactivated MEFs was thawed in a 37°C water-bath, re-suspended in 5ml DMEM 10% FBS and pelleted by centrifugation at 1100rpm for 3 minutes. The pellet was re-suspended in DMEM 10% FBS and seeded into culture vessels at a density of $3x10^5$ / $25cm^2$. The MEF-containing culture vessels were then incubated at 10% CO_2, 37°C to be used within 10 days.

2.3. Cell Culture Growth Mediums

2.3.1. Human Embryonic Stem Cell Medium

The following reagents were sterile-filtered into a 500ml bottle using a 0.22µm Stericup filter (Millipore, SCGPU05RE); 400ml DMEM/F12 (Sigma, DF-041), 100ml GIBCO Knock-out Serum Replacement (KOSR) (ThermoFisher, 10828028), 5ml 100X GIBCO non-essential amino acids (ThermoFisher, 11140050), 5ml 200mM GIBCO L-Glutamine (ThermoFisher, 25030081), 1ml GIBCO 2-mercaptoethanol (ThermoFisher, 21985023) and 0.5ml 100ng/ml bFGF.

2.3.2. Pluriton Reprogramming Medium

Pluriton Supplement 2500X (Stemgent, 01-0016) was aliquoted into single-use 4µl aliquots and stored at -80°C. Pluriton medium (Stemgent, 01-0015) was aliquoted into 40ml aliquots and frozen at -80°C. Upon use, an aliquot of thawed 2500X Pluriton supplement was added to 10ml of thawed Pluriton medium and kept in the fridge at 2-8°C for up to 1 month.

2.3.3. Neuroblastoma and Fibroblast medium

The same medium was used to culture both cell types consisting of DMEM 10% FBS.

2.3.4. Myoblast Growth Medium

Myoblast growth medium comprises DMEM F12 basal media supplemented with 20% FBS, 8ng/ml bFGF and 10ug/ml human insulin solution (Sigma, I9278).

2.3.5. Transdifferentiation Medium

Transdifferentiation medium comprises DMEM F12 containing 10µg/ml human insulin solution.

2.4. Passaging Pluripotent Stem Cells

2.4.1. Passaging on MEFs

Pluripotent stem cells were grown in MEF-coated cell culture vessels, typically T25's or in a 6-Well Plates (6WPs)(Greiner Bio-one, 657160) with hESC medium at 37°C in 5% CO_2. Healthy cultures were passaged every 3-4 days at a split ratio of 1:3. Cell cultures plated on a sub-optimal MEF layer were split less heavily and closer to once per week. Passaging consisted of mechanical scraping with a plastic Pasteur pipette (Alpha Laboratories, LW4728), i.e. using the pipette to score the flask in areas adjudged, by eye, to contain cells that did not appear to be differentiated. Prior to mechanical scraping the culture medium was aspirated until 1ml of medium remained in the flask. After scraping, fresh medium was added to the cell suspension and then plated onto fresh MEF-coated culture flasks containing 6ml or 2ml hESC medium, for a T25 or 6WPs respectively. Typically, 2ml hESC medium was added to the cell suspension following scraping to make the total volume up to 3ml that was then split 1:3.

2.4.2. Passaging on Matrigel

Vials of frozen (-20°C) Matrigel (BD, 354234) were defrosted at 2-8°C in the fridge in a box filled with ice. Once in liquid form the Matrigel was diluted 1:40 in DMEM/F12 and then

aliquoted into culture vessels to be stored at 2-8°C until used. As the water content in Matrigel slowly evaporates at 2-8°C, the volume added was sufficient to coat the culture vessels for up to 1 week, for example, 1.5ml in a well of a 6WP. When required for passaging, refrigerated culture vessels were placed at room temperature for 1 hour after which the Matrigel was aspirated and replaced with 2ml Pluriton medium. Pluripotent stem cells were passaged as described above (Methods 2.4.1). However, the cells were re-suspended in Pluriton medium and split into Matrigel-coated flasks also in Pluriton medium at the volumes described previously (Methods 2.4.1).

2.5 Culture of human dermal fibroblasts

Fibroblasts were grown on gelatine-coated T25 culture flasks (methods 2.1) in 7ml/25cm^2 DMEM 10% FBS at 37°C in 10% CO_2. To passage, the culture medium was aspirated from the culture vessel and replaced with 1ml/25cm^2 0.25% trypsin-EDTA. The cells were then incubated for 1-2 minutes at 37°C. The 0.25% trypsin-EDTA was then neutralised using DMEM 10% FBS and centrifuged at 1000rpm for 3 minutes. Then, the medium was aspirated to the pellet and the cells were re-suspended in typically 3ml DMEM 10% FBS and split into three gelatine-coated T25 culture flasks at a ratio of 1:3.

2.6. SK-N-SH and SKiPS Cell Culture

SK-N-SH cells were grown in T25's or 6WPs in DMEM 10% FBS at 37°C in 5% CO_2. Cultures were passaged once a week at a ratio of 1:6 following a 1-2 minute treatment with 0.25% trypsin-EDTA at 37°C. SK-N-SH cells were obtained from the ATCC (reference number: HTB-11) [157]. SK-N-SH cells that have been reprogrammed using the lentivirus by C. Unger are called SKiPS cells. The SKiPS cells are cultured using the method described in methods 2.4.

2.7. NT2 D1 Cell Culture

NT2 D1 cells [158] were grown in cell culture vessels in DMEM 10% FBS at 37°C in 10% CO_2. Cultures were passaged once a week at a ratio of 1:3 following a 1-2 minute treatment with 0.25% trypsin-EDTA at 37°C.

2.8 Freezing of Cell Cultures

Cell cultures were harvested from their culture vessels by the passaging method appropriate to their cell type and then pelleted by centrifugation at 1000rpm for 3 minutes. The media was then aspirated and the pellet re-suspended in 1ml FBS 10% DMSO per $1x10^6$ cells. The cells were then aliquoted into 1.5ml cryovials and placed in a Mr. Frosty freezing container (ThermoFisher, 5100-0001) at -80°C for 24 hours. The vials were then transferred to liquid nitrogen for long-term storage.

2.9. Thawing of Pluripotent Stem Cell Cultures

Cryovials containing frozen cells were thawed in a water bath set to 37°C and then re-suspended in 5ml fresh hESC medium. The cells were pelleted by centrifugation at 1000rpm for 3 minutes. Meanwhile, the medium was changed on one well of a MEF coated 6WP with 2ml fresh hESC medium which was then placed at 37°C to pre-warm. Once the cells had pelleted, the supernatant was aspirated and the centrifugation tube was gently flicked to dissociate the pellet before being re-suspended in the 2ml hESC medium from the pre-warmed well. The cell suspension was pipetted back in to the MEF-coated 6WP and then the culture vessel was placed in an incubator at 37°C in 5% CO_2 and their growth was monitored.

2.10. Dissociating cell cultures into single cells

Cell culture medium was aspirated from the culture vessel and replaced with 1ml/25cm^2 0.25% trypsin-EDTA or 1X TrypLE Select (ThermoFisher, 12563029). The cells were then incubated for 1-2 or 5 minutes respectively at 37°C. If the cells could not be seen to visibly detach from the surface, the side of the vessel was given a sharp tap. The trypsin-EDTA was then neutralised using a serum-based medium and centrifuged in a Megafuge 1.0R (Heraeus) in a rectangular swinging bucket rotor (Heraeus, 75002252) (radius 16.9cm) at 1000rpm (189 x g) for 3 minutes. The supernatant was aspirated to the pellet and the cells were then re-suspended in the appropriate medium.

2.11. Cell Counting

Cell cultures were dissociated into single cells prior to counting. Fifteen microlitres of single-cell re-suspension was then added to 15µl 0.4%Trypan Blue (Sigma, 15250061). Ten microlitres of this mixture was then added to a haemocytometer (Hawksley, AC1000) and the four corner quadrants were counted (Figure. 2.1). The cell concentration can then be calculated as follows;

Concentration (cells/ml) = Average count of 4 quadrants (outlined in red) x 20,000

Total cell number = concentration (cells/ml) x volume of cell suspension (ml).

Figure 2.1. Schematic of a haemocytometer

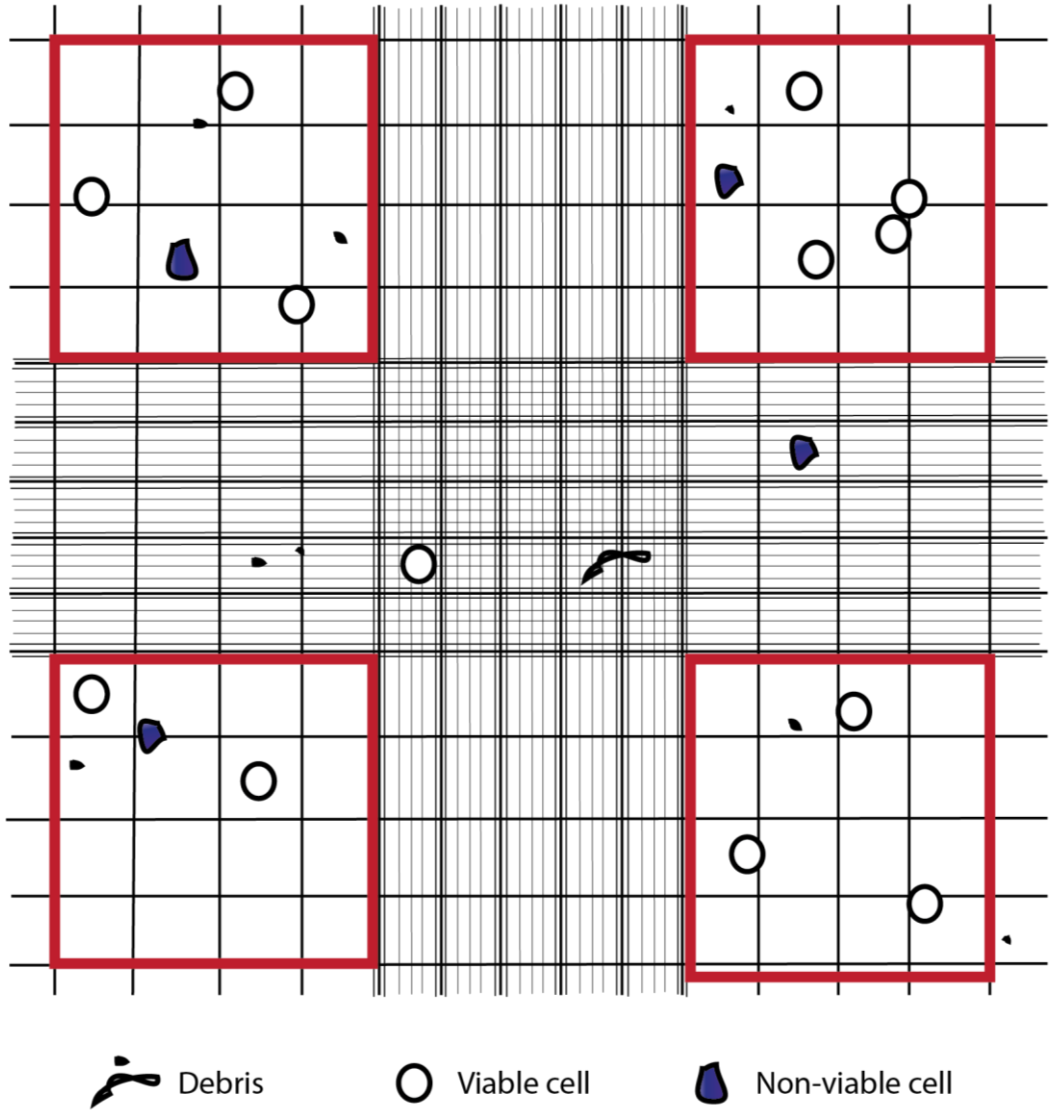

Figure 2.1: The above schematic is representative of a haemocytometer when viewed down the microscope. Cells stained with Trypan Blue are non-viable and should not be counted, nor should cellular debris or dead cells. The viable cells are shown as black circles with a white fill. The quadrants where cells should be counted are highlighted by red squares.

2.12. RNA Extraction

2.12.1. Harvesting Cells

2.12.1.1. Extracting RNA from cells in monolayer culture

Cell medium was aspirated from the cultures and replaced with 1ml Invitrogen™ Trizol (ThermoFisher, 15596026) per $1x10^6$ cells. The cells almost instantly became unattached from the culture vessel and were transferred to a 1.5ml micro-centrifuge tube (STARLAB, E1415-1510). If the sample was not used directly afterwards it was placed at -80°C for long-term storage.

2.12.1.2. Extracting RNA from embryoid bodies

Embryoid bodies were transferred to a $55cm^2$ Corning™ petri dish (Sigma, CLS430293) using a 200µl multi-channel pipette. The cell suspension was then transferred to a 15ml falcon tube (STARLAB, E1415-0200) and pelleted by centrifugation in a Heraeus Megafuge 1.0R at 1000rpm (189 x g) for 3 minutes. The supernatant was aspirated and then the pellet dissociated by flicking the tube. 1ml Trizol per $1x10^6$ cells was added and the cell suspension was transferred to a 1.5ml micro-centrifuge tube. If the sample was not used directly afterwards it was placed at -80°C for long-term storage.

2.12.2. Isolating Total RNA

Frozen Trizol samples were thawed on ice and then 200µl chloroform (Sigma, 288306) was added to the Trizol sample and inverted vigorously until the solution turned pale pink. The samples were left at room temperature for 10 minutes before being placed in a 30-place aerosol-tight fixed-angle rotor (radius 9.5cm) and centrifuged at 10,000rpm (10,621 x g) in an Eppendorf 5417R refrigerated micro centrifuge, for 10 minutes to achieve phase separation. The upper aqueous layer was transferred to a sterile 1.5ml micro-centrifuge tube containing an equal volume of 100% ethanol. The sample was thoroughly mixed using a vortex and total RNA was isolated using the RNA Clean-Up and Concentration Kit (Norgen Biotek, 23600) as per the manufacturer's protocol.

2.13. Reverse Transcription of RNA into cDNA

Reverse transcription reactions were performed using the Applied Biosystems™ High-Capacity cDNA Reverse Transcription Kit (ThermoFisher, 4368814). Reactions were performed in a 0.5ml micro-centrifuge tube (STARLAB, E1405-0610) by adding 2µl of 10X RT buffer, 0.8µl 25X dNTP mix (100mM), 2µl 10X Random Primers, 1µl RNase inhibitor and 3.2µl ddH_2O per sample to be reverse transcribed. An RNA sample was diluted with ddH_2O to 100ng/µl and then 10µl was added to the reverse transcription reaction. The entire 0.5ml micro-centrifuge tube was thoroughly mixed using a vortex and briefly micro-centrifuged to pool the reagents to the bottom of the tube. Finally, 1µl of Applied Biosystems™ MultiScribe Reverse Transcriptase (ThermoFisher, 4368814) was added to the reaction. The sample was briefly spun using a micro-centrifuge and placed in an Applied Biosystems™ 2720 thermal cycler (ThermoFisher, 4359453) to be run using the cycle shown in Figure. 2.2, before being stored at -20°C.

Figure 2.2. The run cycle for reverse transcription reactions

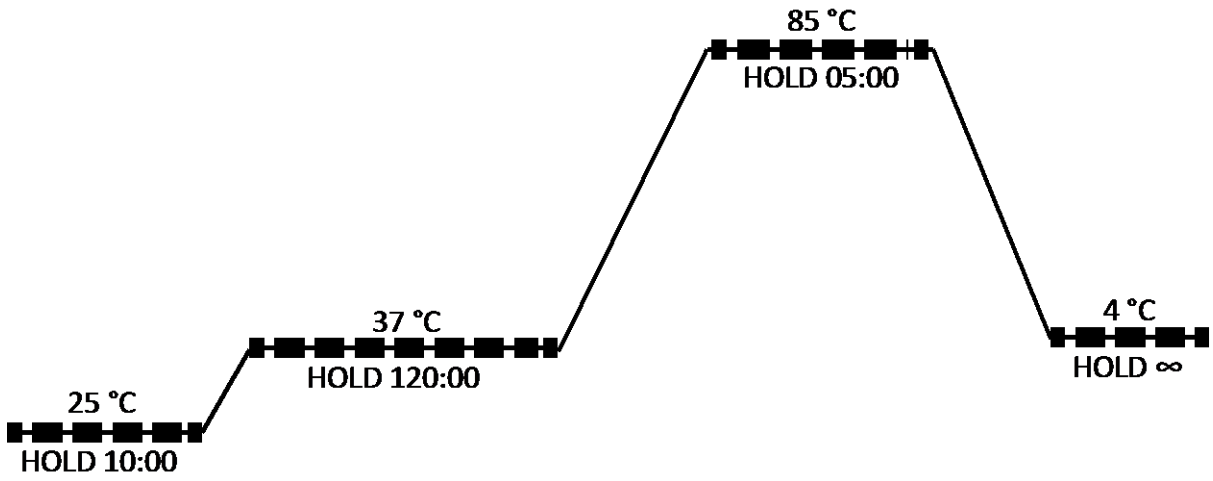

Figure 2.2: The run cycle for reverse transcription reactions includes a 10 minute hold at 25°C to anneal primers followed by a 2 hour hold for reverse transcription to take place. The reaction is terminated by increasing the temperature to 85°C and holding for 5 minutes. The reaction is then cooled to 4°C ready for storage.

2.14. QPCR on cDNA samples

2.14.1. Roche system

Frozen cDNA samples were thawed on ice and their concentration was quantified using a Nanophotometer P330 (Geneflow, discontinued). The cDNA samples were then diluted to 5ng/µl with ddH_2O. This was added to a mixture on ice containing 2.7µl ddH_2O, 5µl Applied Biosystems™ 2X Taqman Fast Universal PCR Master Mix (ThermoFisher, 4352042), 0.2µl Primer mix (containing 5µM sense and antisense oligonucleotides) and 0.1µl Probe (Roche, 04683633001). Eight microliters of the mixture was added to each well of a MicroAmp Optical 96- or 384-well reaction plate (ThermoFisher, 4316813) followed by 2µl of diluted cDNA. The plate was sealed with a MicroAmp Optical Adhesive Film (ThermoFisher, 4311971), and then centrifuged briefly for 5 seconds at 1200rpm. The plate was then analysed on a QuantStudio 12k Flex Real-Time PCR System (ThermoFisher, 4471088) using a standard run cycle setup (Figure. 2.3i). The primer sequences and probes used are detailed in Table 2.1.

2.14.2. TaqMan Gene Expression system

CDNA is diluted to 5ng/µl with ddH_2O and kept on ice. A mixture containing 2.5µl ddH_2O, 5µl 2X TaqMan Fast Universal PCR Master Mix and 0.5µl TaqMan primer (ThermoFisher, Accession numbers provided in Table 2.1) was made per well. Eight microliters of the mixture was added to each well of an optical 96- or 384-well reaction plate followed by 10ng of pre-diluted cDNA. The plate was sealed, spun and analysed as described in the Roche system albeit with an altered run cycle (Figure. 2.3ii). The primer sequences and probes used are detailed in Table 2.1.

Figure 2.3. The two qPCR run cycles when using the Roche Universal Probe Library and the Taqman gene expression systems

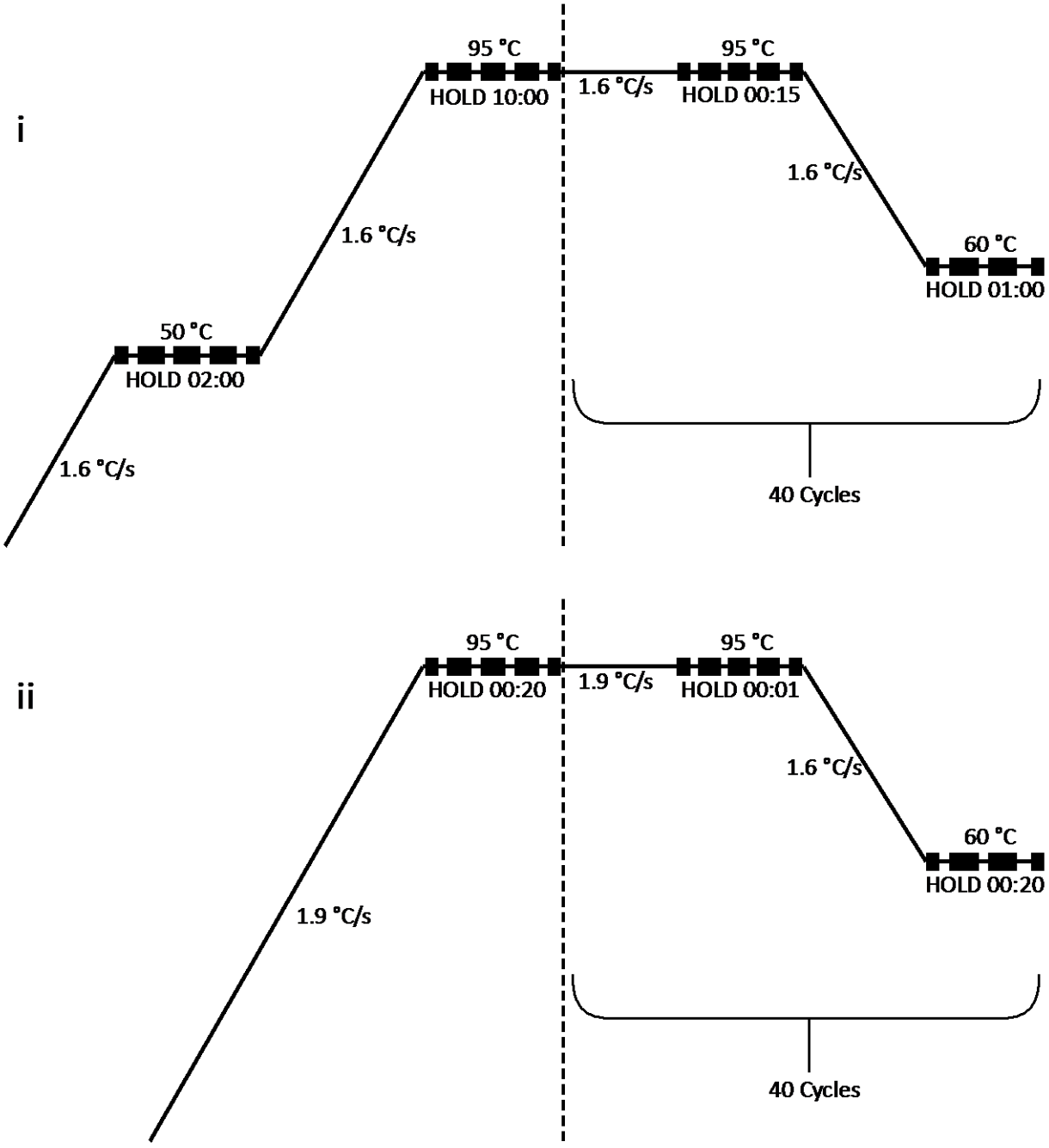

Figure 2.3: The qPCR run cycle setups are shown above. (i) The Roche system includes a hold for 2 minutes at 50°C followed by an increase in temperature to 95°C for 10 minutes to fully denature the cDNA. A further hold at 95°C and then a 1 minute hold at 60°C is performed to allow for annealing and extension of the primers. (ii) The TaqMan system follows the same principals albeit with optimised reagents to allow for the run-time to be completed in a fraction of the time.

2.14.3. Calculating RQ values using the delta CT method.

After running an optical 96- or 384-well reaction plate on the QuantStudio 12k Flex Real-Time PCR System, each well containing a sample will output a Cycle Threshold (CT) value into an excel spreadsheet. The CT values represent the number of PCR cycles it takes for the amplification reaction to accumulate a fluorescent signal above a threshold determined from the background noise. Typically, a CT value below 30 indicates a large amount of target nucleic acid in the sample while a CT value between 30 and 40 indicates a minimal-to-absent level of target nucleic acid in the sample. CT values can be converted to relative quantification (RQ) values that represent changes in gene expression in a cDNA sample relative to a reference cDNA sample, for example, an untreated control. The RQ value calculation process, described below, has been illustrated in Figure. 2.4.

As cDNA samples are often run on a plate in technical triplicate, the mean average of three grouped CT values is calculated before being normalised to a housekeeping gene to obtain a delta CT value that shows the difference in expression between the target gene and the housekeeping gene. Two housekeeping genes, *GAPDH* and *b-ACTIN* were used with the Roche Universal probe library and Taqman gene expression system respectively based on their consistent expression across multiple cell types and experiments (data not shown). The delta CT values were then averaged to give the mean delta CT value. To compare between samples, one sample was selected as the reference sample for all other samples to be compared to, such as an undifferentiated control. The delta-Ct for each gene from the reference sample is subtracted from the corresponding gene in the remaining samples to give for each gene in a sample a so-called delta delta Ct value. The RQ values are finally calculated by using the 2^-delta delta CT formula that reveals the fold change in expression between two samples normalised to a housekeeping gene.

Figure 2.4. Calculating RQ: A worked example

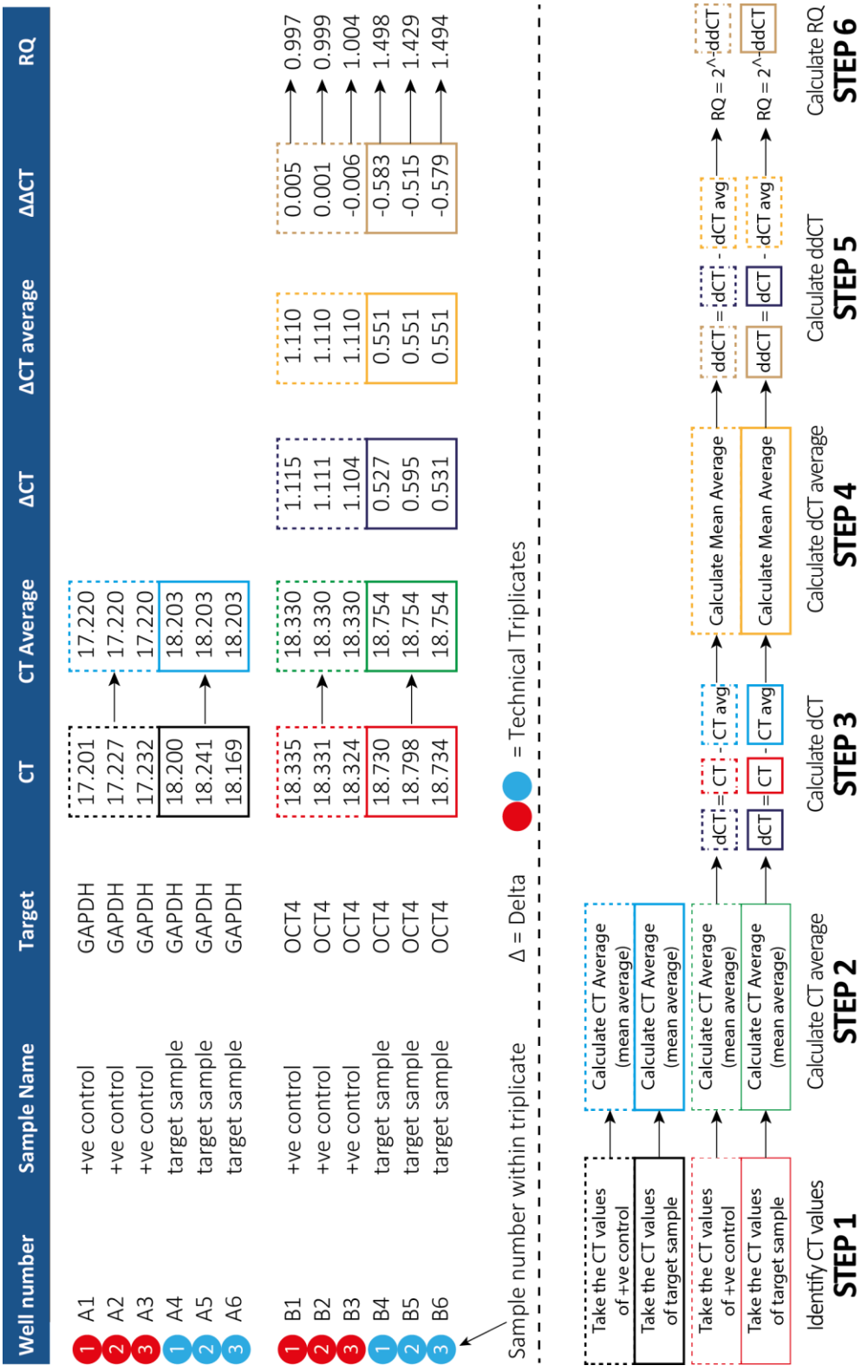

Figure 2.4: An example of calculating RQ values from the output of a qPCR run is shown. A target sample run in technical triplicate is analysed for the abundance of *OCT4* nucleic acid. The target sample is normalised to *GAPDH*. Each cDNA sample within the triplicate is used repeatedly for each target analysed e.g. the cDNA sample in well position A1 has been used again in well position B1 albeit using different primers and probes (*GAPDH* and *OCT4* respectively). A step-by-step, colour-coded process shows how to calculate RQ values from CT values. RQ values are calculated using the 2^-ddCT formula.

Table 2.1. Primer / probe sequences used in qPCR to detect target nucleic acids

Gene	Forward Primer, 5'→3"	Reverse Primer, 3"→5'	Probe #
GAPDH	agccacatcgctcagacac	gcccaatacgaccaaatcc	#60
POU5F1	ccacatcggcctgtgtatatc	agcaaaacccggaggagt	#35
SOX2	atgggttcggtggtcaagt	ggaggaagaggtaaccacagg	#19
KLF4	gccgctccattaccaaga	cgatcgtcttcccctcttt	#82
CMYC	cggttttcggggctttat	ggctcttccaccctagcc	#13
LIN28	gccaaggaatgcaagctg	gaggctaccatatggctgatg	#29
NANOG	agatgcctcacacggagact	tttgcgacactcttctctgc	#31
FOXA2	cgccctactcgtacatctcg	agcgtcagcatcttgttgg	#9
GATA6	aatacttcccccacaacacaa	ctctcccgcaccagtcat	#90
ISL1	gcagcccaatgacaaaactaa	ccgtcgtgtctctctggact	#83
CD34	gcgctttgcttgctgagt	gggtagcagtaccgttgttgt	#8
PECAM	tggaaattggaagagcacaa	ttcaagtttcagaatatcccaatg	#37
GATA2	ccgggagtgtgtcaactgt	caggcattgcacaggtagtg	#76
PAX6	agggcaacctacgcaaga	cgttggaactgatggagttg	#12
COL1A1	gggattccctggacctaaag	ggaacacctcgctctcca	#67
MITF-m	ggtgaaaataatcaactgcatagttc	agcatcaccaatgtttccaag	#61
DCT	cgactctgattagtcggaactca	ggtggttgtagtcatccaagc	#33
c-RET	catcaggggtagcgaggtt	gggaaaggatgtgaaaacagc	#17
SNAI2	tggttgcttcaaggacacat	gcaaatgctctgttgcagtg	#7
PAX3i	ttggcaatggcctctcac	aggggagagcgcgtaatc	#45
SOX10	cccaggtgaagacagagacc	atggctggtcggtgtagtgt	#57
AP2α	acatgctcctggctacaaaac	gtcaagcagctctggatgc	#1
BRN3A	ctccctgagcacaagtaccc	ggcgaagaggttgctctg	#78
FOXD3	gaagccgccttactcgtaca	cgctcagggtcagcttctt	#9
MYOD	cactacagcggcgactcc	taggcgccttcgtagcag	#70
MYOG	ttaaatggcacccagcagtt	gggatgtctcatacagctcca	#66
MYF5	ctatagcctgccgggaca	tggaccagacaggactgttacat	#10
MYH7	acaccctgactaaggccaaa	gtccatgcgcaccttctt	#1
BCL2L1	cccagggacagcatatcag	agcggttgaagcgttcct	#66

Gene	Accession number	Gene	Accession number
β-ACTIN	HS01060665_G1	*BRN3A*	HS00366711_M1
PAX3	HS00240950_M1	*PHOX2B*	HS00243679_M1
SOX10	HS00366918_M1	*FOXD3*	HS00255287_S1
AP2α	HS01029413_M1	*ALK*	HS01058318_M1

Table 2.1: mRNA levels were detected during qPCR using the site specific primer/probe pairs that were designed to span across intronic regions as to not represent genomic DNA. Details of Roche primers and probes (top table, blue boxes) and Taqman Amplicons (bottom table, peach boxes) are given, including; gene name, primer sequences, orientation, primer-matched probe numbers and accession numbers.

2.15. Immunoassays

2.15.1. Flow Cytometry

Cell cultures were dissociated into single cells using 0.25% trypsin-EDTA for 1-2 minutes at 37°C and neutralised using ice cold wash buffer (containing 90% PBS and 10% FBS). The cells were washed from the culture vessel and pelleted at 1200rpm for 3 minutes. The pellet was re-suspended in wash buffer and split equally between a set of BD Falcon round-bottom FACS tubes (BD Falcon, 352063) ensuring a minimum of $1x10^5$ cells per tube. Primary antibody was added (Table 2.2) while flicking to mix and the samples were refrigerated at 2-8°C in darkness for 30 minutes. As a negative control, we used an antibody, P3X, produced by the myeloma P3X63.Ag8 [159], the ultimate parent of all the hybridomas used to produce antibodies used in this study (Table 2.2). The TRA-1-85 primary antibody that has reactivity to a pan-human antigen [160], was used as a positive control for the antibody staining procedure. Three millilitres of wash buffer was added to wash the cells before being spun at 1200rpm for 3 minutes. The supernatant was aspirated down to the 200µl mark on the FACS tube before flicking to break up the pellet. Secondary antibody was then added (Table 2.2) while flicking to mix and the samples were refrigerated for a second time at 2-8°C in darkness for 30 minutes. The cells were washed twice with wash buffer and spun at 1200rpm for 3 minutes. The supernatant was aspirated to the 200µl mark and the cells were re-suspended in 300µl wash buffer. The cells were analysed on a CyAn ADP Analyser (Beckman Coulter, discontinued).

2.15.1.1 Gating strategy

Cells stained with P3X were run through the CyAn ADP Analyser and a forward scatter and side scatter gate was set to exclude cell debris, dead cells and clumps of cells based on cell size and granularity. Typically, clumps of cells have high forward scatter and debris has low forward scatter and high side scatter. Next, a gate was set to filter out doublet cells to ensure only single cell events were being analysed at any one time. Finally, a gate was set, based on the fluorescence profile of those cells stained with the negative control antibody, P3X, such that only 1%-5% of cells stained with the negative control would be scored positive. to determine the threshold between negatively and positively labelled cells.

2.15.2. In-situ Live Cell Staining on the IN cell analyser

Cell culture medium was aspirated and replaced with DMEM without phenol red (ThermoFisher, 21063). Primary antibody was added directly to the cells and incubated at 37°C for 30 minutes. The cells were washed twice with DMEM without phenol red and analysed on the IN Cell Analyser 2200 scanning microscope (GE Healthcare Life Sciences, 29027886). High content Imaging and analysis services were provided by specialist operators from the Centre for Stem Cell Biology, University of Sheffield, and annotated image files provided.

2.15.3. Immunofluorescence method

Cell cultures were fixed by aspirating the culture medium and replacing with 1ml/25cm^2 4% PFA for 15 minutes at room temperature. The PFA was then removed and the cells were blocked with 1ml/25cm^2 PBS containing 10% FBS for 30 minutes at 2-8°C. Then:

For staining with cell surface markers only

PBS containing primary antibody was added to the cells and incubated at 2-8°C in the dark for 1 hour. This was then aspirated, washed three times and then stained with secondary antibody diluted in PBS at 2-8°C in the dark for 1 hour. The cells were counterstained with Hoescht 33342 (ThermoFisher, 62249) during the incubation period with the secondary antibody and then washed a further three times and covered with 3ml PBS. The fixed cells were then visualised using an IN Cell Analyser 2200.

For staining with intracellular markers and cell surface markers

The blocking buffer was removed and replaced with permeabilisation buffer, comprised of 1ml/25cm^2 PBS 5% FBS containing 0.1% Triton X-100 (Sigma, X100), for 1 hour at 2-8°C. The permeabilisation buffer was then removed before the cells were stained with antibodies and washed as described above. All intracellular antibody staining, primary and secondary, took place before cell surface marker antibody staining. Counterstaining with Hoescht 33342 was performed at the same time as the final secondary antibody staining.

Table 2.2. List of primary and secondary antibodies used for flow cytometry and immunofluorescence

Primary Antibody	Secondary Antibody	Procedure	Source, [Origin]
P3X	Alexa Fluor 647 conjugated Goat Anti-Mouse	Flow Cytometry	In house, [159]
SSEA-1	Alexa Fluor 647 conjugated Goat Anti-Mouse	Flow Cytometry	In house, [18]
SSEA-3	Alexa Fluor 647 conjugated Goat Anti-Mouse	Flow Cytometry	In house, [15]
SSEA-4	Alexa Fluor 647 conjugated Goat Anti-Mouse	Flow Cytometry	In house, [16]
TRA-1-60	Alexa Fluor 647 conjugated Goat Anti-Mouse	Flow Cytometry	In house, [161]
TRA-1-81	Alexa Fluor 647 conjugated Goat Anti-Mouse	Flow Cytometry	In house, [161]
TRA-1-85	Alexa Fluor 647 conjugated Goat Anti-Mouse	Flow Cytometry	In house, [160]
OCT4	Alexa Fluor 488 conjugated Goat Anti-Rabbit	Immunofluorescence	C-10, SantaCruz (sc-5279)
TRA-1-60	Alexa Fluor 488 conjugated Goat Anti-Mouse	Immunofluorescence	In house, [161]
NCAM	Alexa Fluor 488 conjugated Goat Anti-Mouse	Immunofluorescence	In house, [18]
DESMIN	Alexa Fluor 488 conjugated Donkey Anti-Rabbit	Immunofluorescence	Cell Signalling Technology (5332)
	Hoescht 33342	Immunofluorescence	ThermoFisher Scientific (62249)

Table 2.2: Table showing a list of the primary and secondary antibodies and their sources used for both flow cytometry and fluorescent activated cell sorting (FACS) (blue) and immunofluorescence experiments (peach) using the IN Cell Analyser 2200 (GE Healthcare Life Sciences). In house antibodies were obtained from stocks prepared by the Centre for Stem Cell Biology from stocks of relevant hybridomas that are referenced above.

2.16. Karyotyping

Cell cultures were provided, as live cell cultures in T25 culture flasks, to the Sheffield Diagnostic Genetics Service at the Sheffield Children's NHS Foundation Trust for karyotyping, to be performed by a UK Health Professionals Clinical Cytogeneticist.

2.17. Isolating Plasmid DNA

2.17.1. Transforming Bacteria

LB Agar Tablets (Sigma, L7275) were diluted in ddH_2O and autoclaved. The liquid agar was cooled and GIBCO Ampicillin (ThermoFisher, 11593027) was added at 50µg/ml and then poured into a 10cm petri dish. The agar was left to solidify before being refrigerated upside down at 2-8°C until needed. Meanwhile, 1µg of plasmid and a 50µl aliquot of One Shot TOP10 chemically competent cells (ThermoFisher, C404010) was mixed and then cooled on ice for 25 minutes. The cells were heat shocked at 42°C for 30 seconds and then immediately placed back on ice for 2 minutes. The mixture was pipetted onto a set agar plate and smeared over the surface using a right-angled 230mm disposable Glass Pasteur pipette (VWR, 14672-380). The agar plate was incubated upside down at 37°C overnight.

2.17.2. Colony Picking

Colonies were picked using a non-filtered 200µl pipette tip (STARLAB, S1121) by hand from the overnight agar plate. The pipette tip was placed into a 15ml bacterial tube containing 5ml of liquid LB broth (Sigma, L3022). This was incubated overnight at 37°C while shaking. LB broth was reconstituted from 10g LB broth powder using 500ml ddH_2O.

2.17.3. Plasmid Extraction

Eighty percent of the overnight bacterial culture was transferred to a 1.5ml micro-centrifuge tube and pelleted at 8000rpm for 2 minutes. Twenty percent of the bacterial culture was mixed with 80% glycerol and stored at -80°C for long-term use. Plasmid DNA was then isolated using the GeneJET Plasmid Miniprep Kit (ThermoFisher, K0502).

2.17.4. Generating *MYOD1* mRNA

The *MYOD1* cDNA clone was contained within a pCMV6-XL5 plasmid (Origene, RG209108). To generate *MYOD1* mRNA the plasmid was initially transformed in to One Shot TOP10 chemically competent E.coli and selected on LB agar plates containing 50µg/ml ampicillin. Ampicillin resistant colonies were picked into LB broth and cultivated overnight in a shaking incubator at 200rpm in 37°C followed by plasmid purification using the GeneJET Plasmid Miniprep Kit. One microgram of purified plasmid was linearised using ten units of XbaI restriction enzyme (New England Biolabs, R0145S) in a 50µl reaction. Linearisation was confirmed prior to in-vitro transcription by running five microlitres of the restriction digest reaction on one percent agarose gels. In an adjacent well, non-linearised DNA was run to confirm the restriction digest had successfully linearised the plasmid. Successfully linearised plasmid was then in-vitro transcribed using the MEGAscript T7 kit (ThermoFisher, AM1333). The transcription reaction was performed as described in methods 2.20, purified and concentrated using the RNA Clean-Up and Concentration Kit (Norgen Biotek, 23600). To verify that *MYOD1* mRNA had been successfully transcribed, one microgram of mRNA was run on a one percent denaturing RNA gel (Methods 2.19.1). A single positive band at 2056 bases long confirms the mRNA has been successfully transcribed.

2.17.5 Generating mRNA from linearised DNA templates

Linearised DNA templates encoding *OCT4*, *SOX2, KLF4, cMYC, LIN28, NANOG* and *mWASABI* were supplied by Allele Biotech as part of their iPS Induction IVT Template Set (ABP-SC-SEIPSSET). Each template structure (shown below) contained a 5' and 3' UTR that flanked the gene of interest (GOI) (sequences unknown) and a 120-nucleotide polyA tail. Transcription was driven by a T7 promoter and the method used for in-vitro transcription is described in methods 2.20.

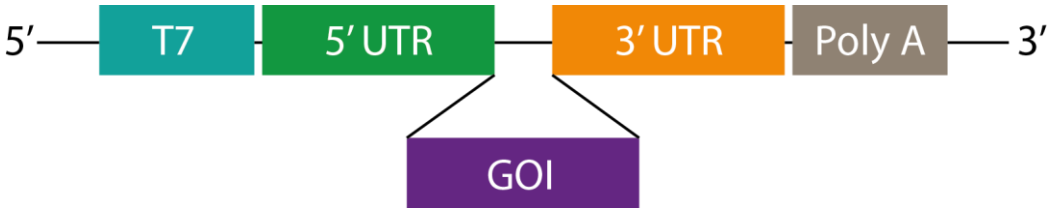

2.17.6 *OCT4-MYOD1* (*M_3O*) mRNA

M_3O mRNA was supplied as part of the 6-factor mRNA reprogramming premix kit (Allele Biotech, ABP-SC-6FMRNA). The gene map below (Figure. 2.5) has been drawn according to Hirai et al [68] and Berkes et al [162] on the understanding that *M_3O* is a fusion between the transcriptional activation domain (TAD) of *MYOD1*, located at its N-Terminus, that has been fused to the N-Terminus of *OCT4*.

Figure 2.5. Generating M_3O, a chimeric protein generated by fusing the transcriptional activation domain of MYOD1 with human OCT4 protein

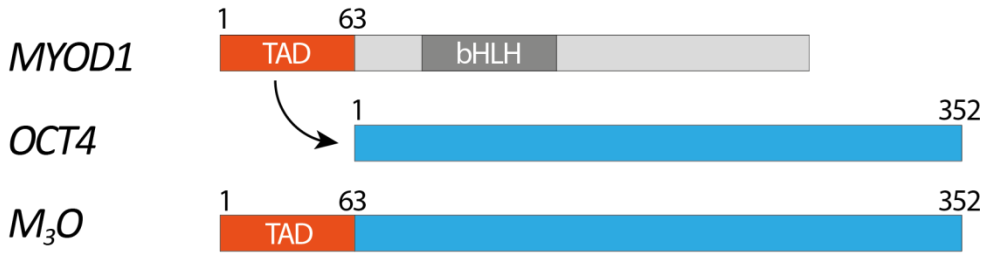

Figure 2.5: Domain structure of *MYOD1*, a transcription factor of the basic helix-loop-helix (bHLH) family, from which the transcriptional activation domain (TAD) is removed and fused to the N-terminus of human OCT4 protein to create a fusion protein called M_3O.

2.17.7 Generating mRNA from the RN3P plasmid

RN3P is an in-house plasmid (Figure. 2.6) that has been modified from pBluescript SK(-) to contain additional linearization sites, PstI and SfiI, and a multiple cloning site that is flanked by 5' and 3' globin untranslated regions [163]. The plasmid contains *eGFP* that is driven by a T3 promoter. Linearisation of the RN3P plasmid is performed by combining 1µg of RN3P plasmid to 10 units of SfiI restriction enzyme (New England Biolabs, R0123S), 5µl 10X NEBuffer (New England Biolabs, B7202S) and 100µg/ml BSA (New England Biolabs, B9000S) in a 1.5ml micro-centrifuge tube. The mixture is made up to 50µl with ddH_2O and then heated to 37°C for 1 hour. IVT reactions were performed from the linearised RN3P plasmid using the T3 MEGAscript Kit (ThermoFisher, AM1338) following the same procedure as described in methods 2.20.

Figure 2.6. Plasmid map for RN3P

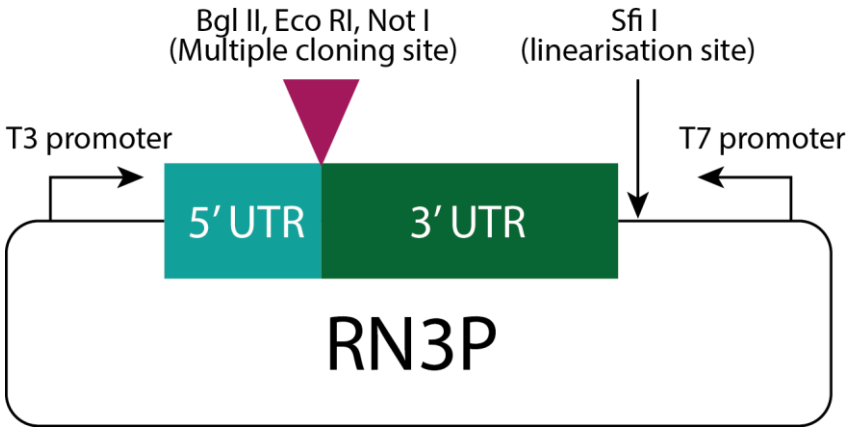

Figure 2.6: eGFP mRNA was transcribed from the RN3P plasmid. The coding region for eGFP was inserted into the RN3P plasmid at a multiple cloning site that is flanked by 5' and 3' untranslated regions of *Xenopus* β-globin. The globin region resides downstream of a T3 promoter that drives the transcription of eGFP and a recombinant polyA tail. Linearisation of the RN3P plasmid was performed using the SfiI restriction enzyme.

2.18. Restriction Digest

A mixture was made containing 1µg of plasmid DNA, 5µl 10x NEBuffer, 0.25µl BSA, 1 unit of restriction enzyme (New England Biolabs) and ddH_2O to 50µl. A larger volume of restriction enzyme was used when its activity was less than 100% in the appropriate buffer. The mixture was placed in a DNA Thermal Cycler 480 (Perkin Elmer, 313002) for 1 hour, typically at 37°C. The plasmid was then ready to be verified by gel electrophoresis.

2.19. Gel Electrophoresis:

2.19.1 DNA gels

An EDTA solution (0.5M) was made by diluting 18.61g of EDTA powder (Fisher Scientific, S311) in 80mls ddH_2O. The pH of the solution was adjusted to 8.0 with 5M NaOH. Then a 10X TBE solution was made by adding 40mls of 0.5M EDTA solution to 108g Trizma Base (Sigma, T1503) and 55g Boric Acid (Sigma, 185094) before making up to 1 litre with ddH_2O. This was diluted to a 1X concentration with ddH_2O to create a working TBE solution. For a 1% agarose gel 1g of Agarose (Fisher Scientific, BP160) was dissolved in 100ml 1X TBE solution. Ethidium Bromide (Fisher Scientific, BP1302-10) was added to a final concentration of 100ng/ml and then poured into a multiSub Mini Horizontal Gel Tray (Cleaver Scientific, MSCHOICETRIO) containing a gel comb. After the gel had set the comb was removed and it was transferred to a multiSub Mini Horizontal gel tank containing a sufficient amount of 1X TBE to cover the upper surface of the gel. A mixture of 25% linearised plasmid DNA, 25% 6X DNA loading dye (Thermo Fisher, R0611), 25% 6X Bromophenol Blue (Sigma, 114391) and 25% ddH_2O was then added to the agarose gel wells alongside 5µl GeneRuler 1kb DNA ladder (Thermo Fisher, SM0312). The gel tank was connected to a PowerPac 300 power supply (Bio-Rad,

164-5050) and run for 40 minutes at 120V. The bands were visualised using an InGenius Bio Imaging trans-illuminator (SYNGENE) and image acquisition was carried out using Genesnap (SYNGENE) software.

2.19.2. Gel Electrophoresis: running RNA gels

RNA was run on a 1% agarose/formaldehyde gel containing 0.5µg/ml ethidium bromide. The Agarose gel was made by combining 20ml 5X MOPS buffer (Sigma, M1254) with 72ml ddH_2O and 1g of Agarose. To make a two-litre stock of 5X MOPS buffer, 83.72g of MOPS and 8.23g of sodium acetate was added to 1.6 litres of ddH_2O. The mixture was stirred until it had completely dissolved. To this, 20ml 0.5M EDTA was added and the pH adjusted to 7.0 using 10M NaOH. The volume was made up to two litres with ddH_2O and then autoclaved. The agarose gel mixture was boiled in a microwave until molten and then cooled to 55°C. To this, 17.6ml 37% formaldehyde (Sigma, F15587) and 0.5µg/ml ethidium bromide was added before the gel was poured into a gel tray (as described in 2.19.1). Once the gel had set it was submersed in 1X MOPS buffer in a multiSub Mini Horizontal gel tank containing a sufficient amount of 1X MOPS buffer to cover the upper surface of the gel. To prepare RNA samples for loading, 5µl RNA was mixed with 10µl RNA buffer. RNA buffer was made by mixing 2ml 5X MOPS buffer with 3.5ml 37% formaldehyde and 10ml Formamide (Sigma, F9037). To this, 5µl RNA loading Dye 2X (New England Biolabs, B0363S) was added before loading into wells of the 1% agarose/formaldehyde gel alongside 5µl ssRNA ladder (New England Biolabs, N0362S). The gel tank was connected to a PowerPac 300 power supply and run at 7V/cm until the loading dye could be seen to have migrated 2/3 the length of the gel. The bands were visualised using an InGenius Bio Imaging trans-illuminator and image acquisition was carried out using Genesnap software.

2.20. In-vitro Transcription of mRNA with modified nucleotides

The enzyme mix and reaction buffer from the T7 MEGAscript Kit (Thermo Fisher, AM1333) was used to *in-vitro* transcribe mRNAs from linearised DNA templates. A mixture was made at room temperature consisting of 2µl 75mM ATP and 2µl 75mM GTP solution (Thermo Fisher, AM1333), 2µl 100mM 5-Methylcytidine-5'-Triphosphate (Stratech, Table 2.3), 2µl 100mM Pseudouridine-5'-Triphosphate (Stratech, Table 2.3), 2µl 60mM Anti-Reverse Cap Analog (Stratech, Table 2.3), 2µl 10X reaction buffer, 1µg linearised template DNA and 2µl enzyme mix. The mixture was made up to 20µl with ddH_2O and pipetted to mix before being micro-centrifuged. The mixture was then incubated in a DNA Thermal Cycler 480 at 37°C for one hour. The mRNA was then purified using the RNA Clean-Up and Concentration Kit and stored at -80°C in working aliquots.

Table 2.3. Commercially sourced reprogramming reagents

Reprogramming Reagent	Catalogue #
Stemgent Reprogramming	**00-0071**
2 vials - Stemgent Oct4 mRNA, Human, 20µg	05-0014
1 vial - Stemgent Klf4 mRNA, Human, 20µg	05-0015
1 vial - Stemgent Sox2, Human, 20µg	05-0016
1 vial - Stemgent Lin28 mRNA, Human, 20µg	05-0017
1 vial - Stemgent c-Myc mRNA, Human, 20µg	05-0018
1 vial - Stemgent nGFP mRNA, 20µg	05-0019
Allele Biotech iPS Induction IVT template set	**ABP-SC-SEIPSET**
Oct3/4 IVT Template 5 µg	ABP-SC-SEOCT34
SOX2 IVT Template 5 µg	ABP-SC-SESOX2
Klf4 IVT Template 5 µg	ABP-SC-SEKLF4
c-Myc IVT Template 5 µg	ABP-SC-SECMYC
Lin28 IVT Template 5 µg	ABP-SC-SELIN28
Nanog IVT Template 5 µg	ABP-SC-SENANOG
mWasabi IVT Template 5 µg	ABP-FP-SEMWASABI
Anti Reverse Cap Analog, 5mg (Stratech)	NU-855-5-JEN
5-Methylcytidine-5'-Triphosphate, 5 µmol (Stratech)	5-0613-295-IBA
Pseudouridine-5'-Triphosphate, L Pack, 5 x 10µl (Stratech)	NU-1139L-JEN
MEGAscript® T7 Transcription Kit (Thermo Fisher)	AM1333
75mM ATP solution (Thermo Fisher), Megascript T7	AM1333
75mM GTP solution (Thermo Fisher), Megascript T7	AM1333
T7 Enzyme Mix (Thermo Fisher), Megascript T7	AM1333
10X reaction buffer (Thermo Fisher), Megascript T7	AM1333
Allele Biotech 6-factor mRNA Reprogramming	**ABP-SC-6FMRNA**
6F mRNA Reprogramming Premix	ABP-SC-6FMRNA
Additional Reagents	
B18R Recombinant Protein, Carrier-Free (eBioscience)	34-8185
Stemfect RNA Transfection Kit	00-0069
MEGAscript® T3 Transcription Kit (Thermo Fisher)	AM1338
B18R Recombinant Protein, Carrier-Free, 50µg	03-0017
0.2 ml of Pluriton™ Supplement 2500X	01-0016
500 ml of Pluriton™ Medium	01-0015

Table 2.3: The reagents used for reprogramming have been listed above. The reagents have been placed in categories: Stemgent reprogramming, Allele Biotech 6-factor mRNA Reprogramming or Allele Biotech iPS Induction IVT template set depending on where they were primarily used.

2.20.1 In-vitro Transcription of mRNA without modified nucleotides

In-vitro transcribing mRNA without modified nucleotides follows the same procedure as *in-vitro* transcribing mRNA with modified nucleotides albeit the modified nucleotides Pseudouridine-5'-Triphosphate (Stratech, NU-1139L-JEN) and 5-Methylcytidine-5'-Triphosphate (Stratech, 5-0613-295-IBA) are substituted with UTP and CTP respectively. Unmodified mRNAs are still capped and polyadenylated.

2.21. mRNA Transfection

Cells were plated in a well of a 6WP on day -1 at a density that would achieve 50-90% confluency after 24 hours. On day 0, Pluriton media was added to a sterile well of a 6WP and equilibrated to 5% CO_2 at 37°C in either low O_2 (5% O_2) or normoxia (normal atmospheric oxygen levels – 21% O_2) for >30 minutes. Meanwhile mRNA was diluted to 100ng/µl with ddH_2O. An mRNA cocktail was then made consisting of 10% mRNA and 90% Stemfect Transfection Buffer (Stemgent, 00-0069). Stemfect RNA transfection reagent (Stemgent, 00-0069) was then added at 4µl / µg of mRNA. The mRNA cocktail was mixed and incubated at room temperature for >15 minutes. It was then added to the equilibrated media and the plate was rocked back and forth by hand to mix. The cell media was aspirated and replenished with the equilibrated media containing the mRNA cocktail. The cells were then put back in a 5% CO_2 incubator at 37°C in normoxia or at low O_2 (5% O_2) for 24 hours.

2.22. Cell Imaging

2.22.1. Fluorescent Microscopy

Cells treated with mRNA encoding a fluorescent protein such as nGFP (Stemgent, 05-0019) or mWASABI (Allele Biotech, ABP-FP-SEMWASABI) would fluoresce upon successful transfection. The monomeric green fluorescent protein, mWASABI, is derived from *Clavularia* coral and is 1.6-fold brighter than eGFP [164]. The fluorescent proteins were visualised in real-time using an EVOS FL Cell Imaging System (ThermoFisher, AMEFC4300).

2.22.2. Whole-well Imaging

When imaging an entire well of a 6WP was necessary, whole-well imaging was undertaken using a BioStation CT (Nikon). This was achieved by setting up a tiling experiment set to capture a grid of 18x18 images at 4X magnification in both phase contrast and the 472-520nm fluorescent channel. Images were then stitched together by importing the tiling micro.CSV file into the CL Quant (Nikon) software to produce a whole-well image.

2.23. Directed Differentiation via Embryoid Body Formation

2.23.1. Pre-attachment Vessel Preparation

A T25 of MEFs was made at least 3 days prior to the harvesting of cell cultures that were to be differentiated as EBs. Cell cultures that were differentiated as EBs included pluripotent stem cells or iPS cells derived from SK-N-SH or fibroblasts. The day before cells were to be

harvested, the conditioned MEF media was transferred to a sterile T25 and incubated at 37°C in 10% CO_2 until required.

2.23.2. Plate Setup

For directed differentiation, four round-bottom CELLSTAR 96-Well Plates (Sigma, M9436) were used for each cell line, constituting the four differentiation conditions; neutral, endoderm, mesoderm and ectoderm containing APEL medium (STEMCELL Technologies, 05270) and combinations of growth factors and inhibitors (Table 2.4). Five millilitres of APEL media was added to 4X 15ml falcon tubes containing different types and amounts of growth factors and inhibitors (Table 2.4). Gentamicin was added at 1:500 and the supplemented media was transferred to a StarTub Reagent Reservoir (STARLAB, S4026-5806) where it was pipetted into the inner 60 wells of the appropriate 96-well plate. One hundred microliters of PBS was added to the outer 36 wells to prevent evaporation. The plates were then transferred to a 37°C incubator in 5% CO_2 until required.

Table 2.4. Growth factor and inhibitor combinations used for directed EB differentiation

	Neutral	Endoderm	Mesoderm	Ectoderm
Activin A		100ng/ml	20ng/ml	
BMP4		1ng/ml	20ng/ml	
SB431542				10µM/ml
DMH-1				1µM/ml
bFGF				100ng/ml

Table 2.4: Pluripotent stem cells, iPS cells derived from SK-N-SH or fibroblasts that were differentiated as embryoid bodies were subjected to four conditions. The neutral condition contained only APEL media to induce spontaneous differentiation to the three germ layers. The three other conditions comprised a mixture of APEL media and combinations of growth factors and inhibitors to direct differentiation to the three primary germ layers. Directed differentiation towards Ectoderm was driven by 100ng/ml bFGF, 1uM/ml DMH1 that inhibits BMP to promote neurogenesis in hESCs and 10uM/ml SB431542 that inhibits differentiation toward mesendodermal lineages by disrupting TGFβ/activin/nodal signalling [164]. Mesoderm differentiation was induced by 20ng/ml Activin A that activates the TGFβ/activin/nodal signalling pathway and 20ng/ml BMP4 that upregulates SLUG to drive the transition of cells from epithelial to mesenchymal derivatives [165]. Endoderm differentiation was induced by 100ng/ml Activin A and 1ng/ml BMP4. While endoderm and mesoderm differentiation both require Activin A and BMP4, the differing concentrations specify the lineage that differentiation is driven towards.

2.23.3. Harvesting cells and pre-attachment

The process for embryoid formation (Figure. 2.7) is as follows. T25 cell culture vessels containing pluripotent stem cells or iPS cells derived from SK-N-SH or fibroblasts were dissociated into a single cell suspension using 0.5mls TrypLE at 37°C for 2 minutes. After 2 minutes the culture vessels were given a sharp tap to dislodge the cells. The TrypLE was neutralised with 3ml hESC media. The media from the pre-attachment vessel (methods 2.23.1) was then aspirated and the single-cell suspension was added to this vessel and then incubated at 37°C for 30 minutes. The media was then aspirated and replaced with a further 3ml hESC media containing Y-27632 dihydrochloride solution (Sigma, Y0503) at a final concentration of 10µM. The Rho-associated kinase (ROCK) inhibitor, Y-27632 aids in cell survival of dissociated pluripotent stem cells at low densities [167]. The vessel was incubated for 30 minutes at 37°C in 5% CO_2 and then scraped using a sterile cell scraper (VWR, 89260-222) into a 15ml falcon tube. The cells were counted and then pelleted at 1000rpm for 3 minutes. Cells were re-suspended at a final concentration of 3000 cells / 50µl and then pipetted into the pre-prepared plates (methods 2.23.2). The plates were then spun at 1000rpm for 3 minutes to collect the cells in the centre of the wells before being transferred into a 5% CO_2 incubator at 37°C for 10 days.

Figure 2.7. Embryoid Body formation process

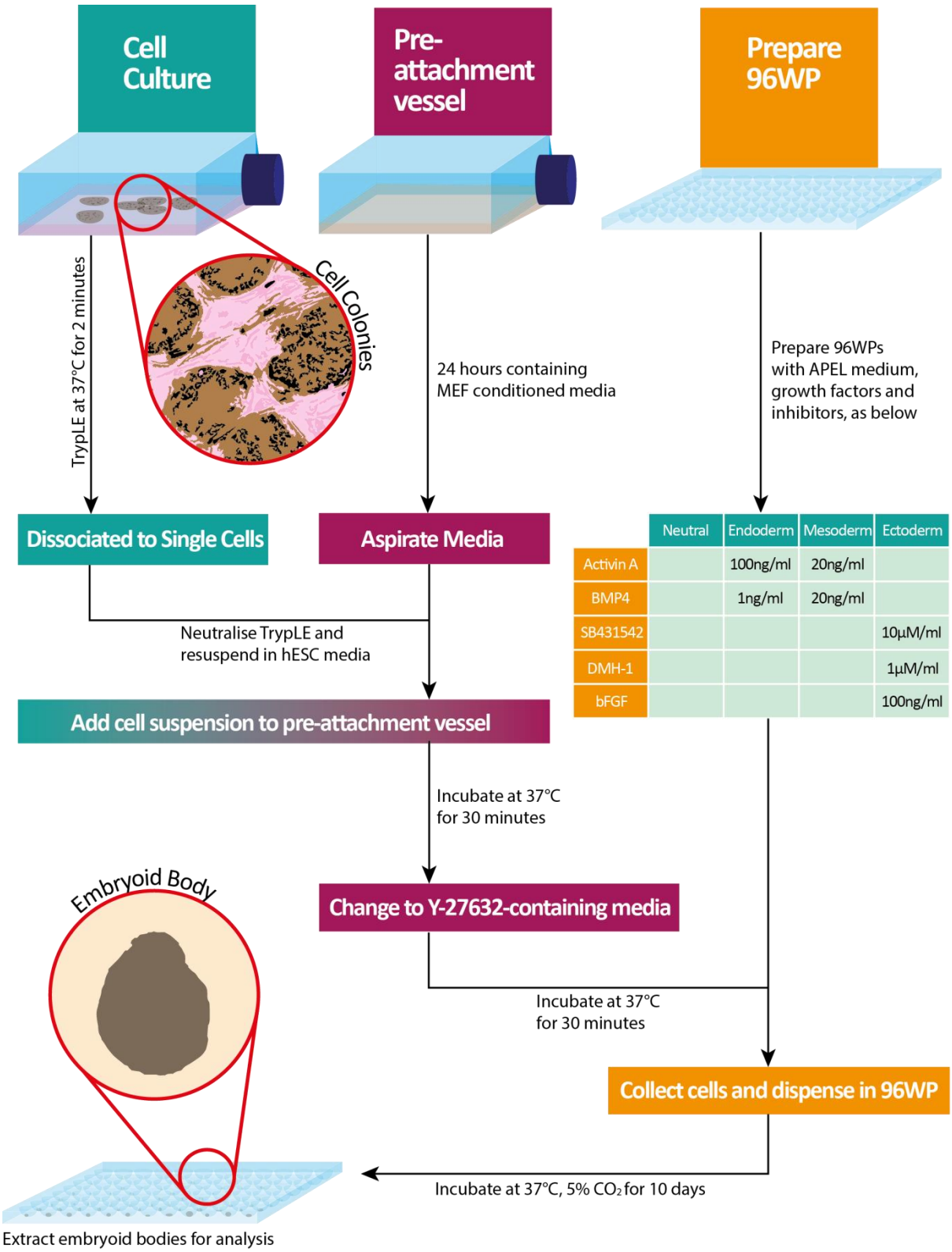

Figure 2.7: Pluripotent stem cells form embryoid bodies (EBs) when differentiated in a low-attachment culture vessel. Differentiation toward endoderm, mesoderm and ectoderm can be directed by creating EBs in medium containing combinations of growth factors and inhibitors (shown in the table provided and Table 2.4). Once EBs are formed they are analysed by qPCR for the presence of markers that distinguish the three germ layers.

Chapter 3.

Developing a reproducible, fast and efficient reprogramming method using non-integrating mRNAs.

3.1. Introduction

Reprogramming has been achieved using a variety of different methods that introduce reprogramming factors into somatic cells such as; retrovirus [36], lentivirus [45], Sendai virus [70], piggyBac transposition [71] and episomal vectors [72]. The reprogramming factors are often constitutively expressed when delivered using these methods and therefore do not need to be repeatedly added to the somatic cells during reprogramming. However, despite the technical simplicity of reprograming using these methods there are potential drawbacks, for example DNA and viruses can integrate freely and at random sites within the genome. This can induce carcinogenic behaviour, lead to insertional mutagenesis and cause undesirable off-target effects [73]. For instance it has been shown that mice will develop tumours following the reactivation of retroviral vectors when the site of integration is downstream of nearby promoter regions. There is also the issue that integrating methods create transgenes and that there is a lack of control over the number of stable integrations that take place, affecting the ability to control gene expression. To circumvent these problems it is necessary to develop reprogramming methodologies that do not interfere with the target cell's underlying genetic code.

Warren et al showed that exogenous mRNA encoding *OCT4, SOX2, KLF4, cMYC and LIN28* [76, 168] could be utilised to efficiently generate human iPS cells in a safe manner. MRNAs offer an integration-free alternative to viruses for reprogramming and directing cell fate. There is also no

requirement to produce viral vectors as mRNAs are created through *in vitro* transcription reactions from linearised DNA templates or from PCR products containing a double stranded promoter region, making them much safer to work with. The main limitation to utilising mRNAs was mitigating against degradation and overcoming the innate interferon immune response induced by single stranded RNAs [84].

Warren et al [76] identified that the limitations to mRNA-mediated reprogramming can be circumvented by performing transcriptional and chemical modifications to mRNAs. Transcriptional modifications included substituting the nucleotides CTP and UTP during *in vitro* transcription reactions with 5-methylcytidine-5'-triphosphate and pseudouridine-5'-triphosphate respectively that decrease the susceptibility of mRNA to degradation by nucleases and deadenylation pathways. Warren polyadenylated and capped mRNAs to further reduce their susceptibility to degradation in addition to flanking the mRNA coding sequence with untranslated regions (UTRs). Untranslated regions are designed to facilitate mRNA localisation, stability, export, and translational efficiency [169]. However, the sequence of the untranslated regions used in this study is unknown and therefore mRNAs transcribed from IVT templates containing different UTRs may have different functional properties. It is therefore important to determine the properties of mRNAs prior to reprogramming to ensure they are capable of being taken up by somatic cells with high efficiency to improve the probability that reprogramming will occur.

Despite the advances in mRNA modifications and the suppression of interferon, mRNA-mediated reprogramming is not without its disadvantages. Firstly mRNA reprogramming takes two weeks and requires the daily addition of mRNA which is both costly and time-consuming and secondly current methods involve splitting the cells mid-way throughout reprogramming. This is done to promote fibroblast proliferation and ease overcrowding in the culture vessel [56] however in

doing so, any reprogramming efficiency statistics are nullified by the possibility that all of the emerging iPS cell colonies have been derived from a single colony that has proliferated from a single iPS cell. In addition, a single clonal cell line does not truly reflect the heterogeneity of the bulk reprogramming culture with respect to gene expression, differentiation capacity or cytogenetics. It is therefore important to develop reprogramming methods that avoid splitting the cells so that better insights into iPS cell heterogeneity can be gained through comparing iPS cell lines of independent clonal origin.

A study by Hanna et al [56] suggested that the kinetics of reprogramming can be accelerated by increasing the number of cell divisions that occur during reprogramming. By inhibiting p53/p21 expression they induced a 2-fold increase in the average cell population doubling rate that correlated to a ~2-fold increase in the kinetics of reprogramming. They attribute this to the acquisition of epigenetic marks during cell division that improve chromatin accessibility so that transcription factors that promote pluripotency are more actively transcribed. The study also describes how measures were taken to avoid reprogramming cultures from becoming over-confluent. Over-confluency induces cells to upregulate p57 expression that inhibits cell proliferation which consequently reduces the efficiency of reprogramming [170].

The suggestion that the success of reprogramming is dependent upon the number of cell divisions [56] but that over-confluency inhibits this process [170], alludes to the notion that reprogramming is most efficiently executed when a balance between cytotoxicity and cellular proliferation is strictly controlled, enabling cells to continually divide without becoming over confluent. Avoiding over-confluency will also negate the requirement to passage the cells during reprogramming. If existing methods were optimised so that there were no requirement to split the cells during reprogramming then this will be advantageous in two ways. Firstly splitting the cells adds confusion to the process as it is unknown whether splitting improves reprogramming

itself or improves the survival and proliferation of emergent iPS cells. For instance, splitting the cells could facilitate the acquisition of epigenetic marks that enhance reprogramming or it could simply increase the amount of space available for iPS cells to emerge and proliferate. Secondly, not splitting the cells during reprogramming allows for the isolation of truly independent iPS cell clones, allowing for reprogramming efficiencies to be accurately calculated. Splitting cells during reprogramming makes it impossible to determine whether the presence of multiple iPS cell colony outgrowths have arisen from a single colony or from individual reprogramming events.

In this chapter, we tried to establish the best possible way for our laboratory to reprogramme cells with mRNA in a quick and efficient manner. Even though protocols exist, they still result in a lot of variability and scientists often fail to achieve reprogramming [54] so we intended to develop our own protocol. We determined the kinetics and efficiency of reprogramming using mRNAs contained within commercial kits from Stemgent and Allele Biotech in addition to being derived from in-house DNA templates. Our findings and the characterisation of the iPS cells generated are presented in this results chapter.

3.2. Results

3.2.1. Characterisation of BJ fibroblasts

In order to establish a gold standard for reprogramming we sought to use a cell line that can be reproducibly reprogrammed into iPS cells using mRNAs. In respect of this, we used the BJ fibroblast cell line (Stemgent, 08-0027) that has been functionally verified by Stemgent to be amenable to reprogramming. Characterisation was performed on BJ fibroblasts to identify endogenous mRNA levels and cell surface markers that are characteristically different between fibroblasts and pluripotent stem cells. The comparison will enable us to monitor the shift toward pluripotency during reprogramming experiments, described throughout Chapter 3.

BJ fibroblasts are a widely utilised human new born foreskin fibroblast cell line that has a longer replicative lifespan than other established human fibroblast cell lines due to slower telomere shortening [104]. In addition, the BJ fibroblast cell line was used for reprogramming as several studies have reproducibly demonstrated that it can be reprogrammed using mRNAs [39, 76, 168]. Upon receipt of the BJ fibroblast cell line, cell banks were created to maintain a low passage working stock for future reprogramming experiments. BJ fibroblasts were analysed for chromosomal abnormalities by karyotype analysis but were found to be karyotypically normal exhibiting a 46XY male karyotype (Figure. 3.1A). BJ fibroblasts were analysed by flow cytometry to confirm a panel of cell-surface markers that are differentially expressed between fibroblasts and iPS cells (Figure. 3.1B). It was found that: SSEA-3, SSEA-4, TRA-1-60 and TRA-1-81, that are known to be expressed in hESCs and iPS

cells in an undifferentiated stem cell state, are not expressed in BJ fibroblasts. SSEA-1 that is expressed when hESCs and iPS cells differentiate is also not expressed in BJ fibroblasts (Figure. 3.1B). One hundred percent of fibroblasts expressed TRA-1-85, a pan-human antigen, that shows the antibody staining procedure was successful.

BJ fibroblasts were further characterised by qPCR to detect endogenous mRNA levels for *OCT4, SOX2, KLF4, cMYC, LIN28* and *NANOG* (Figure. 3.2). There were no detected endogenous mRNA levels for *OCT4, SOX2, LIN28* or *NANOG* in fibroblasts relative to the undifferentiated control hESC line, Shef6, when analysed by qPCR. BJ fibroblasts do however contain a 324-fold higher level of endogenous *KLF4* relative to levels detected in Shef6. It was also shown that endogenous *cMYC* mRNA levels were 1.8-fold higher in fibroblasts than the control hESC line.

Figure 3.1. Karyotyping and flow cytometric analysis of the BJ fibroblast cell line

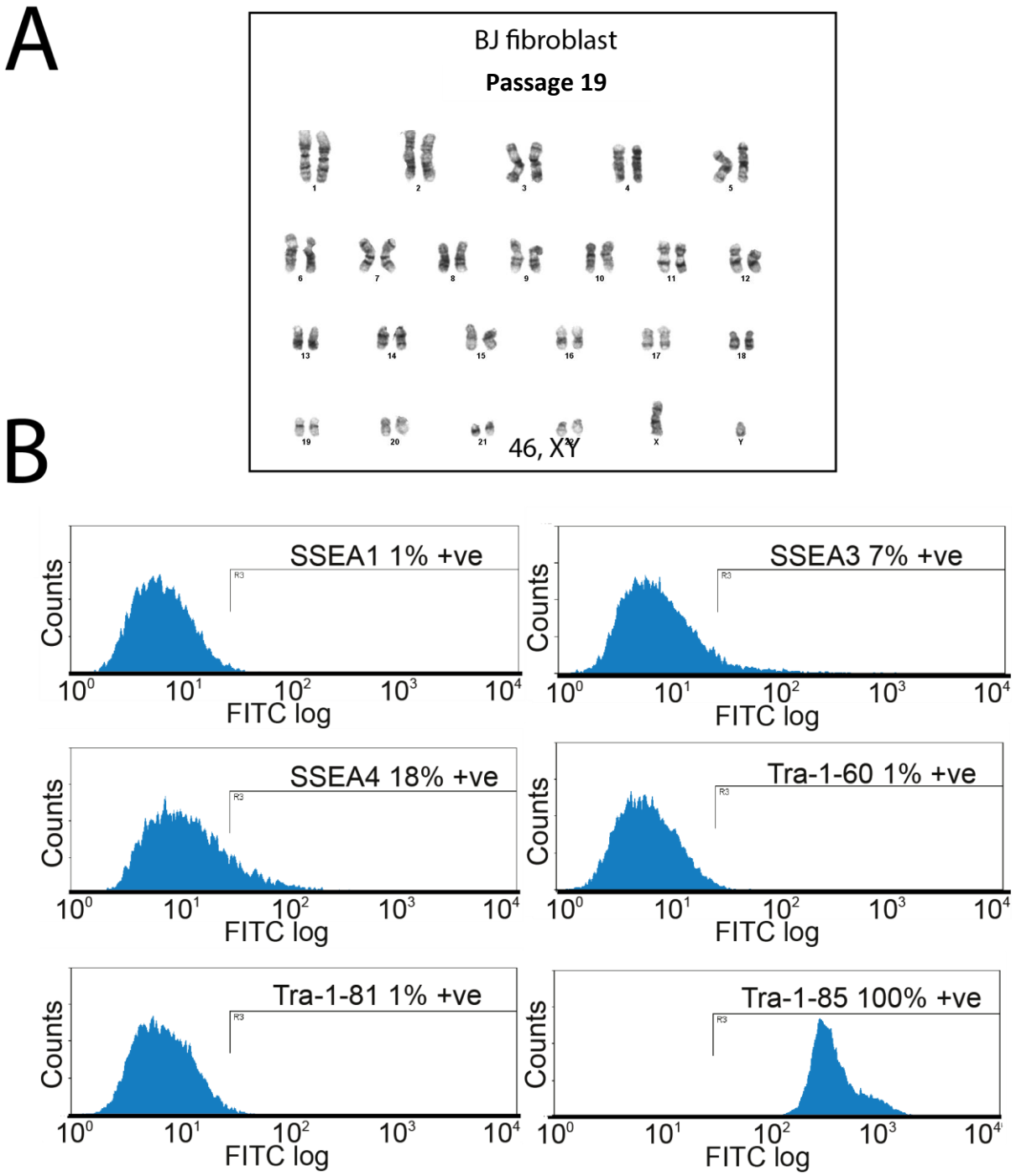

Figure 3.1: (A) Metaphase spread (methods 2.16) of the BJ Fibroblast cell line shows that BJ fibroblasts are karyotypically normal. (B) Flow cytometric analysis of BJ fibroblasts show that they do not express cell surface markers associated with pluripotency in human embryonic stem cells. The blue histograms represent the cell population and the spread of the histogram denotes variations in fluorescent intensity. Gating was performed as described in methods 2.15.1.1. TRA-1-85 is a pan-human marker and 100% expression confirms that the cells are human.

Figure 3.2. Analysis of the BJ fibroblast cell line by qPCR

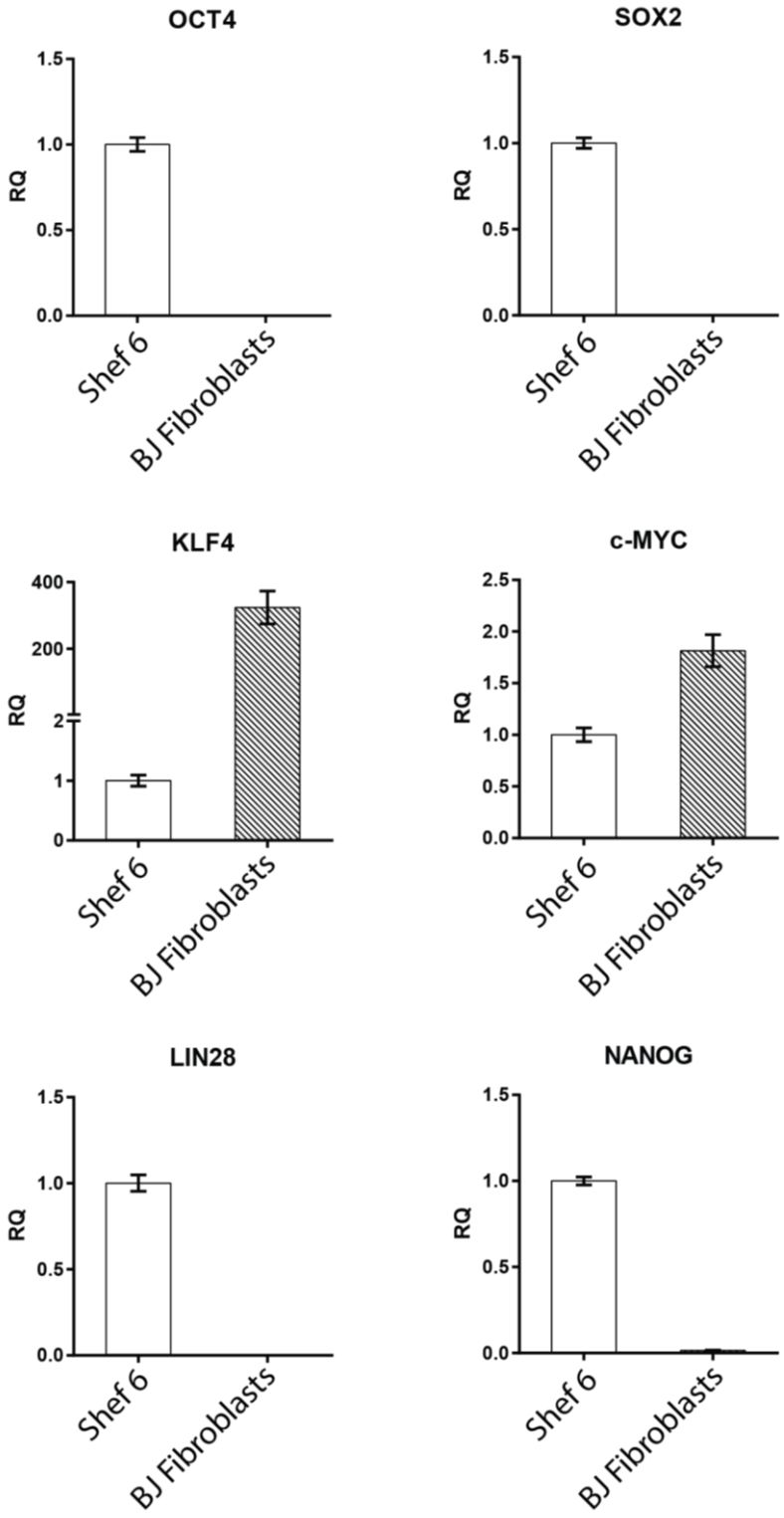

Figure 3.2: The mRNA levels of *OCT4, SOX2, KLF4, CMYC, LIN28* and *NANOG* were compared between the BJ fibroblast cell line at passage +9 and an undifferentiated control hESC line, Shef6, at passage +92. BJ fibroblasts do not express *OCT4, SOX2, LIN28* and *NANOG* but *cMYC* and *KLF4* mRNA levels were found to be ~2-fold and 324-fold higher respectively, relative to Shef6. CT values were normalised to *GAPDH*. N=1 (error bars derived from technical triplicates).

3.2.2. Comparing fluorescence levels and intensities induced by mRNAs derived from the RN3P plasmid and Allele Biotech IVT templates

Does mRNA encoding the mWASABI fluorescent protein, derived from the Allele Biotech iPS induction template (ABP-FP-SEMWASABI), transfect BJ fibroblasts more efficiently than mRNA encoding *eGFP* derived from the RN3P template (methods 2.17.7)? If the Allele Biotech templates generate mRNA that is less susceptible to degradation compared to mRNAs transcribed from RN3P, mRNAs transcribed from Allele Biotech templates may be more appropriate for use in reprogramming experiments that rely on the overexpression of exogenous mRNAs to be sustained.

MRNAs encoding fluorescent proteins mWASABI and eGFP, were transcribed from the Allele Biotech IVT template (ABP-FP-SEMWASABI) and the RN3P DNA template (methods 2.17.7) respectively and introduced into BJ fibroblasts to determine the efficiency that each mRNA was taken up by the cells, based on fluorescence levels and fluorescence intensity. The successful uptake of mRNA by the fibroblasts will cause the fibroblasts to fluoresce. BJ fibroblasts were seeded at a density of $2x10^5$ in Pluriton medium and then 400ng of modified (methods 2.20) or unmodified (methods 2.20.1) *mWASABI* or *eGFP* mRNA was introduced into the cells for 24 hours. After 24 hours, the cells were visualised under an EVOS FL Cell Imaging System (Figure. 3.3). The only well that did not contain visibly fluorescing cells was that introduced to unmodified RN3P *eGFP* mRNA.

After imaging, the percentage of fluorescing cells and the median fluorescent intensities were quantitatively analysed by flow cytometry. It was found that >95%

of fibroblasts were fluorescing following the addition of modified and unmodified *mWASABI* and modified *eGFP* (Figure. 3.3) mRNA, indicating the fibroblasts had taken up both mRNAs successfully. Adding unmodified *eGFP* mRNA into fibroblasts resulted in less than 10% of cells fluorescing. Fewer than 5% of BJ fibroblasts were fluorescing in the untreated and mock transfected controls and were 350-fold and 200-fold dimmer respectively than the well containing modified *mWASABI* mRNA. However, the addition of modified *mWASABI* mRNA into BJ fibroblasts induced fluorescent intensity levels 19-fold brighter compared to when modified *eGFP* was added to BJ fibroblasts. The fluorescent intensities of the other wells that had been introduced to mRNA appeared to diminish in the following order; unmodified *mWASABI*, modified *eGFP* and lastly unmodified *eGFP*. Controls included an un-treated well of BJ fibroblasts and a mock transfected well. The mock transfected well contained Stemfect transfection reagent and buffer to test whether the reagents affected the fluorescence levels or intensities in any way relative to the untreated control.

Figure 3.3. Comparing fluorescence levels and intensities induced by mRNAs derived from the RN3P plasmid and Allele Biotech IVT templates

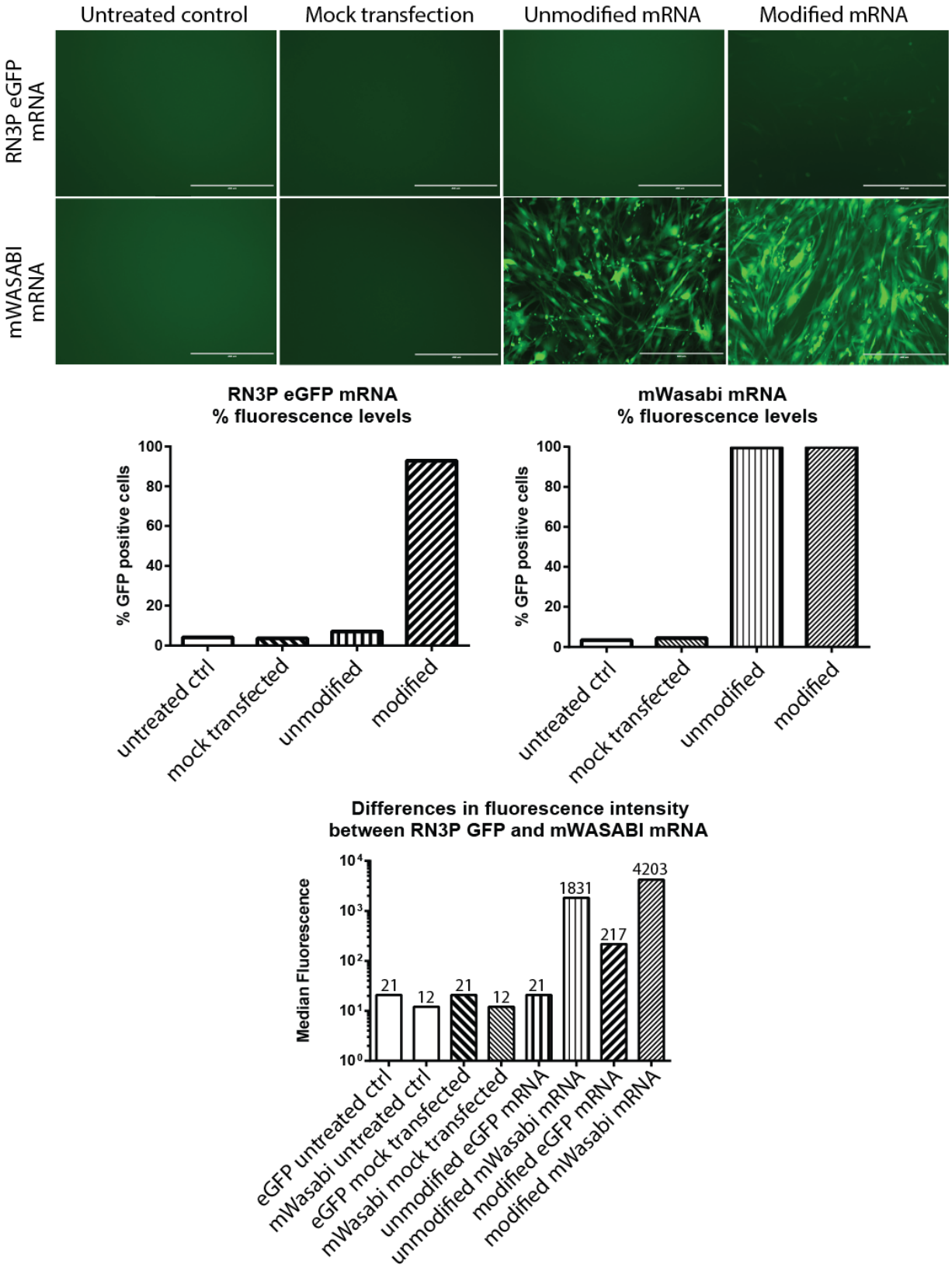

Figure 3.3: A dose of 400ng modified (methods 2.20) and unmodified (methods 2.20.1) *eGFP* and *mWASABI* mRNA was introduced in to BJ fibroblasts for 24 hours. One hundred percent of cells fluoresced when introduced to unmodified and modified *mWASABI* and modified *eGFP*, however the fluorescent intensity of modified *mWASABI* was ~19-fold higher than modified *eGFP*. Untreated and mock transfected controls contained <5% fluorescing cells. N=1. Scale bars = 400µm.

3.2.3 Commercial template-derived mRNAs induce higher levels of mRNA in fibroblasts compared to mRNAs derived from in-house DNA templates after a single transfection

mWASABI mRNA was determined to be 19-fold brighter than _eGFP_ mRNA when introduced in to BJ fibroblasts. One reason this may occur is that the former was better at getting into the cells and thus there were more vectors per cell resulting in a higher fluorescent intensity. Are mRNAs encoding the reprogramming factors that are derived from Allele Biotech IVT templates (ABP-SC-SEIPSET) also better at getting into BJ fibroblasts compared to mRNAs encoding the reprogramming factors derived from RN3P templates (methods 2.17.7)?

To test this I introduced a cocktail of exogenous mRNAs encoding *OCT4, SOX2, KLF4, cMYC, LIN28* and *NANOG* derived from Allele Biotech IVT templates (ABP-SC-SEIPSET) or from RN3P templates (methods 2.17.7) into BJ fibroblasts and assessed mRNA levels by qPCR after 24 hours. This was to determine how efficiently the reprogramming factor mRNA can get in to the cells. The comparison was extended to include Allele Biotech's 6-factor mRNA reprogramming premix (ABP-SC-6FMRNA) that contains pre-made mRNAs encoding the six factors; *M_3O, SOX2, KLF4, cMYC, LIN28* and *NANOG*. *M_3O* is a fusion between the *OCT4* gene and the transcriptional activation domain of *MYOD1* [68], a potent inducer of gene expression [171].

The mRNA cocktails contained a three-fold relative increase of *OCT4* or *M_3O* to *SOX2, KLF4, cMYC, LIN28* and *NANOG*. Human foreskin fibroblasts were seeded at a density of $3x10^5$ on Matrigel in Pluriton medium. After 24 hours, 400ng of each mRNA cocktail derived from the three aforementioned sources (ABP-SC-SEIPSET,

ABP-SC-6FMRNA and RN3P) were added to the cells for a further 24 hours. The cells were then harvested and analysed by qPCR to quantify the mRNA levels in the fibroblasts relative to an undifferentiated hESC control cell line (Figure. 3.4). Un-treated fibroblasts were used as a negative control. The 6-factor reprogramming premix (ABP-SC-6FMRNA) increased mRNA levels in fibroblasts to a greater extent than mRNAs that had been *in vitro* transcribed from the Allele Biotech IVT templates (ABP-SC-SEIPSET) or from RN3P, relative to an undifferentiated Shef6 hESC line (Figure. 3.4). The levels of mRNA in BJ fibroblasts following the introduction of the 6-factor reprogramming premix were between 4-fold and 21-fold higher than those induced by Allele Biotech IVT template-derived mRNAs and were between 1.3-fold and 442-fold higher than mRNA levels induced by RN3P template-derived mRNAs. The addition of *cMYC* mRNA derived from the Allele Biotech IVT template (ABP-SC-SEIPSET) did not increase *cMYC* mRNA levels in BJ fibroblasts after 24 hours. No effect was observed on *LIN28* and *OCT4* mRNA levels after 24 hours following the addition of mRNAs derived from RN3P templates.

Figure 3.4. Comparing mRNA levels in BJ fibroblasts following the introduction of exogenous mRNAs from different sources

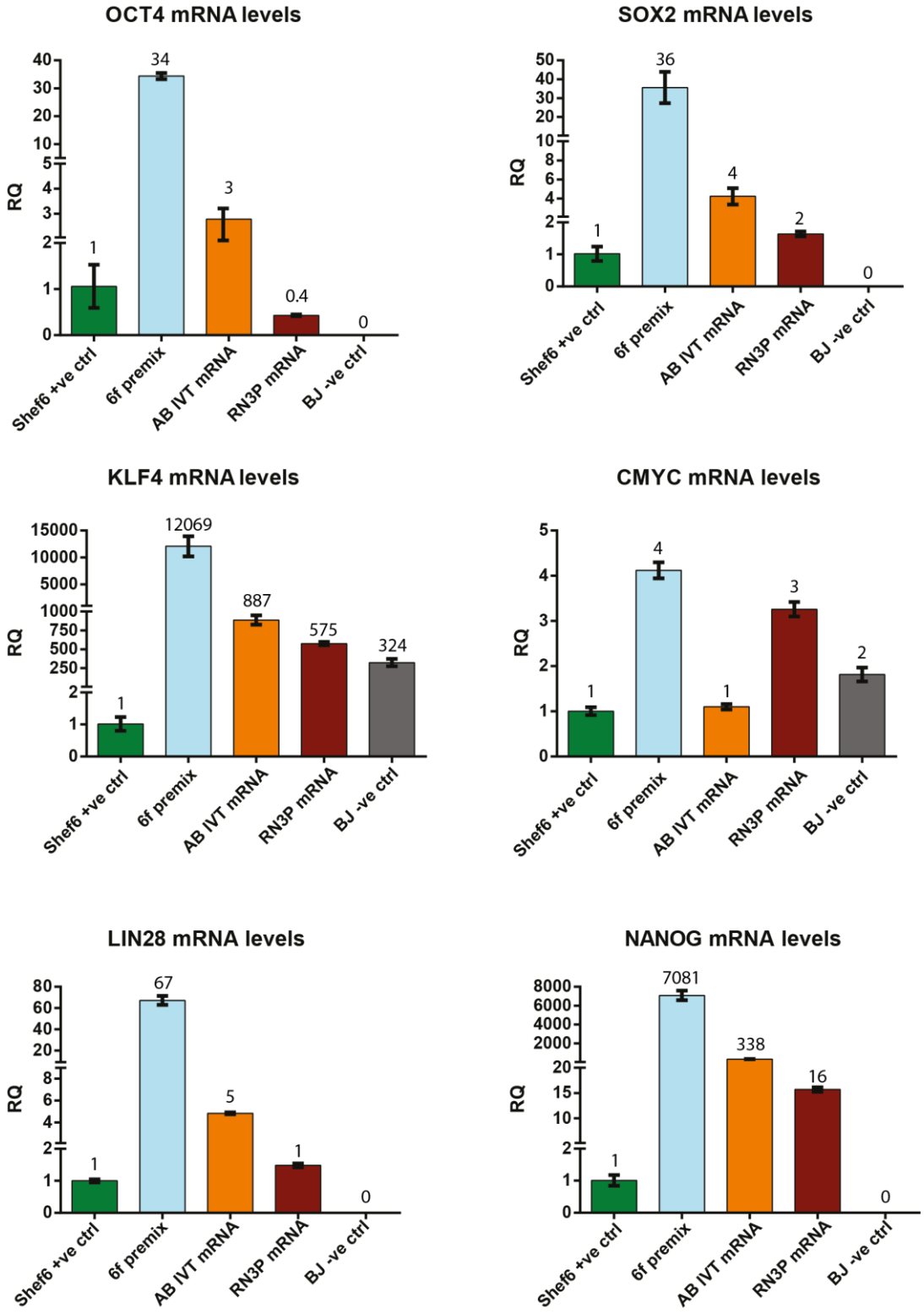

Figure 3.4: Three mRNA cocktails containing *OCT4 / M$_3$O, SOX2, KLF4 CMYC, LIN28* and *NANOG* derived from the 6-factor mRNA reprogramming premix (ABP-SC-6FMRNA), RN3P templates (methods 2.17.7) and Allele Biotech IVT templates (ABP-SC-SEIPSET) were added to separate wells containing BJ fibroblasts at a dose of 400ng and analysed by qPCR to determine the level of each mRNA in the cells. The levels of mRNA in BJ fibroblasts following the introduction of 6f mRNA reprogramming premix were between 4-fold and 21-fold higher than mRNA levels induced by Allele Biotech IVT template-derived mRNAs and were between 1.3-fold and 442-fold higher than mRNA levels induced by RN3P template-derived mRNAs. CT values were normalised to *GAPDH*. N=1 (error bars derived from technical triplicates).

3.2.4 Inactivated mouse embryonic fibroblasts act as a buffer during mRNA transfection by taking up mRNAs

Inactivated MEFs are commonly used to support reprogramming by acting as a feeder layer that releases nutrients into the culture medium. If mRNAs can enter into mitotically inactivated MEFs, it is perceivable that repeated addition of mRNA during reprogramming will trigger an intracellular immune response that will cause the inactivated MEFs to die and thus inhibit reprogramming. Are mRNAs added during reprogramming taken up by inactivated MEFs?

To determine whether mRNAs are taken up into inactivated MEFs, $1x10^5$ MEFs were plated in a 6-well plate in DMEM 10% FBS for 24 hours. Four hundred nanograms of *mWASABI* mRNA was added to the cells for a further 24 hours. The cells were then imaged on an EVOS fluorescent microscope and analysed by flow cytometry to quantify the number of fluorescing cells. It was found that 83% of the inactivated MEFs fluoresced green after 24 hours following the single addition of 400ng *mWASABI* mRNA (Figure. 3.5).

Figure 3.5. Inactivated MEFs are capable of taking up and translating mRNA introduced exogenously

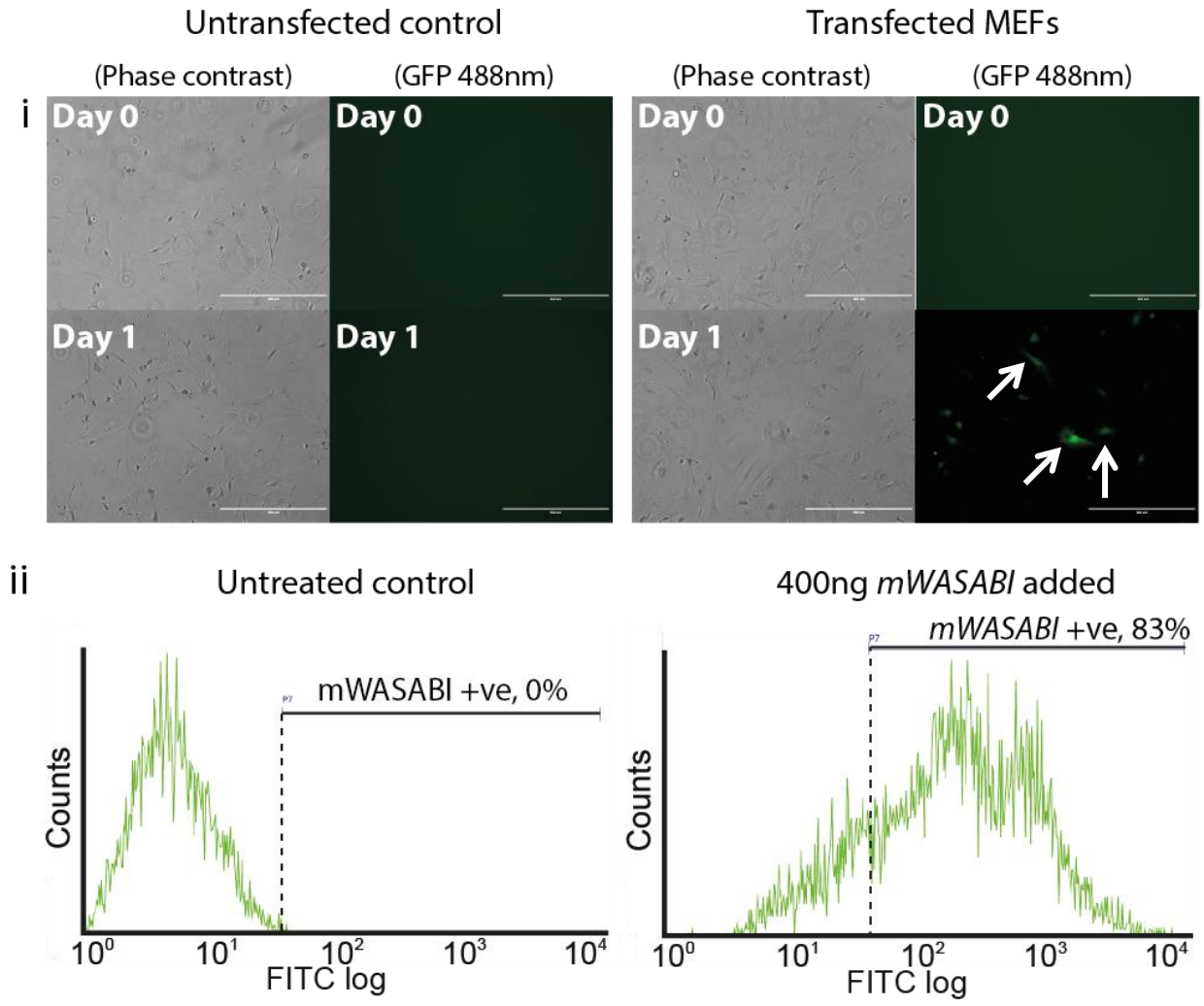

Figure 3.5: Adding *mWASABI* mRNA in to inactivated MEFs causes them to fluoresce. A cell density of $1x10^5$inactivated MEFs were plated in a 6-well culture plate on gelatinised plastic in DMEM 10% FCS for 24 hours. A dose of 400ng of *mWASABI* mRNA was then introduced into the MEFs for a further 24 hours. (i) Images of fluorescent cells (white arrows) were taken on an EVOS FL Cell Imaging System (Life Technologies) (GFP settings: 80% light intensity, 250ms exposure). (ii) Fluorescence levels were assessed by flow cytometry and it was found that 83% of the MEFs expressed *mWASABI* (mWASABI is detectable via the GFP channel at a wavelength of 488nm). The untreated control contained 0% fluorescing cells after 24 hours. White arrows indicate fluorescing MEFs. Scale bars = 400µm.

3.2.5. Initial reprogramming attempt takes 32 days and requires passaging

In order to improve upon the kinetics and efficiency of reprogramming, a 'gold standard' process must first be established. Modifications to this process can then be made to try and improve the speed and efficiency that iPS cells can be generated. In this section (3.2.5) we establish the gold standard process by generating a set of integration-free iPS cells, derived from BJ fibroblasts using the fully tested and validated mRNA reprogramming kit from Stemgent (00-0071).

The mRNAs included within the Stemgent kit (00-0071) encode five reprogramming factors*; OCT4, SOX2, KLF4, cMYC* and *LIN28* that are separately aliquoted to allow for adjustments to be made to individual mRNA concentrations and combined mRNA cocktail stoichiometry if required. An mRNA cocktail containing the five reprogramming factors was created as per the manufacturer's instructions and frozen at -80°C in single use aliquots so that when the mRNA was required during reprogramming, the number of freeze-thaw cycles the mRNA was subjected to would be limited. Each mRNA cocktail contained a three-fold relative increase of *OCT4* on the basis that this improves the efficiency of reprogramming [53]. The mRNA reprogramming kit (00-0071) also contained B18R that was frozen in 2µg aliquots to be used at a final concentration of 200ng/ml.

On day minus-one of reprogramming, BJ fibroblasts were seeded at a density of $1x10^5$ in a 6-well culture plate containing $2x10^5$ inactivated MEFs. From day zero onwards on a once-daily basis, one microgram of the mRNA cocktail was added to the BJ fibroblasts in 2ml Pluriton medium to achieve a final concentration of 500ng/ml. The fibroblasts were cultured in a 37°C incubator at 5% O_2. One hundred

nanograms of nuclear-*GFP* (*nGFP*) was added daily with the *OCT4, SOX2, KLF4, cMYC* and *LIN28* mRNA cocktail to monitor the successful uptake of mRNA in to the cells.

On day three, the fibroblasts had reached near confluency and on day 22, mounds of cells had appeared in the culture (Figure. 3.6B, white arrows) indicating the cell culture had become over-confluent or potentially iPS cells had emerged. On day 32, the BJ fibroblasts began to senesce so the culture was trypsinised and split amongst three wells containing MEF feeder layers that had been seeded at a density of $2x10^5$ in Pluriton medium. Cell counting of the fibroblast cells following the splitting step was not performed as to not lose potential iPS cells in the cell counting process. On day 36, iPS cell colony outgrowths could be seen in the culture (Figure. 3.6B, orange boxes). The iPS cell colonies were isolated from the culture and grown as individual cell lines, characterised and then frozen in liquid nitrogen. The cell lines were named '2SG PiPS X' after the reprogramming experiment from which they were obtained (i.e. 2), the mRNA manufacturer (SG), type of cell line (iPS) and clone number (001 < n < 018).

Figure 3.6. IPS cell generation using the Stemgent Reprogramming Kit

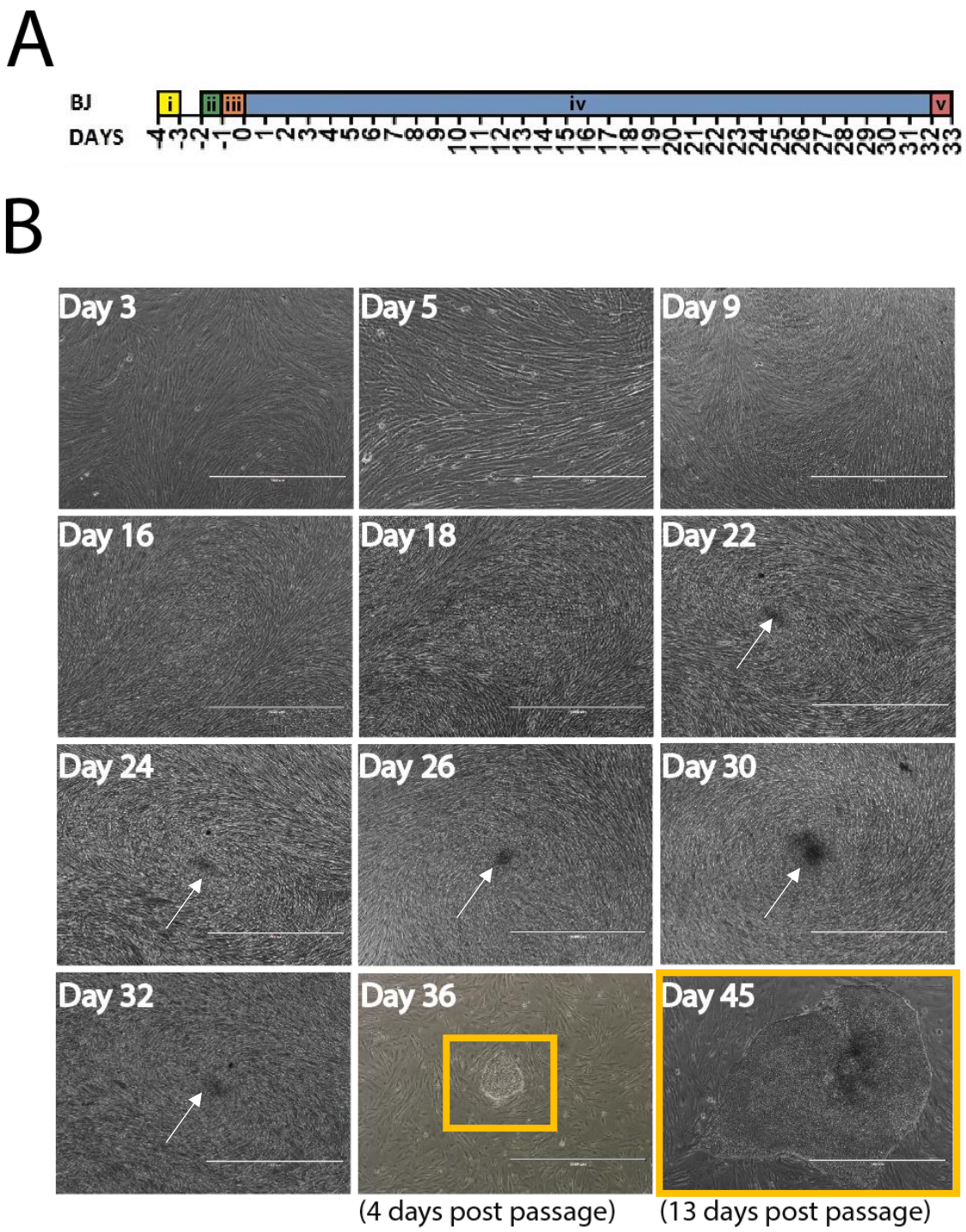

Figure 3.6: (A) Generation of iPS cells using the Stemgent reprogramming kit (00-0071) was achieved in 37 days. (i) Inactivated MEFs were seeded at $2x10^5$ into a 6-well culture plate in 10% DMEM FCS for 48 hours. (ii) BJ fibroblasts were then seeded at a density of $1x10^5$ onto the MEF feeder layer in 10% DMEM FCS for 24 hours. (iii) After 24 hours, the media was replaced with 2mls MEF conditioned hESC media. (iv) Reprogramming factor mRNA from the Stemgent reprogramming kit was added daily until day 32. (v) As the cells had formed a monolayer, they were trypsinised using 0.25% trypsin-EDTA (Sigma) and seeded onto an inactivated MEF feeder layer. (B) Phase contrast images depicting mounding cells (white arrows) and the emergence of iPS cell colonies (orange rectangles). Scale Bars = 1000µm

3.2.6 Characterisation of iPS cell lines

IPS cells were generated using the Stemgent mRNA reprogramming kit (00-0071) however it is necessary to assess the characteristics of these iPS cells to validate that they are representative of pluripotent stem cells. To do this, the phenotype and functional characteristics of the iPS cells was determined by analysing mRNA levels (qPCR analysis), expression of cell surface markers (flow cytometry), presence of chromosomal abnormalities (karyotype analysis) and assessing their capacity to differentiate (embryoid body formation), compared to a positive control pluripotent stem cell line.

Following the successful reprogramming of the BJ fibroblast cell line, two of the iPS cell lines were characterised; 2SG PiPS 006 and 010, to test whether they had truly manifested pluripotency. These clonal lines were selected for characterisation, as they were the quickest to be expanded after isolation from single colonies. The 2SG PiPS 006 and 010 cell lines were analysed by qPCR and flow cytometry at passage six, 30 days after the final addition of mRNA took place during reprogramming. QPCR analysis detected that the 2SG PiPS 006 cell line contained a ~7-fold increase in *NANOG* mRNA levels relative to the control hESC line (Shef6). The mRNA levels for *OCT4, SOX2, KLF4, cMYC* and *LIN28* in the 2SG PiPS 006 cell line were detected at similar levels relative to Shef6 (Figure. 3.9). In the 2SG PiPS 010 cell line, *SOX2* mRNA levels were found to be similar to the hESC control cell line however the remaining factors were detected at elevated levels: *OCT4* (2-fold), *KLF4* (8-fold), *cMYC* (2.5-fold), *LIN28* (4-fold) and *NANOG* (7-fold), relative to the Shef6 control hESC line.

Karyotyping was performed on both iPS cell lines at passage 22. Both cell lines were karyotypically normal (Figure. 3.7). The cell lines were then analysed by flow cytometry and were found to express cell-surface markers typically expressed in pluripotent stem cells including SSEA-3, SSEA-4, TRA-1-60 and TRA-1-81 at similar levels (Figure. 3.8) to the control hESC line.

To test whether the 2SG PiPS 010 cell line was pluripotent, the cells were induced to differentiate spontaneously as embryoid bodies for ten days alongside a control hESC line (Figure. 3.10) in neutral conditions (Table 2.4). After 10 days, RNA was extracted from the embryoid bodies, reverse transcribed to cDNA and then analysed by qPCR to detect the expression of markers characteristic of the three germ layers endoderm, mesoderm and ectoderm. The markers used to identify differentiation toward the three germ layers were *GATA6, FOXA2* and *ISL1*, indicative of differentiation towards endoderm, *CD34* and *COL1A1* to mesoderm and *PAX6* and *GATA2* to ectoderm. The expression of *OCT4*, *NANOG* and *SOX2* was also assessed to determine the differentiation status of the cells. Inducing the 2SG PiPS 010 cell line to differentiate as embryoid bodies resulted in the down-regulated expression of *OCT4, NANOG* and *SOX2* suggesting that the cells were analysed in a differentiated state. In this differentiated state, the 2SG PiPS cell line expressed markers of all three germ layers (Figure. 3.10) thus confirming the iPS cell line's pluripotency status.

Figure 3.7. Karyotype analysis of two clonal iPS cell lines derived using the Stemgent mRNA reprogramming kit: 2SG PIPS 010 and 2SG PIPS 006

i

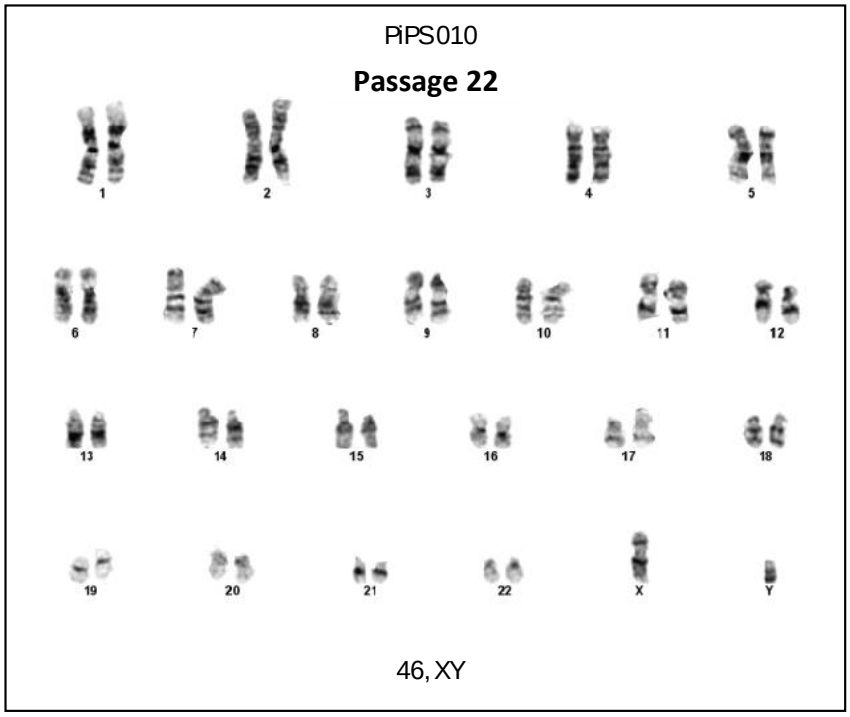

ii

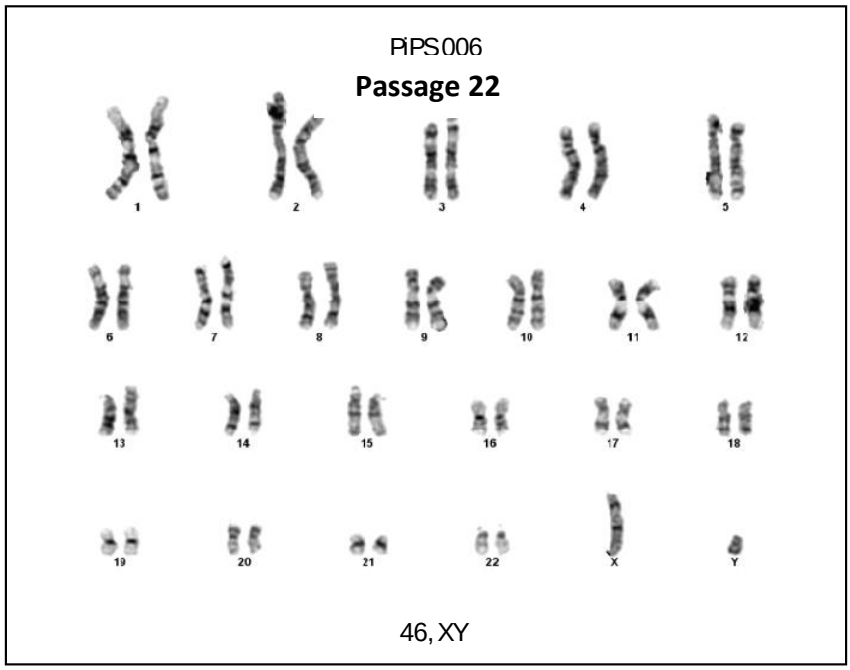

Figure 3.7: Two iPS cell lines of independent clonal origin were isolated from a single reprogramming culture following repeated addition of Stemgent mRNA. The two cell lines, 2SG PiPS 006 and 010 were cultured to passage +22 and following karyotype analysis (methods 2.16) were determined to be karyotypically normal (46XY).

Figure 3.8. The 2SG PiPS 006 and 010 cell lines exhibit similar cell surface marker expression profiles to that of a control hESC line

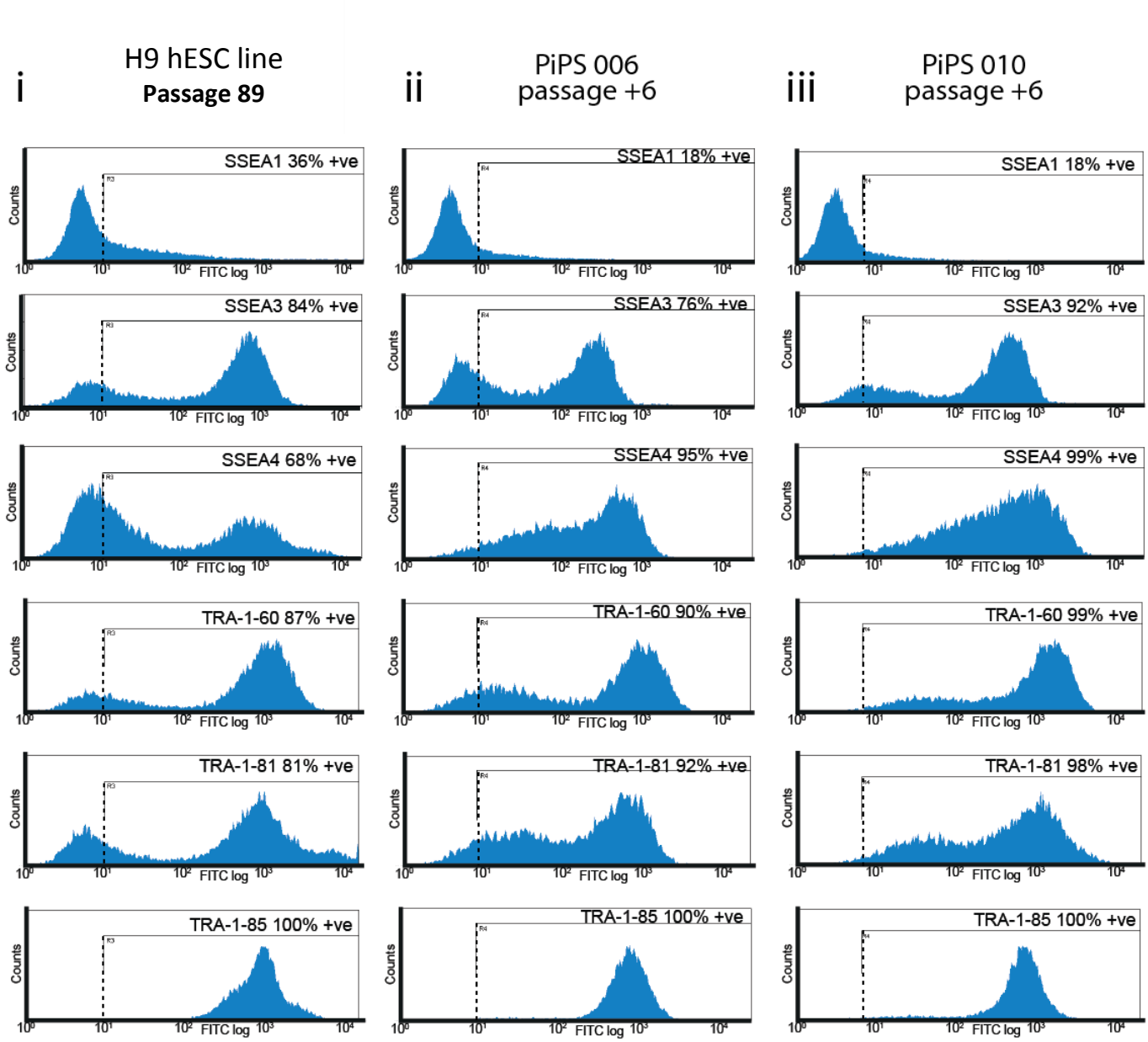

Figure 3.8: Flow cytometric analysis of (i) H9 hESC line passage +89, (ii) 2SG PiPS 006 passage +6 and (iii) 2SG PiPS 010 passage +6 cell lines have similar expression for markers; SSEA-1, SSEA-3, SSEA-4, TRA-1-60, TRA-1-81 and TRA-1-85. Fluorescent cells were determined by gating against a P3X control (dashed line). Gating strategy is described in methods 2.15.1.1. The spread of the histogram denotes variations in fluorescent intensity.

Figure 3.9. Analysis of the 2SG PiPS 006 and 010 cell lines by qPCR

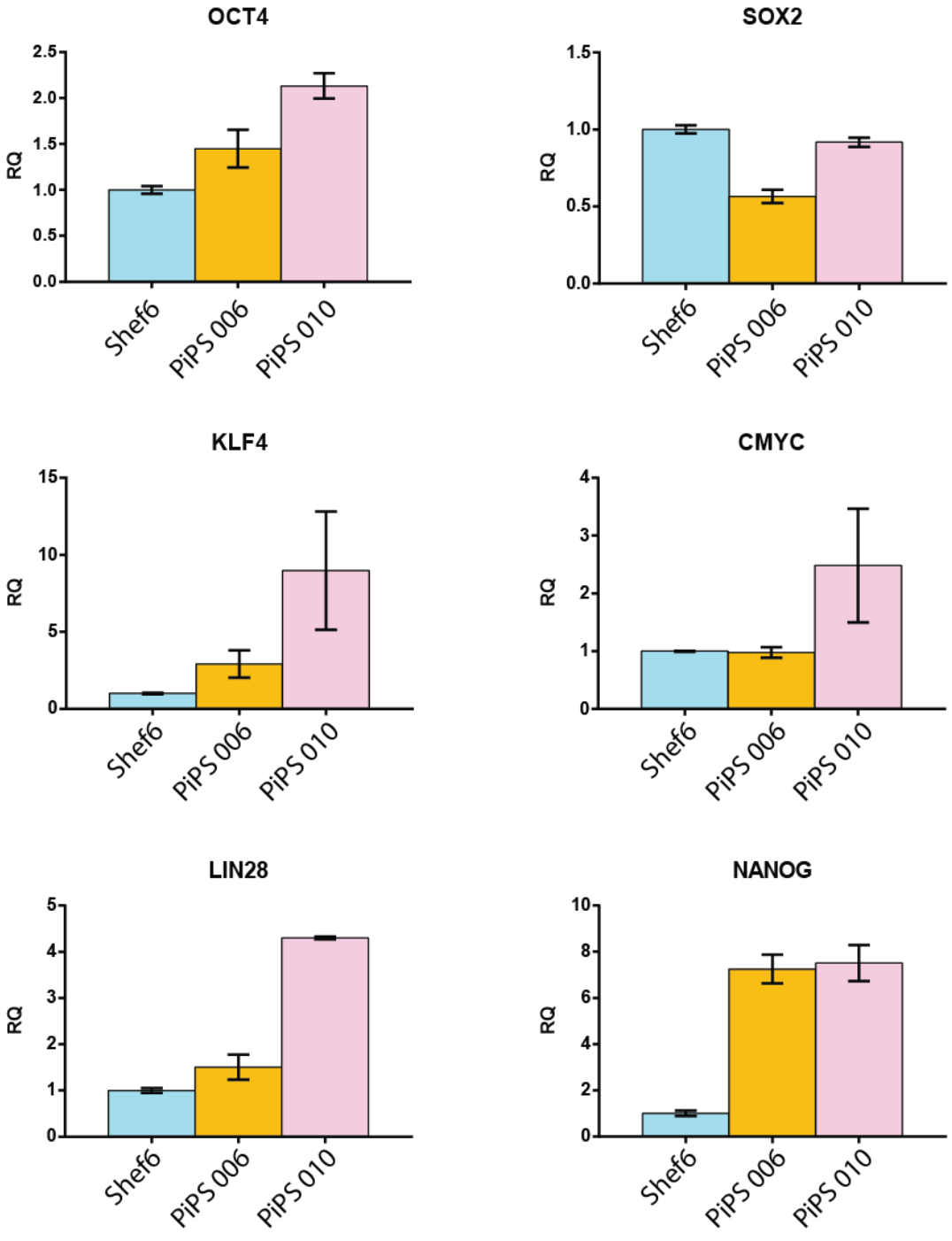

Figure 3.9: qPCR analysis of the 2SG PiPS 006 and 010 cell lines at passage +6 reveal mRNA levels comparable to an undifferentiated control hESC line, Shef6, with respect to genes; *OCT4, SOX2, KLF4, CMYC, LIN28* and *NANOG*. 2SG PiPS 010 has elevated levels of the aforementioned genes compared to both the control hESC line and 2SG PiPS 006. CT values were normalised to *GAPDH*. N=1 (error bars derived from technical triplicates).

Figure 3.10. Spontaneous differentiation of the 2SG PiPS cell line induces gene expression for markers of all three germ layers

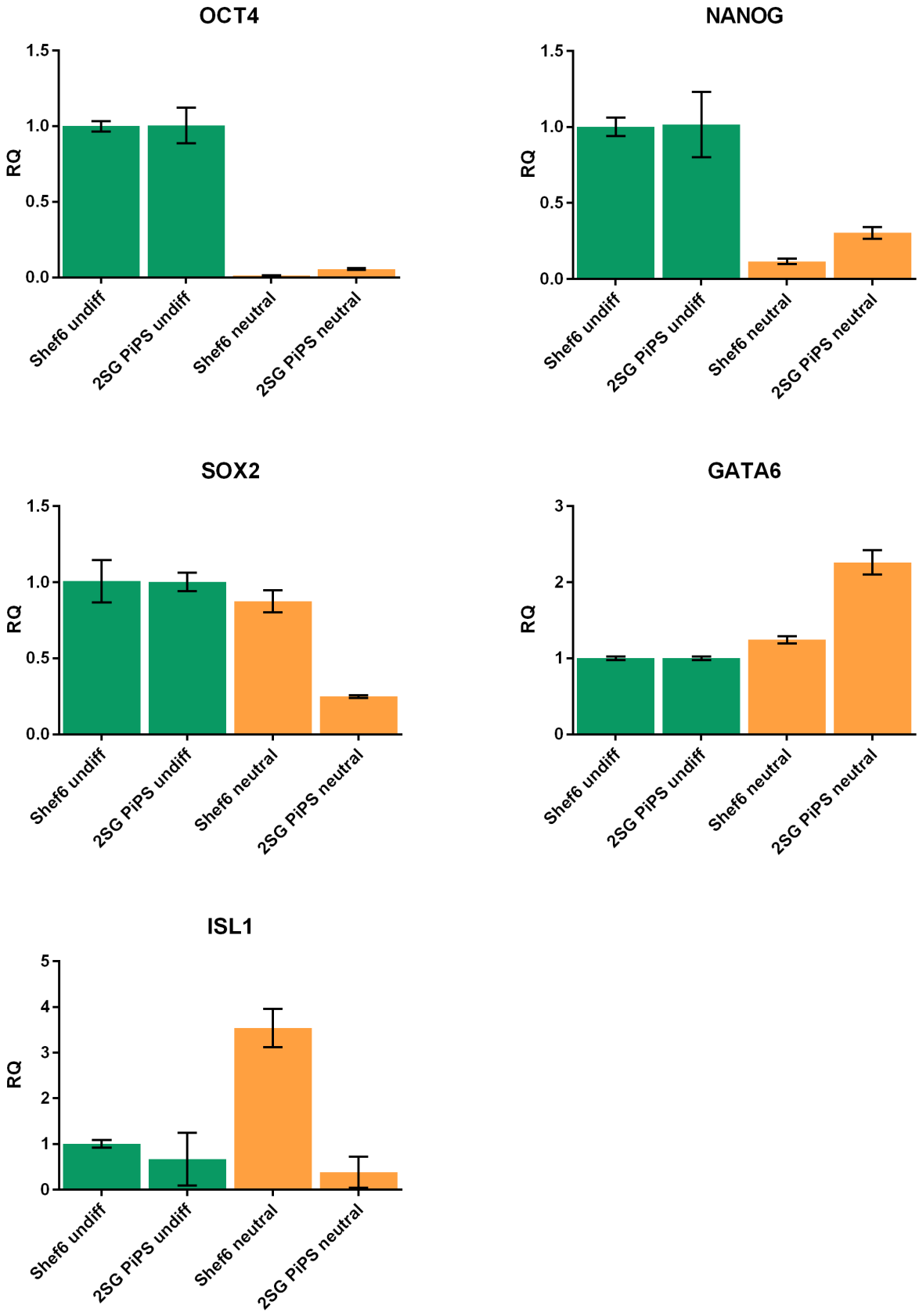

Figure 3.10. Spontaneous differentiation of the 2SG PiPS cell line induces gene expression for markers of all three germ layers

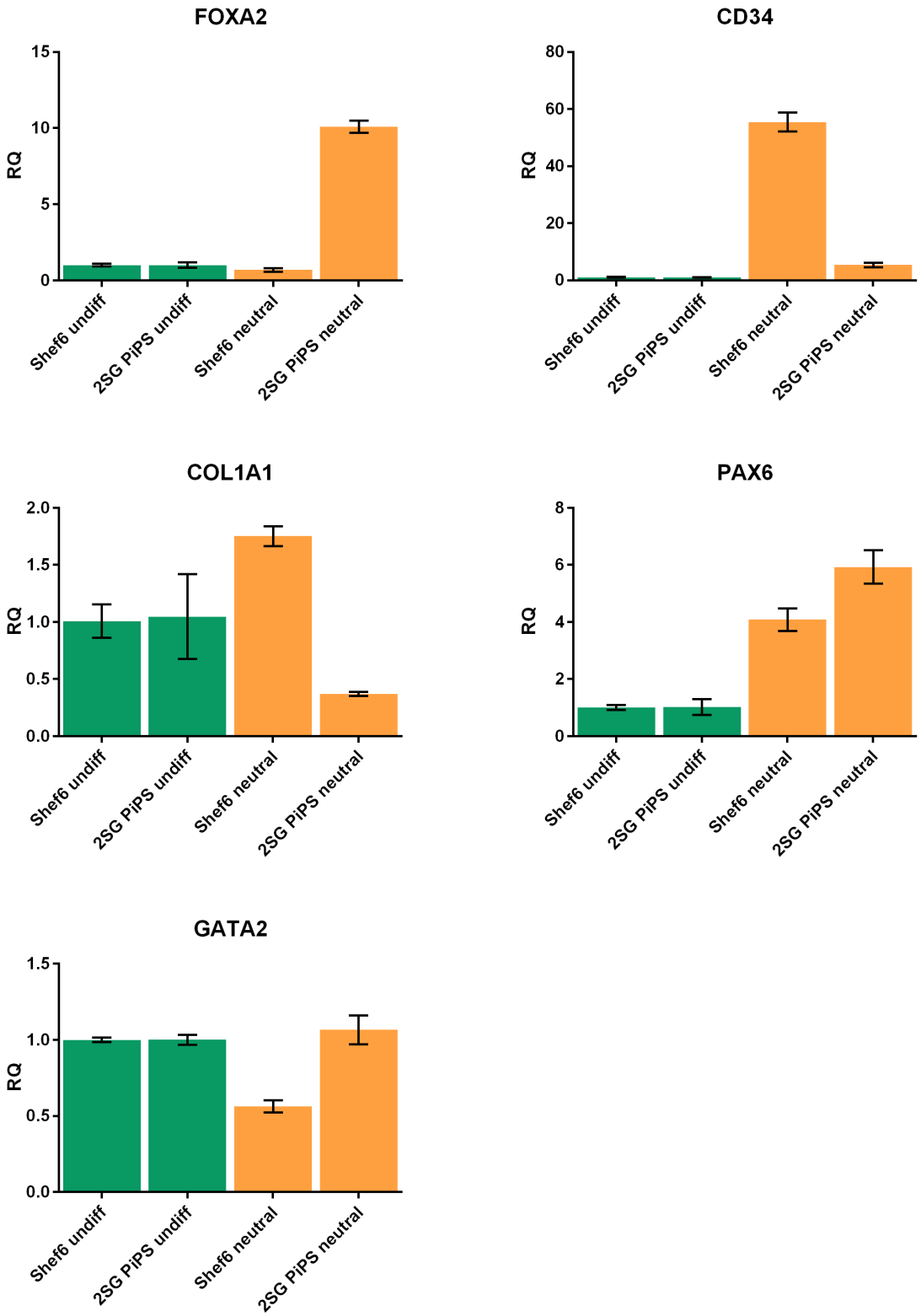

Figure 3.10: The 2SG PiPS 010 cell line was spontaneously differentiated as embryoid bodies for 10 days in the neutral condition (Table 2.4). Following qPCR analysis, the RQ values showed increased gene expression levels for endodermal (*GATA6, FOXA2*), mesodermal (*CD34*) and ectodermal (*PAX6*) markers relative to an undifferentiated control. Under the same conditions, Shef6 cells increased gene expression for *ISL1* (endodermal), *CD34, COL1A1* (mesodermal) and *PAX6* (ectodermal) markers. CT values were normalised to *GAPDH*. N=1 (error bars derived from technical triplicates).

3.2.7. The kinetics of reprogramming can be accelerated by using mRNAs that have been *in vitro* transcribed with modified nucleotides

Successfully reprogramming BJ fibroblasts using the Stemgent mRNA reprogramming kit (00-0071) set a benchmark for the efficiency and kinetics of reprogramming that we can aim to improve through modifications to the process. Here we test whether the incorporation of modified nucleotides in to mRNAs transcribed from the Allele Biotech IVT induction templates (ABP-SC-SEIPSET) can improve upon the speed and efficiency of the reprogramming process.

The Allele Biotech IVT templates (ABP-SC-SEIPSET) are either linearised DNA templates or PCR products containing a double stranded promoter region. As the *in vitro* transcription (IVT) reactions are performed in house, this afforded us control over the incorporation of modified nucleotides, capping and polyadenylation of mRNAs during the IVT reactions. We determined whether these modifications, specifically the incorporation of 5-Methylcytidine-5'-Triphosphate (Stratech, 5-0613-295-IBA) and Pseudouridine-5'-Triphosphate (Stratech, NU-1139L-JEN) modified nucleotides into mRNAs during IVT reactions enhances the reprogramming process.

The IVT templates supplied within the kit (ABP-SC-SEIPSET) contained coding regions for *OCT4, SOX2, KLF4, cMYC and LIN28* as well as a monomeric green fluorescent protein *mWASABI* and *NANOG* that has previously been shown to increase the efficiency of reprogramming [39, 45]. The templates for all seven factors were *in vitro* transcribed using the T7 MEGAscript Kit (Thermo Fisher, AM1333) as described in methods 2.20 and then diluted to a concentration of 100ng/µl. All of the factors with the exception of *mWASABI* mRNA were then combined to form an mRNA cocktail at a molar ratio of 3:1:1:1:1:1,

containing a three-fold relative increase of *OCT4* to the other reprogramming factors and then stored at -80°C. The *mWASABI* mRNA was stored separately from the mRNA cocktail so that it could be introduced independently and intermittently throughout reprogramming to report whether the mRNAs being added to the reprogramming cultures were being taken up by the cells. Single-use aliquots of both the mRNA cocktail and *mWASABI* mRNA were frozen at -80°C until required.

Once the mRNA cocktails had been prepared, reprogramming was executed as follows. BJ fibroblasts were plated onto hESC-qualified Matrigel-coated 6-well plates at a density of $1x10^5$ in Pluriton medium. A Matrigel extra-cellular matrix was used to limit the unwanted transfection of mRNAs into inactivated MEFs (as shown in Figure. 3.5). Eight hundred nanograms of the mRNA cocktail was then added daily for eight days into the BJ fibroblasts and by day three there was evidence of morphological changes in the reprogramming culture in that the fibroblasts had compacted and appeared to lack fibroblastic processes (Figure. 3.11B, white arrows). On day nine the addition of mRNA was ceased and $2x10^5$ inactivated MEFs were added to the reprogramming well to support the emergence of iPS cells. The culture was maintained in Pluriton medium until day 21 and a further $2x10^5$ MEFs were added on day 13. On day 21, it was observed that no iPS cells had emerged so the culture was trypsinised with 0.25% trypsin-EDTA and replated onto a MEF coated 6-well culture plate. After 24 hours, iPS cell colonies could be seen in the culture vessel.

Figure 3.11. Reprogramming BJ fibroblasts with mRNAs from the Allele Biotech iPS induction template set

A

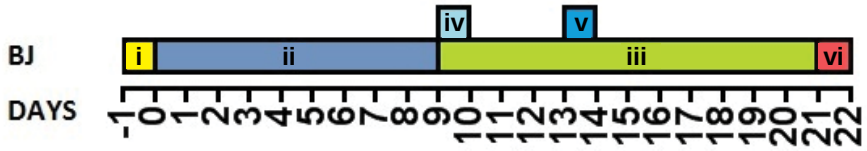

B

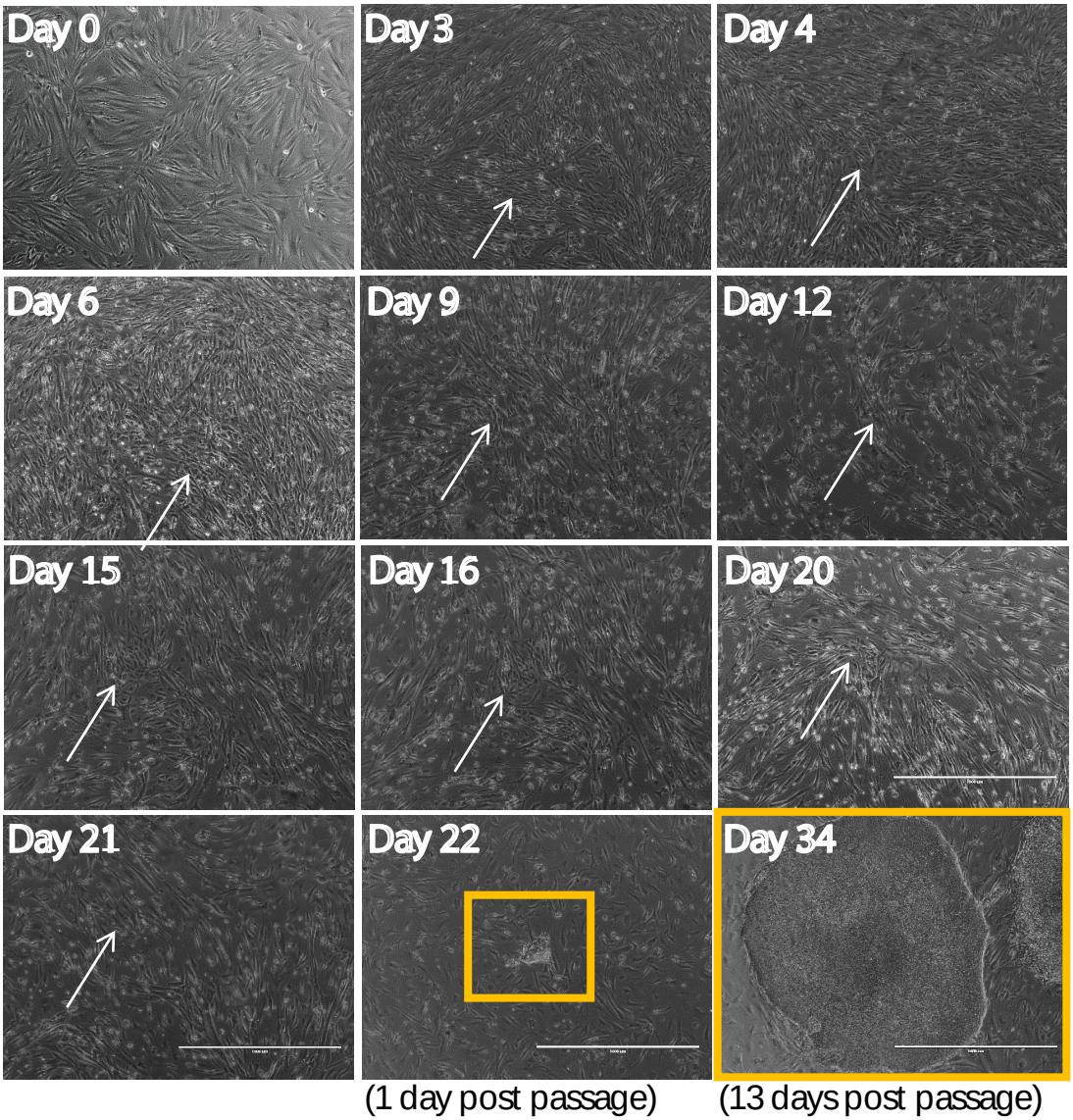

Figure 3.11: (A) Reprogramming using the Allele Biotech iPS induction template set (ABP-SC-SEIPSET) generated iPS cells in 22 days. (i) BJ fibroblasts were seeded at a density of $1x10^5$ onto hESC-qualified Matrigel-coated 6-well culture plates. (ii) mRNAs derived from Allele Biotech templates (*OCT4, SOX2, KLF4, CMYC, LIN28* and *NANOG*) were added daily at a dose of 800ng until day 9. (iii) Between days 9 and 20 no further mRNA was added but the reprogramming culture was fed daily with Pluriton medium supplemented with 1X Pluriton Supplement and 200ng/ml B18R for a further 12 days. (iv) Inactivated MEFs were added at day 9 (v) and day 13 to support emergent iPS cells (vi) The entire culture was trypsinised on day 21 and replated onto a MEF feeder layer. iPS cell colonies (orange rectangles) could be seen to emerge after 24 hours. (B) Phase contrast images depicting morphological changes (white arrows) throughout the reprogramming process. Scale bars = 1000µm.

3.2.8. Emergence of iPS cell colonies without passaging

It has been shown that a fusion protein between *OCT4* and *MYOD1* (called *M_3O*) more effectively recruits chromatin modifying proteins, than *OCT4* alone, to pluripotent loci during reprogramming [68]. We determined whether the reprogramming process could be accelerated by using the 6-factor reprogramming premix (ABP-SC-6FMRNA) that contains the synthetically engineered *OCT4-MYOD* (*M_3O*) fusion gene in replacement for conventional *OCT4*.

Reprogramming was initiated by seeding BJ fibroblasts onto hESC-qualified Matrigel in Pluriton at a cell density of $5x10^4$ for 24 hours. One millilitre of Pluriton medium was added to a sterile 6-well plate and equilibrated for 15 minutes at 37°C in 5% O_2. After equilibration, B18R was added at 200ng/ml and the 6-factor premix (ABP-SC-6FMRNA) was added at 400ng/ml rocking back and forth to mix. The supplemented media was placed onto the target cells on day zero and the process repeated daily until day 11 (Figure. 3.12A). Adding mRNA to the media before it is placed on the cells as opposed to adding the mRNA directly to target cells in a drop-wise fashion prevents pockets of high concentrations of mRNA from accumulating that, if insufficiently mixed into the media, can be toxic to the cells. As cells respond unfavourably to high concentrations of mRNA and are sensitized to environmental cues during reprogramming it is desirable to supplement and mix the media prior to adding it to the target cells, adding the media to the side of the well during each media change. Cytotoxicity was counteracted on day five by increasing the B18R concentration to 400ng/ml and on day six and nine through the addition of $1.5x10^5$ and $3x10^5$ inactivated MEFs respectively. On days 7 through 9, the mRNA concentration was decreased by half to 200ng/ml to mitigate against any mRNA-induced toxicity. The target cells were gradually rescued from cell death via the aforementioned anti-apoptotic measures. Signs of cellular

proliferation ensued and thus the mRNA concentration was increased to 300ng/ml on day 10. Signs of emerging colonies resulted in no further mRNA being added to the cells and the media was switched to un-supplemented Pluriton, containing no B18R or exogenous mRNA, for three days to both encourage iPS cell growth and support non-reprogrammed fibroblasts. Large, undifferentiated iPS cell colonies were picked on day 14 (Figure. 3.12B) into MEF-coated 12-well plates. Prior to passaging, a phase contrast and GFP image of the reprogrammed well was captured to show the location and number of colony outgrowths (Figure. 3.12C). In addition, the GFP image shows the prevalence of cytotoxicity that occurred when using the reprogramming method outlined in Figure 3.12A. Most of the cell death was situated towards the middle of the well possibly due to the use of non-meniscus free culture ware.

Twelve colonies emerged in total, all of which were expanded in culture and frozen down. One of these clonal lines named 5AB PiPS, was further characterised to assess the level of newly manifested pluripotency. This cell line was shown to be karyotypically normal (46 XY) (Figure. 3.13) and expressed cell-surface markers; SSEA-1, SSEA-3 and TRA-1-60 at comparable levels to an undifferentiated control hESC line, H7 S14 (Figure. 3.14). QPCR analysis for genes; *OCT4, SOX2, KLF4, cMYC, LIN28* and *NANOG* confirmed the mRNA levels in 5AB PiPS after four and fifteen passages were similar to those found in Shef6 hESCs (Figure. 3.15). While all the mRNA levels were elevated in the 5AB PiPS cell line after four passages in comparison to undifferentiated Shef6 cells, by passage fifteen the mRNA levels had normalised to levels more closely resembling the hESC control. The differentiation capacity of the 5AB PiPS cell line was then determined by inducing the cells to differentiate as embryoid bodies for ten days in the neutral condition (Table 2.4). Embryoid bodies formed from differentiated 5AB PiPS cells expressed markers of all three germ layers when analysed by qPCR (Figure. 3.16) thus confirming the 5AB PiPS cell line was pluripotent.

Figure 3.12. Generating iPS cells using the Allele Biotech 6-factor reprogramming premix

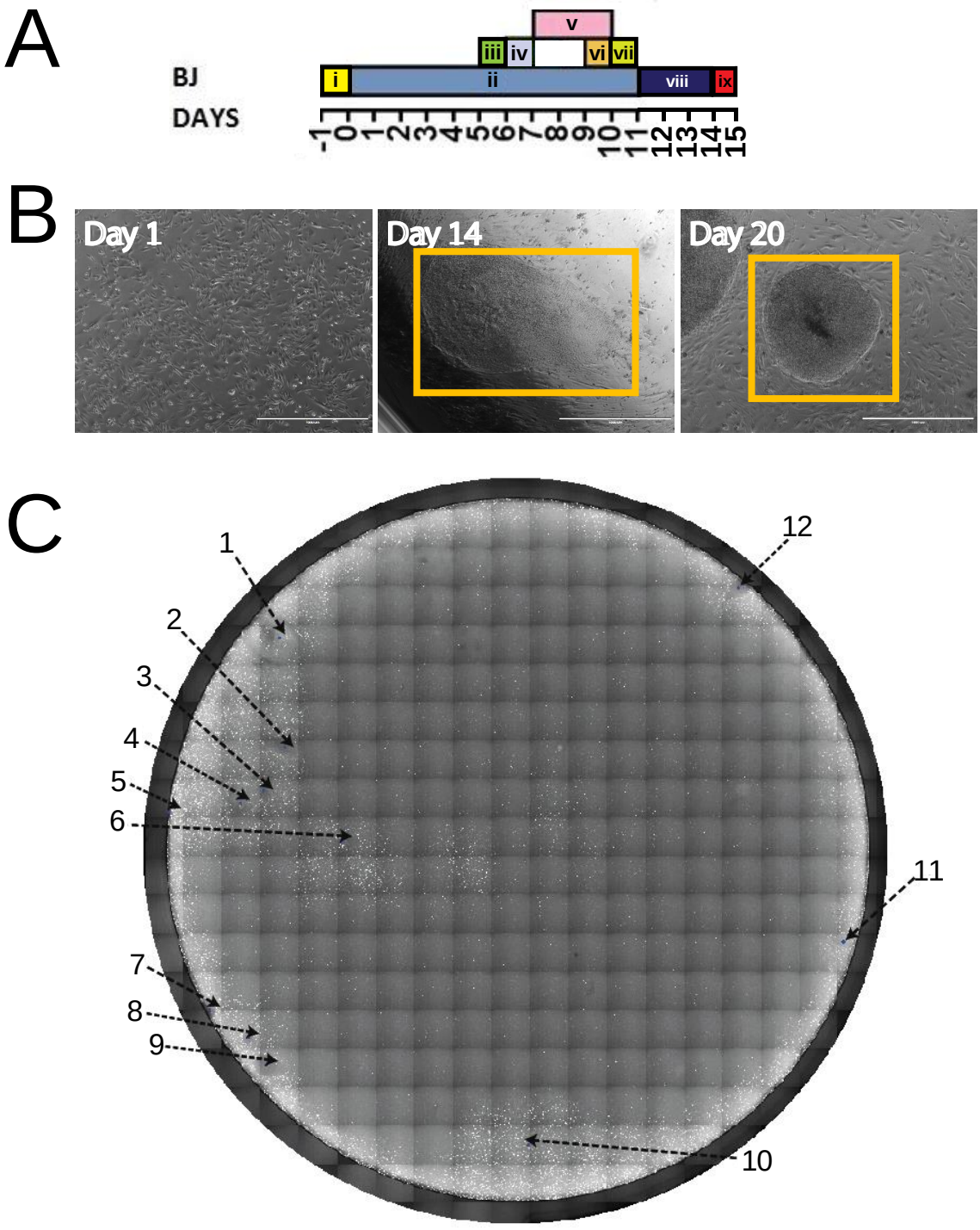

Figure 3.12: (A) Reprogramming timeline using the Allele Biotech 6-factor premix mRNA (ABP-SC-6FMRNA). (i) BJ fibroblasts were seeded at a density of $5x10^5$ onto hESC-qualified Matrigel-coated 6-well culture plates on day -1. (ii) After 24 hours, 400ng/ml 6-factor premix mRNA was added daily for 11 days. (iii) On day 5, a small number of cells were observed to have died so the B18R concentration was increased to 400ng/ml from 200ng/ml. (iv) To further support the cells in the face of apoptosis, inactivated MEFs were added on day 6 at a density of $1.5x10^5$ and (vi) on day 9 at a density of $3x10^5$. (v) The mRNA concentration was also decreased to 200ng/ml between days 7 and 10. (vii) The mRNA concentration was increased to 300ng/ml on the observation that cells had begun to proliferate. (viii) IPS cells appeared on day 11 so no more mRNA was added and the medium was replenished daily with fresh Pluriton medium. (ix) iPS cell colonies were picked on day 14. (B) Phase contrast images of an iPS cell colony on day 14 and six days later following passaging (orange rectangles). (C) Stitched GFP image portraying the extent of toxicity (grey area) and the locations of emergent colonies on day 14 (black arrows).

Figure 3.13. Karyotype analysis of the 5AB PiPS cell line

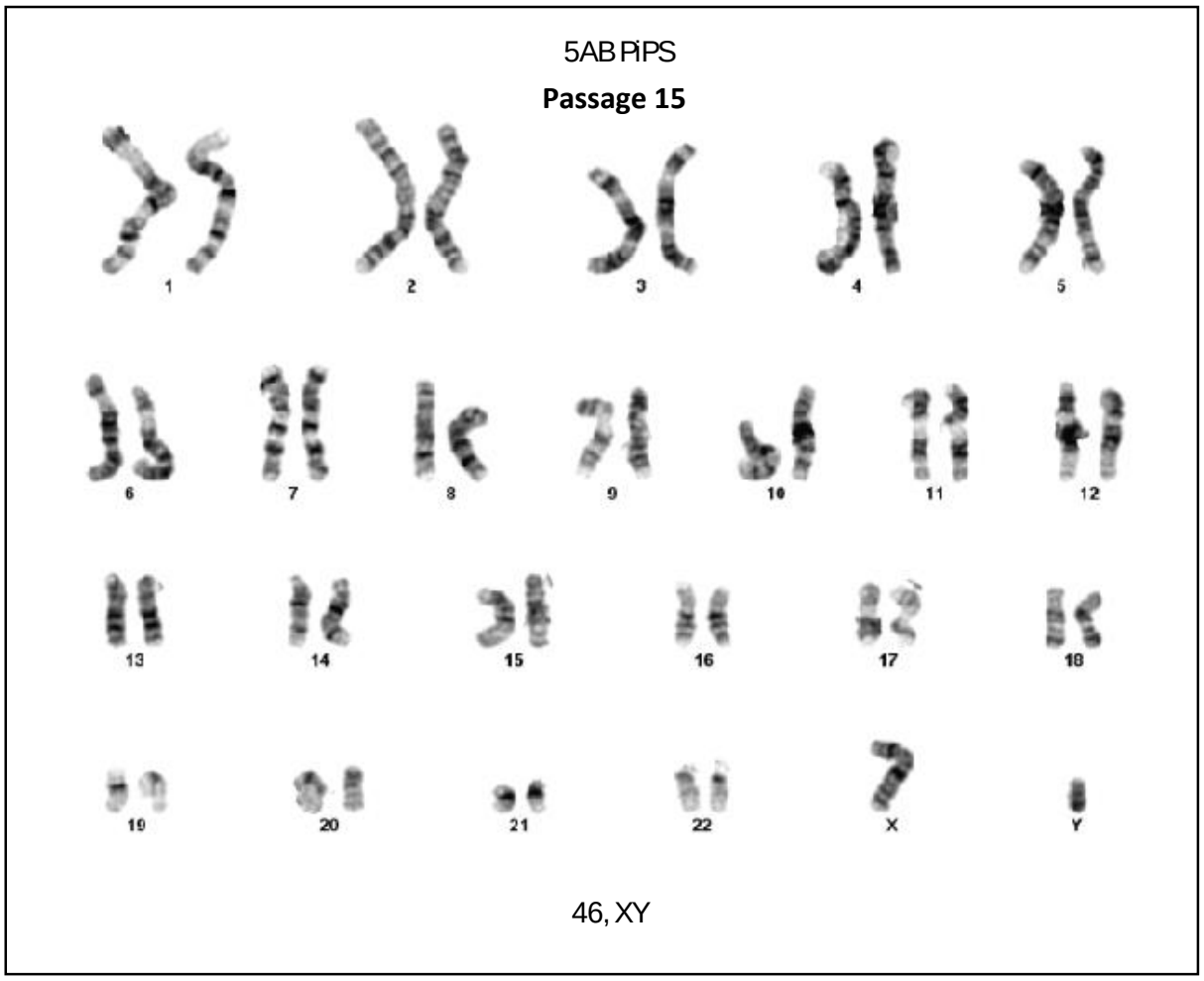

Figure 3.13: Karyotype analysis was performed on the 5AB PiPS cell line that was reprogrammed from BJ fibroblasts using the Allele Biotech 6-factor premix mRNA (ABP-SC-6FMRNA). The cell line was karyotypically analysed (methods 2.16) for chromosomal abnormalities at passage +15 and was determined to be karyotypically normal (46XY).

Figure 3.14. Flow cytometric analysis of the 5AB PiPS cell line compared to a control hESC line and the parental BJ fibroblasts

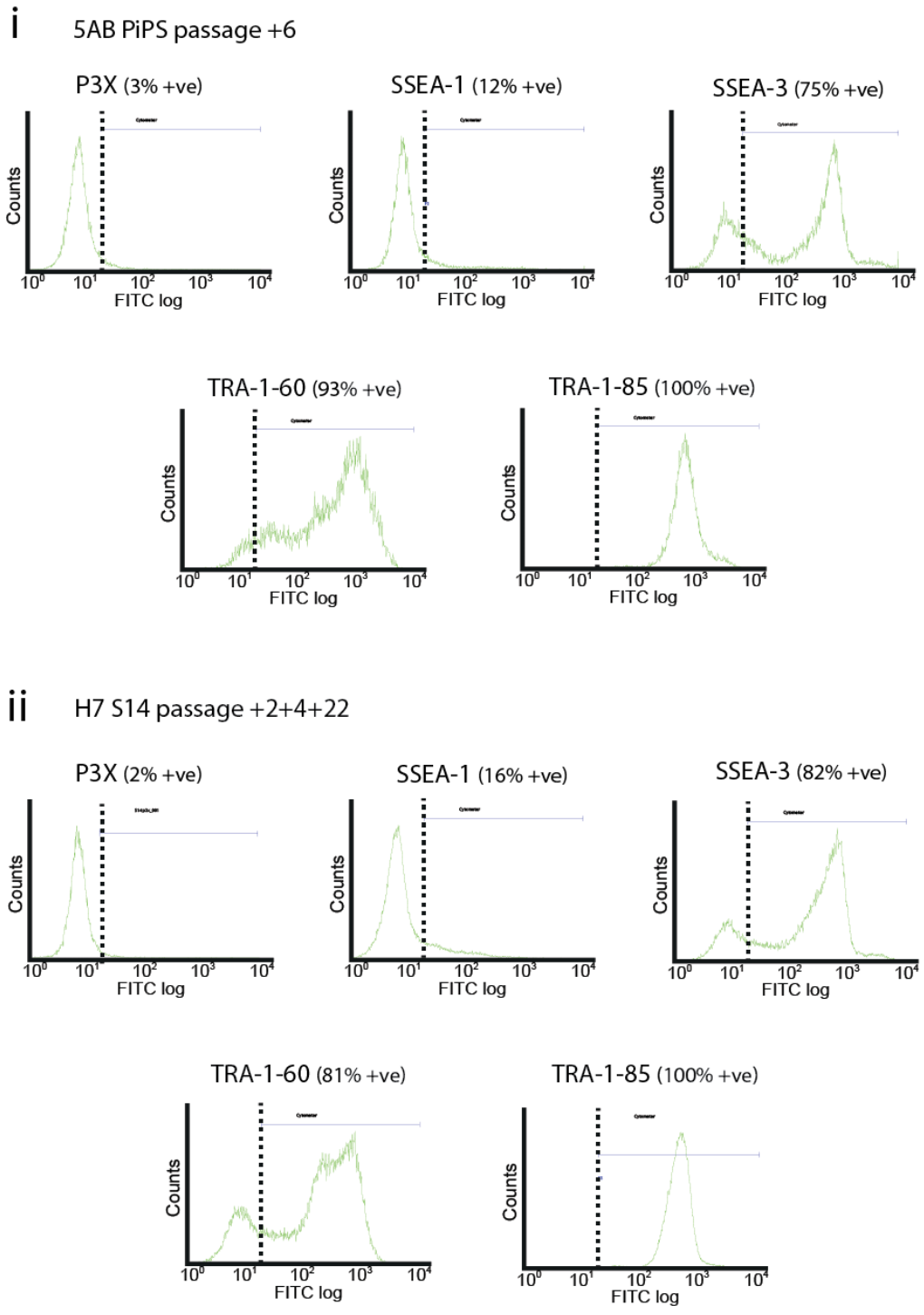

Figure 3.14: Flow cytometric analysis of the 5AB PiPS cell line at passage +6 compared to an undifferentiated hESC control line, H7 S14 at passage +28. Both cell lines express markers of undifferentiated pluripotent stem cells SSEA-3 and TRA-1-60. SSEA-1 is not expressed in either cell line indicating the cells were analysed in an undifferentiated state. P3X was used to gate the cells prior to analysis as described in methods 2.15.1.1. TRA-1-85 was used as a positive control for the antibody staining procedure.

Figure 3.15. Analysis of the 5AB PiPS cell line by qPCR

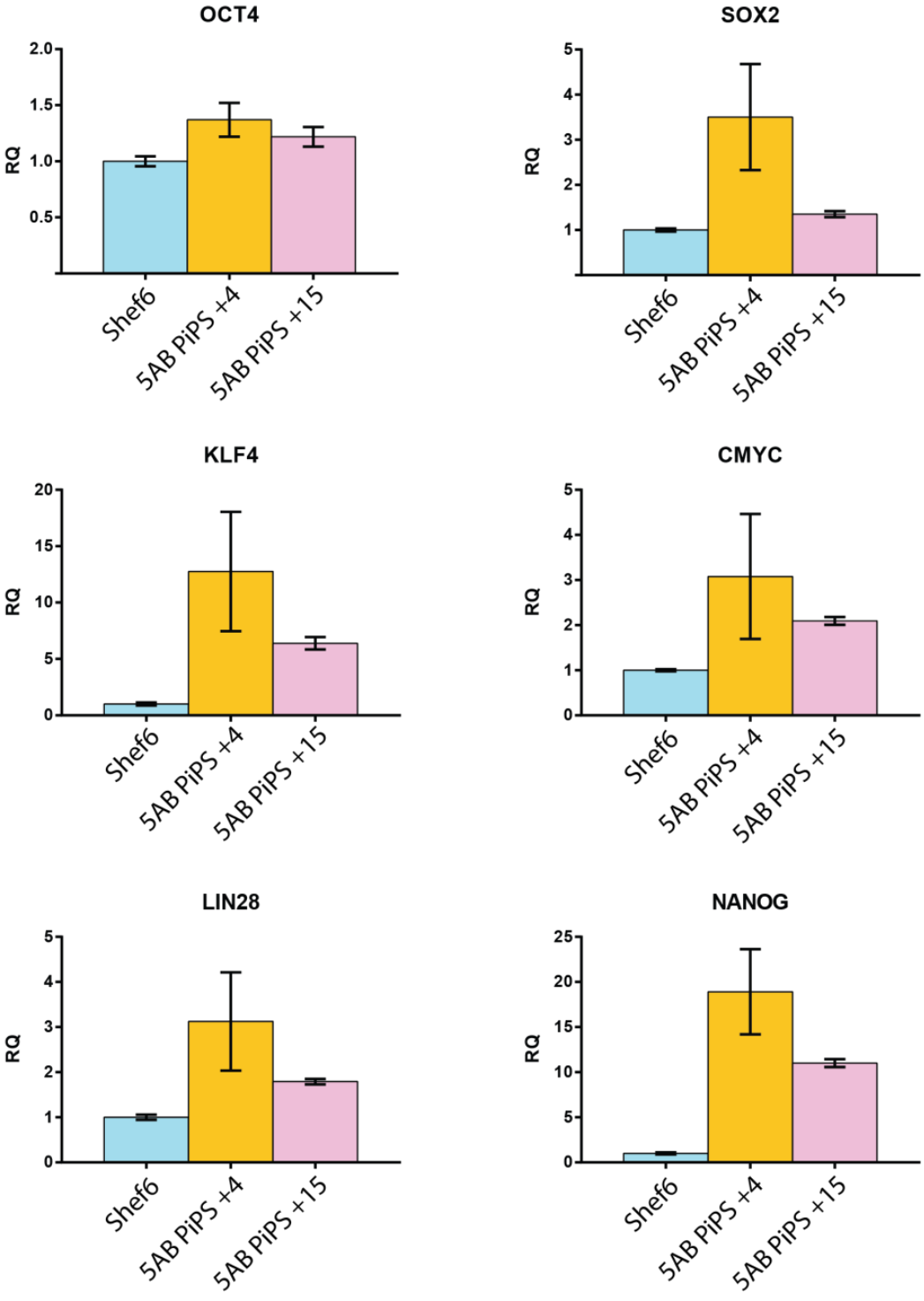

Figure 3.15: The 5AB PiPS cell line at passages +4 and +15 was analysed by qPCR to compare mRNA levels for *OCT4, SOX2, KLF4, CMYC, LIN28* and *NANOG* relative to Shef6, an undifferentiated control hESC line. At passage +4, endogenous mRNA levels were elevated relative to the control hESC line. By passage +15 the previously elevated levels of mRNA had decreased to a level more similar to that of Shef6 with the exception of *KLF4* and *NANOG* which are expressed 6-fold and 11-fold higher respectively. The standard error of measurement on the 5AB PiPS +4 analyses is consistent with a slightly elevated CT value for one of the three technical triplicate repeats for the loading control, *GAPDH*. N=1 (error bars derived from technical triplicates).

Figure 3.16. Spontaneous differentiation of the 5AB PiPS cell line induces gene expression for markers of all three germ layers

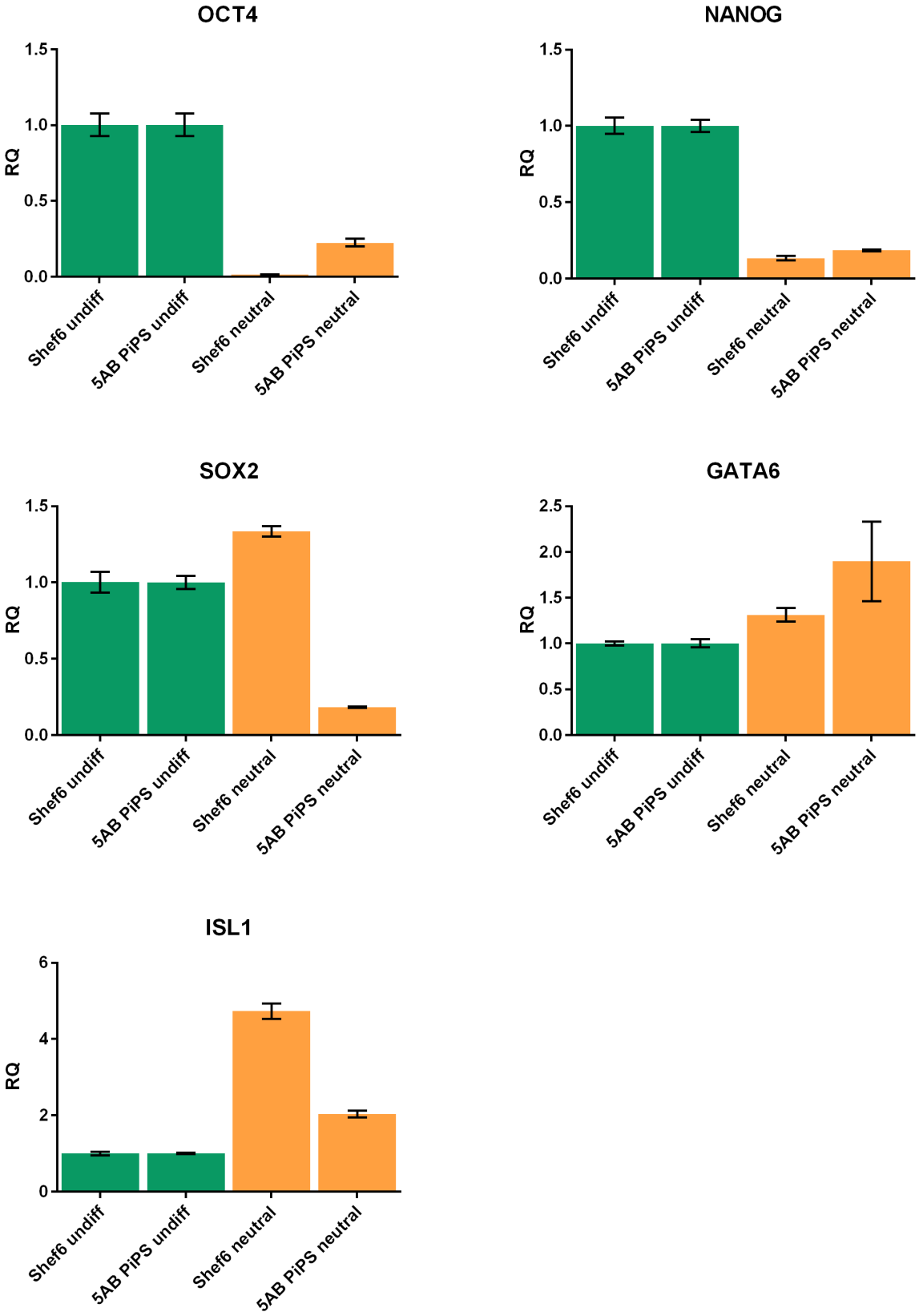

Figure 3.16. Spontaneous differentiation of the 5AB PiPS cell line induces gene expression for markers of all three germ layers

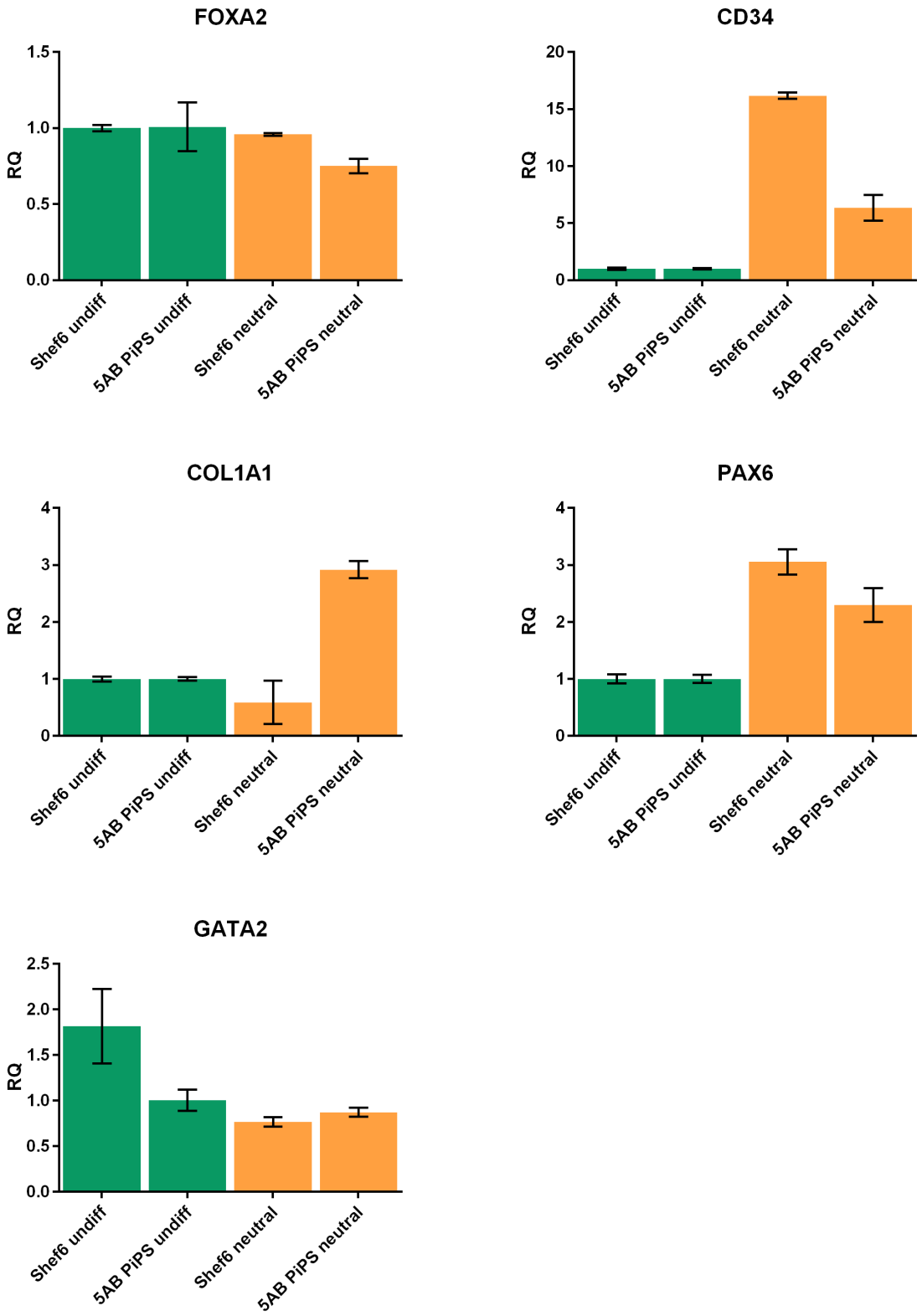

Figure 3.16: The 5AB PiPS 010 cell line was spontaneously differentiated as embryoid bodies for 10 days in the neutral condition (Table 2.4). Following qPCR analysis, the RQ values showed increased gene expression levels for endodermal (*GATA6, ISL1*), mesodermal (*CD34, COL1A1*) and ectodermal (*PAX6*) markers relative to an undifferentiated control. Under the same conditions, Shef6 cells increased gene expression for *ISL1* (endodermal), *CD34* (mesodermal) and *PAX6* (ectodermal) markers. CT values were normalised to *GAPDH*. N=1 (error bars derived from technical triplicates).

3.2.9. mRNA dose ramping and a flexible approach to reprogramming allows for rapid iPS colony generation with reduced cytotoxicity

The Allele Biotech 6-factor reprogramming premix (ABP-SC-6FMRNA) accelerated the kinetics of reprogramming, presumably owing to the inclusion of *M_3O* mRNA that resulted in the generation of iPS cells, without passaging within 11 days. However, cytotoxicity was prevalent (Figure. 3.12C) and is a limiting factor to the success of reprogramming. Could the daily dose of mRNAs during reprogramming be optimised so that the cells would not succumb to apoptosis, were not prevented from proliferating and was sufficient to generate fully reprogrammed iPS cells?

In order to assess whether increased iPS cell colony outgrowth would be achievable if the target cells were not lost to cytotoxic or pro-apoptotic events during reprogramming, mRNA dose-ramping was implemented. The rationale was that dose ramping provides better control over the mRNA dose per cell ratio as mRNAs are added in line with proliferation as opposed to being added irrespective of cell behaviour as most protocols suggest (Figure. 3.17E). BJ fibroblasts were plated onto hESC-qualified Matrigel at a density of $1x10^5$ in Pluriton medium for 24 hours. On days zero and one, 200ng of 6-factor premix mRNA (ABP-SC-6FMRNA) was pipetted into 0.5mls of low oxygen-equilibrated (5% O_2) Pluriton medium containing B18R at 400ng/ml. The supplemented medium was then placed onto the target cells and a further 500µl of Pluriton medium was added four hours later to prevent evaporation. Upon the observation that the cells were continuing to proliferate despite the repeated addition of 6-factor premix mRNA (ABP-SC-6FMRNA (Figure. 3.18B), the mRNA dose was increased to 300ng on days two through eight. On day

four a small percentage of the cell population had died, which is to be expected due to the stresses of reprogramming, so to counteract further cell death, $2x10^5$ MEFs were added to the reprogramming culture and the mRNA dose was not increased. On day seven, clusters of cells that morphologically resembled iPS cell colonies were observed (Figure. 3.18B) and these cells stained positive for TRA-1-60 when analysed via high content screening in-situ (Figure. 3.18C). The reprogramming kinetics of our optimised protocol that incorporates mRNA dose-ramping has been compared to the kinetics of basic commercial protocols supplied with other kits (Figure. 3.17A-D).

Figure 3.17. Optimisation of the basic reprogramming protocol

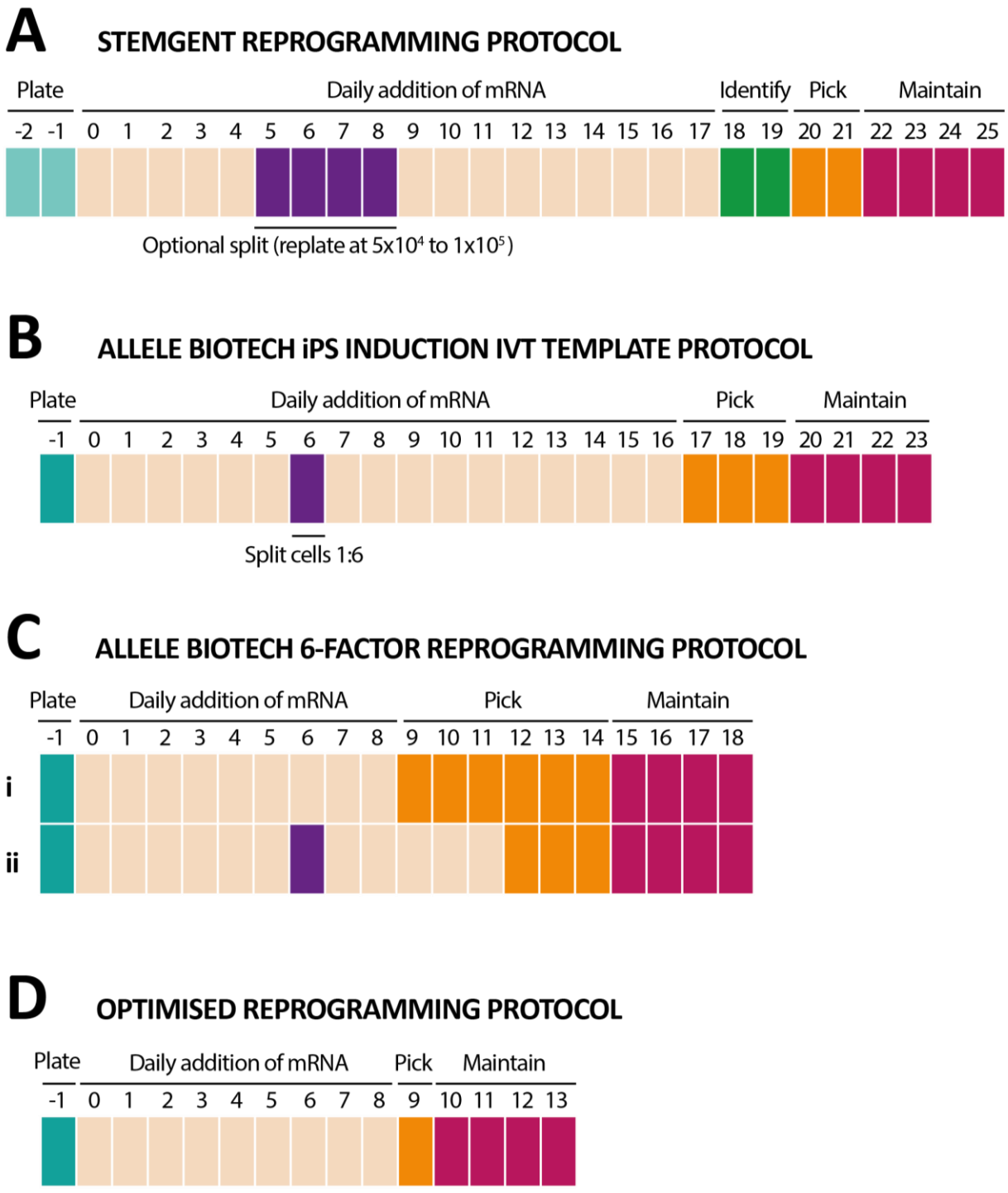

Figure 3.17: (A) The Stemgent protocol (00-0071) comprises 18 days whereby mRNA is repeatedly added to the cells. A splitting step between days 5-8 is recommended to avoid over-confluence. (B) The Allele Biotech iPS induction kit (ABP-SC-SEIPSET) used by Warren et al [76] adds mRNA over 17 days and contains a splitting step at day 6. (Ci) The manufacturer's protocol for the Allele Biotech 6-factor reprogramming premix (ABP-SC-6FMRNA) comprises 9 days where mRNA is added to the cells under a strict dose-ramping regimen. (Cii) The same protocol was modified in a study by Warren [39] whereby mRNA (ABP-SC-6FMRNA) was added for 3 days more than the suggested protocol and a splitting step was used on day 6. (D) Our optimised protocol, that uses 6-factor premix mRNA (ABP-SC-6FMRNA), uses a flexible dose ramping approach and generates iPS cells by day 9 without a splitting step.

Figure 3.17. Optimisation of the basic reprogramming protocol

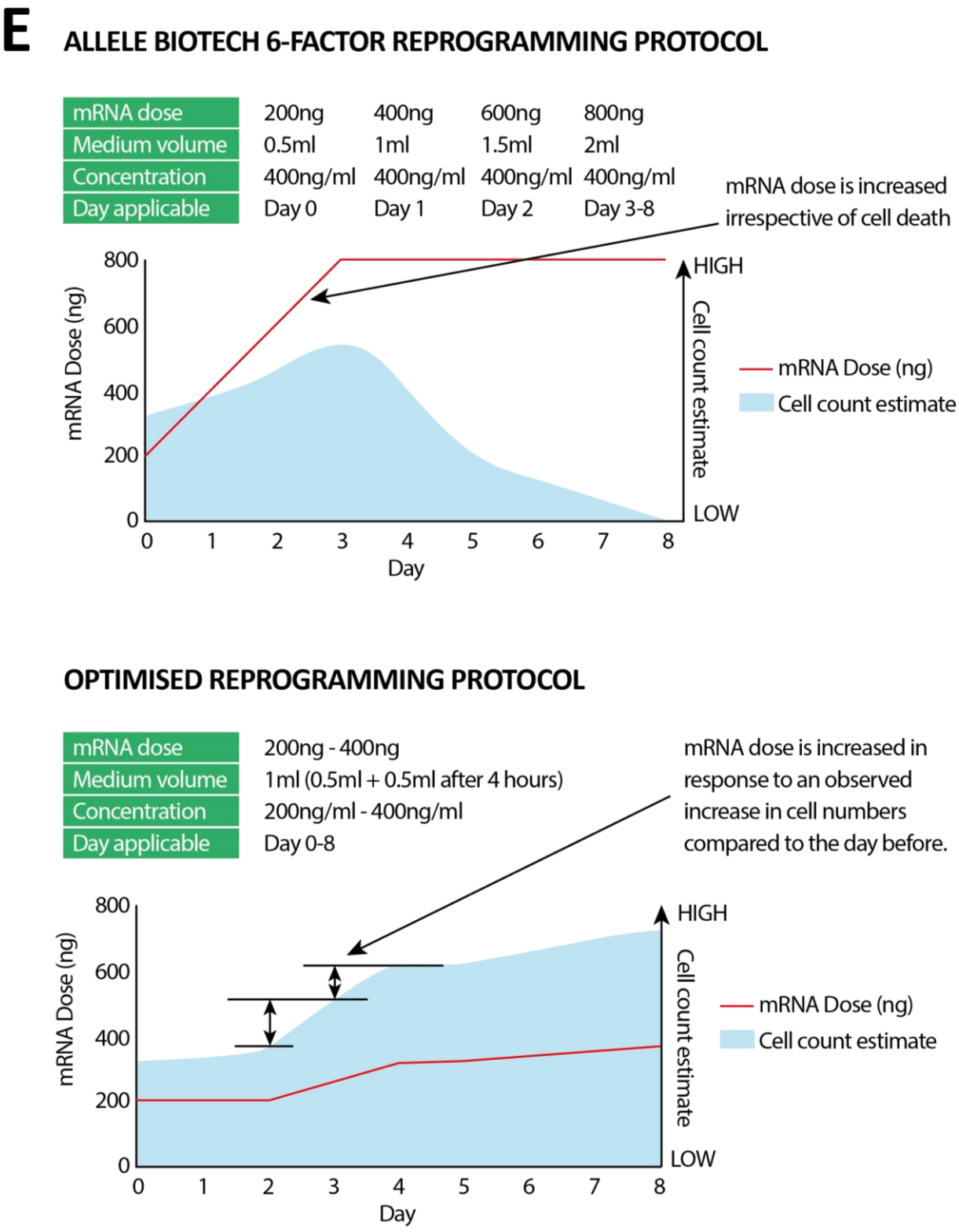

Figure 3.17: (E) The Allele Biotech 6-factor reprogramming premix protocol (top) incorporates a strict dose ramping regimen whereby the mRNA dose (red line) is increased daily by 200ng between days 0 and 3. Our optimised protocol (bottom) increases the mRNA dose in response to an observed increase in cell numbers (increased height of blue area, indicated by arrows) compared to the day before and does not increase by a set amount each day. This modified way of dose-ramping provides greater control over the balance between cell proliferation and apoptosis, thus reducing the probability of over-confluence and cell culture-wide apoptosis that inhibit reprogramming.

Figure 3.18. Reprogramming kinetics are improved using an optimised dose-ramping approach

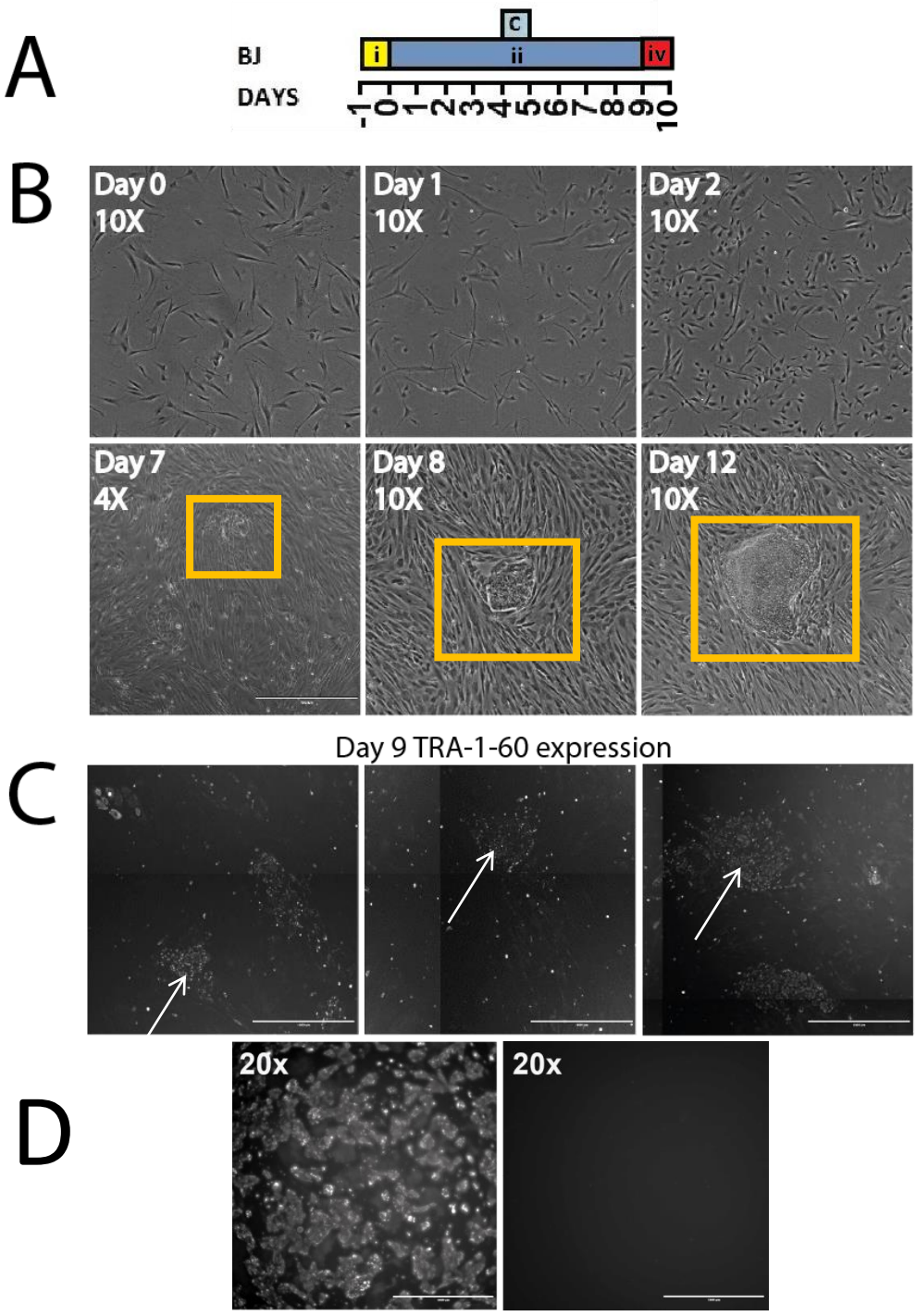

Figure 3.18: (A) The 10-day reprogramming timeline using Allele Biotech 6-factor reprogramming premix (ABP-SC-6FMRNA). (i) BJ fibroblasts were seeded at a density of $1x10^5$ onto hESC-qualified Matrigel-coated 6-well culture plates. (ii) A dose of 200ng mRNA (ABP-SC-6FMRNA) was added on day 0 and 1 and increased to 300ng on days 2 through 8. MRNA was added to 0.5mls of low oxygen-equilibrated (5% O_2) Pluriton medium containing B18R at 400ng/ml and a further 500µl of Pluriton medium was added four hours later to a total volume of 1ml. (iii) Inactivated MEFs were added at a density of $2x10^5$ on day 4 to support fibroblast proliferation. (iv) iPS cell colonies emerged on day 7 and were picked onto a MEF feeder layer on day 9. (B) Phase contrast images of emerging colonies (orange rectangles). (C) The detection of TRA-1-60 positive iPS cell colonies by in-situ live cell staining (methods 2.15.2) on day 9 of reprogramming (white arrows). (D) NT2 cell control positively fluorescing TRA-1-60 (left hand side) and NT2 negative control analysed for secondary antibody binding only. Scale bars =1000µm

3.2.10 Characterisation of iPS cell lines

IPS cells were generated using an optimised mRNA dose-ramping approach in conjunction with the Allele Biotech 6-factor reprogramming premix (ABP-SC-6FMRNA). In this sub-chapter, the phenotype and functional characteristics of these iPS cells was assessed by qPCR, flow cytometry and karyotype analysis. The iPS cells were also subjected to spontaneous differentiation as embryoid bodies for 10 days to assess their capacity to differentiate.

One resultant clonal iPS cell line, named 7AB PiPS, was determined to be karyotypically normal (46 XY) (Figure. 3.19A). The cells were analysed by flow cytometry (Figure. 3.20) which showed that markers; SSEA-3, SSEA-4, TRA-1-60 and TRA-1-81 were expressed in over 96% of cells analysed. SSEA-1 was expressed on only 15% of the cells. Expression of the pan-human marker TRA-1-85 in both 7AB PiPS and the hESC control confirmed the staining procedure worked and was thus performed correctly. Considering the cell markers analysed by flow cytometry were expressed at abnormally high levels, for example SSEA-3 was expressed in 98% of the cells, it is possible that the cells had acquired a genetic mutation that maintains cells in an undifferentiated state. The cells were analysed by qPCR to check for a potential mutation in *BCL2L1*, a common chromosomal abnormality that once overexpressed confers a selective advantage over other cells. It was determined that *BCL2L1* was not overexpressed and did not have an abnormal copy number when compared to negative and positive control cell lines, H7 S14 and H7 S6 respectively (Figure. 3.19B).

The 7AB PiPS cell line was further characterised at passage +5 to determine its gene expression profile compared to that of a control hESC line and the parental BJ fibroblast cell line (Figure. 3.21). QPCR analysis confirmed the 7AB PiPS cells were phenotypically different from the BJ fibroblast cell line from which it was derived, endogenously expressing genes; *OCT4, SOX2, KLF4, cMYC, LIN28* and *NANOG* similar to the hESC control. The mRNA levels for all of the genes analysed were elevated relative to the Shef6 control hESC line. Most notably, *NANOG* mRNA levels were 15-fold higher and *LIN28* mRNA levels were 5-fold higher relative to the hESC control.

To qualitatively confirm the presence of endogenous *OCT4* and TRA-1-60 protein, the cells were analysed by high content screening by staining the cells with *OCT4* and TRA-1-60 primary antibodies, goat anti rabbit AF488 (*OCT4*) and goat anti-mouse AF488 (TRA-1-60) secondary antibodies and counterstaining with Hoescht 33342 (Figure. 3.22). High TRA-1-60 and *OCT4* endogenous expression was confirmed in the cells. Lastly to assess the differentiation capacity of the 7AB PiPS cell line, the cells were subjected to ten days embryoid body differentiation in the neutral condition (Table 2.4). The embryoid bodies were shown to express markers of all three germ layers after qPCR analysis (Figure. 3.23) highlighting the 7AB PiPS cell line's pluripotent capacity.

Figure 3.19. Cytogenetic analysis of the 7AB PiPS cell line

A

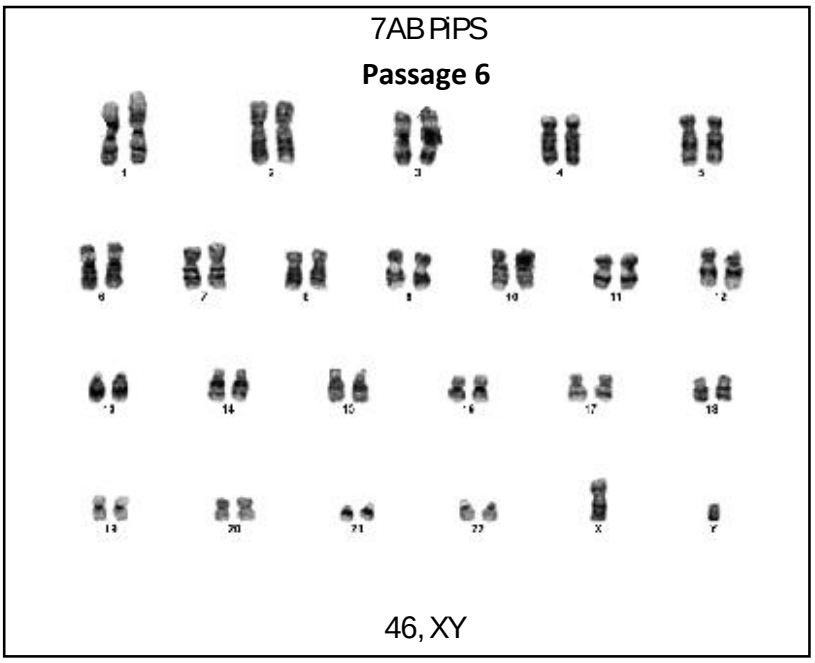

B

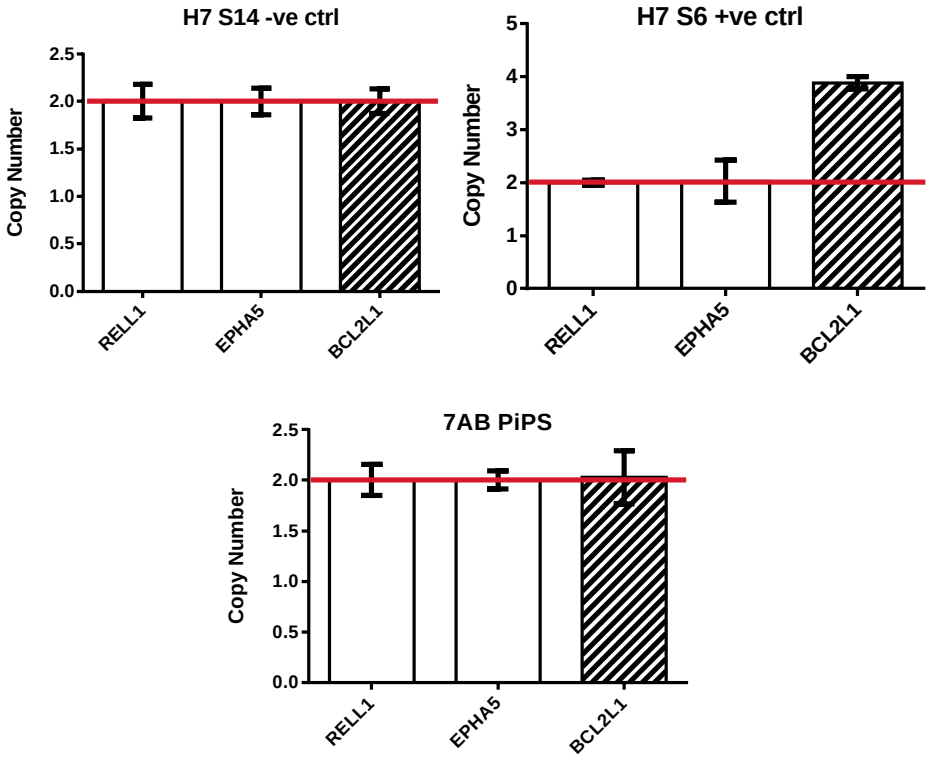

Figure 3.19: (A) Karyotype analysis (methods 2.16) on the 7AB PiPS cell line at passage +6 revealed that it is karyotypically normal (B) 7AB PiPS+6 were subjected to a genomic qPCR assay to determine the copy number for BCL2L1, a gene commonly expressed in karyotypically abnormal hESCs. The copy number analysis detected no amplification of BCL2L1 in the 7AB PiPS cell line. H7 S14 was used as a negative control and H7 S6 was used a positive control for the BCL2L1 amplification. CT values were normalised against the housekeeping gene RELL1, a gene that displays a low incidence of genomic instability in hESCs. EPHA5 confirms the suitability of the first control. N=1 (error bars derived from technical triplicates).

Figure 3.20. Flow cytometric analysis of the 7AB PiPS cell line compared to an undifferentiated hESC line

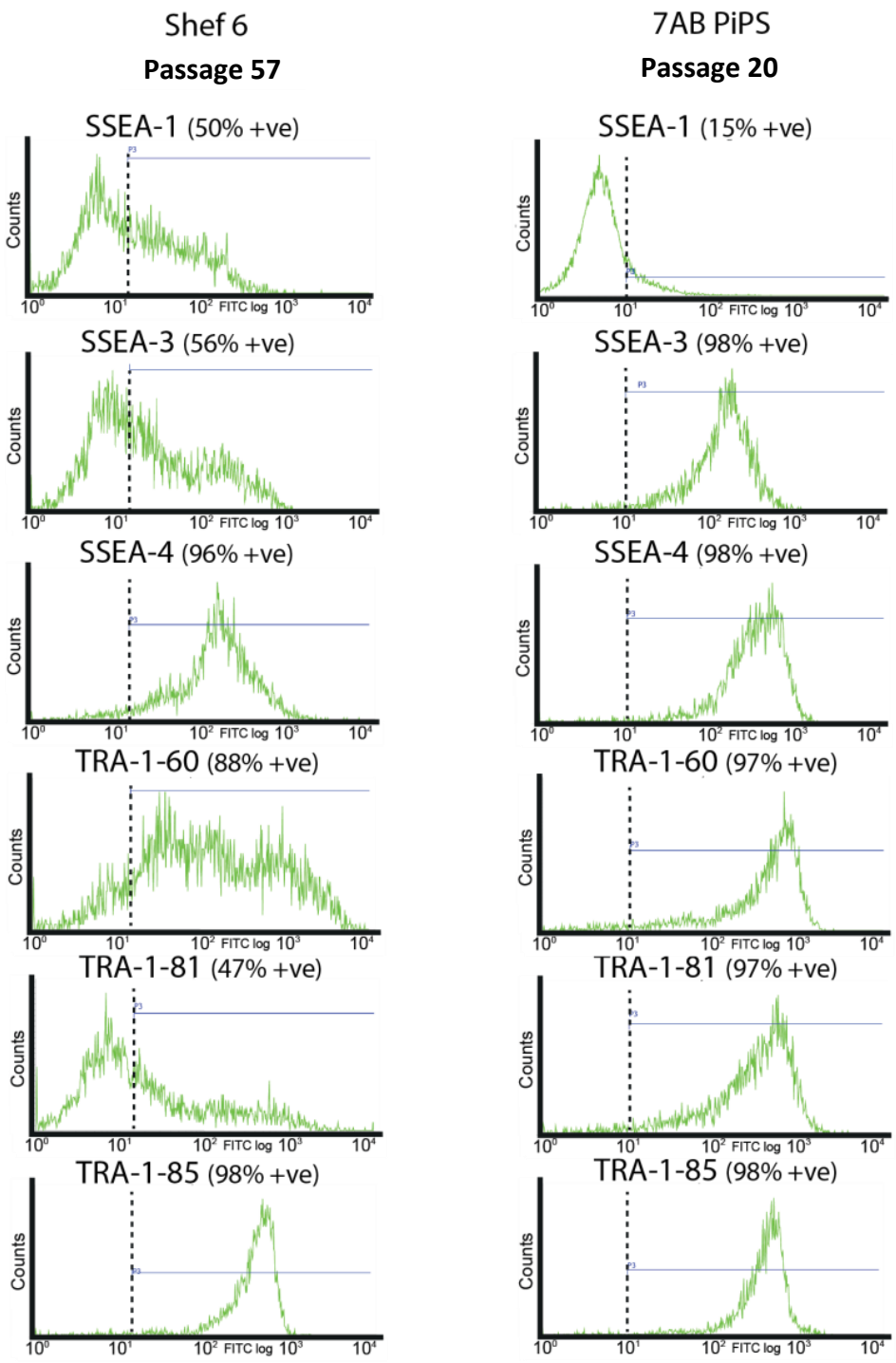

Figure 3.20: Flow cytometric analysis of the 7AB PiPS cell line compared to an undifferentiated hESC control, Shef6. Both cell lines positively express markers: SSEA-3, SSEA-4, TRA-1-60 and TRA-1-81 that are associated with an undifferentiated stem cell state. Fifteen percent of 7AB PiPS cells expressed SSEA-1, a marker of differentiated hESCs / iPS cells, indicating the cells were predominantly undifferentiated when analysed. SSEA-3 was expressed in 56% of Shef6 cells compared to 98% of 7AB PiPS cells suggesting that Shef6 had begun to differentiate sooner than 7AB PiPS cells given they were both cultured in the same conditions (MEF feeder layer in hESC medium) for 5 days prior to the analysis. TRA-1-85 was used a positive control for the antibody staining. Gating (dashed line) was performed as described in methods 2.15.1.1 using P3X.

Figure 3.21. Analysis of the 7AB PiPS cell line by qPCR

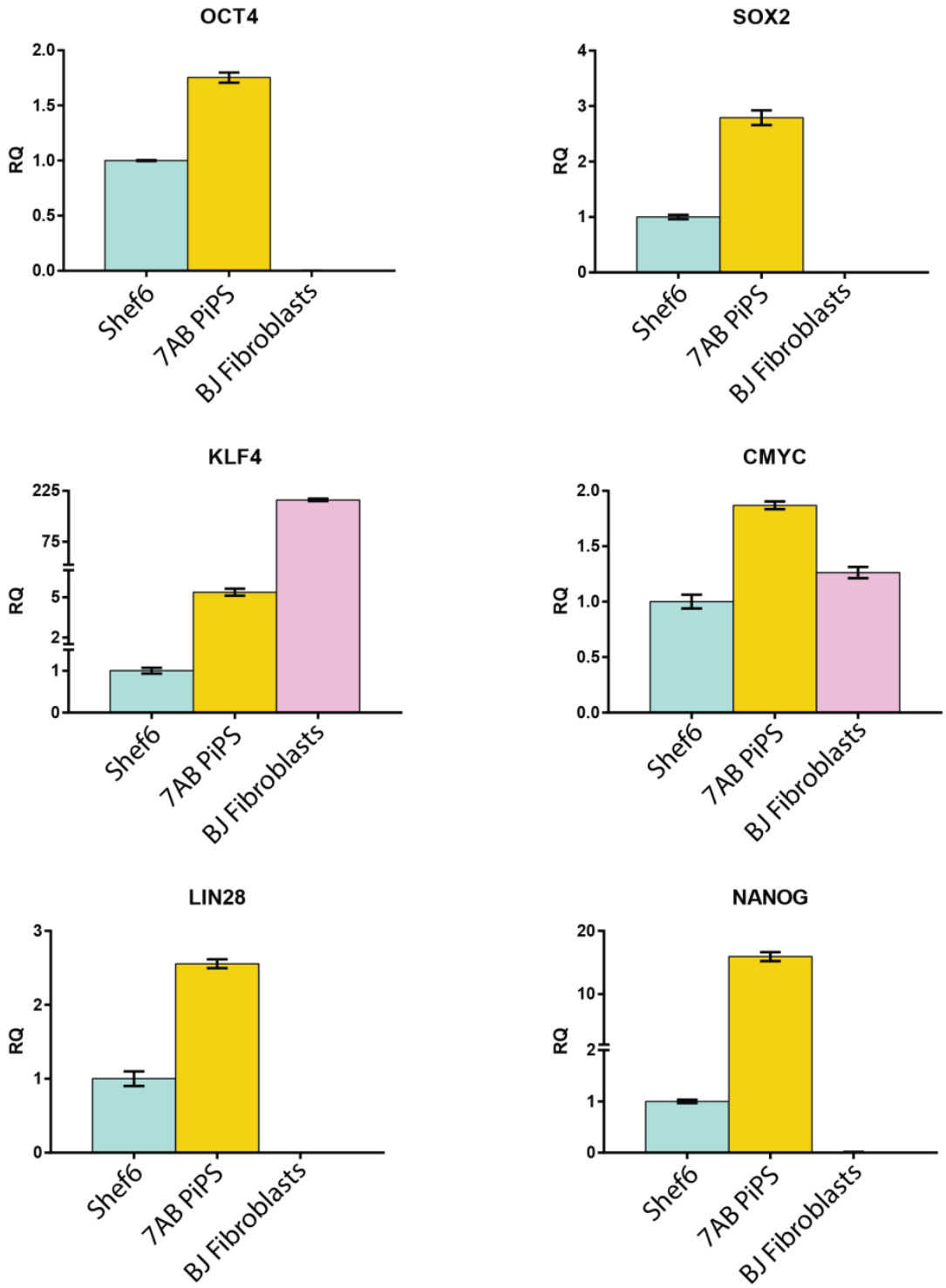

Figure 3.21: qPCR analysis of the 7AB PiPS cell line at passage +5 shows mRNA levels comparable to the hESC control cell line, Shef6, and dissimilar to the parental BJ fibroblast line at passage +9. The mRNA levels for; *OCT4, SOX2, cMYC* and *LIN28* are expressed 1.7-fold, 2.7-fold, 1.7-fold and 2.5-fold higher respectively in 7AB PiPS cells compared to Shef6 while *KLF4* and *NANOG* mRNA levels are 5-fold and 15-fold higher respectively. Analysing 7AB PiPS cells in a pristine, undifferentiated stem cell state or Shef6 cells that had begun to differentiate may be the reason for elevated levels of *NANOG* in 7AB PiPS cells relative to Shef6. BJ fibroblasts endogenously express *cMYC* and *KLF4* as shown in Figure 3.2. CT values were normalised to *GAPDH*. N=1 (error bars derived from technical triplicates).

Figure 3.22. The 7AB PiPS cell line endogenously expresses OCT4 and TRA-1-60

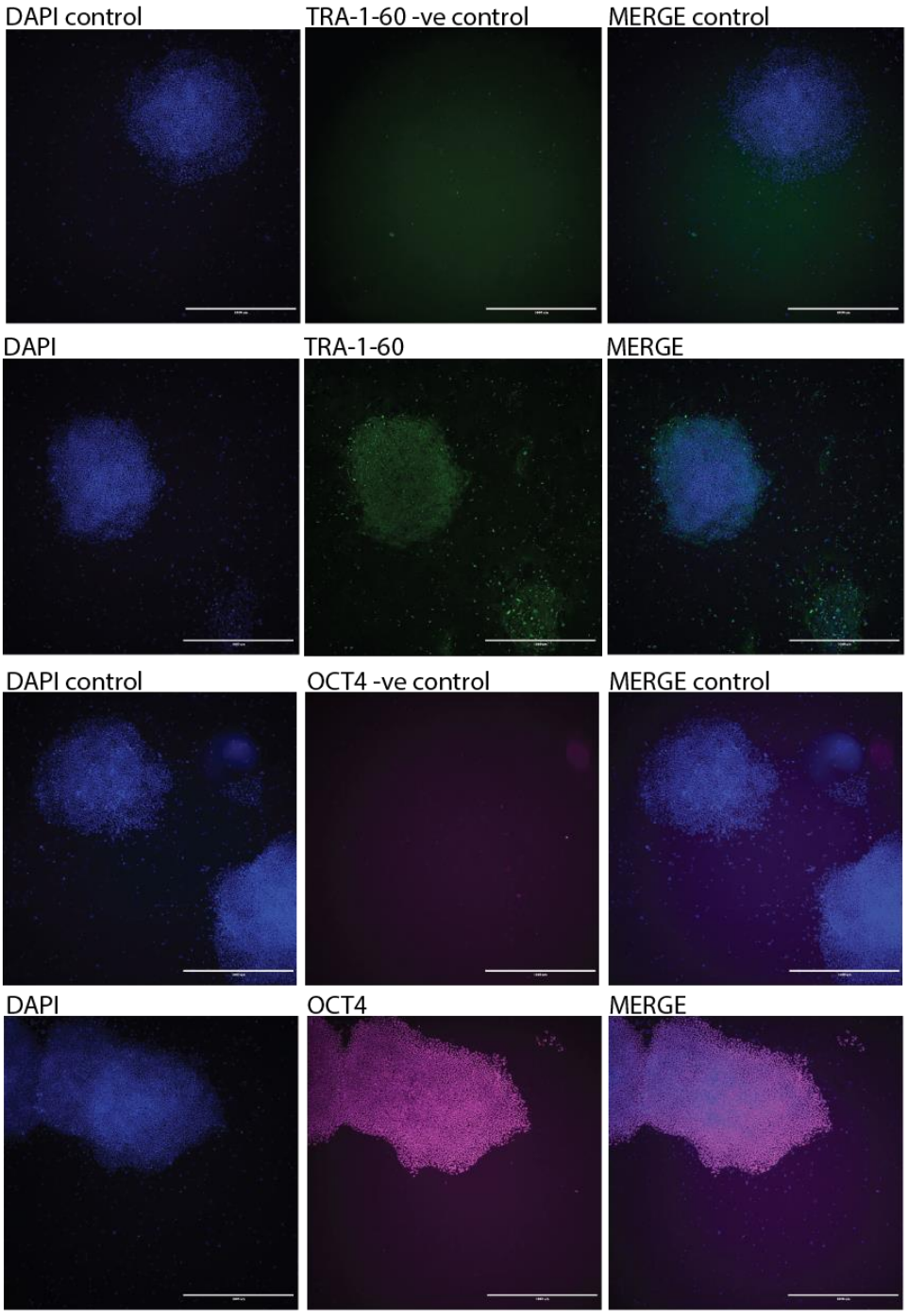

Figure 3.22: 7AB PiPS express intracellular OCT4 and TRA-1-60 cell surface marker as assessed by immunomicroscopy. 7AB PiPS were grown on MEFs in hESC medium for 4 days then fixed with 4% PFA. Cell surface marker staining was performed prior to permeabilisation with 0.1% Triton X followed by intracellular staining. Primary antibodies used were OCT4 (rabbit) at 1:100 and TRA-1-60 (mouse) at 1:10. Secondary antibodies used were goat anti rabbit AF488 (OCT4) at 1:100 and goat anti-mouse AF488 (TRA-1-60) at 1:100. Controls were dual stained with the secondary antibodies only and all wells were stained with Hoescht 33342 at 1:1000. Scale bars = 1000µm.

Figure 3.23. Spontaneous differentiation of the 7AB PiPS cell line induces gene expression for markers of all three germ layers

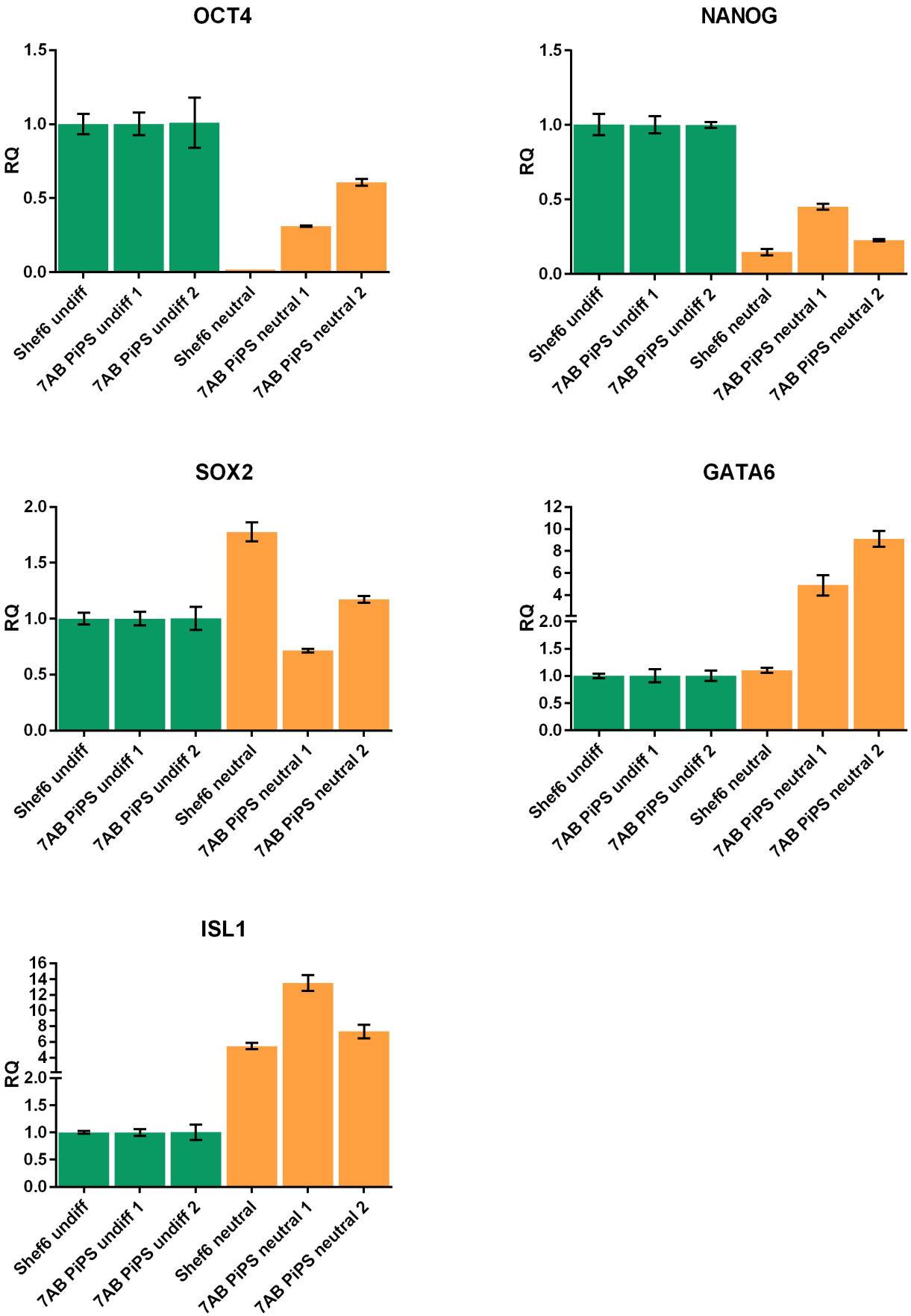

Figure 3.23. Spontaneous differentiation of the 7AB PiPS cell line induces gene expression for markers of all three germ layers

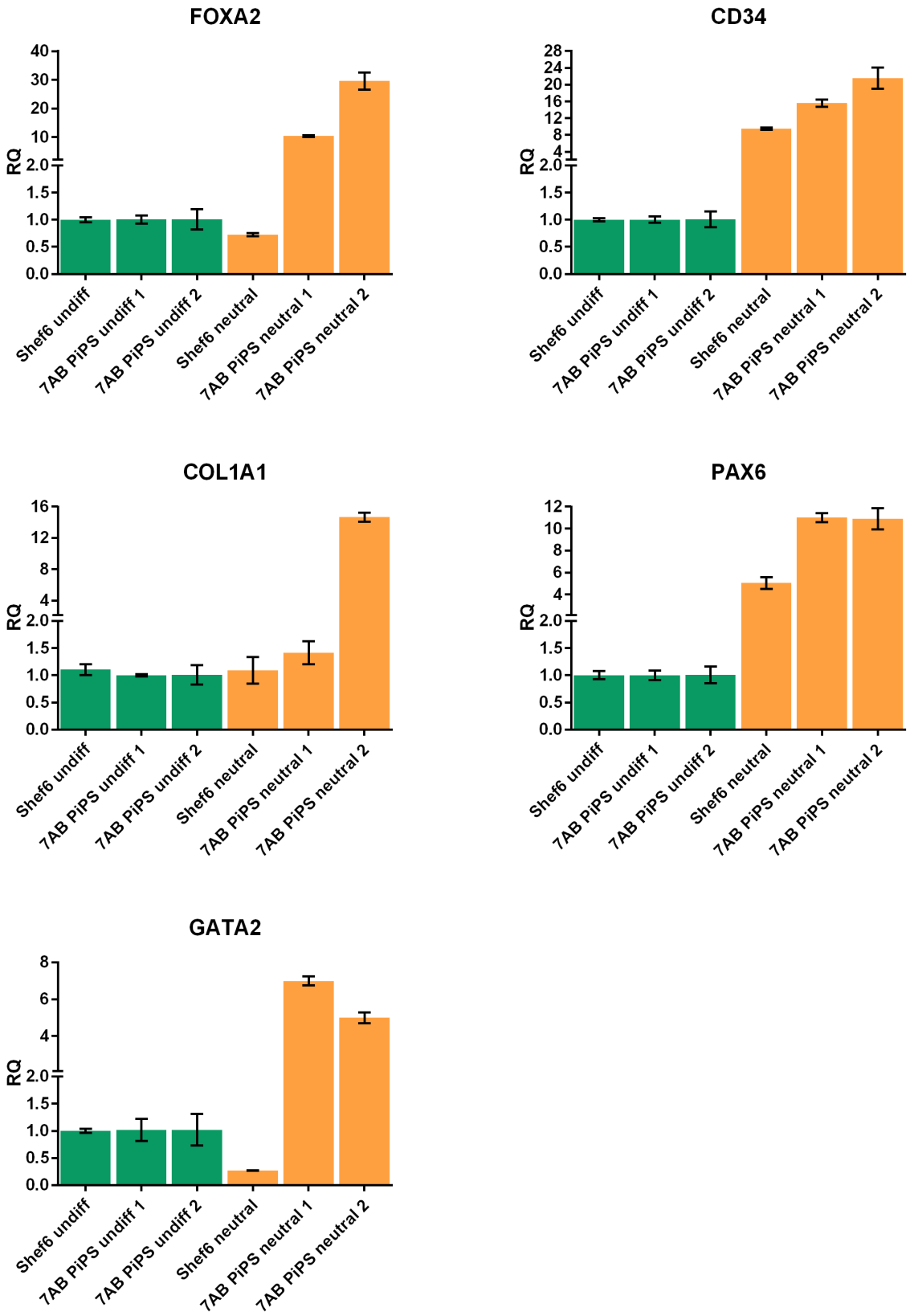

Figure 3.23: Two biological replicates of the 7AB PiPS cell line were spontaneously differentiated as embryoid bodies for 10 days in the neutral condition (Table 2.4). Following qPCR analysis, the RQ values for both replicates showed increased gene expression levels for endodermal (*GATA6, ISL1, FOXA2*), mesodermal (*CD34, COL1A1*) and ectodermal (*PAX6,GATA2*) markers relative to an undifferentiated control. Under the same conditions, Shef6 cells increased gene expression for *ISL1* (endodermal), *CD34* (mesodermal) and *PAX6* (ectodermal) markers. CT values were normalised to *GAPDH*. N=1 (error bars derived from technical triplicates).

3.3. Discussion

MRNAs derived from different sources were found to exhibit different efficiencies in terms of their ability to get into the fibroblast cells and the number of vectors that enter each cell. In fibroblasts, the addition of *mWASABI* mRNA containing modified nucleotides derived from an Allele Biotech IVT template (ABP-SC-SEIPSET) and *eGFP* mRNA derived from the RN3P plasmid (methods 2.17.7) resulted in >95% of the cells exhibiting fluorescence. However, the addition of mRNAs into fibroblasts that were derived from the RN3P plasmid and did not contain modified nucleotides resulted in less than ten percent of the cells fluorescing. Possible reasons for this include mRNA degradation or a failure for mRNAs to successfully enter the cells following lipofection. Considering that the mRNAs used were flanked by identical untranslated regions (UTRs), capping structure and polyA tail, suggests the mRNA open reading frame where the modified nucleotides are incorporated is the specific region whereby differences regarding the susceptibility to degradation may occur, possibly via miRNAs and endonucleases. It is unlikely that the reason why mRNAs that were not transcribed with modified nucleotides had low fluorescence levels was attributable to an inability to enter the cells. This is reinforced by the finding that mRNAs derived from Allele Biotech templates (ABP-SC-SEIPSET) that were transcribed without modified nucleotides could achieve near 100% transfection efficiency.

Fibroblasts that were subjected to the addition of *mWASABI* mRNA transcribed with modified nucleotides were determined to be 19-fold brighter than when *eGFP* mRNA containing modified nucleotides was added. While this could be due to an increased mRNA per cell ratio or by virtue of its derivation from *Clavularia* coral, it is more likely that *mWASABI* mRNA is more resilient to degradation or is more easily translated. Firstly *mWASABI* protein has been reported to fluoresce only 1.6-fold brighter than eGFP [164] which does not then account for the 19-fold difference in median fluorescent intensity. Secondly, the same transfection reagent and amounts were used

for all transfections concerning both *eGFP* and *mWASABI* mRNAs therefore making the transfection reagent a non-limiting factor as to why cells transfected with *mWASABI* were brighter than those transfected with *eGFP*. It is therefore more likely that *mWASABI* fluoresces at a higher intensity than *eGFP* because the Allele Biotech IVT template (ABP-SC-SEIPSET) from which it was transcribed is more efficiently designed to improve the half-life of the mRNA transcript, prevent degradation by nucleases and / or increase how efficiently the mRNA is translated. To further this point it was found that mRNAs encoding *OCT4*, *SOX2*, *KLF4*, *cMYC*, *LIN28* and *NANOG* derived from Allele Biotech IVT templates (ABP-SC-SEIPSET) increased mRNA levels on average to 206-fold higher than what is endogenously expressed in undifferentiated hESCs. In comparison, mRNAs encoding *OCT4*, *SOX2*, *KLF4*, *cMYC*, *LIN28* and *NANOG* derived from the RN3P template induced a 99-fold increase in mRNA levels relative to the same control hESC line. This supports the hypothesis that mRNAs derived from Allele Biotech IVT templates (ABP-SC-SEIPSET) facilitate mRNA localisation, stability, export or translational efficiency more efficiently that mRNAs transcribed from linearised RN3P plasmids.

Prior to reprogramming using mRNAs derived from Allele Biotech IVT templates (ABP-SC-SEIPSET) (results 3.2.3), I showed that mitotically inactive MEFs are capable of taking up exogenous mRNA. Considering reprogramming protocols require the use of an inactivated / irradiated fibroblast feeder layer, I investigated whether mRNAs would be taken up by the feeder layer. This could be problematic for the following reason. If mRNAs can enter into mitotically inactivated MEFs, it is likely that the repeated addition of single-stranded mRNAs would trigger an intracellular immune response that would cause the inactivated MEFs to die. As a result, the feeder layer would be eradicated, inhibiting the emergence of iPS cell colonies. I tested whether this was the case by adding a single dose of *mWASABI* mRNA into inactivated MEFs and analysed the fluorescence levels by flow cytometry after 24 hours. I found that the MEFs were positively expressing mWASABI protein in that they were fluorescing after 24 hours

indicating they do take up exogenous mRNA. Considering MEFs are transfected at the same time as the intended fibroblast cells it is important to add MEFs to cell cultures where a MEF layer is used and when repeated transfection of mRNAs is necessary, so that the supportive feeder layer can be replenished.

I have successfully shown reprogramming of the BJ fibroblast cell line firstly with the Stemgent reprogramming kit (00-0071), secondly using mRNAs in-vitro transcribed from the Allele Biotech IVT templates (ABP-SC-SEIPSET) and then on two occasions with the 6-factor premix mRNA (ABP-SC-6FMRNA). IPS cells were generated after 32, 21, 14 and 9 days respectively indicating a consistent improvement in the kinetics of reprogramming. I found that reprogramming using the 6-factor premix mRNA (ABP-SC-6FMRNA) gave rise to iPS cells in a shorter timeframe than mRNA from other sources. This could be attributable to a reduced susceptibility to degradation or a higher translational efficiency. It could also be that the 6-factor premix (ABP-SC-6FMRNA) contains codon-optimised mRNAs. Codon optimisation is a technique used to modify mRNAs to enhance mRNA stability that results in an increase in protein expression compared to their non-codon-optimised counterparts. Achieving a sufficient level of exogenous transcription factor expression is a necessity in driving target cells to reprogramme and may explain why mRNAs that produce insufficient expression levels have difficulty in activating an endogenous pluripotency network that leads to the emergence of iPS colonies. The 6-factor premix (ABP-SC-6FMRNA) also contains M_3O mRNA as opposed to *OCT4*, which has been shown to facilitate reprogramming [39] via chromatin remodelling and protein recruitment to pluripotency genes [68] and may explain variability in reprogramming success between cocktails that utilise *OCT4-MYOD1* mRNA and those that contain endogenous *OCT4* transcripts. Speculatively the 6-factor premix mRNA (ABP-SC-6FMRNA) may also contain antagomirs that irreversibly bind to miRNAs, known to inhibit the reprogramming process such as miR-29 and mir-21 [172], to prevent mRNA degradation via the RNA-induced silencing complex.

The final two reprogrammings using the 6-factor premix mRNA (ABP-SC-6FMRNA) did not require passaging to yield iPS cells thus represents an improvement upon existing reprogramming efficiencies. The first of these reprogrammings took eleven days before iPS cell colonies could be identified while the latter reprogramming took only seven days. The difference can be attributed to a key optimisation that I implemented during the reprogramming process. This was a flexible dose-ramping approach for the addition of mRNAs during reprogramming. What this means is that mRNAs were not added at a certain amount on a certain day as most protocols suggest but instead, the mRNA dose would be determined by an approximation of the number of cells in the culture compared to the previous day. As the cells proliferated, the mRNA dose would increase. If the confluency markedly increased then too little mRNA was added the previous day, conversely if there was less cells than the day before then too much mRNA was added. This optimisation allowed for better control over the mRNA dose per cell ratio by using cellular cues as opposed to strict protocols to more optimally determine the mRNA dose on a given day. Typical mRNA-reprogramming methods result in a large amount of cell death following repeated addition of mRNA however, mRNA dose-ramping ameliorates this effect. MRNA dose ramping can therefore help increase the number of viably reprogrammable target cells to enhance the efficiency of reprogramming.

These findings show that by utilising highly modified mRNAs in a dose-dependent manner while tightly regulating cellular proliferation and rapidly responding to cellular cues in the face of pro-apoptotic and cytotoxic events is key to a more efficient, accelerated reprogramming. We have employed two simple method adaptations to limit reprogramming toxicity and generate iPS cells with accelerated kinetics from fibroblasts. Firstly, we used an optimised dose ramping approach that starts with a lower mRNA dose in the first couple of days and increases to a larger dose only if the cells continue to proliferate. Secondly, we add extra human fibroblasts during reprogramming if cell death was higher than cell proliferation. Future mRNA-based

reprogramming methodologies would benefit from implementing a similar approach when trying to produce informative iPS cells in a reduced timeframe.

Chapter 4.

Determining the applicability of mRNA reprogramming in a neuroblastoma cell line.

4.1. Introduction

We have previously demonstrated that SK-N-SH-derived iPS cell lines can be obtained (named SKiPS) by overexpressing the reprogramming factors: *OCT4*, *SOX2*, *KLF4*, *cMYC*, using lentivirus vectors. However, the resultant neuroblastoma-iPS cell lines contained irremovable transgenes. Informative analyses on disease-derived iPS cells ideally do require that the cells are devoid of transgenes so that the characterisation and functional analyses on the cells can more accurately model aspects of disease development. So I decided to test whether integration free neuroblastoma-derived iPS cells could be created following the repeated addition of mRNAs. Fibroblasts were most efficiently reprogrammed with mRNAs when using the 6-factor reprogramming premix (ABP-SC-6FMRNA) so this provides a good basis to test whether this mRNA cocktail could reprogramme the SK-N-SH neuroblastoma cell line to generate integration-free neuroblastoma-iPS cells. The decision to select this neuroblastoma cell line was based on its amenability to the reprogramming process. The resultant iPS cells could then be functionally analysed, for example, by differentiating the cells as embryoid bodies in defined conditions (Figure. 2.7 and Table 2.4) to test whether the disease genome has affected the resultant iPS cells ability to differentiate, a finding that would mirror a small aspect of early neuroblastoma development.

Early neuroblastoma development has been modelled *in vivo* in mouse [134]. This study demonstrated that neuroblastoma can be initiated by overexpressing Myc-n in migrating neural

crest under the control of a tyrosine hydroxylase promoter. There are, however, at the time of writing, no *in vitro* models for neuroblastoma development that are iPS cell-based. To establish such models, in addition to mRNA reprogramming, the SK-N-SH cell line was sent to a collaborative group at the Karolinska Institutet in Sweden to be reprogrammed using the Sendai virus. There were two reasons for this. Firstly, the Sendai virus provides an additional method for reprogramming and secondly it allows for comparisons to be made between methods that introduce transgenes as mRNA or as viral RNA.

4.2. Results

4.2.1. Reprogramming SK-N-SH cells using mRNAs induces TRA-1-60 expression in over a third of the cell population that form iPS-cell like colonies after cell sorting.

It is unknown what the consequences are for forcing a human cancer genome to operate in the context of a distinct lineage. We can begin to address this by applying the optimised reprogramming method that successfully reprogrammed BJ fibroblasts, to a neuroblastoma cell line. The resultant neuroblastoma-derived iPS cells will create a platform from which we can improve our understanding of the molecular mechanisms underlying neuroblastoma development.

In order to obtain a set of integration-free neuroblastoma-derived iPS cells, an mRNA cocktail containing *OCT4*, *SOX2*, *KLF4*, *cMYC*, *LIN28* and *NANOG* derived from Allele Biotech IVT templates (ABP-SC-SEIPSET) was added into the SK-N-SH cell line at a stoichiometry containing a relative three-fold increase of *OCT4* to the other factors. SK-N-SH cells were plated at a density of $3x10^5$ on to an inactivated MEF layer for 24 hours. A higher plating density was used in comparison to that of BJ fibroblasts after finding that SK-N-SH cells fail to proliferate on Matrigel in Pluriton medium when seeded at low densities (Figure. 4.1). The target cells were transfected daily until day eight with the mRNA cocktail (ABP-SC-SEIPSET) at a dose of 800ng in 2 ml of Pluriton medium to a final concentration of 400ng/ml (Figure. 4.2A). In addition, *mWASABI* mRNA was introduced periodically throughout reprogramming to report whether the reprogramming factor mRNA cocktail being added to the reprogramming cultures was being taken up by the cells. B18R was added to the media every day at a concentration of 400ng/ml. The target cells grew to 100% confluency by day five and by day eight the cells had begun to mound on

top of one another (Figure. 4.2B). The cells were passaged as single cells using 0.25X trypsin-EDTA at a split ratio of 1:3 on day eight onto fresh MEF-coated culture dishes. This was done to firstly promote iPS cell survival in the event that any of the SK-N-SH cells had been reprogrammed and secondly to create space for further cell divisions to take place. After passaging, the addition of mRNA was ceased and the growth medium was switched to hESC media to promote cell survival and encourage iPS cell growth. On day 16, it became difficult to visually detect the presence of iPS cells as the reprogramming culture had become over-confluent and formed a monolayer. To isolate any putative iPS cells from the culture, the cell population was sorted for TRA-1-60. Upon sorting it was observed that 36% of the population was TRA-1-60^{+ve} (Figure. 4.3iii). TRA-1-60 positive (6.5x10^{4} cells) and negative fractions were seeded onto MEFs in hESC media to compare phenotypic differences between the two fractions.

The replated TRA-1-60^{-ve} cells were indistinguishable from SK-N-SH cultures made up of small, spiny neuronal cells. However, the TRA-1-60^{+ve} cells were morphologically dissimilar to SK-N-SH cells and more closely resembled iPS cells. The iPS-like cells were characterised by the way they formed tightly packed epithelial-like colonies, with domed centres and jagged borders (Figure. 4.2B, white arrows). Upon subsequent passaging, the TRA-1-60^{+ve} cells lost their iPS cell-like colony morphology and returned to a TRA-1-60^{-ve} SK-N-SH phenotype indicating that the reprogrammed cells had not formed a stable cell line. One reason for this could be that the cells were in a partially reprogrammed state. To determine whether this could be the case, the original sort data was re-analysed to assess the fluorescence levels of *mWASABI* present in the TRA-1-60^{+ve} sorted cells. As found in my fibroblast reprogrammings and in line with other reports, cells that express TRA-1-60 tend not

to co-express mWASABI protein or other fluorescent proteins translated from vectors that have been added during reprogramming to monitor transfection efficiency. To re-evaluate the original sort data, the original histograms and gates used to control for cell size, granularity and doublet discrimination were maintained and this population was plotted against the GFP channel that detect *mWASABI* expression. It was found that 36% of the gated population positively expressed *mWASABI* (Figure. 4.4i). This was then gated against TRA-1-60 to quantify the number of cells that co-expressed TRA-1-60 and *mWASABI* (Figure. 4.4ii). The resultant TRA-1-60 histogram showed that the re-seeded population after sorting contained two sub-populations, one that was 50% TRA-1-60^{+ve} / *mWASABI*$^{+ve}$ and the other that was 50% TRA-1-60^{+ve} / *mWASABI*$^{-ve}$.

Figure 4.1. Seeding SK-N-SH cells at low densities on Matrigel in Pluriton affects its ability to proliferate

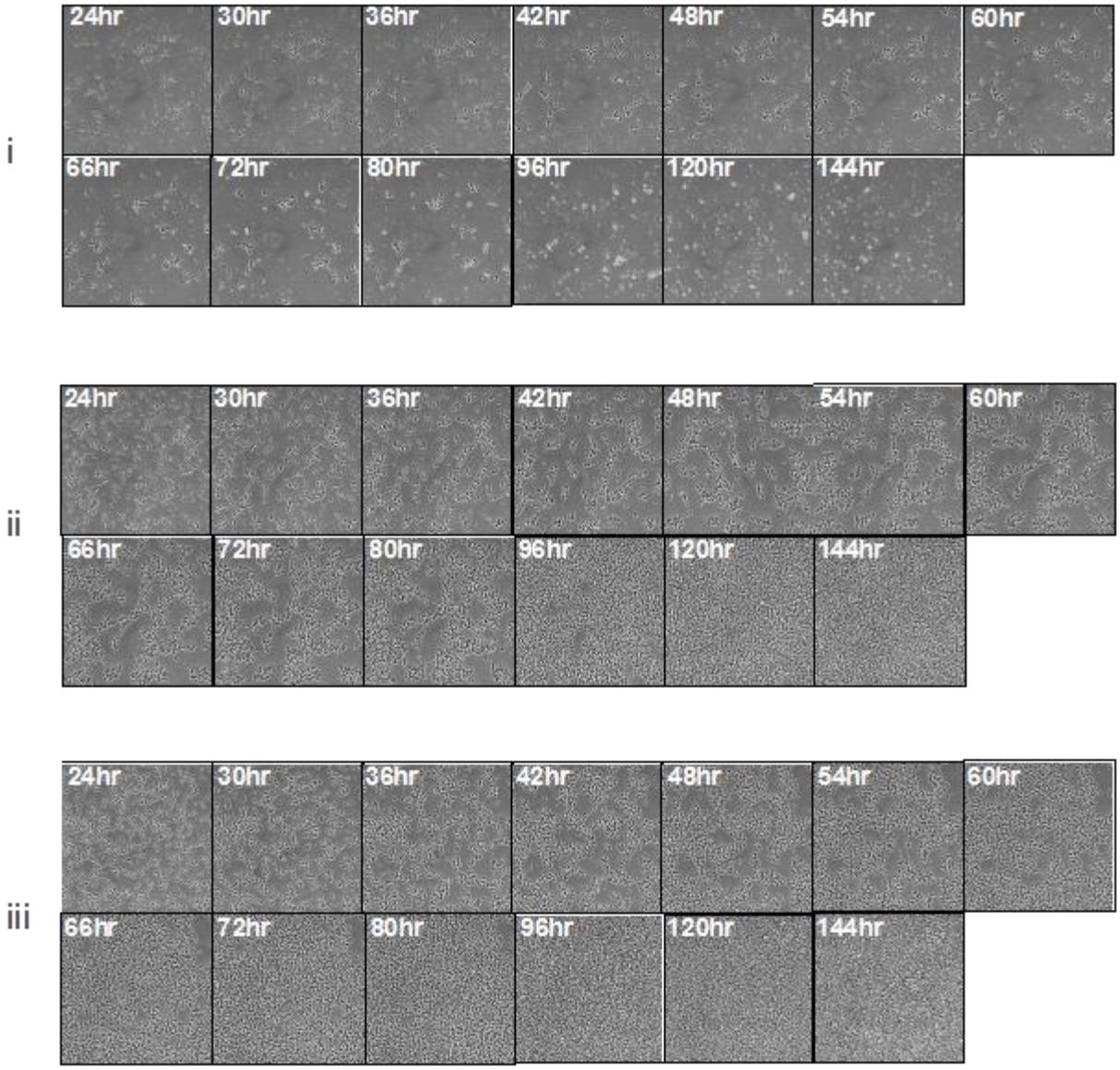

Figure 4.1: SK-N-SH cells do not proliferate on Matrigel in Pluriton medium at sub-optimal densities. SK-N-SH cells were plated down at a density of (i) $5x10^4$, (ii) $1.5x10^5$ or (iii) $2.5x10^5$ in Pluriton medium on Matrigel. The cells were placed in a Biostation CT (Nikon) at 37°C in 5% CO_2 and phase contrast images at co-ordinates (x000000, y000000) were taken every 6 hours for 6 days. The cells succumbed to apoptosis within 4 days at a density of $5x10^4$. Near-confluency was reached at days 4 and 3 at densities of $1.5x10^5$ and $2.5x10^5$ respectively. SK-N-SH cells plated at a density of $5x10^4$ failed to proliferate.

Figure 4.2. Reprogramming SK-N-SH cells using mRNAs from the Allele Biotech iPS induction template set

A

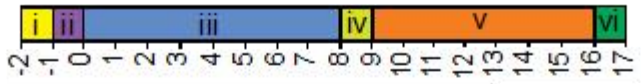

B

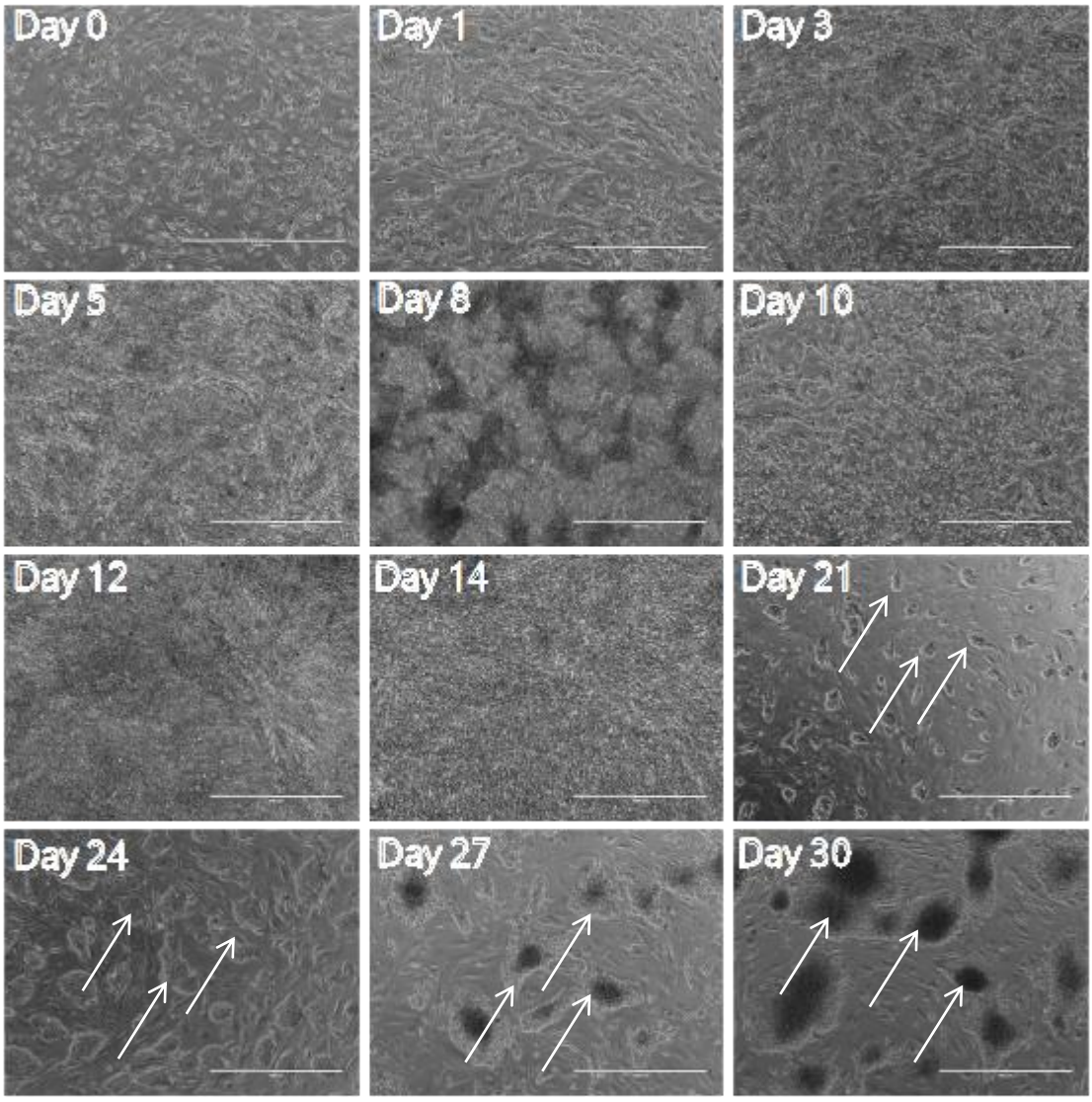

Figure 4.2: (A) SK-N-SH reprogramming timeline using mRNAs derived from the Allele Biotech iPS induction templates (ABP-SC-SEIPSET). (i) Inactivated MEFs were seeded at a density of $1x10^5$ onto a gelatinised 6-well culture plate for 24 hours (ii) SK-N-SH cells were plated onto this at a density of $3.5x10^5$ in hESC media. (iii) mRNAs from the Allele Biotech iPS induction kit (ABP-SC-SEIPSET) encoding *OCT4, SOX2, KLF4, CMYC, LIN28, NANOG* and *mWASABI* were added daily at a dose of 800ng until day 8. (iv) On day 8, the culture became over confluent and was split at a ratio of 1:3 with 0.25% trypsin-EDTA (Sigma) onto a MEF coated 6-well plate in hESC media. (v) On day 9 until day 16, the passaged reprogramming culture was fed with hESC media without the addition of further mRNAs. (vi) On day 16, the cells were sorted for TRA-1-60, and replated onto a MEF feeder layer in hESC medium. (B) Phase contrast images showing iPS cell-like colonies (white arrows). Scale bars = 1000µm

Figure 4.3. Sorting reprogrammed SK-N-SH cultures for cells that express TRA-1-60

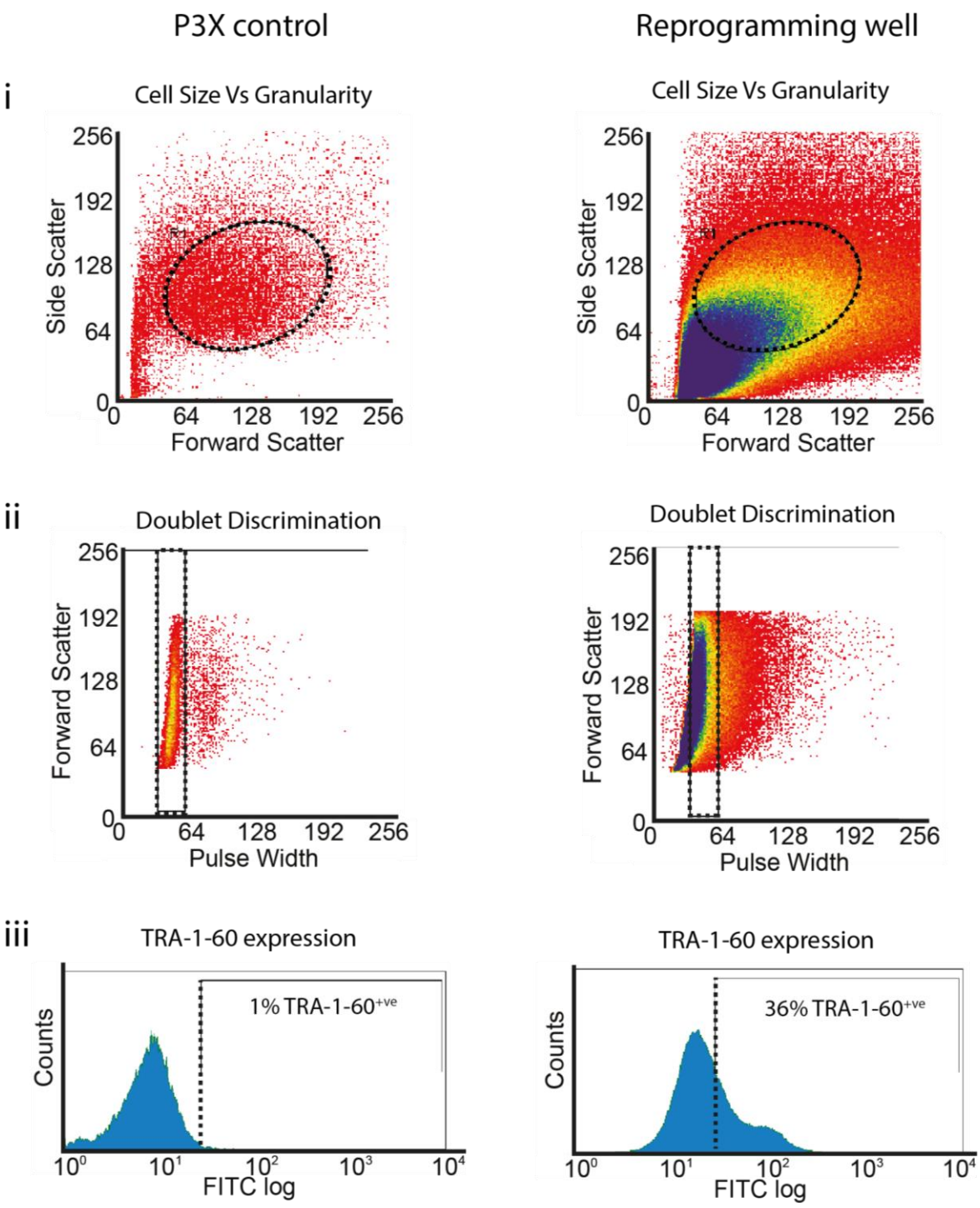

Figure 4.3: Histograms and gate parameters used to sort out a TRA-1-60+ population during SK-N-SH reprogramming. (Left Hand Side, i) A population of viable cells (62%) based on cell size (forward scatter) and granularity (side scatter) were identified in the control well that had been stained with P3X as described in methods 2.15.1.1. (Left Hand Side ii) This population was plotted on a pulse width Vs. forward scatter histogram and gated to remove doublet cells that represented 15% of the gated population. (Left Hand Side iii) This population was finally gated to determine a threshold for positively and negatively labelled cells. (Right Hand Side, i-iii) Once the gates were set on the control well, the SK-N-SH reprogramming well was analysed to determine the number of cells that expressed TRA-1-60. It was found that 36% of the cells were TRA-1-60^{+ve}.

Figure 4.4. Emergent cell populations that express TRA-1-60 following SK-N-SH reprogramming contain sub-populations of GFP^{+ve} and GFP^{-ve} cells

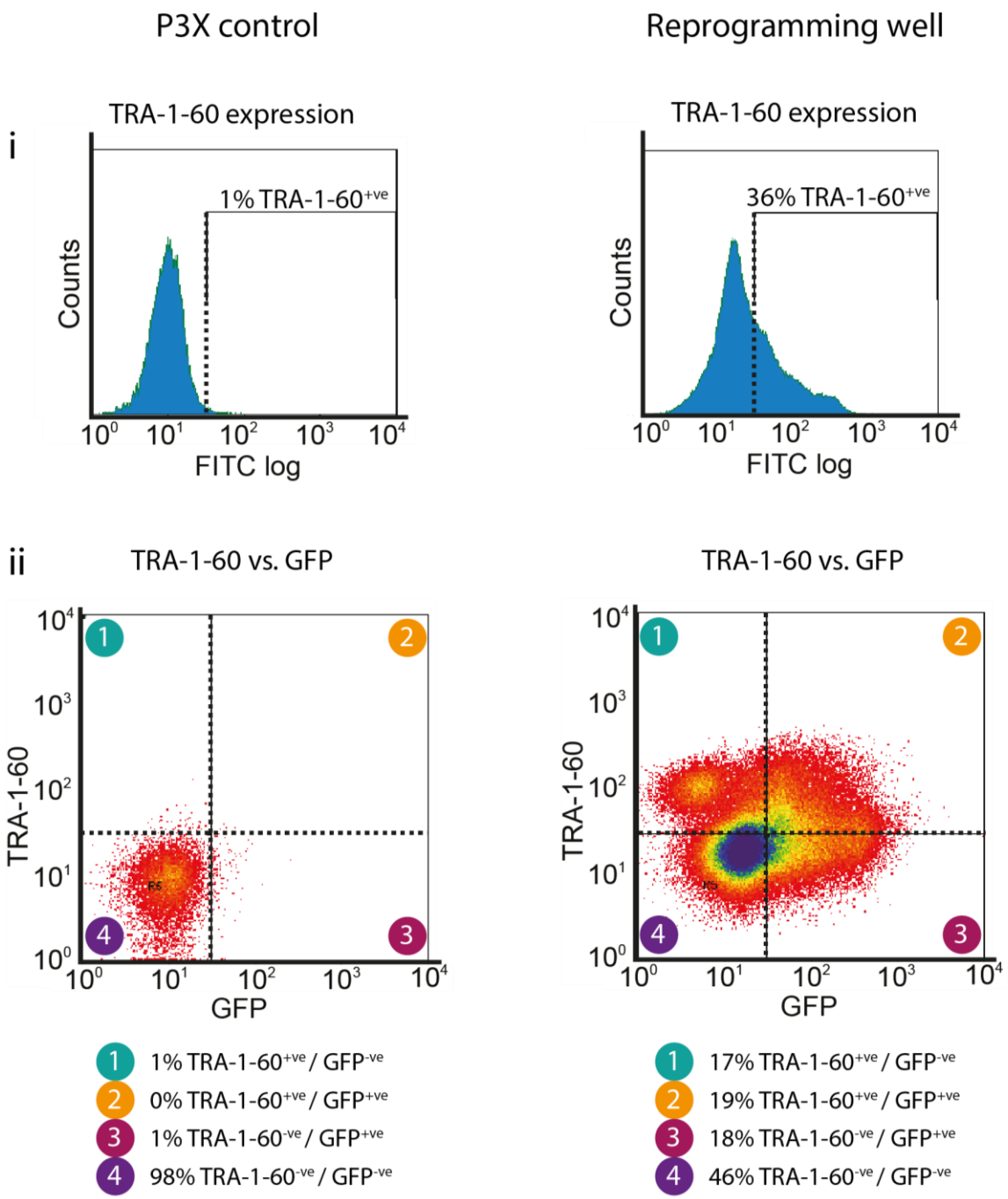

Figure 4.4: Histograms and plots showing sub-populations of mWASABI^{+ve} and mWASABI^{-ve} cells within the TRA-1-60^{+ve} population. (i) One percent of cells in the control well expressed TRA-1-60 compared to 36% in the reprogramming well. (ii) The TRA-1-60^{+ve} population in the reprogramming well was then plotted against cells that expressed mWASABI. mWASABI had been added throughout reprogramming to monitor the efficiency of mRNAs getting into the cells. Cells that were mWASABI^{+ve} were detected through the GFP channel, that detects mWASABI expression. The percentage of cells in the TRA-1-60^{+ve} population in the reprogramming well that also expressed mWASABI was 53%. The control well contained no mWASABI^{+ve}/TRA-1-60^{+ve} cells.

4.2.2. Retinoic Acid treated SK-N-SH cells exhibit perturbed growth that may elongate the transfection phase of reprogramming

When reprogramming SK-N-SH cells, the cell culture became confluent within three days when seeded at a density determined to prevent cells from succumbing to apoptosis (Figure. 4.1). Over confluency could inhibit reprogramming by decreasing the mRNA dose per cell ratio to a level that is insufficient to generate fully reprogrammed iPS cells. In order to generate fully reprogrammed iPS cells we need to decrease the rate that SK-N-SH cells proliferate. Retinoic acid has been shown to induce growth arrest in neuroblastoma cells [173] including the SK-N-SH cell line *in vitro* [174]. We determined the levels of growth arrest that occur in SK-N-SH cells following treatment with varying concentrations of RA.

MRNA-mediated reprogramming of SK-N-SH cells induced 36% of the population to express TRA-1-60 but none of these cells formed a stable iPS cell line. It was found that it is necessary to plate SK-N-SH cells prior to reprogramming at higher cell densities than fibroblasts to prevent cell death (Figure. 4.1) but this resulted in the cells reaching confluency within three days. In order to determine if the proliferative capacity of SK-N-SH cells could be decreased to maintain a more optimal mRNA dose per cell ratio over an extended period of time, the cells were treated with retinoic acid (RA) (Figure. 4.5A). RA was dissolved in DMSO to a working concentration of 10^{-2}M and then further diluted in tenfold decreasing concentrations to 10^{-6} M. These RA working stocks were then added to SK-N-SH cultures at 1:1000 to yield final concentrations between 10^{-5} and 10^{-9}M. The cells were maintained in RA-containing Pluriton medium on Matrigel for seven days, replenishing the media and supplementing fresh RA on days zero and four. The number of viable cells were

counted on day seven and quantified as a percentage of the cell growth achieved in a control well that was treated with 0.1% DMSO (Table 4.1). Growth arrest was inhibited in a concentration dependent manner. In the experiment, 80% growth inhibition of SK-N-SH cells was detected when using a RA concentration of 10^{-5}M.

Figure 4.5. Dose response relationship between Retinoic Acid induction and growth inhibition of SK-N-SH after 7 days

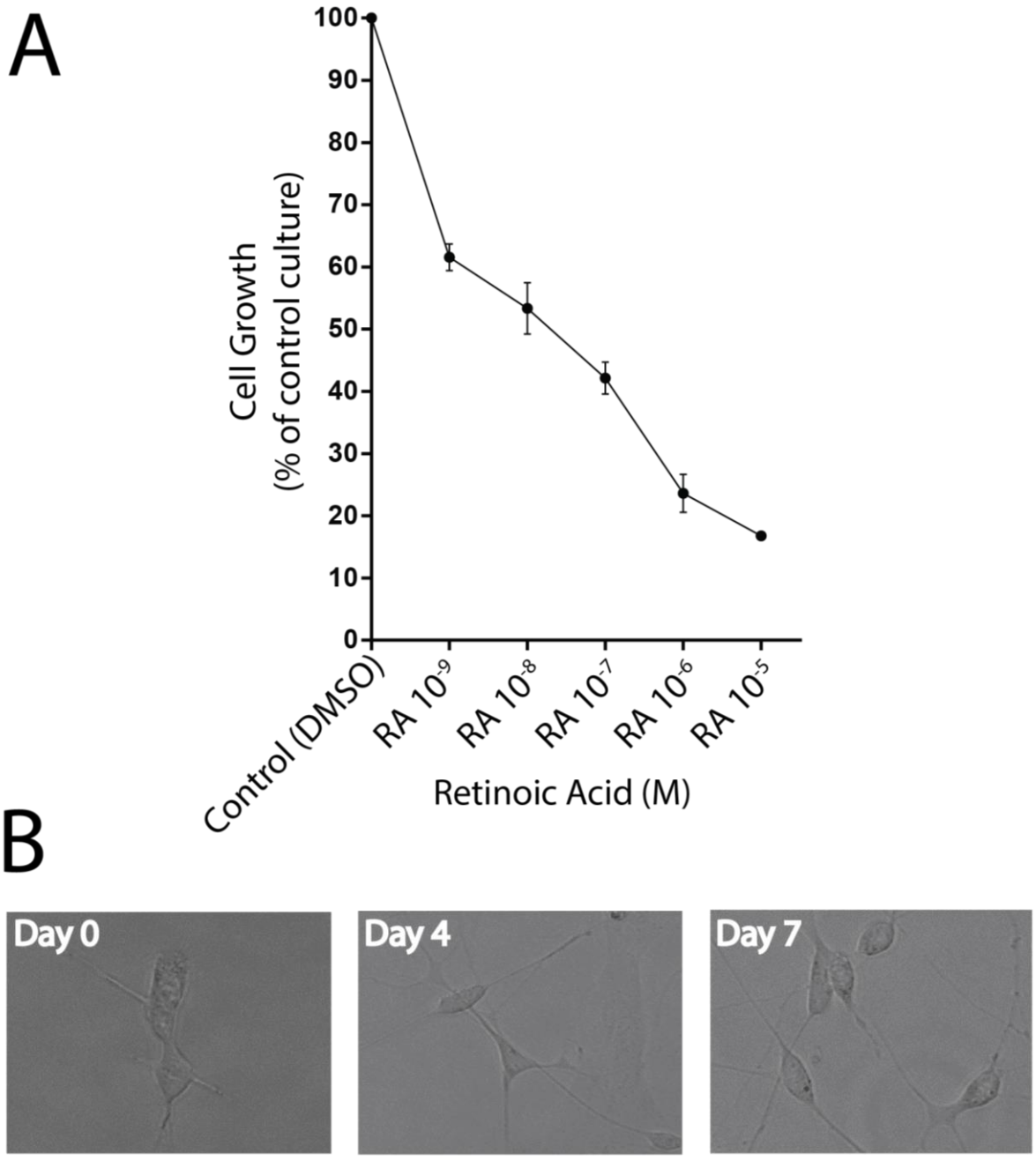

Figure 4.5: Retinoic Acid induces growth arrest and neuronal differentiation in SK-N-SH. (A) Retinoic Acid was dissolved in DMSO to a concentration of 10^{-2} and then diluted in tenfold decreasing concentrations to 10^{-6}. This was then added daily for 7 days at 1:1000 (0.1% vol/vol) to SK-N-SH cells plated at a density of $3.85x10^{4}$ in 2mls of Pluriton media to yield the final range of concentrations 10^{-5} to 10^{-9}. The level of growth arrest is determined by comparing the mean cell counts from 3 biological replicates (shown on the next page), from treated cultures to that of an untreated control. (B) Phase contrast images showing SK-N-SH with neurite-like extensions after treatment with RA. N=3

Table 4.1. Dose response relationship between Retinoic Acid induction and growth inhibition of SK-N-SH after 7 days

Biological Repeat 1

Parameter	Count 1	Count 2	Count 3	Count 4	Average Count	Cells/ml	Total cells	Cell growth (% of control culture)
Control (DMSO 0.1% vol/vol)	39	54	20	27	35	350000	700000	100.0%
RA 10^{-5}	6	5	9	3	6	57500	115000	16.4%
RA 10^{-6}	12	4	12	4	8	80000	160000	22.9%
RA 10^{-7}	23	7	14	14	15	145000	290000	41.4%
RA 10^{-8}	14	17	20	19	18	175000	350000	50.0%
RA 10^{-9}	22	18	20	25	21	212500	425000	60.7%

Biological Repeat 2

Parameter	Count 5	Count 6	Count 7	Count 8	Average Count	Cells/ml	Total cells	Cell growth (% of control culture)
Control (DMSO 0.1% vol/vol)	33	42	29	37	35	352500	705000	100%
RA 10^{-5}	5	7	6	6	6	60000	120000	17%
RA 10^{-6}	7	8	9	6	8	75000	150000	21%
RA 10^{-7}	19	15	14	13	14	140000	280000	40%
RA 10^{-8}	18	19	23	14	19	185000	370000	52%
RA 10^{-9}	24	19	21	20	21	210000	420000	60%

Biological Repeat 3

Parameter	Count 9	Count 10	Count 11	Count 12	Average Count	Cells/ml	Total cells	Cell growth (% of control culture)
Control (DMSO 0.1% vol/vol)	25	35	31	41	33	330000	660000	100%
RA 10^{-5}	4	7	5	6	6	55000	110000	17%
RA 10^{-6}	10	8	7	10	9	87500	175000	27%
RA 10^{-7}	17	9	16	18	15	150000	300000	45%
RA 10^{-8}	18	21	18	19	19	190000	380000	58%
RA 10^{-9}	19	24	20	22	21	212500	425000	64%

Average of three biological repeats

Parameter	Average Count	Cells/ml	Total cells	Cell growth (% of control culture)
Control (DMSO 0.1% vol/vol)	34	344167	688333	100.0%
RA 10^{-5}	6	57500	115000	16.7%
RA 10^{-6}	8	80833	161667	23.5%
RA 10^{-7}	15	145000	290000	42.1%
RA 10^{-8}	18	183333	366667	53.3%
RA 10^{-9}	21	211667	423333	61.5%

Table 4.1: SK-N-SH cells treated with retinoic acid for 7 days were counted (as described in methods 2.11) and compared to a control sample that had been treated with DMSO 0.1% vol/vol. It was found that the population of SK-N-SH cells that had been treated with the highest dose of RA (10^{-2}) contained the fewest amount of cells after 7 days. RA treatment inhibits cell proliferation in a dose dependent manner. N=3.

4.2.3. Reprogramming SK-N-SH cells following treatment with Retinoic Acid

We found that growth inhibition of SK-N-SH cells can be induced by 80% following treatment with 10^{-5}M RA. If we treated SK-N-SH cells with RA prior to reprogramming, could this reduce the rate that SK-N-SH cells proliferate and thus increase the number of times that mRNA could be added to the cells before the culture became confluent, so that fully reprogrammed iPS cells can be generated?

To test this hypothesis, SK-N-SH cells were plated at a density of $1.5x10^5$ onto Matrigel in Pluriton (Figure. 4.6Bi). The cells were treated for four days prior to reprogramming-day zero with 10^{-5}M RA. In this reprogramming attempt, we decided to use the 6-factor reprogramming premix (ABP-SC-6FMRNA), instead of mRNAs derived from Allele Biotech IVT templates (ABP-SC-SEIPSET). This was based on the finding that the 6-factor premix (ABP-SC-6FMRNA) generated iPS cells from BJ fibroblasts more efficiently in that a splitting step was not required and iPS cells were generated with accelerated kinetics (Figure. 3.17 and 3.18). The addition of 800ng 6-factor premix mRNA (ABP-SC-6FMRNA) at a final concentration of 400ng/ml was performed between days zero to six and eleven to fourteen with a decreased concentration of 200ng/ml used between days seven to ten in response to cytotoxicity. Cytotoxicity was further alleviated through the addition of $1.5x10^5$ MEFs on day seven and by increasing the B18R concentration to 400ng/ml from 200ng/ml on days six and nine. In addition, 100ng *mWASABI* mRNA was periodically added to the reprogramming culture to verify that the exogenous mRNA was being successfully taken up by the cells. By day 15, the target well could be separated into regions that expressed distinctly different levels of confluency (Figure. 4.6Bii). For example some areas were densely compacted in multiple layers, others were absent

of cells and some regions represented clusters of cells in a single layer. Morphological transformations could be observed on the periphery of clusters of cells that were centrally located. These cells appeared to look more epithelial than neuronal (Figure. 4.6Biii) and may be indicative of an initial phase in reprogramming but their incidence was rare. The culture was sorted for TRA-1-60^{+ve} / *mWASABI*$^{-ve}$ cells to isolate any fully reprogrammed iPS cells however no cells were found within these parameters. The cells were then re-plated onto MEFs in hESC medium and cultured for ten days to encourage iPS cell outgrowths. No iPS cell colonies were seen to emerge, so the 6-factor premix mRNA (ABP-SC-6FMRNA) was repeatedly added to the cells at a dose of 800ng (400ng/ml) for a further 18 days. On day 43, the reprogramming was terminated since there was a lack of emergent colonies and cell death was ubiquitously prevalent (Figure. 4.6Ci and ii).

Figure 4.6. Reprogramming SK-N-SH cells using the Allele Biotech 6-factor reprogramming premix

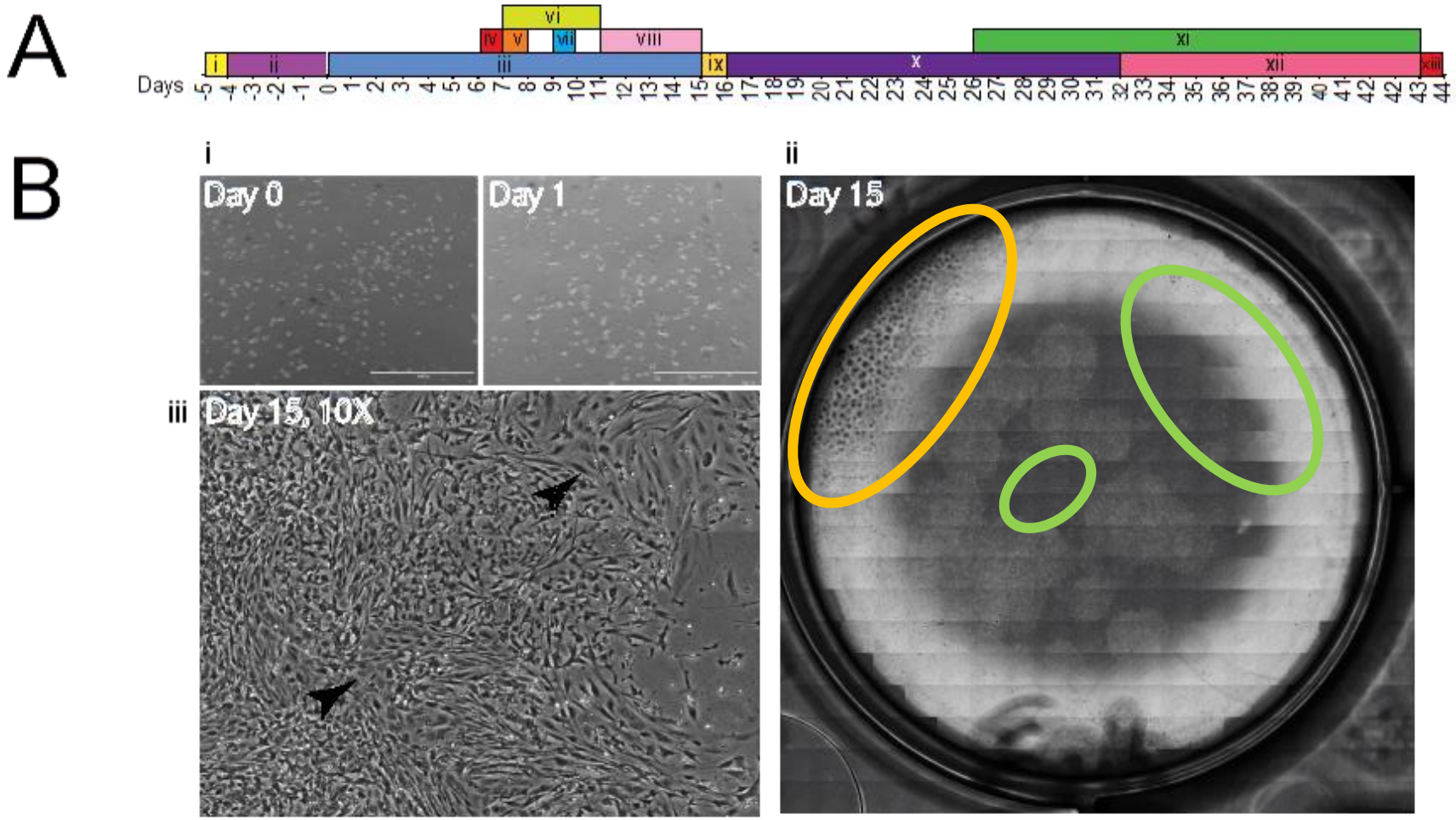

Figure 4.6: (A) Timeline schematic for SK-N-SH reprogramming. (i) SK-N-SH cells were seeded at a density of $1.5x10^5$ onto Matrigel-coated 6-well culture plates in Pluriton medium. (ii) Retinoic acid (10^{-2}) was added at 0.1% vol/vol on day -4 for four days then (iii) on day 0 the cells were transfected with 800ng Allele Biotech 6-factor premix mRNA (ABP-SC-6FMRNA) in 2ml Pluriton until day 7. (viii) As the cells restored health, the mRNA was subsequently increased to 400ng/ml. (ix) The cells were sorted for TRA-1-60 on day 15 but none were positive. (x) The cells were replated in to hESC medium to encourage the emergence of iPS cell colonies. (xi) Repeated daily addition of 400ng/ml mRNA recommenced on day 26 until day 43 and (xii) the media was switched back to Pluriton. (xiii) Cytotoxicity was prevalent and the reprogramming was terminated on day 43. (B) Phase contrast images during reprogramming depict (i) RA-treated SK-N-SH cells on days 0 and 1 of reprogramming and (ii) areas of overgrowth (orange circle) and death (green circles) on day 15. (iii) A 10X magnification at day 15 showing areas of morphological transformation (black arrowheads).

Figure 4.6. Reprogramming SK-N-SH cells using the Allele Biotech 6-factor reprogramming premix

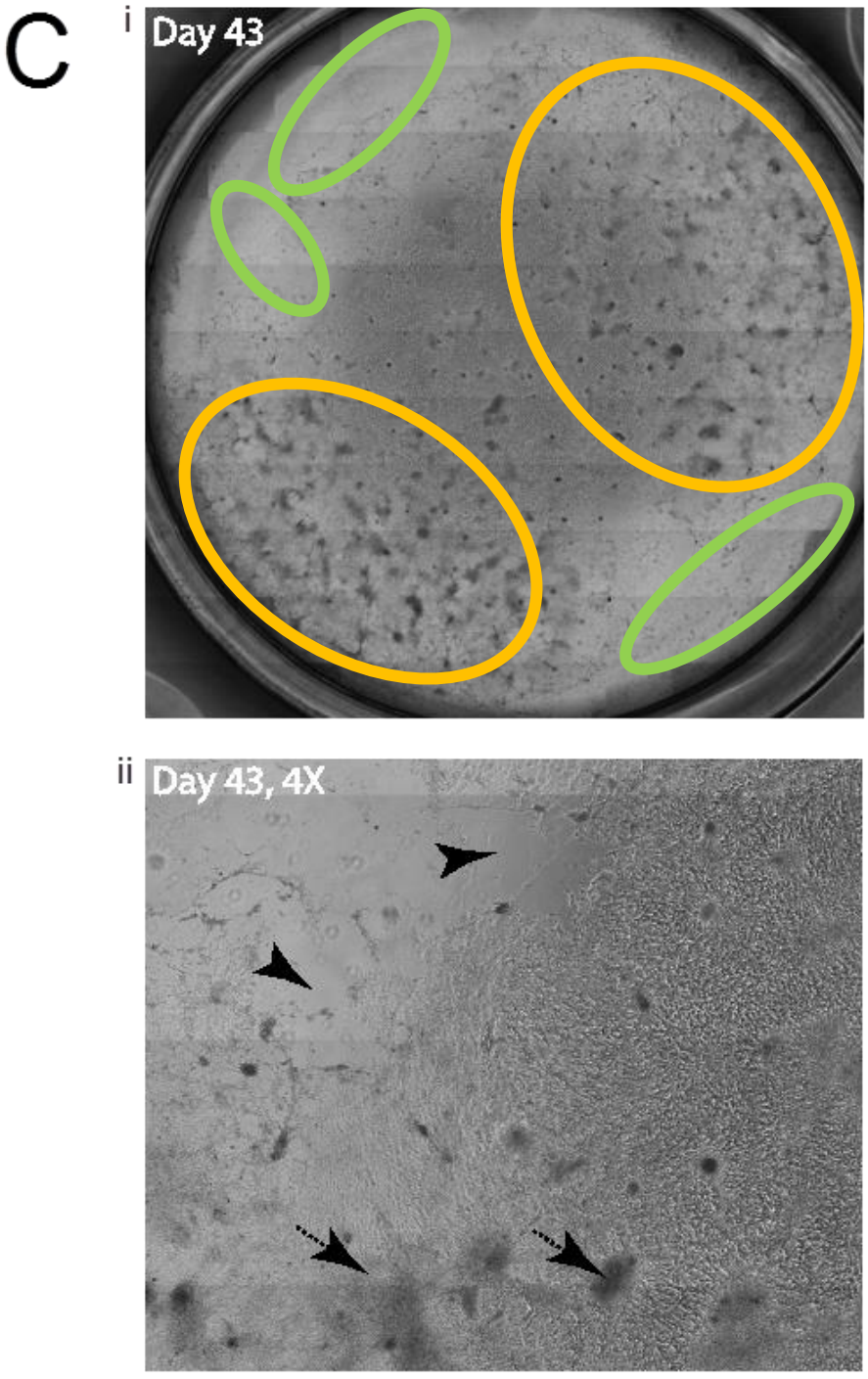

Figure 4.6: (C) On day 43 of the SK-N-SH reprogramming using the Allele Biotech 6-factor premix mRNA (ABP-SC-6FMRNA), (i) a stitched whole-well image captured on a Biostation CT (Nikon) shows large areas of cell death (green circles) and overgrowth (orange circles). (ii) An enlarged section of the stitched image showing areas of cytotoxicity (black arrowheads) and areas of differentiation (arrows).

4.2.4. SK-N-SH cells are less tolerant to the conditions of mRNA reprogramming compared to BJ fibroblasts

Treating SK-N-SH cells with retinoic acid prior to reprogramming induced growth arrest sufficient to increase the number of days that mRNA could be added prior to the cells reaching confluency. However, the cells succumbed to apoptosis that may have been caused by an overdose of the 6-factor premix mRNA (ABP-SC-6FMRNA). When reprogramming BJ fibroblasts, mRNA dose ramping improved the survivability of cells by providing greater control over the mRNA dose per cell ratio. We tested whether the optimised mRNA dose-ramping protocol (Figure. 3.17D) improved the survivability of SK-N-SH cells during reprogramming, sufficient to generate fully reprogrammed iPS cells.

On day minus one of the reprogramming protocol, SK-N-SH cells were plated on to hESC-qualified Matrigel at a density of $1.5x10^5$ in Pluriton medium. On day zero, the 6-factor premix mRNA (ABP-SC-6FMRNA) was then added to the cells at a dose of 200ng to a final concentration of 400ng/ml in 0.5ml Pluriton medium. MRNA dose ramping was implemented thereafter whereby the 6-factor premix mRNA (ABP-SC-6FMRNA) was added to the cells at a dose that was determined by comparing an estimate of the number of cells in the culture from one day to the next. To prevent evaporation of the medium, a further 0.5ml of Pluriton medium was added four hours after the addition of mRNA. The Pluriton medium used throughout the reprogramming was supplemented with 300ng/ml B18R. Twenty four hours after the first addition of the 6-factor reprogramming premix mRNA (ABP-SC-6FMRNA) the cells had proliferated yet showed early signs of toxicity (Figure. 4.7B) therefore the mRNA dose on day one was kept to 200ng. This was in contrast to when 200ng

of *mWASABI* mRNA was added to the reprogramming control in parallel that showed no signs of toxicity (Figure. 4.7C). On day 2 of reprogramming, the cell density was judged to be less than that observed 24 hours prior therefore the mRNA dose was not increased and instead, $5x10^4$ inactivated MEFs were added as a supportive measure. MRNA transfections were ceased on day four on the finding that ~95% of the cells had died. The cells were maintained in Pluriton medium until day eight and further supplemented with $1x10^5$ MEFs however the extent of toxicity obligated the termination of reprogramming.

We found that SK-N-SH cells succumbed to apoptosis during reprogramming following the addition of the 6-factor premix mRNA (ABP-SC-6FMRNA) but not when *mWASABI* mRNA was added at an identical dose to a control well in parallel. We determined whether cell death is dependent upon the dose of mRNA added to the cells and whether this could be exacerbated by increasing the dose of mRNA. To test this, we treated SK-N-SH cells with an increasing dose of *mWASABI* mRNA between 1µg and 5µg for 24 hours. SK-N-SH cells were seeded at a density of $1.5x10^5$ in Pluriton medium and a dose between 1µg and 5µg of *mWASABI* mRNA was added to the cells for 24 hours. After 24 hours, fluorescing cells were imaged using an EVOS FL Cell Imaging System and then analysed by flow cytometry on a CyAn ADP Analyser. Fluorescence levels were detected on the GFP channel at a wavelength of 488nm and gating using the P3X antibody was performed as described in methods 2.15.1.1. The cells were simultaneously stained with propidium iodide to detect the number of dead cells relative to an untreated SK-N-SH control. It was found that a dose of 1µg *mWASABI* mRNA induced cell death in 15% of the cells, suggesting that the widespread cell death induced during reprogramming of SK-N-SH cells (Figure. 4.7B) is not due to the mRNA dose but more likely due to a specific mRNA.

Figure 4.7. Adding a low (200ng) daily dose of 6-factor premix mRNA to SK-N-SH cells during reprogramming induces apoptosis

A

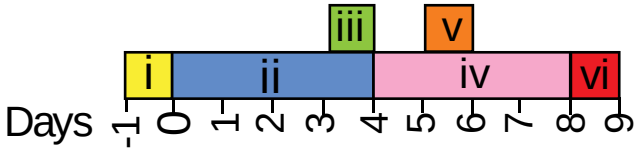

B

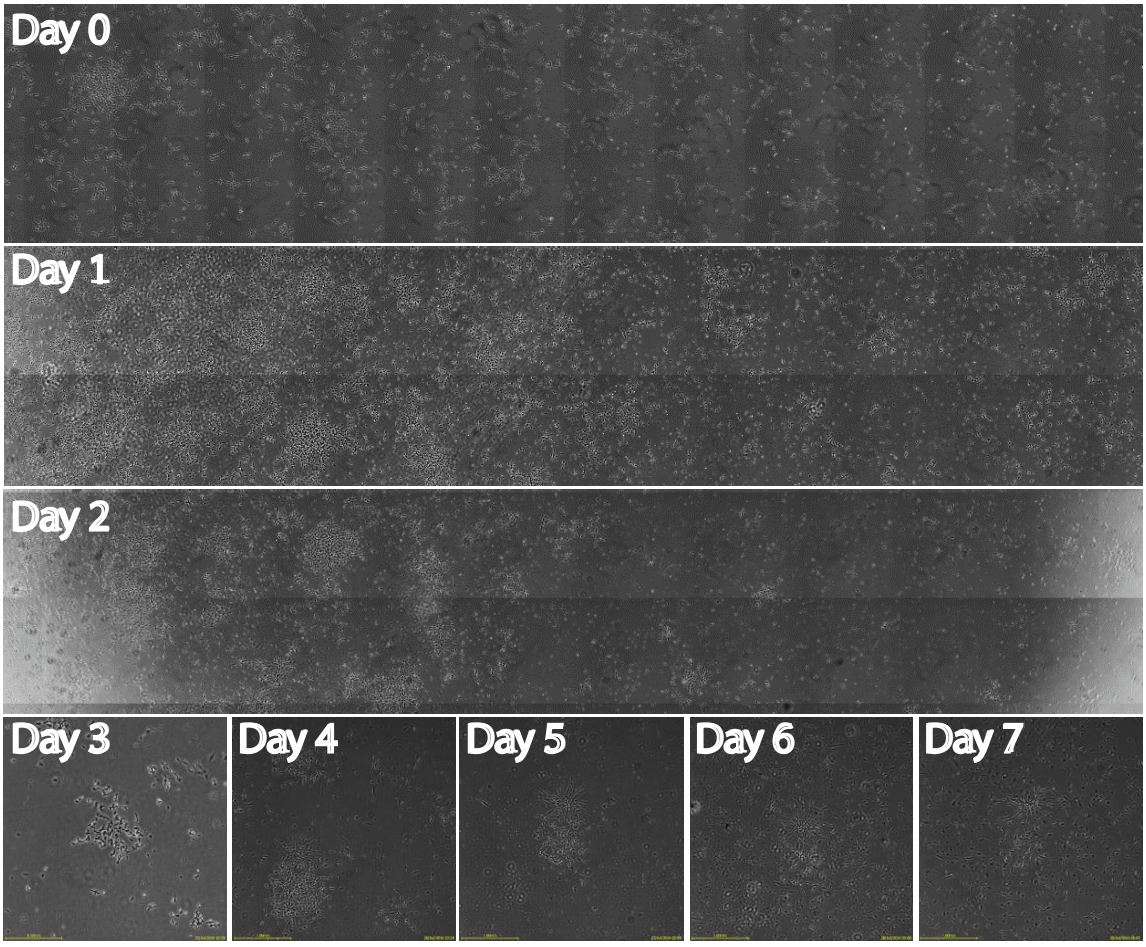

Figure 4.7: (A) SK-N-SH reprogramming timeline using the Allele Biotech 6-factor premix mRNA (ABP-SC-6FMRNA). (i) SK-N-SH cells were plated at a density of $1.5x10^5$ onto Matrigel-coated 6-well culture plates. (ii) Between days 0 and 4, 200ng mRNA was added to 1ml low-oxygen (5% O_2) equilibrated Pluriton medium containing 300ng/ml B18R. Inactivated MEFs at a density of $5x10^5$ and $1x10^5$ were added on (iii) day 3 and (v) day 9 respectively. (iv) On day 4, the addition of mRNA was stopped on the observation that cells had begun to die however the Pluriton medium was continually replenished daily until day 8. (vi) The reprogramming was terminated on day 8 due to severe cytotoxicity. (B) Phase contrast images taken on the Biostation CT (Nikon) showing the onset of apoptosis between day 0 and 7.

Figure 4.7. Adding a low (200ng) daily dose of 6-factor premix mRNA to SK-N-SH cells during reprogramming induces apoptosis

C

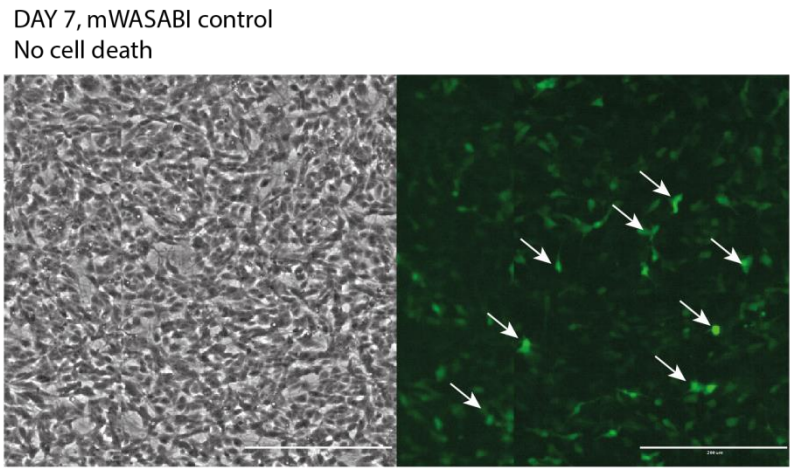

D

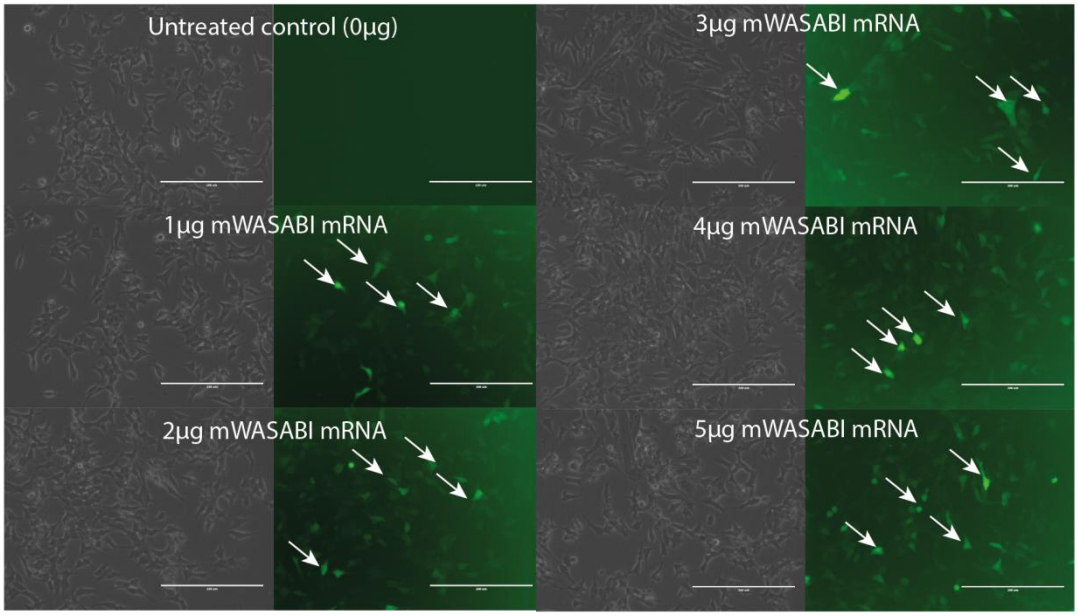

mRNA dose	mWASABI fluorescence levels (%)	Dead cells (%)
0µg	3.91	2.16
1µg	88.78	15.27
2µg	94.67	19.65
3µg	87.71	18.12
4µg	94.95	28.41
5µg	87.52	30.8

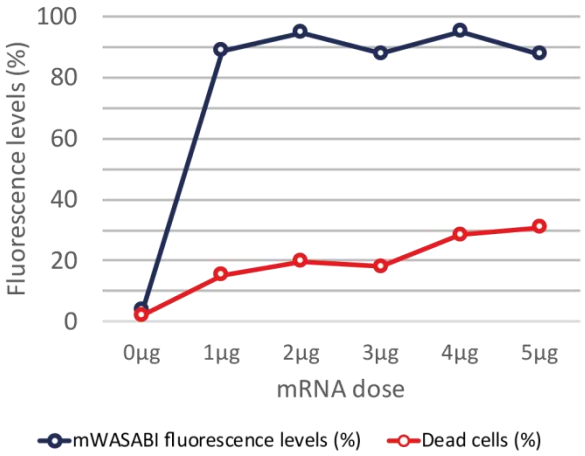

Figure 4.7: (C) *mWASABI* mRNA was added to a control well containing $1.5x10^5$ SK-N-SH cells during reprogramming to monitor the uptake of mRNAs. After 7 days, SK-N-SH cells can be seen fluorescing (white arrows) and no cell death was observed. (D) SK-N-SH cells were treated with 1-5µg of mWASABI mRNA for 24 hours to test whether the cells would succumb to apoptosis. After 24 hours, the cells were analysed by flow cytometry to detect the number of cells that were positively fluorescing mWASABI and were simultaneously stained with Propidium Iodide (ThermoFisher, P3566) to detect the number of dead cells relative to an untreated control. A dose of 1µg mWASABI mRNA induced cell death in 15% of the cells that gradually rose to 30% at a dose of 5µg. Scale bars = 200µm

A second reprogramming was initiated under the same conditions as the previous reprogramming attempt (Figure. 4.7) albeit SK-N-SH cells were plated at an increased density of $2.5x10^5$ (Figure. 4.8). It appeared that SK-N-SH cell death was less prevalent when reprogramming of SK-N-SH cells was conducted using the higher plating density of $2.5x10^5$ cells. An mRNA dose of 200ng 6-factor premix mRNA (ABP-SC-6FMRNA) was added on days zero and one. This was increased to 300ng on day two upon the observation that the cells were continuing to proliferate despite the repeated addition of mRNA. This dosage (300ng) was added daily and stopped on day 12, as there was no observed incidence of morphological transformations that suggest reprogramming was taking place(Figure. 4.8Bi), such as the compaction of cells, that had been previously found during SK-N-SH cell reprogramming (Figure. 4.2B). Cytotoxicity was observed on the periphery of cell clusters (Figure. 4.8B, white arrows) and was mitigated against by the addition of $2x10^5$ MEFs on day 2 and 4. On day eleven, the reprogramming culture was analysed by in-situ live-cell staining (methods 2.15.2) for TRA-1-60 however it was found that no cells were positive for TRA-1-60 (Figure. 4.8Bii) suggesting that the cells were not transitioning toward pluripotency.

Figure 4.8. Plating SK-N-SH cells at high densities ($2.5x10^5$) prior to reprogramming, promotes cell survival

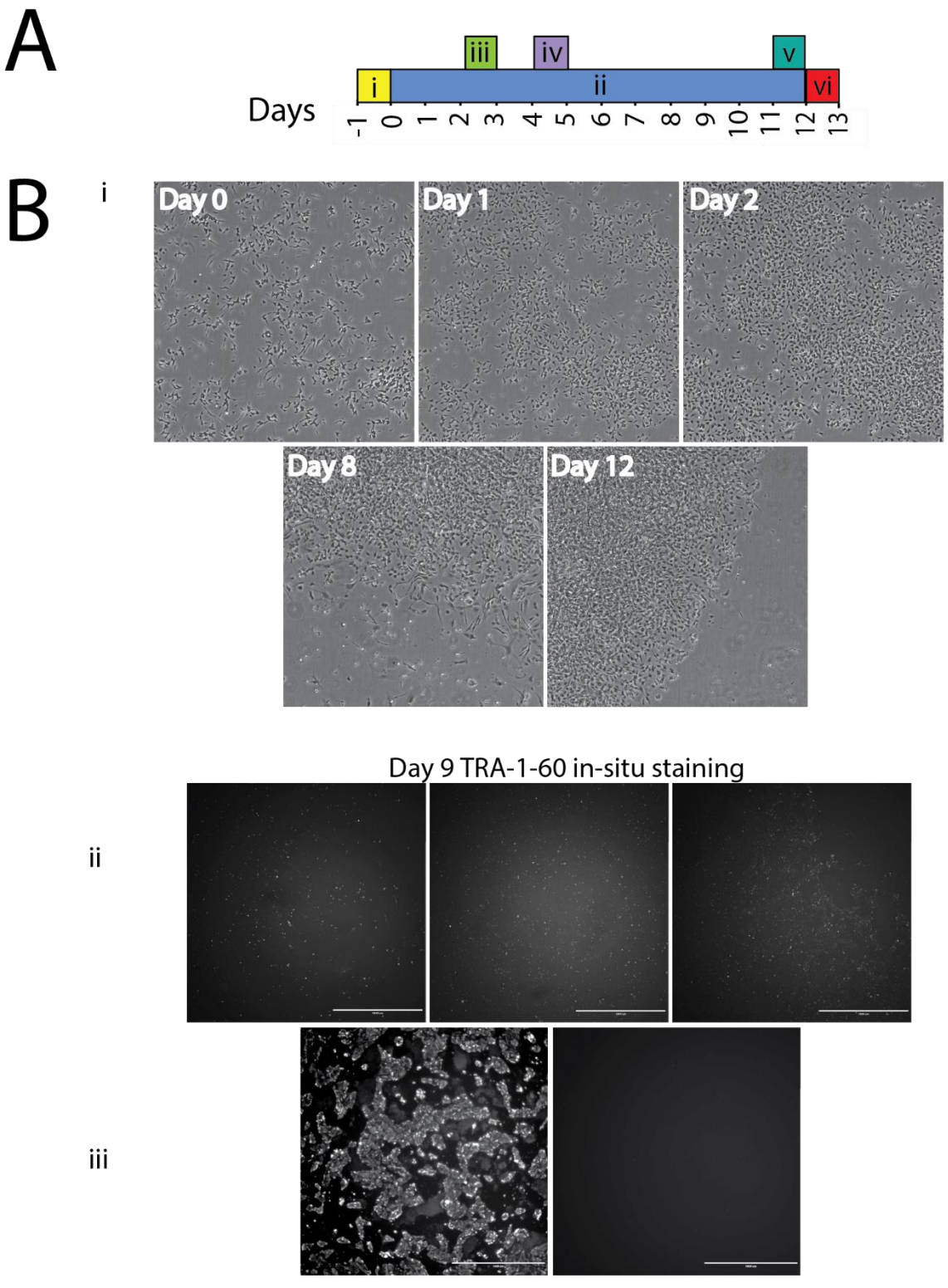

Figure 4.8: (A) SK-N-SH reprogramming using 6f premix mRNA. (i) $2.5x10^5$ SK-N-SH cells were plated onto Matrigel-coated 6-well culture plates and (ii) transfected in Pluriton containing 300ng/ml B18R with 200ng mRNA on days 0 and 1 and 300ng on days 2 to 11. MEFs were added at $2x10^5$ on (iii) day 2 and (iv) day 4. (v) Live-cell in-situ TRA-1-60 staining was performed revealing no positive colonies for TRA-1-60. (vi) Reprogramming was terminated on day 12. (B) Brightfield images depicting (i) areas of variable cell densities. (ii) Live-cell staining for TRA-1-60 reveals no emerging colonies, (iii) NT2 cell control positively fluorescing TRA-1-60 (left hand side) and NT2 negative control analysed for secondary antibody binding only. Scale Bars = 1000µm.

4.2.5. SK-N-SH cells downregulate endogenous cMYC following the addition of mRNA

One of the limiting factors to reprogramming SK-N-SH cells is that they respond poorly to the addition of mRNAs (Figures. 4.7, 4.8 and 4.9) and the culture conditions (Figure. 4.1) proven to successfully reprogramme BJ fibroblasts. However, SK-N-SH cells do not succumb to apoptosis when *mWASABI* mRNA is added to the cells (Figure. 4.7C & D). Therefore, we tested whether the toxicity that is induced in SK-N-SH cells during reprogramming is due to a specific mRNA.

During SK-N-SH cell reprogramming, *mWASABI* mRNA derived from the Allele Biotech iPS induction template (ABP-FP-SEMWASABI) is added to an SK-N-SH control well in parallel at the same dose that the mRNA cocktail, containing *OCT4/M_3O*, *SOX2, KLF4, cMYC, LIN28* and *NANOG* mRNA, is added to the main reprogramming well. In all of the SK-N-SH reprogrammings performed, none of the control wells treated with *mWASABI* mRNA succumbed to apoptosis. This suggests that it was not the mRNA dose that resulted in cell death of SK-N-SH cells during reprogramming but more likely a specific mRNA-induced toxicity. In order to determine whether this was the case, each individual mRNA factor that amasses to make up the reprogramming cocktail (*OCT4*, *SOX2, KLF4, cMYC, LIN28* and *NANOG*) was added separately into SK-N-SH cells. The dose of each factor added to the cells was 100ng with the exception of *OCT4* that was added at a dose of 300ng that corresponds to the mRNA dosage used during reprogramming. SK-N-SH cells were seeded onto Matrigel coated plates in Pluriton at a density of $1x10^5$ in 5% O_2 at 37°C. Individual mRNAs encoding one of the six factors (*OCT4*, *SOX2, KLF4, cMYC, LIN28* and *NANOG*) from the iPS induction kit were added daily to the SK-N-SH cells for seven days to a

final concentration of 100ng/ml or 300ng/ml for *OCT4*. It was found that minimal cell death had resulted from the addition of each factor independently into SK-N-SH cells over a seven day period.

Upon finding that the addition of each independent factor did not induce cell death in SK-N-SH cells after 24 hours, further addition of mRNA was performed daily over a seven day period to determine whether each individual factor had an effect on the expression of any of the other factors. This was investigated to see whether the addition of one exogenous factor can affect the mRNA levels of another factor postulating that the SK-N-SH cell death may be attributable to a cumulative effect between multiple factors. To assess this, the SK-N-SH cells that had been treated with mRNA for 24 hours were treated under the same conditions for a further 6 days and then analysed by qPCR (Figure. 4.9) to detect *OCT4, SOX2, KLF4, cMYC, LIN28* and *NANOG* mRNA levels. QPCR analysis showed that the addition of *OCT4, SOX2, KLF4, LIN28* and *NANOG* mRNA in to SK-N-SH cells, increased mRNA levels for none of the factors other than their own with the exception of *cMYC*. Interestingly, *cMYC* mRNA levels decreased 3-fold comparable to endogenous levels of *cMYC* in SK-N-SH cells following the independent addition of each of the six factors.

Figure 4.9. QPCR analysis following the addition of individual mRNAs in to SK-N-SH cells to determine a possible cause for cytotoxicity

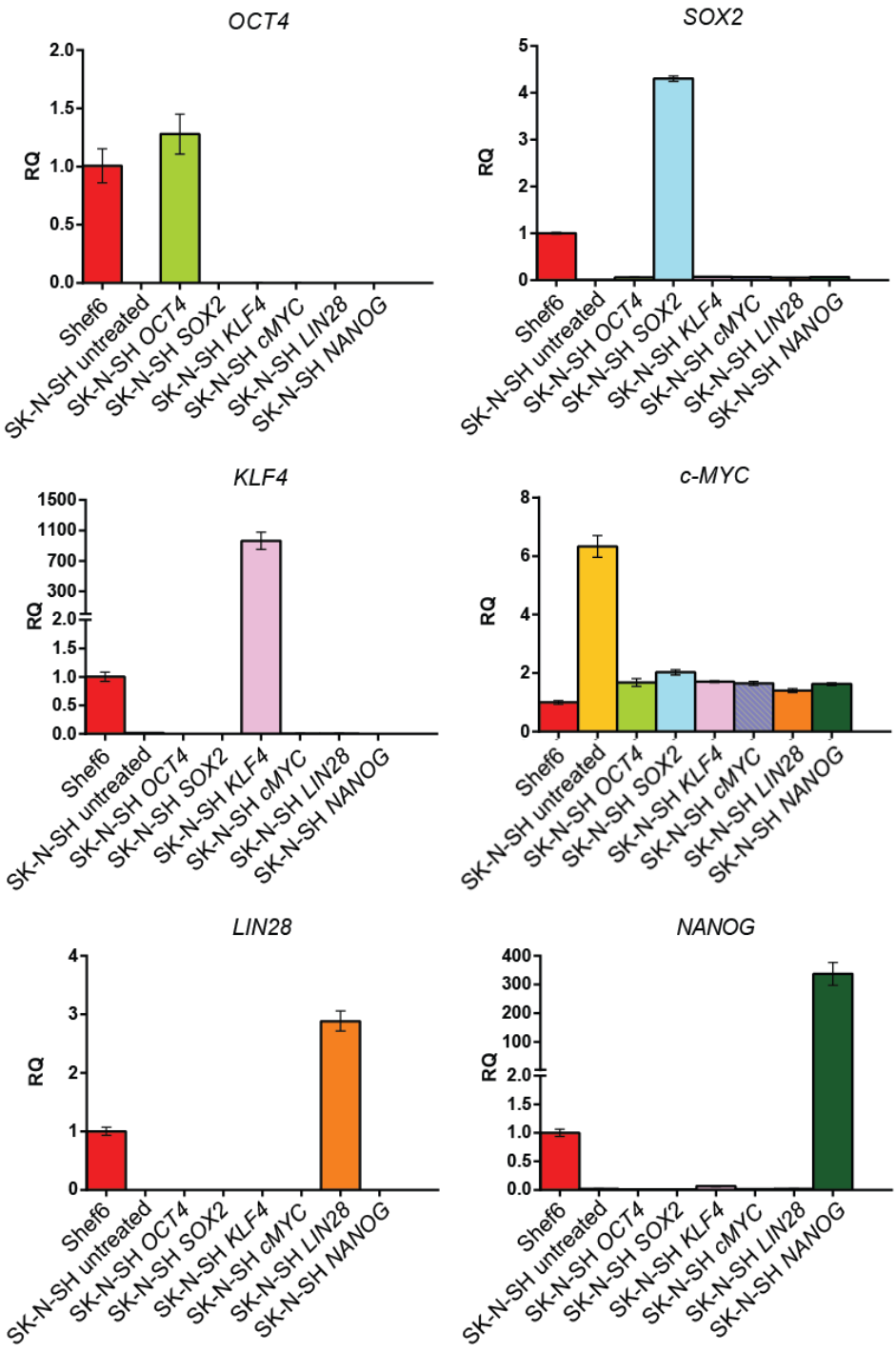

Figure 4.9: mRNAs encoding *OCT4, SOX2, KLF4, CMYC, LIN28* and *NANOG* derived from the Allele Biotech iPS induction templates (ABP-SC-SEIPSET) were added individually at a concentration of 100ng/ml (300ng/ml for *OCT4*) into SK-N-SH cells to verify the uptake of mRNA into the cells and to test whether mRNA levels for other reprogramming factors are affected. If one mRNA leads to the upregulation of another, this may lead to mRNA-induced cytotoxicity that inhibits reprogramming. SK-N-SH cells were seeded on Matrigel-coated 6-well culture plates at a density of $1x10^5$ in 5% O2 at 37°C. A dose of 100ng mRNA encoding the aforementioned factors was added daily into the cells for 6 days into 1ml of Pluriton medium. The cells were analysed by qPCR on day 7. It was found that mRNAs added to SK-N-SH cells were successfully taken up with the exception of *cMYC*. SK-N-SH cells endogenously express *cMYC* however adding mRNA, encoding any of the reprogramming factors, reduced the *cMYC* mRNA levels in SK-N-SH cells ~3-fold. CT values were normalised to *GAPDH*. N=1 (error bars derived from technical triplicates).

4.2.6. Characterisation of iPS cells derived from the SK-N-SH cell line using the Sendai virus.

Despite failing to create neuroblastoma-derived iPS cells using mRNA we were able to obtain, from our collaborators at the Karolinska Institutet, an iPS cell line (named SeViPS-NB2) that had been reprogrammed from SK-N-SH cells by overexpressing *OCT4, SOX2, KLF4* and *CMYC* using non-integrating Sendai viral vectors. We determined the extent to which the SeViPS-NB2 cells resembled undifferentiated pluripotent stem cells and assessed, via embryoid body formation in defined conditions, whether genotypic differences affected their ability to differentiate.

The SeViPS-NB2 cell line was generated using the Cytotune kit (Invitrogen) as per the manufacturer's instructions. The Cytotune kit was used by the Karolinska Institutet to also reprogram fibroblasts yielding a reprogramming efficiency of ~0.1%. The efficiency of the SK-N-SH reprogramming is not known but it is believed to be less than 0.1%. Upon receiving the SeViPS-NB2 cell line we performed an initial characterisation to establish the extent to which they resembled undifferentiated human pluripotent stem cells. Characterisation of the SeViPS-NB2 cell line included analysis through qPCR, flow cytometry and karyotyping. In addition, the differentiation capacity of the cells was assessed *in vitro* by inducing the cells to differentiate as embryoid bodies in defined conditions that differentiate cells toward the three germ layers: endoderm, mesoderm and ectoderm (Table 2.4).

The SeViPS-NB2 cell line was analysed by qPCR (Figure. 4.10) to determine the mRNA levels of *OCT4, SOX2, KLF4, cMYC, LIN28* and *NANOG* in the cells compared to

the parental SK-N-SH cell line and to an undifferentiated hESC control line, Shef6. We found that the SeViPS-NB2 cell line exhibited mRNA levels of the aforementioned genes that more closely resembled undifferentiated hESCs than SK-N-SH cells.

The SeViPS-NB2 cell line was then analysed by flow cytometry to determine the percentage of cells that expressed, SSEA-1, SSEA-3, SSEA-4, TRA-1-60 and TRA-1-81 compared to SK-N-SH and NT2 D1 cell lines (Figure. 4.11). We found that SeViPS-NB2 and NT2 D1 cells expressed the cell surface markers at similar levels. Comparatively SK-N-SH cells had high SSEA-1 expression but did not express the other cell-surface markers analysed.

The SeViPS-NB2 cell line was karyotyped to check for chromosomal abnormalities and to compare metaphase spreads between the parental SK-N-SH cells and the SKiPS cell line (Figure. 4.12) that is an iPS cell line reprogrammed from SK-N-SH cells using lentivirus. It was found that SK-N-SH cells exhibited a gain of whole chromosome 7, deletion on the short arm of chromosome 14 between q13 and q22 and translocations from 2p21 to 9q34 and 17q21 to 22q13. In contrast, the SeViPS-NB2 cell line exhibited a gain of whole chromosome 12 and loss of trisomy 7 while the SKiPS cell line maintained trisomy 7 but gained a whole chromosome 1 and lost whole chromosomes 3, 13 and 15.

The differentiation capacity of SeViPS-NB2 was assessed by inducing the cells to differentiate as embryoid bodies (Figure. 4.13) for ten days in defined conditions as described in Table 2.4. The embryoid bodies were harvested and analysed by qPCR to determine the gene expression levels for markers of the three germ layers

compared to SeViPS-NB2 cells in an undifferentiated state (Figure. 4.14). In addition, MIFF1 iPS cells were differentiated in the same conditions to act as a control. The endodermal genes analysed were; *GATA6, ISL1* and *FOXA2*, mesodermal; *CD34, COL1A1* and *PECAM* and ectodermal; *PAX6, GATA2, SOX10, AP2α, BRN3A PHOX2B, ALK* and *FOXD3*. The expression of *OCT4*, *NANOG* and *SOX2* was also analysed. As these genes are typically upregulated in undifferentiated hESCs and iPS cells, their down-regulation serves as a positive control for differentiation. QPCR analysis represented as delta CT values showed expression levels for *OCT4* and *NANOG* had decreased indicating that the cells had differentiated while the expression levels for all of the differentiation markers tested had increased. Combining the results of the SeViPS-NB2 characterisation and then comparing it to the genotype and phenotype of SK-N-SH and control hESC/iPS cell lines indicated that the SeViPS-NB2 cell line had activated an endogenous pluripotency network that was absent prior to reprogramming.

Figure 4.10. Analysis of SeViPS-NB2 cells by qPCR

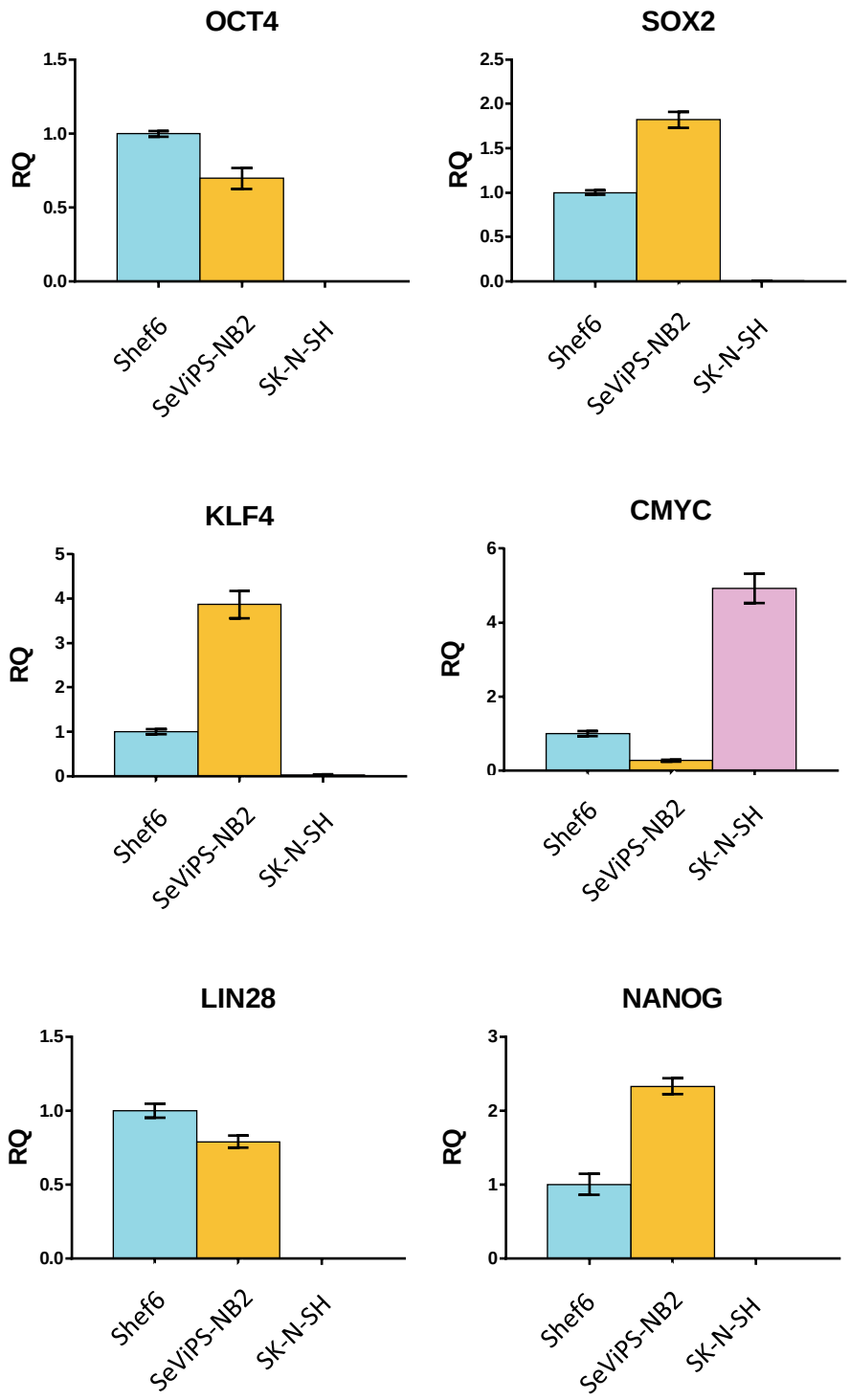

Figure 4.10: qPCR analysis of the SeViPS-NB2 cell line at passage +47 shows mRNA levels comparable to the hESC control cell line, Shef6, and dissimilar to the parental SK-N-SH cell line at passage +70. The mRNA levels for *KLF4* and *NANOG in* SeViPS-NB2 cells relative to Shef6 are ~3.5-fold and ~2-fold higher respectively. SK-N-SH cells endogenously express *cMYC* ~5-fold higher than expressed in Shef6. CT values were normalised to *GAPDH*. N=1 (error bars derived from technical triplicates).

Figure 4.11. Flow cytometric analysis of the SeViPS-NB2 cell line compared to SK-N-SH and NT2-D1 cells

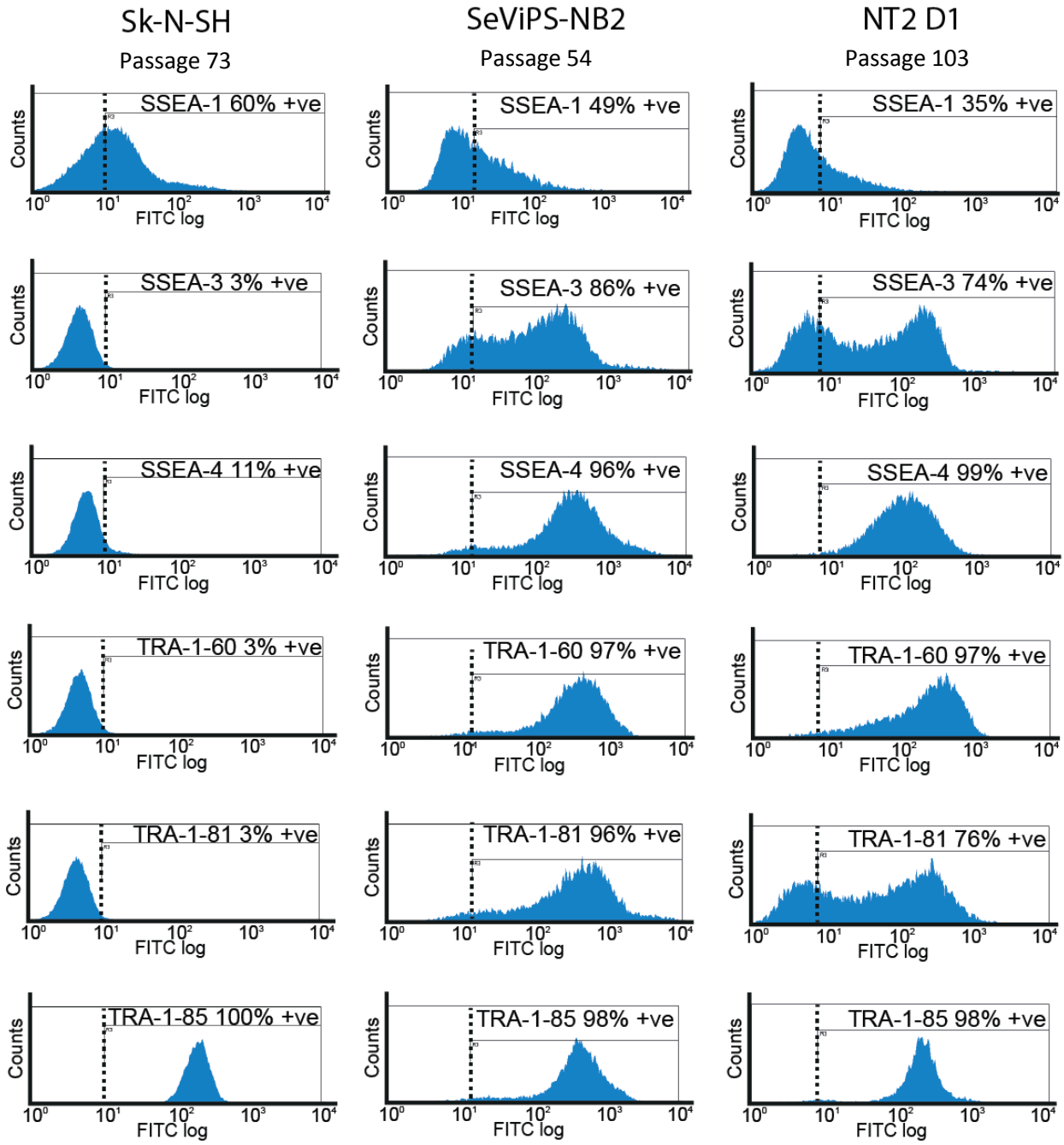

Figure 4.11: SeViPS-NB2 cells at passage +54 express cell surface markers SSEA-3, SSEA-4, TRA-1-60 and TRA-1-81 that are expressed in undifferentiated pluripotent stem cells. The NT2 D1 cell line at passage +103 was used as a positive control and exhibits a similar cell surface marker expression profile to that of the SeViPS-NB2 cell line. The parental cell line, SK-N-SH at passage +73 from which SeViPS-NB2 was derived does not express markers associated with undifferentiated pluripotent stem cells. P3X was used to gate the cells (shown by the dashed line) as described in methods 2.15.1.1.

Figure 4.12. Karyotype analysis of SeViPS-NB2 cells compared to SK-N-SH and SKiPS cell lines

SK-N-SH Passage 73

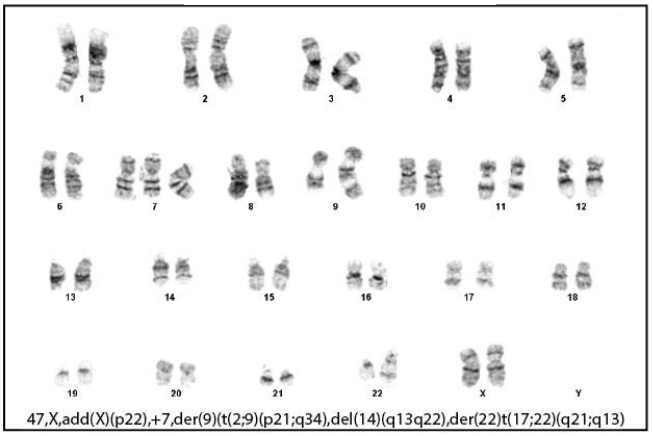

SeViPS-NB2 Passage 52

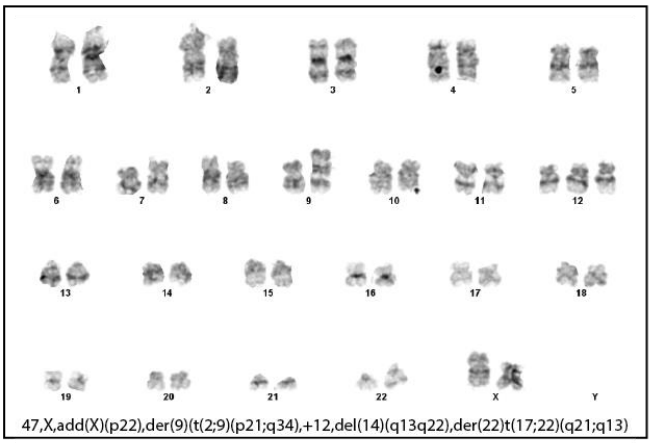

SKiPS-1.5-2 Passage 13

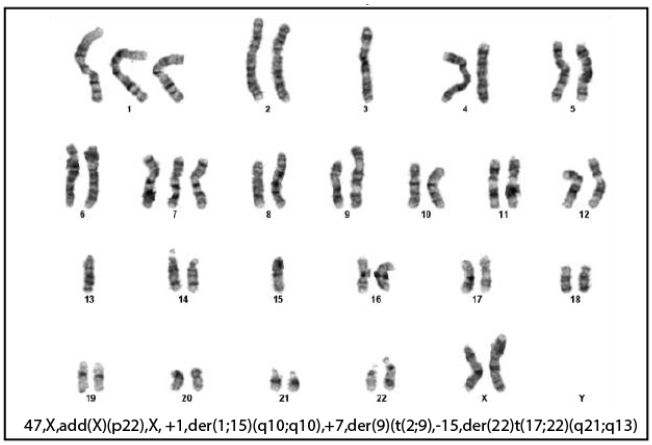

Figure 4.12: Karyotype analysis was performed on the SeViPS-NB2 cell line that was reprogrammed from SK-N-SH cells by the Karolinska Institutet using the Cytotune Sendai Virus Kit (Invitrogen). The karyotype was compared to the parental SK-N-SH cell line and a cell line reprogrammed from SK-N-SH using the lentivirus, SKiPS-1.5-2. The SK-N-SH cell line shows a gain of whole chromosome 7, deletion on 14p between q13 and q22 and translocations from 2p21 to 9q34 and 17q21 to 22q13. SeViPS-NB2 cells show a gain of whole chromosome 12 and loss of trisomy 7. The SKiPS 1.5-2 cell line maintains trisomy 7, but exhibits gains of whole chromosome 1 and loss of chromosome 15. Each cell line is karyotypically abnormal and different from one another.

Figure 4.13. Embryoid bodies formed from SeViPS-NB2 are morphologically dissimilar to those formed from MIFF1 iPS cells

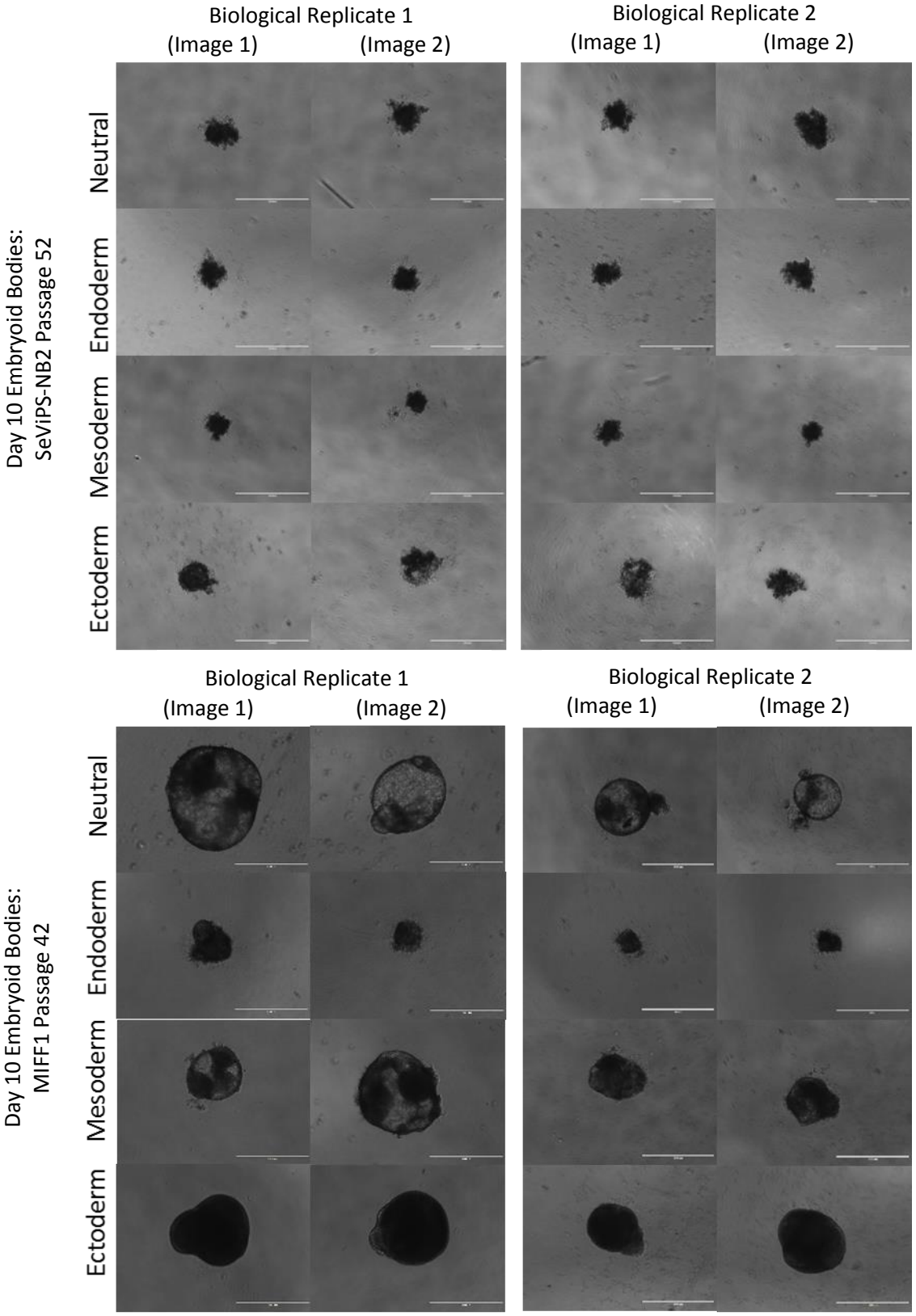

Figure 4.13: Directed differentiation of SeViPS-NB2 toward the three germ layers: endoderm, mesoderm and ectoderm in defined conditions (Table 2.4), results in the formation of small, fragmented embryoid bodies after 10 days. This is dissimilar to the control iPS cell line, MIFF1, which forms compact, large embryoid bodies when induced to differentiate following the same protocol. Two phase contrast images of each biological replicate was taken. Scale bars = 1000µm. N=2

Figure 4.14. Comparing gene expression levels between SeViPS-NB2 and a control iPS cell line, MIFF1

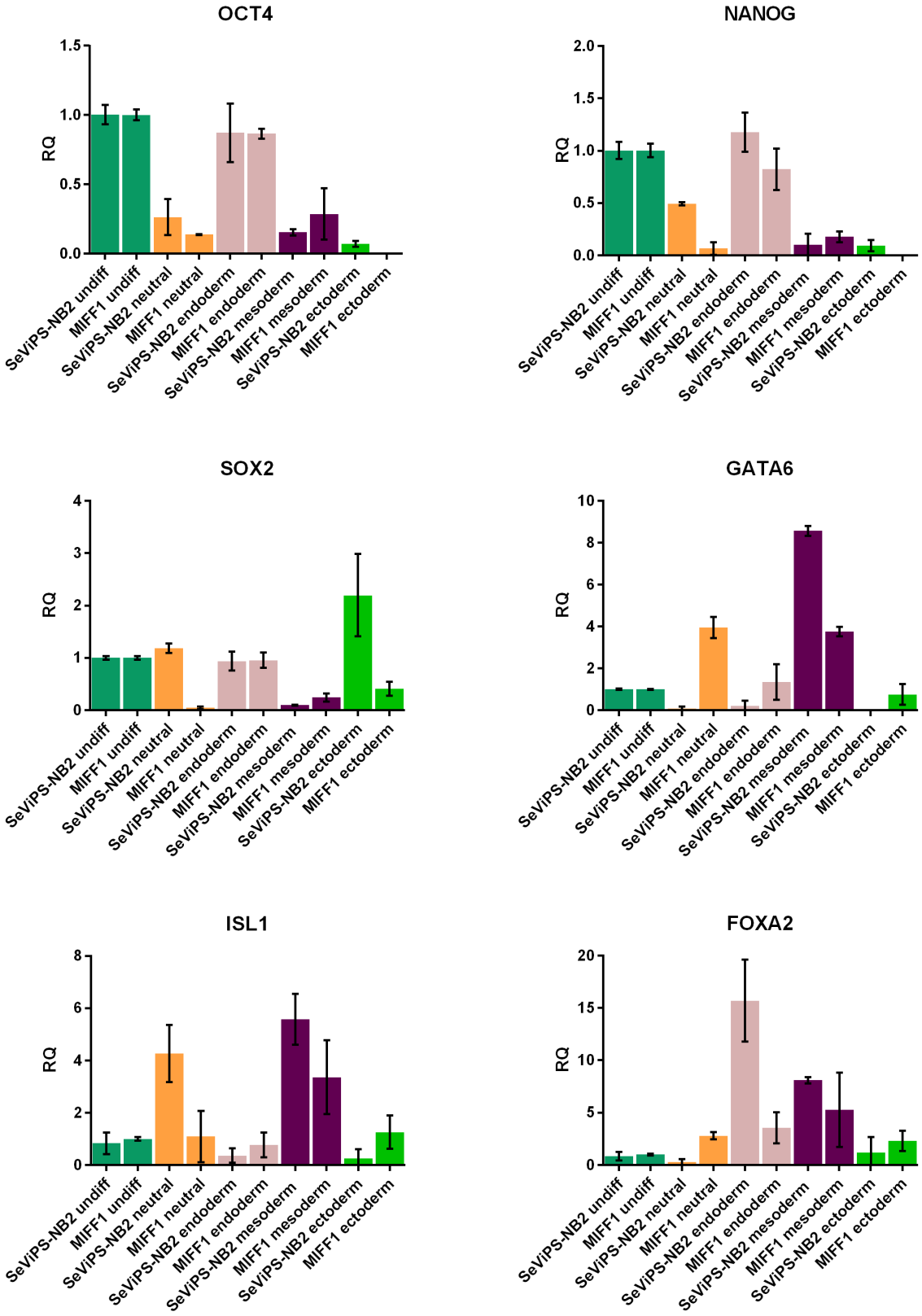

Figure 4.14: SeViPS-NB2 cells were differentiated as embryoid bodies for 10 days toward the three germ layers (endoderm, mesoderm and ectoderm) in defined conditions (Table 2.4). Differentiated SeViPS-NB2 cells were analysed by qPCR and expressed elevated levels of endodermal (*GATA6, ISL1, FOXA2)*, mesodermal (*CD34, PECAM*) and ectodermal (*PAX6*) genes relative to an undifferentiated control. MIFF1 iPS cells were differentiated under the same conditions and increased gene expression levels for *GATA6, ISL1, FOXA2* (endodermal), *CD34, COL1A1, PECAM* (mesodermal) and *PAX6, GATA2* (ectodermal). QPCR was performed using the Roche system (methods 2.14.1) and CT values were normalised to *GAPDH*. N=2.

Figure 4.14. Comparing gene expression levels between SeViPS-NB2 and a control iPS cell line, MIFF1

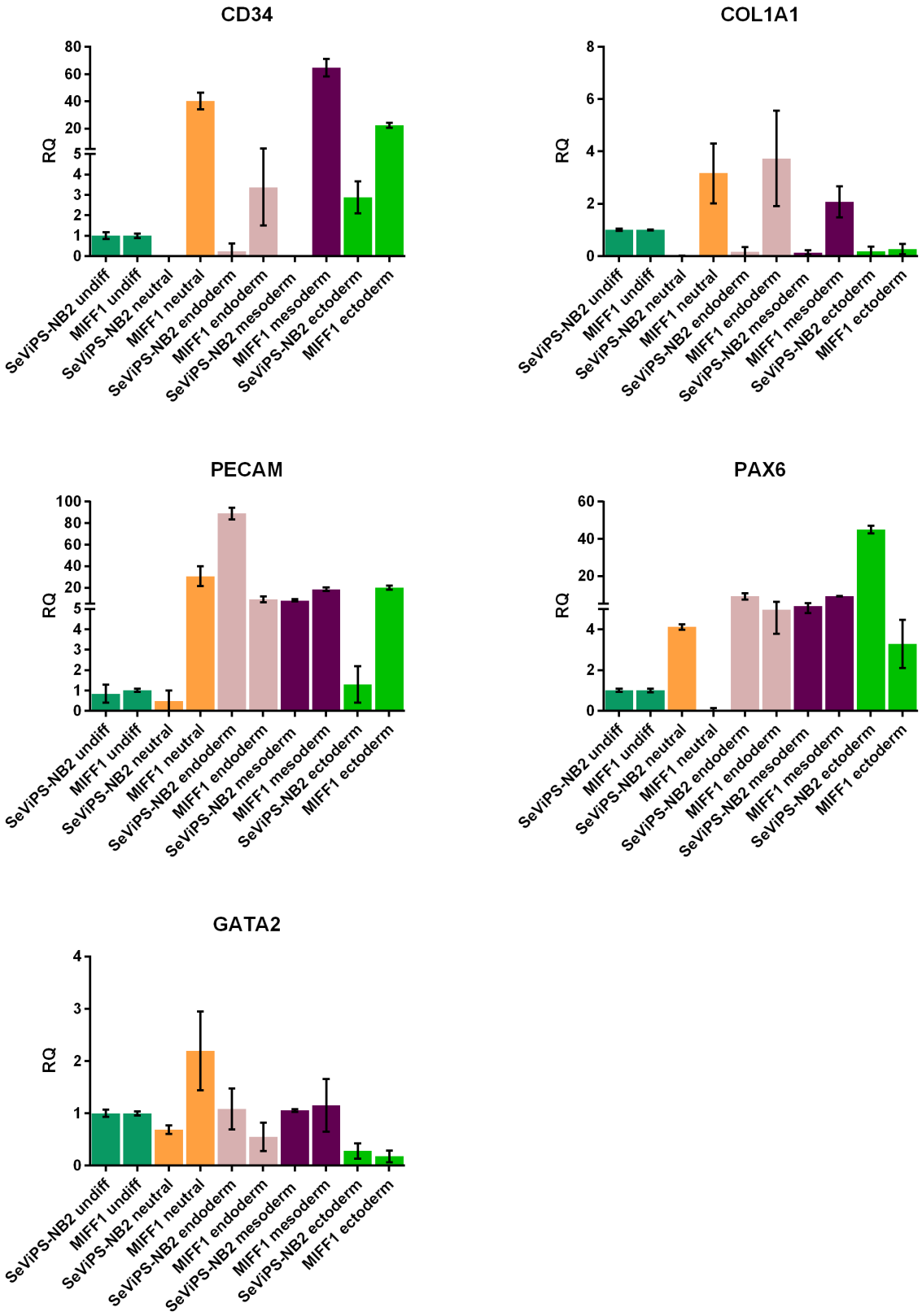

Figure 4.14: The expression levels for *OCT4, NANOG* and *SOX2* did not decrease as much when SeViPS-NB2 or MIFF1 cells were differentiated in the defined condition for endoderm (Table 2.4). Differentiation may be counteracted by the levels of Activin A (100ng/ml) supplemented in the medium. Activin A could be signalling via the TGFβ pathway to drive the transcription of pluripotency genes that are preventing the cells from differentiating (Figure. 1.1). It was found that the defined conditions did not always drive differentiation toward the desired germ layer however, the SeViPS-NB2 did express markers for all three germ layers. N=2

Figure 4.14. Comparing gene expression levels between SeViPS-NB2 and a control iPS cell line, MIFF1

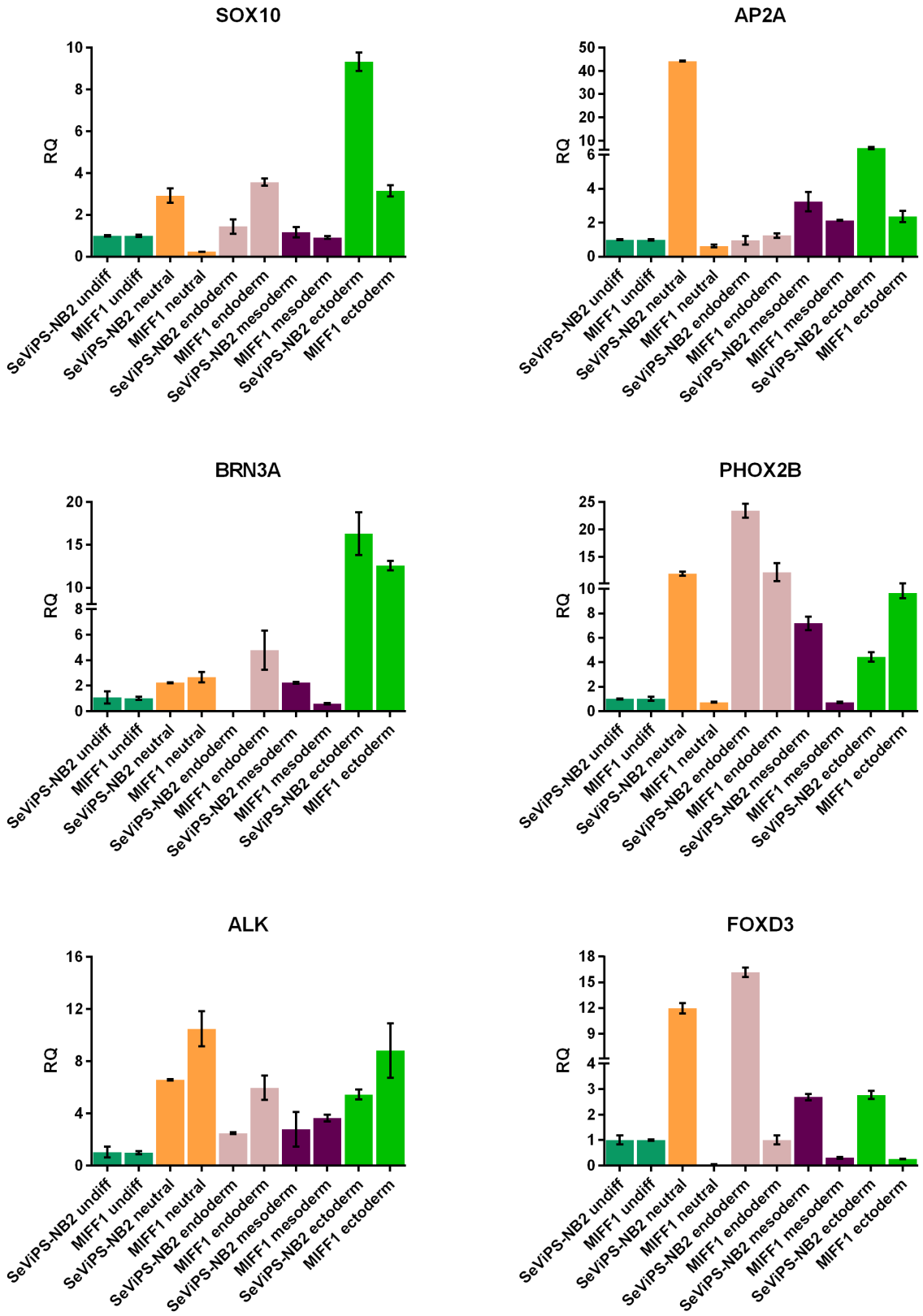

Figure 4.14: The cDNAs isolated from the differentiated SeViPS-NB2 and MIFF1 cells were also analysed by qPCR using the TaqMan system (methods 2.14.2) to determine the expression levels for a further panel of ectodermal markers: *SOX10, AP2α, BRN3A, PHOX2B, ALK* and *FOXD3.* It was found that all of the aforementioned genes were upregulated in SeViPS-NB2 cells when differentiated in the ectodermal condition (Table 2.4). CT values were normalised to β-ACTIN. N=2

4.3. Discussion

We have successfully demonstrated that the SK-N-SH cell line can be successfully reprogrammed to a pluripotent state. This has been achieved using lentiviral vectors to generate the SKiPS cell lines (unpublished work by Christian Unger) and as described in this report using the Sendai virus vector. The SeViPS-NB2 cell line, which was reprogrammed by overexpressing *OCT4, SOX2, KLF4* and *cMYC* using Sendai Viral vectors to introduce the reprogramming factors, was shown to possess a capacity to differentiate similar to hESCs in that it was capable of forming embryoid bodies that expressed markers for each of the three germ layers. One noticeable difference, however, was the morphology of the embryoid bodies. It was observed that the SeViPS-NB2 embryoid bodies were small and fragmented in both repeats, which is dissimilar to the Shef6-derived embryoid bodies that were induced to differentiate under the same conditions. The difference in embryoid body morphology may be as a result of perturbed differentiation, for example, via persistent replication of the Sendai virus inducing *OCT4* and *NANOG* to be constitutively expressed, although this was not tested. Even though *OCT4* and *NANOG* were downregulated during the differentiation process, it was not to the same extent to which *OCT4* and *NANOG* was downregulated in the control MIFF1 iPS cell line. If the Sendai virus was persistently replicating *OCT4* and *NANOG*, two genes that promote and maintain a pluripotent state, this may have affected the embryoid body's ability to differentiate.

It is also possible that following reprogramming the SeViPS-NB2 cells have retained what is called an 'epigenetic memory' whereby the reprogrammed cells have inherited characteristics of the epigenome of the parental cells, which can influence the properties of iPS cells [175], for example, their differentiation capacity. We did not perform RNA-sequencing analysis to compare the transcriptome profile of SeViPS-NB2 and SK-N-SH cells but this may help to identify RNAs that are exhibited at similar levels. Candidate RNAs can then be tested to determine the extent

to which they affect the differentiation capacity of the SeViPS-NB2 cells. It is also possible that genomic differences between the SeViPS-NB2 cells, which contain the neuroblastoma genome and the MIFF1 cells, which contain a normal diploid karyotype are affecting the differentiation capacity of the SeViPS-NB2 cells. It would be pertinent to identify the role that *MYCN* [129], *PHOX2B* [130] and *ALK* [131] have on the SeViPS-NB2 cells given they regulate neural crest development in normal cells.

The SeViPS-NB2 cell line was further characterised by analysing its karyotype. The results of this karyotype compared to one previously performed by our collaborators at the Karolinska Institute showed the cells had altered their karyotype, showing a gain of whole chromosome 12 and loss of trisomy 7, during continued maintenance in culture (Figure. 4.12). Long-term culturing of iPS cells reprogrammed using Sendai viral methods is necessary to dilute out the presence of viral vectors introduced into the cell cytoplasm. Unfortunately, the time taken to achieve this in the SeViPS-NB2 cell line overlapped with the onset of chromosomal alterations, specifically in chromosomes 7 and 12. Whole gains of chromosome 12 in human embryonic stem cells are typically associated with adaptation to an in vitro culture environment while the loss of whole chromosome 7 (trisomy to diploid) in the SeViPS-NB2 cell line indicates the loss of a pertinent mutation that is prevalent in the majority of neuroblastomas [176, 177]. It is possible that the SeViPS-NB2 cells have acquired chromosomal aberrations as a mechanism associated with culture adaptation to provide a selective advantage over non-adapted cells, which is a common consequence of maintaining hESCs and iPS cells in culture for prolonged periods of time [178]. Genomic alterations can influence a cell's capacity to differentiate [111] and therefore may affect the ability to recreate the developmental conditions required to model aspects of neuroblastoma development. It may be possible to clone out non-adapted cells from a chromosomally mosaic culture, but it was my intent to generate a set of neuroblastoma-derived iPS cells that maintained genomic integrity by using non-integrating mRNAs.

Repeated addition of an mRNA cocktail containing: *OCT4, SOX2, KLF4, cMYC, LIN28* and *NANOG* mRNAs transcribed from Allele Biotech IVT templates (ABP-SC-SEIPSET) into the SK-N-SH cell line induced 36% of the population to express cell-surface marker TRA-1-60 (Figure. 4.3 and 4.4). Given that TRA-1-60 is expressed on bona fide iPS cells [179] but not on neuroblastoma cells, suggests that the SK-N-SH cells had shifted towards a pluripotent state. Following cell sorting and re-plating of TRA-1-60^{+ve} cells from reprogrammed SK-N-SH cultures, the cells formed iPS cell-like colonies. This highlighted a phenotypic change as SK-N-SH cells do not grow in colonies. Nevertheless, the iPS cell-like colonies appeared to contain neural-looking cells that were indistinguishable from SK-N-SH cell cultures. After a few passages, the iPS-like cells reverted back to the SK-N-SH phenotype, forming a monolayer of neural cells that did not grow as colonies and did not express TRA-1-60. It is possible that a subset of TRA-1-60^{+ve} iPS-like cells may have been only partially reprogrammed. It is possible to determine via FACS analysis whether a cell is likely to be partially or fully reprogrammed by analysing cells that express TRA-1-60 and the reporter gene *mWASABI* [179]. It is known that iPS cells and hESCs are difficult to transfect with a reporter gene [180], such as *mWASABI* and as a result when mWASABI is added to reprogramming cultures, the cells that surround emergent iPS colonies, such as neuroblastoma cells, fluoresce while the cells within the iPS colony itself do not, even after repeated addition of the reporter gene. I determined that a subset of the TRA-1-60^{+ve} cells that we sorted out from the reprogramming culture via FACS also expressed *mWASABI*, which had been added into the reprogramming culture repeatedly to monitor mRNA getting in to the cells. This suggests there is a possibility that partially reprogrammed, *mWASABI*$^{+ve}$ cells were sorted out from the reprogramming culture along with bonafide, fully reprogrammed TRA-1-60^{+ve} cells, which may have resulted in the culture of sorted cells reverting back to a neuroblastoma phenotype. Any future strategies to sort iPS cells from neuroblastoma reprogramming cultures would greatly benefit from using a combination of cell surface and intracellular markers. Sorting for cells based

on a TRA-1-60^{+ve}, SSEA-4^{+ve} , *mWASABI*$^{-ve}$ and *NANOG*$^{+ve}$ phenotype may represent a reliable combination to isolate fully reprogrammed cells [179].

Neuroblastoma cells were successfully reprogrammed over a period of time exceeding ten weeks using lentiviral and Sendai viral methods. This is problematic for mRNA-mediated approaches considering that SK-N-SH cells would reach confluency prior to ten weeks in culture and that mRNA penetrance is inhibited when added to cells that are densely compacted. This is made worse by the fact that unlike fibroblasts, SK-N-SH cells are non-contact inhibited. This means that during SK-N-SH reprogramming, if transfections are required beyond the cells reaching confluency, maintaining a sufficient mRNA dose per cell ratio may require large doses of mRNA. Large doses of mRNA encoding the reprogramming factors may become toxic to the cells and thus inhibit reprogramming. This led to treating the cells with Retinoic Acid (RA) as RA has been found to induce growth arrest in SK-N-SH cells due to the down-regulation of cell cycle-promoting cyclins and cyclin-dependent kinases (CDKs) [181]. After treatment with RA, SK-N-SH cells were found to have an inhibited proliferative capacity which increased the number of transfections that could be performed prior to the cells reaching confluency. After 15 days of repeatedly adding mRNAs to SK-N-SH cells (Figure. 4.6), a small number of larger, flatter cells appeared which were morphologically distinguishable from the neuronal cell phenotype that populates the majority of the culture. This possibly indicated that these cells had entered an early phase of reprogramming based on the finding that fibroblasts also change morphology during the initial phase. Unfortunately, after the further addition of mRNAs over a 43-day protocol, SK-N-SH cells did not reprogramme to iPS cells. These findings highlight that the expression of mRNAs in the current reprogramming cocktail is insufficient to allow for the transition to pluripotency and possibly more mRNAs encoding further transcription factors may be required to execute reprogramming. It may also be that additional events are required to

overcome major epigenetic barriers that inhibit reprogramming of neuroblastoma cells such as chromatin inaccessibility.

In an attempt to increase chromatin accessibility, I performed reprogramming using the 6-factor premix mRNA cocktail (ABP-SC-6FMRNA) that contained *M_3O* mRNA instead of conventional *OCT4* transcripts. However, adding the *M_3O* mRNA cocktail to SK-N-SH cell cultures resulted in most of the cells succumbing to apoptosis. Under the same conditions in fibroblasts this did not happen, highlighting different survival thresholds between SK-N-SH cells and fibroblasts following the addition of exogenous mRNAs. However, the addition of *mWASABI* mRNA to SK-N-SH cultures did not succumb the cells to apoptosis (Figure. 4.7C and D) highlighting that it is not the dose of mRNA but more likely a specific mRNA or combination of mRNAs that induce cytotoxicity in SK-N-SH cells. Cytotoxicity induced by the 6-factor mRNA cocktail (ABP-SC-6FMRNA) in SK-N-SH cells can be partially mitigated by reducing the mRNA dose-per-cell ratio during reprogramming. However, lowering the mRNA dose to promote SK-N-SH cell survival did not result in the emergence of iPS-like cells that were morphologically dissimilar from SK-N-SH cells or that expressed TRA-1-60. My findings indicate that the method optimised for reprogramming fibroblasts is not directly translational to neuroblastoma cells considering that iPS cells failed to emerge following the same protocol that induced pluripotency in fibroblasts. However, the method should act as a reprogramming template when attempting to reprogramme the SK-N-SH cell line on the finding that following the method did induce over a third of SK-N-SH cells to endogenously express TRA-1-60, indicative of a shift towards pluripotency. It is conceivable that further optimisations to the current method possibly alterations that better facilitate chromatin remodelling of the disease genome may overcome epigenetic barriers to allow for the generation of mRNA-mediated disease-iPS cells.

Chapter 5.

Transdifferentiation of fibroblasts using mRNAs.

5.1. Introduction

MRNA-mediated reprogramming is an established integration-free method for converting somatic cells in to iPS cells but there is little experience of using transfection of mRNAs as a tool for transdifferentiating somatic cells into specialised cells. Unlocking this potential would be invaluable for generating integration-free differentiated cell types that could be used in the future not only for cell replacement therapies but also as a tool for investigating mechanisms that underlie the conversion of cell states. Converting somatic cells from one lineage to another while bypassing an intermediate pluripotent state is advantageous over reprogramming for a couple of reasons. Firstly, the process is much simpler, because it can be executed using as little as one defined factor in a simple defined medium. Secondly, transdifferentiation protocols tend to require much less time to acquire the desired cell type in comparison to reprogramming methods that first require conversion of somatic cells to a pluripotent state before being subsequently differentiated.

MYOD1 is a transcription factor that has binding sites in the promoter regions of myoblast-associated genes, such as *MYOGENIN,* and once bound induces a cascade of events (Figure. 5.1) that is sufficient to convert fibroblasts into myoblasts. Through DNA methylation, the transcription of myoblast-associated genes is typically repressed in fibroblasts. However, it has been shown that *MYOD1* is able to remodel the chromatin structure and directly activate genes, such as *MYOGENIN* and *MCK* (muscle creatine kinase) [182] that are involved in myogenic conversion. *MYOD1* achieves this through the recruitment of histone acetyltransferase (HAT)

p300, which acetylates H3K27 (H3K27ac) and methyltransferase Set7 that methylates histone H3K4 (H3K4me1) at myogenic enhancer regions [183]. In addition, *MYOD1* recruits the SWItch/Sucros Non-Fermentable (SWI/SNF) complex that uses enzymatic activity to remodel the way chromatin is packed. The SWI/SNF complex possesses an ATPase that breaks down ATP to destabilise the interaction between histones and DNA in the promoter regions of muscle-specific genes, brahma-related gene-1 (*BRG1*) and human brahma (*BRM*) [184]. When chromatin becomes unstable it opens up previously inaccessible binding sites that allow for transcription factors to easily bind to DNA and initiate transcription.

Transdifferentiating fibroblasts to myoblasts has been demonstrated in mouse [150-153] and human [76] by overexpressing *MYOD1* using different delivery mechanisms: cDNA transfection [150], lentivirus [151] retrovirus [152] and mRNA [116]. The conversion frequency for generating myoblasts from fibroblasts is high, ranging from 5% [112] to 50% [111] [87] in addition to being a technically uncomplicated 6-day process. I therefore set out to transdifferentiate human fibroblasts to myoblasts because this transdifferentiation model can be achieved by overexpressing a single factor, *MYOD1*, has a high conversion frequency and is an established model in mouse fibroblasts but not human fibroblasts. This model will provide the most suitable platform to determine whether mRNA can be used for transdifferentiation but also to provide proof of concept that mRNA can be used as a tool to drive the conversion of cell states.

Figure 5.1. Mechanism of Action for *MYOD1*

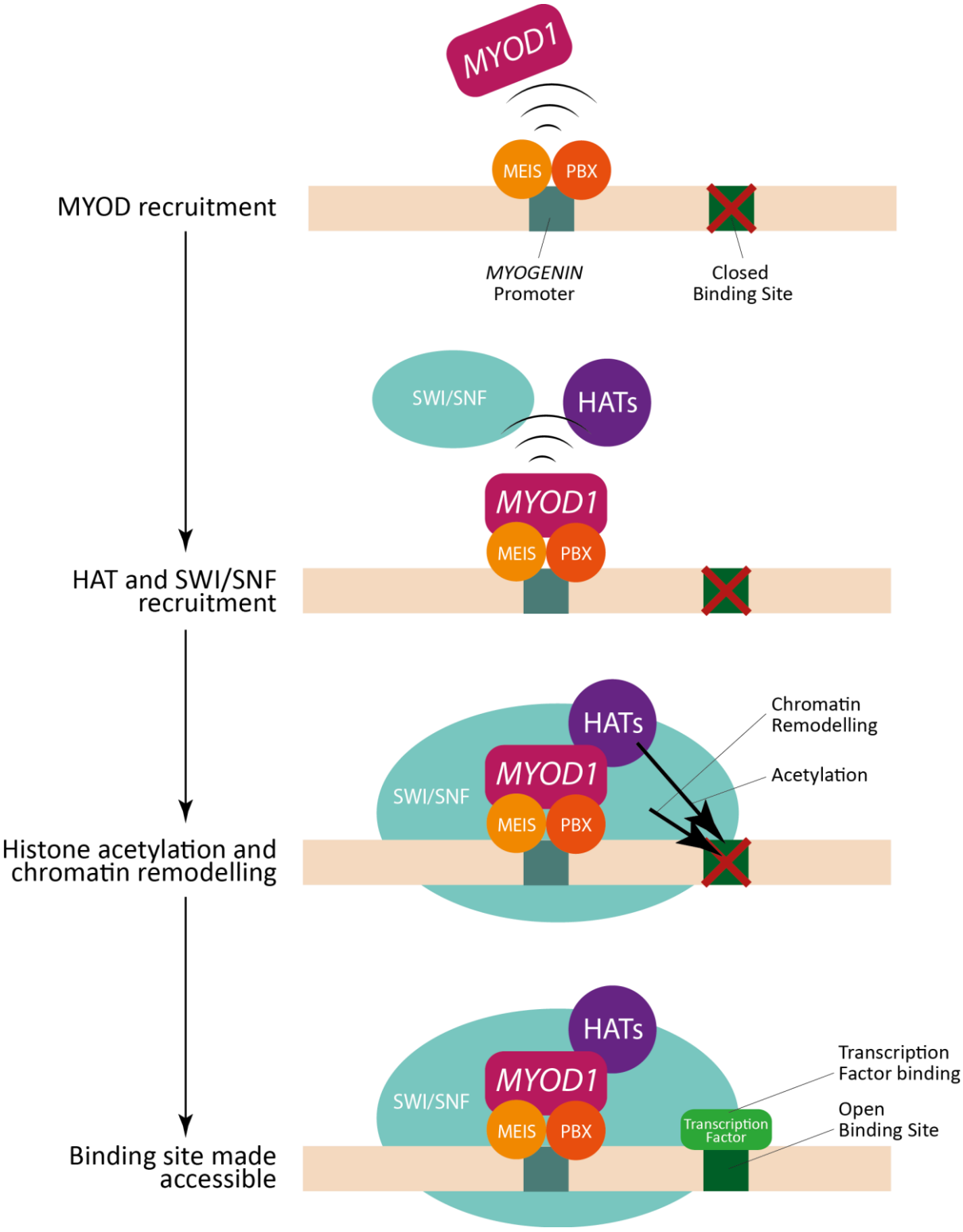

Figure 5.1: *MYOD1* is recruited to the *MYOGENIN* promoter by MEIS and PBX that are constitutively bound to the *MYOGENIN* promoter. *MYOD1* then recruits histone acetyltransferases (HATs) and the SWI/SNF complex to acetylate and repackage chromatin respectively. The chromatin undergoes remodelling and closed transcription binding sites are opened.

5.2. Results

5.2.1. Generation and validation of *MYOD1* mRNA

We have shown that the repeated introduction of reprogramming factor mRNAs into BJ fibroblasts is capable of converting them into iPS cells (Figures. 3.6, 3.11, 3.12, 3.18). We decided to test whether the repeated introduction of an mRNA encoding a gene associated with a myoblastic phenotype (*MYOD1*), could transdifferentiate fibroblasts into muscle cells without the need to enter a pluripotent state. The first step to achieving this involves testing the capacity of fibroblasts to uptake *MYOD1* mRNA.

We sought to transdifferentiate fibroblasts to myoblasts through the repeated addition of *MYOD1* mRNA. In order to obtain the necessary mRNA, we obtained the pCMV6-XL5 MYOD1 DNA plasmid from Origene (Methods 2.17.4) (Figure. 5.2A) that contained a cDNA clone for *MYOD1*. Generating *MYOD1* mRNA from this plasmid, including the linearization process and the parameters of the restriction digest are described in methods 2.17.4. Prior to linearisation, the sequence of pCMV6-XL5 *MYOD1* was inputted into a plasmid editor (ApE) software and a virtual restriction digest was performed using the XbaI restriction enzyme to predict the band sizes that would be expected when performing gel electrophoresis (Figure. 5.2B). A predicted band size of 6179 base pairs was suggested. The plasmid was then linearised as described in methods 2.17.4 and verified, prior to performing *in-vitro* transcription reactions, by running 5µl of the restriction digest reaction on a one percent agarose gel (Figure. 5.2C). An undigested DNA control was run in a well adjacent to this to verify that the restriction digest had successfully linearised the pCMV6-XL5 MYOD1 plasmid. We found that the linearised plasmid, that was 6.2kb in length, migrated as a single band while the undigested plasmid failed to migrate as a single band or at the same speed

through the gel, possibly because the undigested plasmid was circular in shape or nicked that can result in slower migration [185] (Figure. 5.2C). The single band coupled with a faster migration through the gel suggests that the plasmid had been successfully linearised. The linearised pCMV6-XL5 *MYOD1* plasmid was then *in-vitro* transcribed using the MEGAscript T7 kit using modified nucleotides (methods 2.20). To verify that *MYOD1* mRNA had been successfully transcribed, one microgram of mRNA was run on a one percent denaturing RNA gel (Figure. 5.2D) alongside an ssRNA ladder. *MYOD1* mRNA was identified by a band at ~2056 base pairs in length that was consistent with what was expected.

To test the ability for *MYOD1* mRNA to enter fibroblasts, a dose of 400ng *MYOD1* mRNA was added to HFFs that had been plated at a density of $1x10^5$ in plastic wells of a 6-well plate in 10% DMEM FCS for 24 hours. To serve as controls, HFFs in separate wells were mock transfected with Stemfect and Stemfect buffer, left untreated or contained 100ng *mWASABI* mRNA for 24 hours. After 24 hours, RNA was extracted from the cells, reverse transcribed into cDNA and then analysed by qPCR to detect the mRNA levels for *MYOD1* (Figure. 5.3). It was found that *MYOD1* mRNA levels in the well in which *MYOD1* mRNA was added, increased $9.7x10^4$-fold relative to the untreated control.

Figure 5.2. Linearizing and in-vitro transcribing *MYOD1* mRNA from the pCMV6-XL5 plasmid

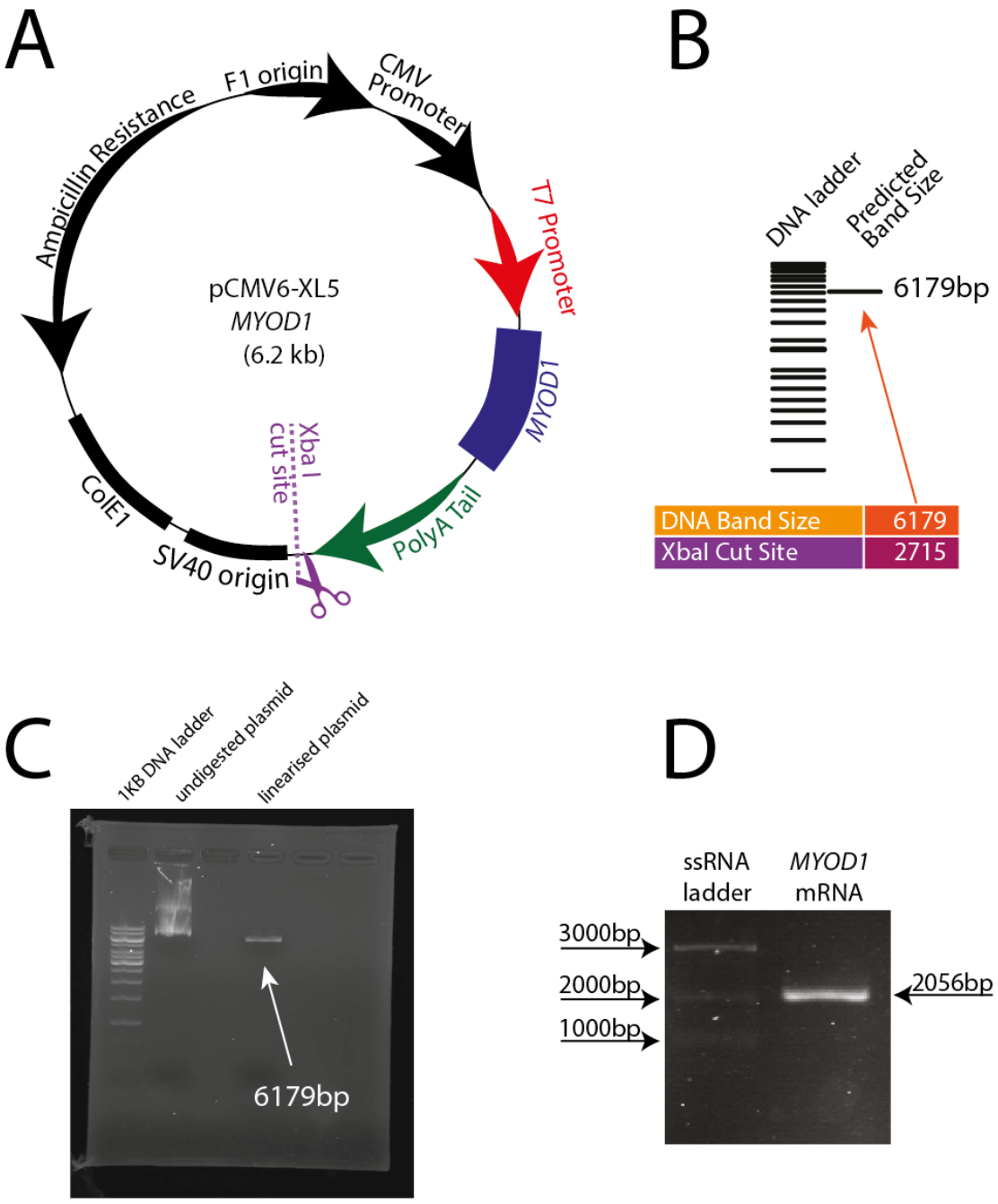

Figure 5.2: *MYOD1* mRNA was *in-vitro* transcribed from a linearised pCMV6-XL5 *MYOD1* plasmid. (A) The plasmid map shows a linearisation site, XbaI, downstream of a polyA tail that is incorporated at the 3' end of mRNA following *in vitro* transcription. IVT reactions are driven by a T7 promoter upstream of the *MYOD1* coding sequence. (B) The sequence of pCMV6-XL5 *MYOD1* was inputted into a plasmid editor (ApE) software that performed a virtual restriction digest on the plasmid using the XbaI restriction enzyme. A predicted band size of 6179 base pairs was suggested. (C) The plasmid was linearised using 5 units of XbaI restriction enzyme as described in methods 2.17.4. Linearisation was verified by running the plasmid on a 1% agarose DNA gel and single band size at ~6179 base pairs, as predicted, is shown (methods 2.19). (D) An in-vitro transcription reaction was then performed on the linearised plasmid. The resultant modified *MYOD1* mRNA was verified on a 1% denaturing RNA gel (methods 2.19.1). A 1kb DNA ladder and an ssRNA ladder were used for DNA and RNA gels respectively.

Figure 5.3. *MYOD1* mRNA levels increase 9.7x10^4-fold following its addition into human fibroblasts

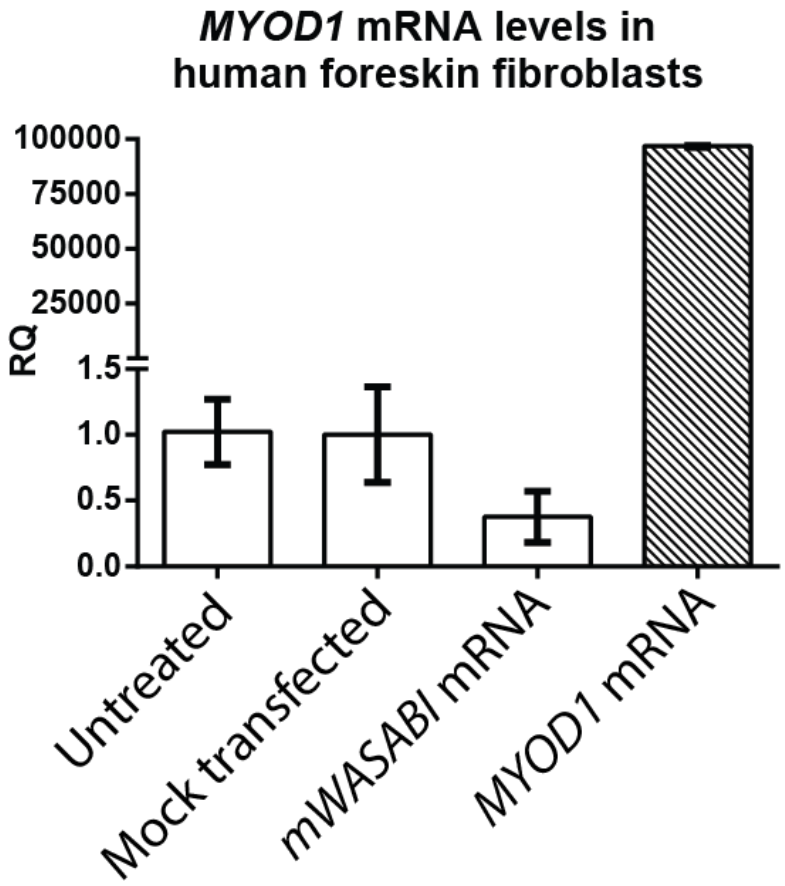

Figure 5.3: *MYOD1* mRNA at a dose of 400ng was introduced into HFF cells at passage +15 for 24 hours and then analysed by qPCR to verify that it was taken up by the cells. *MYOD1* mRNA levels were 9.7x10^4-fold higher compared to untreated HFFs verifying that *MYOD1* mRNA is highly penetrant in HFFs. Controls included untreated HFFs, mock transfected HFFs that had been treated with Stemfect and Stemfect buffer (Stemgent, 00-0069) and HFFs where *mWASABI* mRNA had been added at a dose of 400ng for 24 hours. CT values were normalised to *GAPDH*. N=1 (error bars derived from technical triplicates).

5.2.2. MYOD1 mRNA induces human fibroblasts to transdifferentiate to myoblasts

It was found that *MYOD1* mRNA is highly penetrant in fibroblasts. We tested whether the repeated introduction of *MYOD1* mRNA into fibroblasts would cause them to transdifferentiate into myoblasts.

Firstly, HFFs were dissociated into single cells using 0.25% trypsin-EDTA and seeded down onto untreated 6-well plates at a density of $5x10^3$ / cm^2 in DMEM containing 10% FBS. Controls were also included to ensure that any myoblasts that formed following the transdifferentiation process were not as a result of spontaneous differentiation. The controls included an untreated well that was maintained in DMEM 10% FBS, a well controlling for phenotypic changes that may occur due to media changes i.e. switching from DMEM 10% FBS to myoblast growth medium and then to transdifferentiation medium and finally a mock transfected well that was treated with Stemfect transfection reagent and buffer.

For transdifferentiation, twenty four hours after the HFFs had been plated the medium was changed to myoblast growth medium (methods 2.3.4) containing 200ng/ml B18R. The cells were grown in this medium until the cells reached 80% confluency which took typically 72 hours. During this time period, *MYOD1* mRNA at a dose of 200ng was repeatedly added into HFFs daily to a final concentration of 200ng/ml. After 72 hours, the media was switched to transdifferentiation medium for three days (methods 2.3.5) to encourage any transdifferentiated myoblasts to fuse together to from multinucleated myotubes. Cells that morphologically resembled myoblasts appeared in the culture one day after the first addition of *MYOD1* mRNA (Figure. 5.4A, Day 1, indicated by white arrows). These cells were characteristically compact, irregularly shaped with a large nucleus to cytoplasm ratio and granular edges. This is distinctly different to fibroblasts that have a typically elongated cell

body, contain fibroblastic processes and exhibit little granularity. Following the transdifferentiation process the cells were fixed and stained, on day 7, with NCAM and DESMIN and analysed via high content screening to detect the presence of cells that had converted to a myoblast-like phenotype (Figure. 5.4B). It was determined on day seven that 0.08% of cells had transdifferentiated to myoblast-like cells, based on NCAM expression.

Figure 5.4. Transdifferentiation of fibroblasts to myoblast-like cells after repeated addition of MYOD1 mRNA

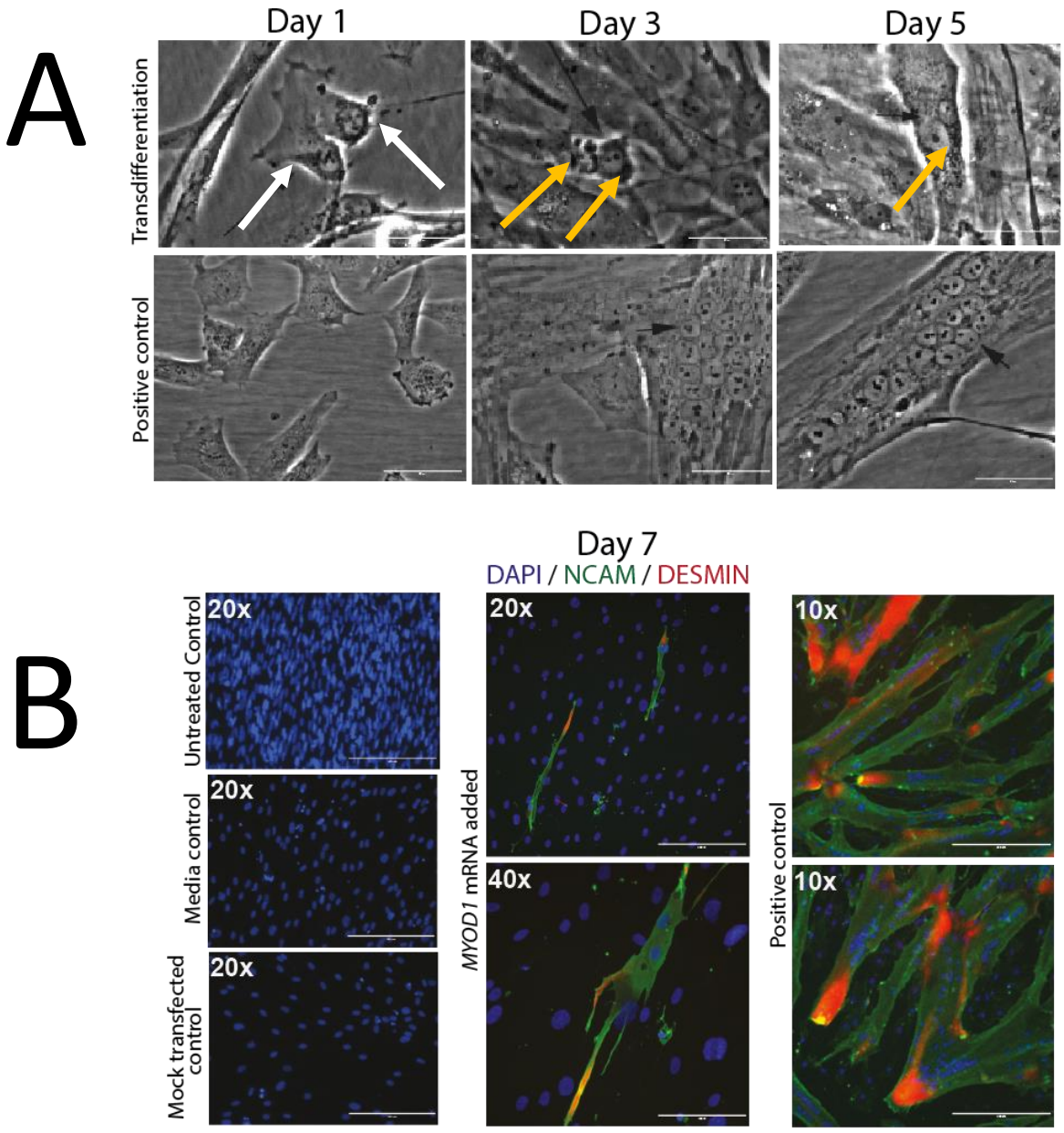

Target Set	Nuclei Count	NCAM positive cells	Conversion Frequency (%)
MYOD1 mRNA transfected	151900	125	0.08
Untransfected control	202967	0	0
Media control	215397	0	0
Mock transfected control	266112	0	0

Figure 5.4: Fibroblasts that were introduced to a dose of 200ng *MYOD1* mRNA for four days were induced to transdifferentiate into myoblasts which stain positive for NCAM and DESMIN. One day after the first addition of *MYOD1* mRNA, the cell population contained myoblast-like cells (white arrows). On day three and five, cells containing multiple nuclei emerged (orange arrows). Immunofluorescence analysis was performed on day seven using the IN Cell Analyser 2200 (GE Healthcare Life Sciences) that found that 0.08% of the population expressed NCAM and DESMIN. The KMISS human myoblast cell line was used as a positive control. Cells were counterstained with Hoescht at 1:1000. Scale bars = 50µm (day 1-5), 200µm (day 7, 20X), 100µm (day 7, 40X) 400µm (day 7, 10X)

5.2.3. The NCAM cell surface marker and DESMIN intracellular marker are expressed on myoblasts and myotubes but not on fibroblasts

Cultures of fibroblasts and myoblasts are distinguishable by morphology however this characteristic alone is insufficient to confirm that fibroblasts have transdifferentiated to myoblasts. In order to facilitate the unambiguous identification of myoblasts within transdifferentiated fibroblast cultures, we determined the expression levels of two markers, a cell-surface marker NCAM and an intracellular marker DESMIN.

In order to distinguish between fibroblasts, myoblasts and myotubes, HFFs and a myoblast positive control cell line named KM155 were obtained [186]. Myotubes form following the fusion between multiple myoblasts and were obtained by seeding KM155 cells at a density of $2x10^5$ in a 6-well plate in myoblast growth medium (methods 2.3.4) until the cells reached approximately 80% confluency. The media was then switched to transdifferentiation medium (methods 2.3.5) for 48-72 hours to give rise to multinucleated myotubes. HFFs, KM155 myoblast cells and KM155-derived myotubes were then analysed by flow cytometry, qPCR and high content screening for the expression of NCAM and DESMIN, two markers that have been reported to distinguish fibroblasts from myoblasts and myotubes.

Analysis by flow cytometry was performed by seeding HFFs and KM155 cells at a density of $2x10^5$ in a 6-well plate in either fibroblast growth medium, DMEM 10% FBS or in myoblast growth medium containing DMEM F12, 20% FBS, 8ng/ml bFGF and 10µg/ml human insulin solution. After 24 hours the cells were dissociated into single cells and stained for 30 minutes primarily with NCAM monoclonal antibody at a dilution of 1:10 followed by a further 30 minutes with Alexa Fluor 488 (AF488) goat anti-mouse secondary antibody at 1:100. Throughout the process the cells were maintained at 2-8°C. The cells were analysed

by flow cytometry and it was found that fibroblasts do not express NCAM however 98% of myoblasts positively expressed NCAM (Figure. 5.5A).

To visually illustrate the difference in NCAM and DESMIN expression between fibroblasts, myoblasts and myotubes, the cells were subject to high content screening. In separate wells, HFFs and myoblasts were plated down as previously described for flow cytometry for 24 hours. HFFs, myoblasts and myotubes were then fixed with 4% PFA for 15 minutes at room temperature. The PFA was then removed and the cells were blocked with PBS containing 10% FBS for 30 minutes. The cells were then stained with NCAM or DESMIN, washed three times and then stained with secondary antibodies AF488 or AF647 respectively. The cells were counterstained with Hoescht 33342 during the incubation period with the secondary antibody before being washed a further three times. NCAM and DESMIN expression was assessed by an INCELL Analyser 2200 and it was clearly visible that fibroblasts do not express NCAM or DESMIN yet they are ubiquitously expressed in myoblasts and myotubes (Figure. 5.5B). DESMIN mRNA levels in HFFs, KM155 myoblasts and differentiated myotubes were then analysed by qPCR. DESMIN mRNA levels were found to be 115-fold higher and 223-fold higher in myoblasts and myotubes respectively relative to fibroblasts. NCAM and DESMIN can therefore be used to distinguish between fibroblasts and proliferating or differentiated myoblasts.

Figure 5.5. Myoblasts and myotubes but not fibroblasts express NCAM and DESMIN

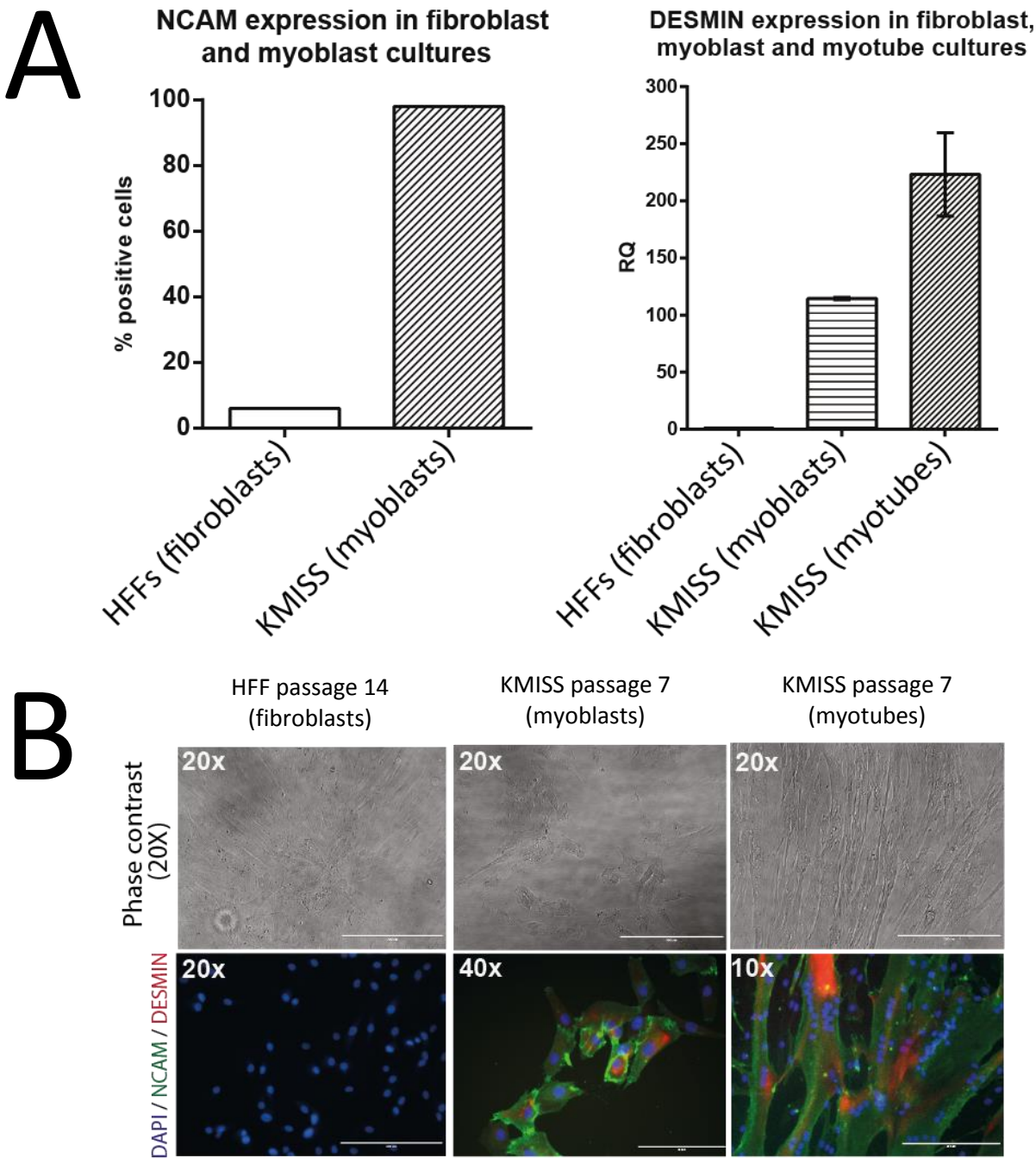

Figure 5.5: Myoblasts and myotubes express NCAM and DESMIN but fibroblasts do not. (A) HFFs and KMISS myoblast cells were analysed by flow cytometry for the expression of the cell surface marker, NCAM. Staining was performed as described in methods 2.15.1. Flow cytometric analysis showed that NCAM was not expressed on fibroblasts but was expressed on 98% of myoblasts. HFFs, KMISS myoblasts cells and KMISS myotubes that were differentiated from myoblasts using transdifferentiation medium (methods 2.3.5) were then analysed by qPCR for the expression of intracellular marker DESMIN. It was found that fibroblasts do not express DESMIN but it is expressed ~120-fold and ~220-fold higher in myoblasts and myotubes respectively, relative to HFFs. CT values were normalised to *GAPDH*. N=1 (error bars derived from technical triplicates). (B) NCAM and DESMIN expression was visualised by analysing HFFs, KMISS myoblasts cells and KMISS myotubes by immunofluorescence on the IN Cell Analyser 2200 (GE Healthcare Life Sciences). It was confirmed that fibroblasts do not express NCAM or DESMIN however both markers are expressed on myoblasts and myotubes derived from KMISS cells. Cells were counterstained with Hoescht at 1:1000. Scale bars = 200µm (20X), 100µm (40X), 400µm (10X).

5.2.4. NCAM expressing cells transdifferentiated from fibroblasts can be terminally differentiated to form multinucleated myotubes confirming they are myoblasts

We have provided a proof-of-concept that mRNAs can be used to direct cell fate by successfully transdifferentiating fibroblasts to myoblasts through the repeated addition of *MYOD1* mRNA. A functional property of myoblasts is the ability to fuse with other myoblasts to form multinucleated myotubes. Do the myoblast cells that we have converted from fibroblasts possess the functional capacity to form multinucleated myotubes?

Myoblasts require close contact with other myoblasts to fuse to form myotubes. Given the previous transdifferentiation experiment achieved a conversion frequency of 0.08%, we decided to sort the cells following the phase in which mRNAs are added to the cells to enrich the population with myoblast-like cells. Re-plating the enriched myoblast-like cell population should decrease the space between converted cells and improve the probability of myoblast fusion events occurring. However, cell sorting cannot be performed on cells that have been fixed, the purpose of which is to identify the presence of NCAM and DESMIN expressing myoblast cells within transdifferentiated cultures. Therefore, transdifferentiation was performed in two wells under the same conditions, one to be fixed and analysed in-situ for the presence of cells expressing NCAM and DESMIN and the other for sorting cells based on NCAM expression.

Myoblast induction was performed as previously described via the repeated addition of *MYOD1* mRNA albeit the mRNA dose in both wells was increased to 300ng to test whether an increased mRNA dose-per-cell ratio would increase the conversion frequency. After four days of repeated transfection with MYOD1 mRNA, one well was analysed by high-content

screening to determine the number of myoblast-like cells that expressed DESMIN and NCAM. On day four it was determined that 0.4% of cells had transdifferentiated to myoblast-like cells, based on NCAM expression (Figure. 5.6ii). At this point, the second well was sorted into NCAM positive and negative fractions containing $4x10^4$ and $2x10^5$ cells respectively (Figure. 5.6iii). The positive and negative fractions were re-plated into separate wells of a 6-well plate at a cell density of $4x10^4$ in myoblast growth medium. On day 7, the cells had proliferated to a confluency of ~80% so the media was then changed to transdifferentiation medium for a further 72 hours, to day 10. On day 10, the cells were fixed and stained with NCAM, DESMIN and Hoescht 33342 as previously described (Figure. 5.6iv). It was determined that the NCAM positive fraction contained myoblasts that had fused to form multinucleated myotubes. The myotubes had multiple nuclei, stained positive for NCAM and morphologically resembled large fibres (Figure. 5.6iv). The cells in the negative fraction did not form myotubes or myoblasts and did not express NCAM or DESMIN.

Figure 5.6. In-vitro differentiation of myoblast-like cells transdifferentiated from fibroblasts to multinucleated myotubes

i

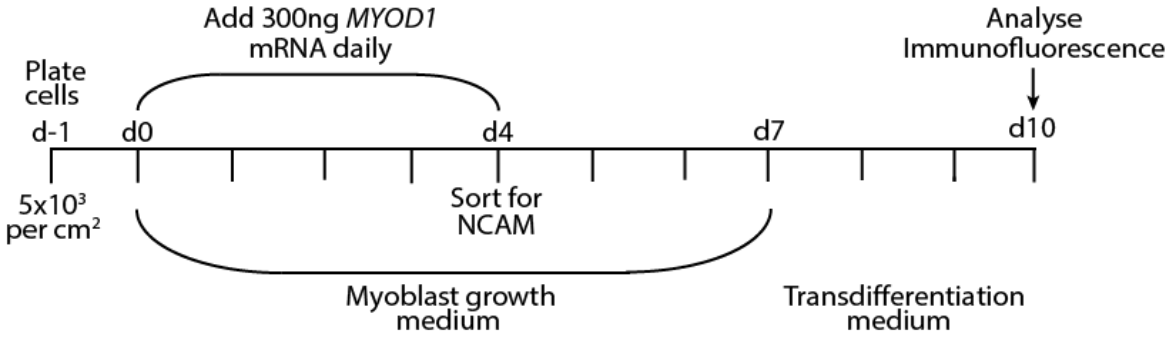

ii

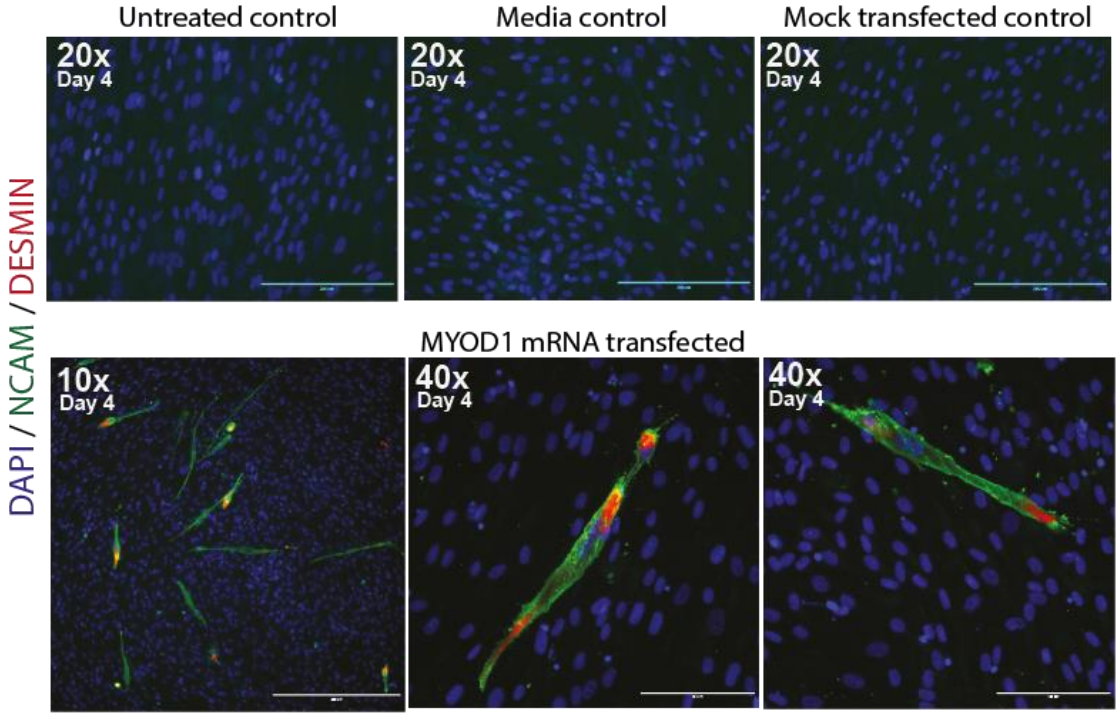

Target Set	Nuclei Count	NCAM positive cells	Conversion Frequency (%)
Untransfected control	539238	0	0.0
Media control	561564	12	0.0
Mock transfected control	540376	9	0.0
MYOD1 mRNA transfected	625259	2697	0.4

Figure 5.6. In-vitro differentiation of myoblast-like cells transdifferentiated from fibroblasts to multinucleated myotubes

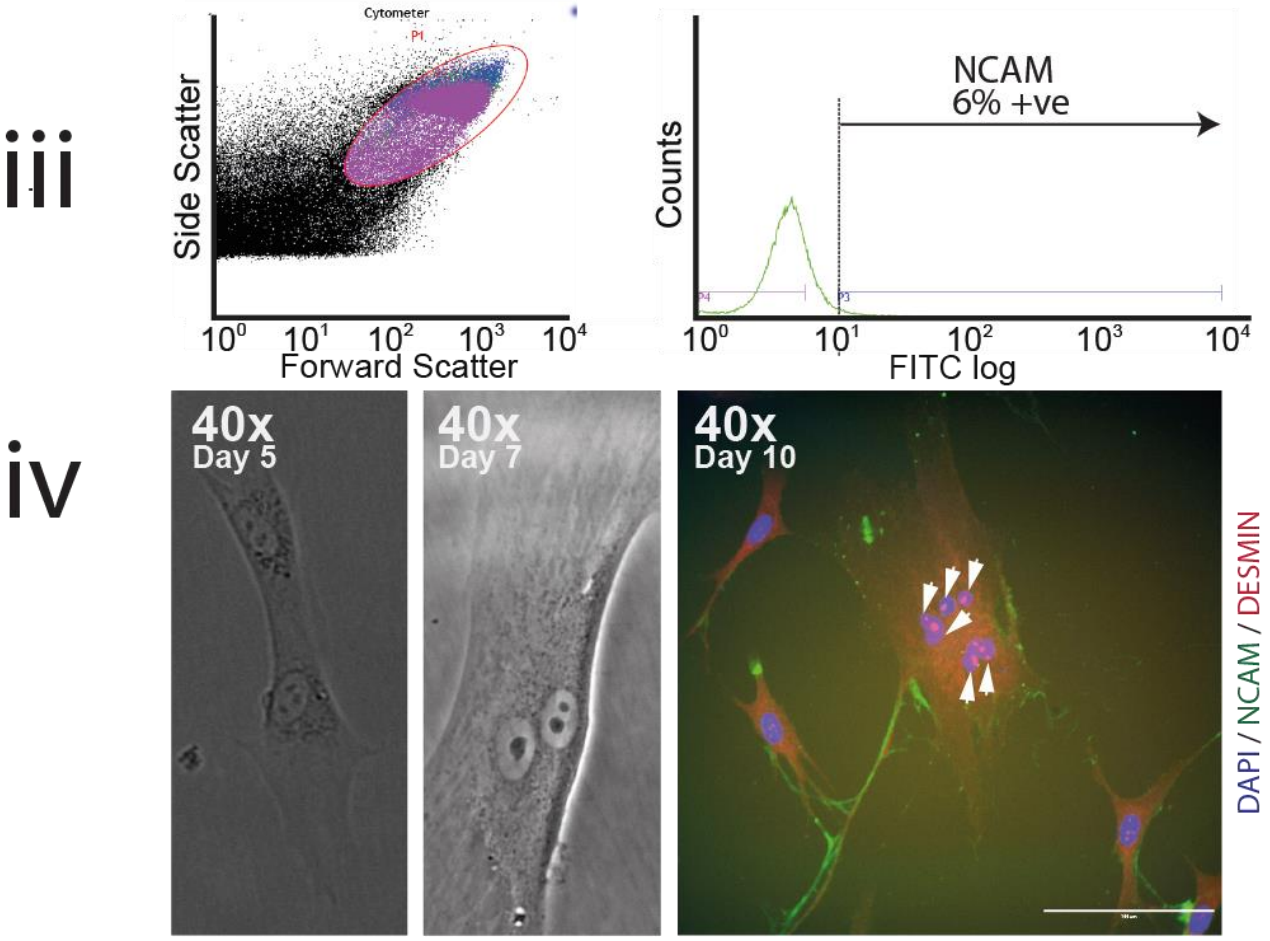

Figure 5.6: Fibroblasts were transdifferentiated to NCAM expressing myoblast-like cells which can be differentiated to form multinucleated myotubes. (i) Schematic of the experimental design. Fibroblasts were seeded at a density of $5x10^3/cm^2$ on day-1 in to two wells of a 6-well plate in myoblast growth medium (methods 2.3.4). A dose of 300ng *MYOD1* mRNA was added to both wells daily for four days. (ii) On day 4, one well was analysed by the IN Cell Analyser 2200 (GE Healthcare Life Sciences) to assess whether fibroblasts had begun to convert to myoblasts. It was found that 0.4% of fibroblasts had converted to NCAM-expressing myoblast cells. (iii) The second well, also on day 4, was therefore sorted via fluorescent activated cell sorting (FACS) for cells that positively expressed NCAM ($NCAM^{+ve}$) and those that did not express NCAM ($NCAM^{-ve}$). Gating was performed as described in methods 2.15.1.1. FACS analysis isolated 6% of the gated population that expressed NCAM ($NCAM^{+ve}$). Both the $NCAM^{+ve}$ enriched and $NCAM^{-ve}$ cells were plated into separate wells containing myoblast growth medium until day 7 and then the medium was switched to transdifferentiation medium (methods 2.3.5) for 3 days. (iv) On day 10, immunofluorescence analysis was performed to detect NCAM and DESMIN-expressing cells. It was found that in the $NCAM^{+ve}$ fraction, cells had fused to form DESMIN-expressing myotube-like fibres containing multiple nuclei (white arrowheads). The $NCAM^{-ve}$ cells did not express NCAM, DESMIN or contain multiple nuclei. Scale bars = 200µm (20X), 100µm (40X), 400µm (10X).

5.3. Discussion

The successful entry of *MYOD1* mRNA into HFFs is evidenced by a $9.7x10^4$-fold increase in *MYOD1* mRNA levels relative to untreated HFFs that occurs following the single addition of mRNA. The large increase in mRNA levels may be attributable to the ability for *MYOD1* protein to activate its own transcription [187]. One mechanism by which *MYOD1* reportedly achieves this is by increasing p21 expression which represses cyclin dependent kinases (CDKs) that inhibit the transcription of *MYOD1* [188] thus creating an auto-regulatory loop for self-activated transcription. A second mechanism is that *MYOD1* increases the expression of myogenic transcription factors such as *MYOGENIN* and *MYF5* which subsequently auto- and cross-regulate one another's expression [150, 189]. The combination of these mechanisms may explain how *MYOD1* can achieve sufficiently high levels of MYOD1 protein following a single addition of mRNA. Generating an abundance of protein in a short space of time may represent one contributing factor that allows for rapid conversion of fibroblasts to a myoblast-like phenotype.

Fibroblasts were converted to myoblasts following the daily addition of *MYOD1* mRNA for three days. Comparing the kinetics of transdifferentiation to our reprogramming experiments on BJ fibroblasts, iPS cells were generated more rapidly in the reprogramming experiments that utilised M_3O mRNA (Figures 3.12, 3.18), a fusion protein between *OCT4* and the transcriptional activation domain of *MYOD1*. Conversely, using *OCT4* instead of M_3O increased the time it took to generate iPS cells (Figures 3.6, 3.11). These results complement the notion that the conversion of cell states can be enhanced when transcription factors are bound to or contain the transcriptional activation domain (TAD) of *MYOD1*. Our current thinking is that the TAD of *MYOD1* improves the accessibility of chromatin through the recruitment of epigenetic modifiers that facilitate transcription factor binding and activation

of genes at target loci, through chromatin remodelling and the erasure and re-establishment of epigenetic marks. With respect to myoblast transdifferentiation, the conversion of one cell state to another, for example fibroblasts to myoblasts, relies on the activation of an endogenous myogenic gene network that is facilitated by an increase in transcriptional activity at genes important for myogenesis. Our transdifferentiation experiments suggest that an endogenous myogenic gene network had been activated (Figures 5.4, 5.6) in that two markers, NCAM and DESMIN that fibroblasts do not express were upregulated following the addition of *MYOD1* mRNA. It would be beneficial to further these experiments by identifying epigenetic and genetic changes that occur in fibroblasts following the introduction of *MYOD1* mRNA to facilitate our understanding of the mechanisms that underlie the conversion of cell states.

Conversion of fibroblasts to myoblasts can be achieved after repeated addition of *MYOD1* mRNA but myogenic transcription factors or cell-surface markers are required to distinguish between myoblasts and unconverted fibroblasts. NCAM and DESMIN were found to be good markers that can distinguish between myoblasts and fibroblasts [190]. Interestingly DESMIN protein expression levels appear higher in myotubes than myoblasts when analysed by high-content screening. This suggests that increased DESMIN expression levels may be associated with a more terminally differentiated myoblastic state as myotubes represent a later developmental stage during myogenesis. DESMIN could therefore be used to determine the differentiation status of myoblasts during transdifferentiation.

The repeated addition of *MYOD1* mRNA into fibroblasts was found to induce transdifferentiation towards NCAM-expressing myoblast-like cells. Increasing the *MYOD1* mRNA dose from 200ng to 300ng per $5x10^3$ / cm^2 cells increased the myoblast conversion frequency that is probably attributable to a more efficient mRNA dose-per-cell ratio. Control

wells of fibroblasts that were left untreated, placed in myoblast and transdifferentiation medium or mock transfected with Stemfect transfection reagent and buffer did not contain NCAM-expressing cells based on two biological replicates. This confirms that *MYOD1* mRNA is the causative factor for driving myoblast transdifferentiation and not the components in the growth medium, the transfection reagent or due to spontaneous differentiation.

To functionally test whether the NCAM-expressing cells were indeed myoblasts, subpopulations of cells that did and did not express NCAM were sorted, through Fluorescence Activated Cell Sorting (FACS), into positive and negative fractions respectively and replated in myoblast growth medium. This was to done to enrich the population for myoblasts and to encourage the cells to proliferate in close proximity to one another. Placing the cells in transdifferentiation medium caused the cells plated from the positive fraction to fuse together to form multinucleated myotubes. The representative image provided (Figure. 5.6iv) verified that myotubes had formed as they expressed both NCAM and DESMIN and contained multiple nuclei (six shown) that had co-located within one cell. Cells replated from the negative fraction did not fuse nor form myotubes.

This research demonstrates a novel mRNA-mediated strategy for directly converting human fibroblasts to myoblasts. It also provides proof of concept that this controlled approach could be used to look at the function of a whole range of genes delivered by mRNA. The approach enables the study of other differentiation pathways and for the creation of other cell types free of genomic integrations.

Chapter 6.

General Discussion.

6.1 mRNA dose ramping enhances existing mRNA reprogramming methods by allowing iPS cells to be generated without passaging with accelerated kinetics and improved efficiencies

The aim of Chapter 3 was to determine whether we could develop a reprogramming method utilising mRNAs that could generate iPS cells from fibroblasts with greater efficiency and accelerated kinetics compared to existing methods. With regard to this objective, we successfully reprogrammed BJ fibroblasts four times with each successive reprogramming taking less time than the previous to generate iPS cells, owing to the modifications to the process that were implemented. The implementation of a flexible mRNA dose ramping approach to the reprogramming process was a key innovation that improved the survivability of cells over the course of reprogramming. This optimised method may benefit future reprogramming's by reducing the probability that cells succumb to apoptosis following the repeated daily addition of mRNAs.

Our results show that iPS cells can be generated from fibroblasts through mRNA-mediated reprogramming in seven days without passaging, compared to 16 days without passaging reported in the original mRNA reprogramming study [76]. This can be attributable to a technical improvement to the method regarding the dosing of mRNA into cells over the course of reprogramming. Rather than following a strict regime that dictates the mRNA dose to be added per day, our method relies on cellular cues to determine the amount of mRNA to be added. This means that the cells are introduced to gradually increased amounts of

mRNA in line with the rate of proliferation to attenuate cell death from overdosing cells with mRNA. This technical improvement helped to improve the kinetics of reprogramming compared to previous studies [39, 76, 168], cutting the time taken for mRNA-mediated iPS cells to emerge by as much as 11 days. Improving the kinetics of mRNA-mediated reprogramming is an important aspect in that it makes the process more high throughput and cuts down on the workload requirements. Most studies aim to accelerate the kinetics of reprogramming by incorporating a single passaging step in the methodology [39, 76] while some studies continuously passage the cells throughout reprogramming [56]. However, splitting the cells nullifies the efficiency of reprogramming as iPS cell colonies of independent clonal origin cannot be confirmed. It is reported that increasing the rate at which cells divide during reprogramming can shorten the time it takes to generate iPS cells [56]. That study attributes this to an increased probability for undefined stochastic events to occur that are necessary for reprogramming to take place. However, a consequence of encouraging cells to divide more rapidly is the diluting effect that cell division has on mRNA levels within the cells. This may lower mRNA levels in cells containing exogenous mRNAs to insufficient levels required to generate iPS cells, which has been avoided in our approach that does not implement a splitting step. Our method, that does not rely on a splitting step, may sustain sufficient mRNA levels in the cells for a longer period of time, which may explain why our method can generate iPS cells in a shorter timeframe. If splitting the cells is desirable then perhaps increasing the mRNA dose or more frequently adding mRNAs to the cells will ensure that sufficient levels of mRNA are maintained throughout reprogramming. However, increasing the daily dose of mRNAs or the frequency of mRNA additions to reprogramming cultures could add to the prevalent cytotoxic and pro-apoptotic pressures that cells already face during reprogramming. We focused on generating iPS cells without a passaging step and found that mRNA dose ramping efficiently maintains cells in a balance between a proliferative and apoptotic state allowing for more optimal control over the

mRNA dose per cell ratio. This approach better sustains a consistent concentration of mRNA throughout reprogramming, a finding that has been shown to improve the efficiency of generating iPS cells [39]. Striking this balance efficiently generated iPS cells with improved kinetics and efficiency compared to reprogrammings that did not employ a dose ramping regimen. A study by Warren et al [39] employed a strict dose ramping regimen however there were three key differences to our method. Firstly, we removed a splitting step, secondly the mRNA concentration we used throughout was much lower (200-300ng/ml compared to 600ng/ml) and finally our reprogramming cell cultures were maintained in 1ml of media, as opposed to 0.5ml, in a 6-well plate format during the early stages of reprogramming. This is interesting because even though we used the same BJ fibroblast cell line and the 6-factor reprogramming premix mRNA (ABP-SC-6FMRNA) that is referenced in their study, I found that the addition of this mRNA to a concentration of 400ng/ml or higher would reproducibly induce widespread cell death. This occurred even in the presence of increased B18R levels or additional MEFs that act to counteract cytotoxicity. This suggests that there are other variables for example cell density, age and viability that impact a cell's ability to tolerate the stresses induced by the addition of mRNA and furthermore its ability to be reprogrammed. In essence, reprogrammings can exhibit variations in kinetics and efficiencies despite using the same cell line and the same mRNAs highlighting either the process is stochastic or that there are potential unconsidered variables that impact the process. Our method is more accommodating than existing methods as it considers more of these variables such as proliferative capacity and cell viability throughout reprogramming.

While efforts have been made to gain insights in to the mechanisms that drive reprogramming including the role of the reprogramming factors *OCT4, SOX2, KLF4* and *cMYC* [52, 58, 61-63], basic research is still required that is focused on obtaining detailed, molecular insights into the reprogramming process. It has been shown that reprogramming

is facilitated when transcription factors are bound to potent transcriptional activation domains such as that of *MYOD1* [68]. We also found this to be the case and demonstrated that the kinetics of reprogramming could be improved when *OCT4* was replaced with M_3O, comprising a fusion protein between *OCT4* and the TAD of *MYOD1*, and thus supports the notion that reprogramming can be accelerated via better recruitment of chromatin modifying proteins.

In addition to reprogramming kinetics, the efficiency is also important. Low efficiencies hinder the ability to study reprogramming intermediates that provide insights into the mechanisms that underlie the process. Improving the efficiency of reprogramming is important considering that iPS cells exhibit heterogeneity, genetic instability and display varying levels of epigenetic reprogramming [191]. In a study that characterised 20 hESC lines and 12 iPS cell lines it was found that each cell line contained several genes that were expressed at notably different levels [191]. Another study found that heterogeneity could be observed in iPS cell lines that had been derived from the same individual [192]. In line with these findings, we found that two iPS cell lines we had created displayed notable differences. For example, the 5AB PiPS and 7AB PiPS cell lines reproducibly displayed differences in the expression of SSEA-3, 75% and 98% respectively despite expressing similar levels of SSEA-1. This could suggest that the 7AB PiPS cells are more refractory to differentiation or that they may contain a genomic abnormality despite being karyotypically normal and not displaying an abnormal copy number for *BCL2L1*. The 5AB PiPS cell line also did not express *GATA2, ISL1* or *PAX6* when induced to differentiate spontaneously as embryoid bodies for ten days highlighting differences regarding their capacity to differentiate. Functional heterogeneity amongst iPS cell lines has been previously documented [192]. In this study, it was suggested that differences in the functional properties of iPS cells may have been caused by epigenetic differences. It is conceivable that

the epigenetic status of the 5AB PiPS and 7AB PiPS cell lines had been erased and remodelled to different extents, which may have influenced their characteristic differences. Bisulphite sequencing would have helped to evaluate the phenotypic differences observed between iPS cell lines. For example, why were there differences in mRNA levels between two clonal lines (Figure. 3.9) derived from the same reprogramming? In addition, why did the 7AB PiPS cell line express SSEA-3 in 98% of the cells after 5 days in culture – is it less susceptible to differentiation? Analysing patterns of DNA methylation in the iPS cell lines derived from BJ fibroblasts through bisulphite sequencing would have complemented their characterisation. It would allow for the epigenetic status of the iPS cell lines generated to be compared between each other and to control pluripotent stem cell lines to provide insights into the similarities and differences between their epigenetic landscapes. It may transpire that the characteristic differences observed between iPS cell lines is attributable to varying levels of epigenetic remodelling that has occurred following reprogramming.

6.2 mRNAs can achieve partial reprogramming of neuroblastoma cells while fully reprogrammed iPS cells can be generated when the Sendai virus delivery vector is used

Following rounds of mRNA-mediated neuroblastoma reprogramming, neuroblastoma-derived iPS cells (SeViPS-NB2) were successfully generated using Sendai viral methods. SK-N-SH cells were sent to Anna Falk's group at the Karolinska Institute in Sweden to be reprogrammed using the Sendai virus as a means for introducing the reprogramming factors: *OCT4, SOX2, KLF4, cMYC* into SK-N-SH cells. The neuroblastoma-derived iPS cells generated were sent back to us at passage fifteen. When characterised by qPCR these cells were found to endogenously express genes associated with pluripotency, *OCT4, SOX2, KLF4, cMYC, LIN28* and *NANOG*. The cells were also capable of tri-lineage differentiation when directly differentiated as embryoid bodies for ten days in defined conditions (Table 2.4). The cells also expressed SSEA-1, SSEA-3, SSEA-4, TRA-1-60 and TRA-1-81 to similar levels expressed in undifferentiated hESCs signifying that the SeViPS-NB2 cells were indeed pluripotent. The gene expression and cell surface marker expression profile of the SeViPS-NB2 cell line is consistent with another study that derived iPS cells from neuroblastoma cell lines [193].

In addition to reprogramming SK-N-SH cells using Sendai viral vectors, we also tested the applicability of using mRNAs to reprogramme SK-N-SH cells and we have demonstrated that a population of cells within the cancer cell population can be induced to express TRA-1-60, a marker of pluripotent stem cells, following the repeated addition of reprogramming factor mRNAs (ABP-SC-SEIPSET). Interestingly, this was achieved when using an mRNA cocktail that did not include M_3O mRNA, which raises a question over the suitability of using potent transcriptional activation domains to open up chromatin when reprogramming SK-N-SH cells. Transcription factors bound to TADs improve chromatin accessibility through the recruitment of epigenetic modifiers that facilitate the activation of repressed genes, in some

cases thousands of genes [194]. However this is somewhat uncontrolled in that the genes that are activated are either consistent with the role of the transcription factor that is bound to the TAD or through indirect interactions. It is possible that transcription factors bound to TADs can activate the transcription of apoptosis-inducing genes in SK-N-SH cells and this may inhibit the success of reprogramming. However, the induction of TRA-1-60 expression within a subpopulation of SK-N-SH cells indicated that the SK-N-SH cell line may be reprogrammable using non-integrating techniques. Despite the induction of TRA-1-60, these cells did not form a stable iPS cell line and following continuous passaging reverted back to a phenotype indistinguishable from the parental SK-N-SH cells. This suggests that the cells had undergone partial reprogramming or that the TRA-1-60 population contained a sub-population of cells that were incompletely reprogrammed and may have outcompeted any bona fide iPS cells that had emerged. The TRA-1-60 population was found to contain a sub-population of cells that may have been partially reprogrammed. During reprogramming, *mWASABI* mRNA is added in to the cell cultures to monitor the uptake of mRNA into the cells and is lost in the cells that convert to a fully reprogrammed state [179, 195]. We found that the TRA-1-60^{+ve} cells induced during SK-N-SH reprogramming contained a subpopulation of *mWASABI*$^{+ve}$ cells that may have represented a partially reprogrammed state, which contributed to a reduction in reprogramming efficiency.

Another study that sought to reprogramme a set of neuroblastoma cell lines reported difficulties in establishing iPS cell lines, reporting only one of four neuroblastoma cell lines examined successfully generating iPS cells [193]. There is a possibility that not all cancer cell lines possesses the ability to obtain the characteristics of iPS cells, however our work suggests that the mechanisms required to execute reprogramming of the SK-N-SH cell line are not well understood. Several reports suggest that somatic cell lines that endogenously express combinations of the reprogramming factors *OCT4, SOX2, KLF4* and *cMYC* are more

susceptible to reprogramming [196-198]. We found that SK-N-SH cells endogenously express *cMYC* but do not express any of the other reprogramming factors and this may contribute in part to the difficulties encountered in reprogramming this cell line.

Two reasons why mRNA transfection, unlike Sendai viral delivery of the reprogramming factors, was incapable of generating iPS cells from SK-N-SH cells, possibly include transfection reagent-related cytotoxicity and the transient nature of mRNAs during the transfection procedure. Considering that 200ng/ml of 6-factor premix mRNA (ABP-SC-6FMRNA) was enough to succumb SK-N-SH cells to apoptosis suggests that perhaps a lower mRNA dose-per-cell ratio is more favourable when reprogramming this particular cell line. Using a smaller dose however may fail to achieve sufficient mRNA levels required to execute reprogramming as discussed previously.

Incomplete reprogramming may occur as a result of cells receiving insufficient levels of mRNA [76] that can occur if the mRNA dose is not increased as the cells proliferate. To combat this, neuroblastoma reprogramming was initiated on SK-N-SH cells following a period of treatment with retinoic acid. We found that retinoic acid induced growth arrest in treated cells (Figure. 4.5), an effect observed in both SK-N-SH cells [174] and other neuroblastoma cell lines [173]. This allowed for the transfection phase of reprogramming to be elongated but this had no positive effect on the outcome of reprogramming. Reprogramming could not be achieved in SK-N-SH cells following the addition of the Allele Biotech 6-factor reprogramming premix (ABP-SC-6FMRNA), a finding that was shown in our work and in agreement with others [39] to enhance the reprogramming of fibroblasts. This highlights disparities between fibroblast and neuroblastoma reprogramming in that while iPS cell induction from fibroblasts can be enhanced by optimising the mRNA type, cell densities and dose ramping, this is not directly translational to neuroblastoma cells.

We found that *cMYC* mRNA levels decreased following the independent or collective addition of reprogramming factor mRNAs (*OCT4, SOX2, KLF4, cMYC, LIN28* and *NANOG*) into SK-N-SH cells. This finding was consistent between both the Allele biotech 6-factor reprogramming premix mRNA (ABP-SC-6FMRNA) and the mRNAs in-vitro transcribed from the Allele Biotech IVT templates (ABP-SC-SEIPSET). One report explains that *cMYC* and *MYCN* expression levels are inversely correlated [199] therefore the repression of endogenous *cMYC* mRNA levels may be as a result of *MYCN* amplification. It is unknown whether the introduction of exogenous mRNAs in SK-N-SH cells results in *MYCN* amplification although this mechanism may explain why *cMYC* mRNA levels are repressed following the addition of exogenous mRNAs. Whether *MYCN* amplification in SK-N-SH cells inhibits reprogramming, is something that requires testing. It has recently been demonstrated that *cMYC* has a general role in amplifying gene expression for genes with an active promoter in tumour cells [200]. Overexpressing *cMYC* in tumour cells may prevent the cells from being reprogrammed by encouraging the active transcription of oncogenes [201] that have been reported to interfere with mechanisms, such as the mesenchymal to epithelial transition, that are necessary for reprogramming to take place. Considering it has been reported in mouse that cMyc is dispensable for reprogramming mouse fibroblasts [202], it would be appropriate to determine whether reprogramming without *cMYC* promotes reprogramming of neuroblastoma cells. A greater understanding of the complex genetic and epigenetic barriers to reprogramming would greatly assist in the generation of mRNA-mediated neuroblastoma-derived iPS cells.

We showed that reprogramming BJ fibroblasts can be achieved in 7 days following the repeated addition of mRNAs encoding the reprogramming factors: *M_3O, SOX2, KLF4, cMYC, LIN28* and *NANOG*. This increases to ~17 days when the reprogramming factors are introduced into BJ fibroblasts using the Sendai virus [203] or 6 weeks when introduced into

SK-N-SH cells, a length of time consistent with other reports [193]. One reason why it may take longer to reprogramme SK-N-SH cells compared to BJ fibroblasts is due to epigenetic differences between the two cell lines. A larger degree of chromatin remodelling is necessary in SK-N-SH cells before an endogenous pluripotency network can be activated. Therefore it may be beneficial to use an epigenetic modifier, such as 5-azacytidine, during the reprogramming of SK-N-SH cells to facilitate the generation of iPS cells. The other option would be to reprogramme a neuroblastoma cell line that endogenously expresses one or more of the reprogramming factors such as SK-N-AS or SK-N-DZ that express *NANOG*, *KLF4* and *NANOG* (SK-N-AS) and *OCT4,* and *KLF4* (SK-N-DZ) respectively [193].

Overall, our findings support the possibility that mRNA reprogramming can generate iPS cells from cell lines other than fibroblasts, such as those with a disease genotype, and this in the future may lead to the creation of integration-free iPS cells that provide insights into the molecular mechanisms that underlie disease development.

6.3 *MYOD1* mRNA transdifferentiates fibroblasts to myoblasts that fuse to form multi-nucleated myotubes

We have provided proof-of-principle that mRNAs can be used to direct cell fate by successfully and reproducibly transdifferentiating fibroblasts to myoblasts through the repeated addition of *MYOD1* mRNA. The resultant myoblasts were functionally characterised by their ability to differentiate to form multinucleated myotubes. We have also provided a methodology involving cell sorting that facilitates the fusing of myoblasts that can be used to validate the differentiation capacity of these cells. Validating the formation of myotubes was based on the co-location of multiple nuclei in one cell that expressed muscle markers, NCAM and DESMIN. The success of our study warrants the exploration of a broader number of mRNAs that may be used to direct cell fate, to facilitate a greater understanding of the mechanisms involved during transdifferentiation.

Myotubes are derived from mono-nucleated myoblasts that have fused together and share a single cell membrane [204]. This is the only mRNA approach on human fibroblasts that has been reported and therefore provides proof of principle that mRNAs can directly convert fibroblasts to an alternative somatic cell type. The timescale for this approach was consistent with two other reports that used mRNA to transdifferentiate somatic cells to myoblasts although these reports used alternative transfection and transdifferentiation mediums and did not use human fibroblasts. The first report [76] isolated myoblasts by differentiating iPS cells to an unknown cell type(s) before transdifferentiating with *MYOD1* mRNA and the second report [205] transdifferentiated murine fibroblasts. It is impossible to determine whether the spontaneously differentiated population in the first report was indeed enriched for fibroblasts as no characterisation on this population was performed. Another problem is that it is conceivable that the starting population may have contained

myoblasts as a result of spontaneous differentiation. Without any characterisation on the differentiated population of cells it is difficult to ascertain the somatic cell type(s) that were transdifferentiated and therefore it cannot be said that fibroblasts were indeed the cell type that converted to myoblasts. The second report was performed on murine fibroblasts providing proof of principle for investigating whether the same could be achieved in human fibroblasts, the results of which have been shown here. Our results show direct conversion of human fibroblasts to myoblasts but also provide proof of concept that mRNAs can be used a tool to convert one cell type to another. There is no obvious reason as to why this approach could not be used to look at differentiation pathways or the function of other genes, particularly when other reports of transdifferentiation, for example to the neural crest [93] or cardiomyocytes [91], can be achieved by overexpressing a select few defined factors.

Myoblast transdifferentiation has been performed using an inducible system comprising a tetracycline-regulated lentiviral delivery vector encoding *MYOD1* [194] that allows for the timing and magnitude of *MYOD1* expression to be controlled. This study tested whether the kinetics of transdifferentiation could be improved by using engineered variants of the *MYOD1* vector containing different transcriptional activation domains (TADs). All constructs containing variants of the TAD had improved kinetics compared to wildtype *MYOD1* however the fastest conversion rate was achieved after 10 days. We found that myoblasts could be generated from fibroblasts using wildtype *MYOD1* mRNA by day 7. The difference in kinetics may be attributable to the different delivery mechanisms used to introduce the *MYOD1* transcription factor into fibroblasts, a finding consistent between delivery methods used for reprogramming [206].

In addition to high-content screening, which is typically performed to identify the presence of transdifferentiated myoblast-like cells, I extended the characterisation to functionally test the myoblast-like cell's capacity to differentiate in to multinucleated myotubes. This presented a problem given the myoblast conversion frequencies from two separate experiments were 0.08% and 0.4% based on $NCAM^{+ve}$ expression. This meant that there was considerable space between converted myoblasts that limited the number of myoblast fusion events that could take place. Two other studies have reported myogenic conversion frequencies of 25% using cDNA [148] and 10%-40% using *MYOD1* mRNA [76]. In the mRNA study, the quantification of efficiency was calculated based on adding the number of nuclei that expressed Myogenin to the number of cells that expressed Myosin Heavy Chain, making comparison difficult to our work that based efficiency on the number of cells that expressed NCAM. In our work, generating myotubes was made possible by sorting the cells for NCAM prior to the addition of the transdifferentiation medium to enrich the population for myoblasts and therefore increasing the likelihood that myoblasts fusion events would occur. Following this strategy gave rise to multinucleated myotubes, presumably because multiple myoblasts were now within close proximity to one another. As myoblasts and myotubes both express NCAM and DESMIN it would be beneficial to have expanded the panel of markers to further distinguish between the two cell phenotypes. Immunostaining with myosin heavy chain and Phalloidin would have demonstrated the striated pattern that is characteristic of *ACTIN-MYOSIN* banding found in myotubes [207]. The electrophysiological competence of myotubes could be characterised through patch clamping that would test whether the myotubes contract when electrically stimulated, a characteristic of functional skeletal muscle. Staining the myotubes for Myosin Heavy Chain, a skeletal muscle marker, and Phalloidin that binds to filamentous-Actin to highlight the striated pattern characteristic of muscle fibres [208], would have further facilitated unambiguous validation.

Further alterations to the methodology that we had implemented that are in contrast to the reports of other transdifferentiation experiments include the use of different mediums used throughout transdifferentiation. The medium we used when mRNAs were added to the cells had the composition of a typical myoblast growth medium containing bFGF and human insulin solution while the transdifferentiation medium contained only DMEM F12 and insulin. These mediums had distinctly different compositions to the DMEM 10% FCS or Opti-MEM-based mediums that have been used in other studies but were chosen because previous attempts to transdifferentiate fibroblasts in DMEM 10% FCS had proven unsuccessful. Nevertheless, myoblast conversion did not occur in the absence of *MYOD1* mRNA when fibroblasts were cultured in the myoblast growth medium or transdifferentiation mediums alone. Nor did they convert to myoblasts following four, once-daily mock transfections or as a result of spontaneous differentiation determined by the absence of NCAM and DESMIN expressing cells in these conditions. This suggests that *MYOD1* mRNA is they key component required for myoblast conversion and acts as proof of principle for mRNA-mediated transdifferentiation. This opens up the door for further transdifferentiation studies to be performed using other differentiation-specific mRNAs to direct fibroblasts or other somatic cell types to alternative cell fates.

6.4 Concluding Remarks

We have shown that mRNAs are an efficient tool for reprogramming and transdifferentiating fibroblasts. Reprogramming can be enhanced by using mRNAs encoding transcription factors bound to potent transcriptional activation domains that better facilitate the recruitment of chromatin modifying proteins. Reprogramming can also be accelerated by employing a dose ramping approach that improves the survivability of cells during the addition of mRNAs by reducing the number of cells that succumb to mRNA-induced apoptosis. Further improvement to the kinetics and efficiency of reprogramming could be facilitated by improving our understanding of the underlying mechanisms, such as the temporal requirements of factor expression, required to successfully generate iPS cells. One study investigated the temporal requirements of the reprogramming factors required to generate iPS cells using lentiviral vectors encoding four reprogramming factors (*OCT4, SOX2, KLF4* and *cMYC*) bound to fluorescent proteins [53]. However, the study did not elucidate the timings that the reprogramming factors should be added or the length of sustained overexpression required for each reprogramming factor. Understanding when the reprogramming factors are and are not required will benefit reprogramming in two ways. Firstly, it will mitigate mRNA-induced cytotoxicity by lowering the daily dose of mRNA used throughout reprogramming as a consequence of removing unnecessary reprogramming factors from the mRNA cocktail. Secondly, it will enable us to gain insights into the mechanisms involved in the induction of pluripotency that may help to make it easier to reprogramme disease cell lines in the future.

Following on from the successful generation of iPS cells derived from the SK-N-SH neuroblastoma cell line using the Sendai virus (SeViPS-NB2), it is conceivable that with further optimisation, an mRNA approach to reprogramming SK-N-SH cells will be achieved

quickly and efficiently. Neuroblastoma cells appear to be more resistant to cellular reprogramming induced by exogenous factors translated from mRNA compared to those delivered using Sendai viral vectors. Gaining insight into the mechanisms involved in epigenetic reprogramming of cancer cells may reveal underlying mechanisms involved in cancer cell resistance to reprogramming when using different delivery methods, such as mRNA or the Sendai virus. In addition, it would be interesting to assess the consequences of differentiating the SeViPS-NB2 cell line in the context of the neural crest to study the behaviour of iPS cells carrying a neuroblastoma genome. Differentiation toward the disease cell of origin may help to recreate the developmental conditions required to model aspects of neuroblastoma development.

The success of mRNA-mediated transdifferentiation acts as a proof-of-concept for using mRNAs as a tool for converting the phenotype of one cell to another. It would be beneficial to apply this proof-of-concept to an array of other genes so that further platforms for studying the mechanisms that underlie differentiation pathways can be created. Recently it has been demonstrated that the overexpression of *SOX10* in the presence of epigenetic modifiers and growth factors within human fibroblasts is sufficient to induce a neural crest phenotype [155]. In line with generating a panel of integration-free iPS cells derived from SK-N-SH cells, it would seem pertinent to determine whether *SOX10* mRNA could be used to differentiate SeViPS-NB2 cells toward the neural crest.

Chapter 7.

References.

1. Thomson, J.A., et al., *Embryonic Stem Cell Lines Derived from Human Blastocysts.* Science, 1998. **282**(5391): p. 1145-1147.
2. James, D., et al., *TGFbeta/activin/nodal signaling is necessary for the maintenance of pluripotency in human embryonic stem cells.* Development, 2005. **132**(6): p. 1273-82.
3. Gaarenstroom, T. and C.S. Hill, *TGF-beta signaling to chromatin: how Smads regulate transcription during self-renewal and differentiation.* Semin Cell Dev Biol, 2014. **32**: p. 107-18.
4. Pauklin, S. and L. Vallier, *Activin/Nodal signalling in stem cells.* Development, 2015. **142**(4): p. 607.
5. Jin, G.P., et al., *Stem cell pluripotency and transcription factor Oct4.* Cell Res, 2002. **12**(5-6): p. 321-329.
6. Rodda, D.J., et al., *Transcriptional Regulation of Nanog by OCT4 and SOX2.* Journal of Biological Chemistry, 2005. **280**(26): p. 24731-24737.
7. Boyer, L.A., et al., *Core transcriptional regulatory circuitry in human embryonic stem cells.* Cell, 2005. **122**(6): p. 947-56.
8. Liu, N., et al., *Molecular mechanisms involved in self-renewal and pluripotency of embryonic stem cells.* J Cell Physiol, 2007. **211**(2): p. 279-86.
9. Itskovitz-Eldor, J., et al., *Differentiation of human embryonic stem cells into embryoid bodies compromising the three embryonic germ layers.* Mol Med, 2000. **6**(2): p. 88-95.
10. Thomson, J.A., et al., *Isolation of a primate embryonic stem cell line.* Proceedings of the National Academy of Sciences of the United States of America, 1995. **92**(17): p. 7844-7848.
11. Graves, K.H. and R.W. Moreadith, *Derivation and characterization of putative pluripotential embryonic stem cells from preimplantation rabbit embryos.* Mol Reprod Dev, 1993. **36**(4): p. 424-33.
12. Notarianni, E., et al., *Derivation of pluripotent, embryonic cell lines from the pig and sheep.* J Reprod Fertil Suppl, 1991. **43**: p. 255-60.
13. Notarianni, E., et al., *Maintenance and differentiation in culture of pluripotential embryonic cell lines from pig blastocysts.* J Reprod Fertil Suppl, 1990. **41**: p. 51-6.
14. Evans, M.J. and M.H. Kaufman, *Establishment in culture of pluripotential cells from mouse embryos.* Nature, 1981. **292**(5819): p. 154-156.
15. Shevinsky, L.H., et al., *Monoclonal antibody to murine embryos defines a stage-specific embryonic antigen expressed on mouse embryos and human teratocarcinoma cells.* Cell, 1982. **30**(3): p. 697-705.
16. Kannagi, R., et al., *Stage-specific embryonic antigens (SSEA-3 and -4) are epitopes of a unique globo-series ganglioside isolated from human teratocarcinoma cells.* Embo j, 1983. **2**(12): p. 2355-61.
17. Andrews, P.W., *Retinoic acid induces neuronal differentiation of a cloned human embryonal carcinoma cell line in vitro.* Developmental Biology, 1984. **103**(2): p. 285-293.
18. Draper, J.S., et al., *Surface antigens of human embryonic stem cells: changes upon differentiation in culture.* Journal of Anatomy, 2002. **200**(3): p. 249-258.
19. Shamblott, M.J., et al., *Derivation of pluripotent stem cells from cultured human primordial germ cells.* Proceedings of the National Academy of Sciences of the United States of America, 1998. **95**(23): p. 13726-13731.
20. Hanna, J., et al., *Human embryonic stem cells with biological and epigenetic characteristics similar to those of mouse ESCs.* Proc Natl Acad Sci U S A, 2010. **107**(20): p. 9222-7.

21. Brons, I.G., et al., *Derivation of pluripotent epiblast stem cells from mammalian embryos.* Nature, 2007. **448**(7150): p. 191-5.
22. Martin, G.R., *Isolation of a pluripotent cell line from early mouse embryos cultured in medium conditioned by teratocarcinoma stem cells.* Proc Natl Acad Sci U S A, 1981. **78**(12): p. 7634-8.
23. Ying, Q.L., et al., *BMP induction of Id proteins suppresses differentiation and sustains embryonic stem cell self-renewal in collaboration with STAT3.* Cell, 2003. **115**(3): p. 281-92.
24. Silva, J. and A. Smith, *Capturing Pluripotency.* Cell, 2008. **132**(4): p. 532-536.
25. Silva, J., et al., *Nanog Is the Gateway to the Pluripotent Ground State.* Cell, 2009. **138**(4): p. 722-737.
26. Takahashi, K., et al., *Induction of Pluripotent Stem Cells from Adult Human Fibroblasts by Defined Factors.* Cell, 2007. **131**(5): p. 861-872.
27. Maherali, N., et al., *Directly reprogrammed fibroblasts show global epigenetic remodeling and widespread tissue contribution.* Cell Stem Cell, 2007. **1**(1): p. 55-70.
28. Papp, B. and K. Plath, *Epigenetics of reprogramming to induced pluripotency.* Cell, 2013. **152**(6): p. 1324-1343.
29. Apostolou, E. and K. Hochedlinger, *Chromatin Dynamics during Cellular Reprogramming.* Nature, 2013. **502**(7472): p. 462-471.
30. Dong, X. and Z. Weng, *The correlation between histone modifications and gene expression.* Epigenomics, 2013. **5**(2): p. 113-116.
31. Olins, D.E. and A.L. Olins, *Chromatin history: our view from the bridge.* Nat Rev Mol Cell Biol, 2003. **4**(10): p. 809-14.
32. Eberharter, A. and P.B. Becker, *Histone acetylation: a switch between repressive and permissive chromatin: Second in review series on chromatin dynamics.* EMBO Reports, 2002. **3**(3): p. 224-229.
33. Zhou, Y., et al., *Epigenetic modifications of stem cells: a paradigm for the control of cardiac progenitor cells.* Circ Res, 2011. **109**(9): p. 1067-81.
34. Vierbuchen, T., et al., *Direct conversion of fibroblasts to functional neurons by defined factors.* Nature, 2010. **463**(7284): p. 1035-1041.
35. Ieda, M., et al., *Direct Reprogramming of Fibroblasts into Functional Cardiomyocytes by Defined Factors.* Cell, 2010. **142**(3): p. 375-386.
36. Takahashi, K. and S. Yamanaka, *Induction of pluripotent stem cells from mouse embryonic and adult fibroblast cultures by defined factors.* Cell, 2006. **126**(4): p. 663-76.
37. Fidalgo, M., et al., *Zfp281 mediates Nanog autorepression through recruitment of the NuRD complex and inhibits somatic cell reprogramming.* Proc Natl Acad Sci U S A, 2012. **109**(40): p. 16202-7.
38. Hahn, S. and H. Hermeking, *ZNF281/ZBP-99: a new player in epithelial-mesenchymal transition, stemness, and cancer.* J Mol Med (Berl), 2014. **92**(6): p. 571-81.
39. Warren, L., et al., *Feeder-Free Derivation of Human Induced Pluripotent Stem Cells with Messenger RNA.* Sci. Rep., 2012. **2**.
40. Solozobova, V. and C. Blattner, *p53 in stem cells.* World Journal of Biological Chemistry, 2011. **2**(9): p. 202-214.
41. Kawamura, T., et al., *Linking the p53 tumor suppressor pathway to somatic cell reprogramming.* Nature, 2009. **460**(7259): p. 1140-1144.
42. Banito, A., et al., *Senescence impairs successful reprogramming to pluripotent stem cells.* Genes Dev, 2009. **23**(18): p. 2134-9.
43. Rasmussen, M.A., et al., *Transient p53 suppression increases reprogramming of human fibroblasts without affecting apoptosis and DNA damage.* Stem Cell Reports, 2014. **3**(3): p. 404-13.
44. Brosh, R., et al., *p53 counteracts reprogramming by inhibiting mesenchymal-to-epithelial transition.* Cell Death Differ, 2013. **20**(2): p. 312-20.

45. Yu, J., et al., *Induced pluripotent stem cell lines derived from human somatic cells.* Science, 2007. **318**(5858): p. 1917-20.
46. Hu, Q., et al., *Memory in induced pluripotent stem cells: reprogrammed human retinal-pigmented epithelial cells show tendency for spontaneous redifferentiation.* Stem Cells, 2010. **28**(11): p. 1981-91.
47. Bar-Nur, O., et al., *Epigenetic memory and preferential lineage-specific differentiation in induced pluripotent stem cells derived from human pancreatic islet beta cells.* Cell Stem Cell, 2011. **9**(1): p. 17-23.
48. Kim, J.B., et al., *Direct reprogramming of human neural stem cells by OCT4.* Nature, 2009. **461**(7264): p. 649-653.
49. Gurdon, J.B., *The Developmental Capacity of Nuclei taken from Intestinal Epithelium Cells of Feeding Tadpoles.* Journal of Embryology and Experimental Morphology, 1962. **10**(4): p. 622-640.
50. Tsialikas, J. and J. Romer-Seibert, *LIN28: roles and regulation in development and beyond.* Development, 2015. **142**(14): p. 2397-404.
51. Nakagawa, M., et al., *Generation of induced pluripotent stem cells without Myc from mouse and human fibroblasts.* Nat Biotechnol, 2008. **26**(1): p. 101-6.
52. Li, R., et al., *A Mesenchymal-to-Epithelial Transition Initiates and Is Required for the Nuclear Reprogramming of Mouse Fibroblasts.* Cell Stem Cell, 2010. **7**(1): p. 51-63.
53. Papapetrou, E.P., et al., *Stoichiometric and temporal requirements of Oct4, Sox2, Klf4, and c-Myc expression for efficient human iPSC induction and differentiation.* Proceedings of the National Academy of Sciences of the United States of America, 2009. **106**(31): p. 12759-12764.
54. Schlaeger, T.M., et al., *A comparison of non-integrating reprogramming methods.* 2015. **33**(1): p. 58-63.
55. Eminli, S., et al., *Differentiation stage determines reprogramming potential of hematopoietic cells into iPS cells.* Nature genetics, 2009. **41**(9): p. 968-976.
56. Hanna, J., et al., *Direct cell reprogramming is a stochastic process amenable to acceleration.* Nature, 2009. **462**(7273): p. 595-601.
57. Rais, Y., et al., *Deterministic direct reprogramming of somatic cells to pluripotency.* Nature, 2013. **502**(7469): p. 65-70.
58. Buganim, Y., D.A. Faddah, and R. Jaenisch, *Mechanisms and models of somatic cell reprogramming.* Nature reviews. Genetics, 2013. **14**(6): p. 427-439.
59. Smith, Z.D., C. Sindhu, and A. Meissner, *Molecular features of cellular reprogramming and development.* Nat Rev Mol Cell Biol, 2016. **17**(3): p. 139-154.
60. Unternaehrer, Juli J., et al., *The Epithelial-Mesenchymal Transition Factor SNAIL Paradoxically Enhances Reprogramming.* Stem Cell Reports, 2014. **3**(5): p. 691-698.
61. Rahl, P.B., et al., *c-Myc regulates transcriptional pause release.* Cell, 2010. **141**(3): p. 432-45.
62. Xu, B., K. Zhang, and Y. Huang, *Lin28 modulates cell growth and associates with a subset of cell cycle regulator mRNAs in mouse embryonic stem cells.* RNA, 2009. **15**(3): p. 357-361.
63. Chappell, J. and S. Dalton, *Roles for MYC in the Establishment and Maintenance of Pluripotency.* Cold Spring Harbor Perspectives in Medicine, 2013. **3**(12): p. a014381.
64. Papp, B. and K. Plath, *Reprogramming to pluripotency: stepwise resetting of the epigenetic landscape.* Cell Research, 2011. **21**(3): p. 486-501.
65. Jaenisch, R. and R. Young, *Stem cells, the molecular circuitry of pluripotency and nuclear reprogramming.* Cell, 2008. **132**(4): p. 567-582.
66. Darr, H., Y. Mayshar, and N. Benvenisty, *Overexpression of NANOG in human ES cells enables feeder-free growth while inducing primitive ectoderm features.* Development, 2006. **133**(6): p. 1193-201.
67. Feng, B., et al., *Molecules that promote or enhance reprogramming of somatic cells to induced pluripotent stem cells.* Cell Stem Cell, 2009. **4**(4): p. 301-12.

68. Hirai, H., et al., *Radical Acceleration of Nuclear Reprogramming by Chromatin Remodeling with the Transactivation Domain of MyoD.* Stem cells (Dayton, Ohio), 2011. **29**(9): p. 1349-1361.
69. Becker, P.B. and J.L. Workman, *Nucleosome Remodeling and Epigenetics.* Cold Spring Harbor Perspectives in Biology, 2013. **5**(9): p. a017905.
70. Ban, H., et al., *Efficient generation of transgene-free human induced pluripotent stem cells (iPSCs) by temperature-sensitive Sendai virus vectors.* Proc Natl Acad Sci U S A, 2011. **108**(34): p. 14234-9.
71. Woltjen, K., et al., *piggyBac transposition reprograms fibroblasts to induced pluripotent stem cells.* Nature, 2009. **458**(7239): p. 766-70.
72. Yu, J., et al., *Human induced pluripotent stem cells free of vector and transgene sequences.* Science, 2009. **324**(5928): p. 797-801.
73. Okita, K., T. Ichisaka, and S. Yamanaka, *Generation of germline-competent induced pluripotent stem cells.* Nature, 2007. **448**(7151): p. 313-317.
74. Okita, K., et al., *Generation of mouse-induced pluripotent stem cells with plasmid vectors.* Nat. Protocols, 2010. **5**(3): p. 418-428.
75. Kim, D., et al., *Generation of Human Induced Pluripotent Stem Cells by Direct Delivery of Reprogramming Proteins.* Cell stem cell, 2009. **4**(6): p. 472-476.
76. Warren, L., et al., *Highly efficient reprogramming to pluripotency and directed differentiation of human cells with synthetic modified mRNA.* Cell Stem Cell, 2010. **7**(5): p. 618-30.
77. Leight, E.R. and B. Sugden, *Establishment of an oriP Replicon Is Dependent upon an Infrequent, Epigenetic Event.* Molecular and Cellular Biology, 2001. **21**(13): p. 4149-4161.
78. Harui, A., et al., *Frequency and Stability of Chromosomal Integration of Adenovirus Vectors.* Journal of Virology, 1999. **73**(7): p. 6141-6146.
79. Stadtfeld, M. and K. Hochedlinger, *Without a trace? PiggyBac-ing toward pluripotency.* Nat Meth, 2009. **6**(5): p. 329-330.
80. Li, X., et al., *Generation of pluripotent stem cells via protein transduction.* Int J Dev Biol, 2014. **58**(1): p. 21-7.
81. Robinton, D.A. and G.Q. Daley, *The promise of induced pluripotent stem cells in research and therapy.* Nature, 2012. **481**(7381): p. 295-305.
82. Bowman, M.C., S. Smallwood, and S.A. Moyer, *Dissection of individual functions of the Sendai virus phosphoprotein in transcription.* J Virol, 1999. **73**(8): p. 6474-83.
83. Feller, J.A., et al., *Comparison of identical temperature-sensitive mutations in the L polymerase proteins of sendai and parainfluenza3 viruses.* Virology, 2000. **276**(1): p. 190-201.
84. Angel, M. and M.F. Yanik, *Innate Immune Suppression Enables Frequent Transfection with RNA Encoding Reprogramming Proteins.* PLoS ONE, 2010. **5**(7): p. e11756.
85. Wong, M.-T. and S.S.L. Chen, *Emerging roles of interferon-stimulated genes in the innate immune response to hepatitis C virus infection.* Cell Mol Immunol, 2014.
86. Chakrabarti, A., B.K. Jha, and R.H. Silverman, *New insights into the role of RNase L in innate immunity.* J Interferon Cytokine Res, 2011. **31**(1): p. 49-57.
87. Durbin, A.F., et al., *RNAs Containing Modified Nucleotides Fail To Trigger RIG-I Conformational Changes for Innate Immune Signaling.* 2016. **7**(5).
88. Colamonici, O.R., et al., *Vaccinia virus B18R gene encodes a type I interferon-binding protein that blocks interferon alpha transmembrane signaling.* J Biol Chem, 1995. **270**(27): p. 15974-8.
89. Fusaki, N., et al., *Efficient induction of transgene-free human pluripotent stem cells using a vector based on Sendai virus, an RNA virus that does not integrate into the host genome.* Proceedings of the Japan Academy. Series B, Physical and Biological Sciences, 2009. **85**(8): p. 348-362.

90. Decker, C.J. and R. Parker, *A turnover pathway for both stable and unstable mRNAs in yeast: evidence for a requirement for deadenylation.* Genes Dev, 1993. **7**(8): p. 1632-43.
91. Shyu, A.B., M.E. Greenberg, and J.G. Belasco, *The c-fos transcript is targeted for rapid decay by two distinct mRNA degradation pathways.* Genes Dev, 1989. **3**(1): p. 60-72.
92. Nadeau, J.H. and B.A. Taylor, *Lengths of chromosomal segments conserved since divergence of man and mouse.* Proceedings of the National Academy of Sciences of the United States of America, 1984. **81**(3): p. 814-818.
93. Barbazuk, W.B., et al., *The Syntenic Relationship of the Zebrafish and Human Genomes.* Genome Research, 2000. **10**(9): p. 1351-1358.
94. Pandey, U.B. and C.D. Nichols, *Human Disease Models in Drosophila melanogaster and the Role of the Fly in Therapeutic Drug Discovery.* Pharmacological Reviews, 2011. **63**(2): p. 411-436.
95. Hackam, D.G. and D.A. Redelmeier, *Translation of research evidence from animals to humans.* Jama, 2006. **296**(14): p. 1731-2.
96. Perel, P., et al., *Comparison of treatment effects between animal experiments and clinical trials: systematic review.* BMJ : British Medical Journal, 2007. **334**(7586): p. 197-197.
97. Seok, J., et al., *Genomic responses in mouse models poorly mimic human inflammatory diseases.* Proc Natl Acad Sci U S A, 2013. **110**(9): p. 3507-12.
98. Suntharalingam, G., et al., *Cytokine storm in a phase 1 trial of the anti-CD28 monoclonal antibody TGN1412.* N Engl J Med, 2006. **355**(10): p. 1018-28.
99. Mak, I.W.Y., N. Evaniew, and M. Ghert, *Lost in translation: animal models and clinical trials in cancer treatment.* American Journal of Translational Research, 2014. **6**(2): p. 114-118.
100. Ebert, A.D., et al., *Induced pluripotent stem cells from a spinal muscular atrophy patient.* Nature, 2009. **457**(7227): p. 277-80.
101. Li, Li B., et al., *Trisomy Correction in Down Syndrome Induced Pluripotent Stem Cells.* Cell Stem Cell, 2012. **11**(5): p. 615-619.
102. Miyoshi, N., et al., *Defined factors induce reprogramming of gastrointestinal cancer cells.* Proc Natl Acad Sci U S A, 2010. **107**(1): p. 40-5.
103. Ebert, A.D., P. Liang, and J.C. Wu, *Induced pluripotent stem cells as a disease modeling and drug screening platform.* J Cardiovasc Pharmacol, 2012. **60**(4): p. 408-16.
104. Lorenz, M., et al., *BJ fibroblasts display high antioxidant capacity and slow telomere shortening independent of hTERT transfection.* Free Radic Biol Med, 2001. **31**(6): p. 824-31.
105. Miyoshi, N., et al., *Defined factors induce reprogramming of gastrointestinal cancer cells.* Proceedings of the National Academy of Sciences, 2010. **107**(1): p. 40-45.
106. Brennand, K.J., et al., *Modelling schizophrenia using human induced pluripotent stem cells.* Nature, 2011. **473**(7346): p. 221-5.
107. Moretti, A., et al., *Patient-specific induced pluripotent stem-cell models for long-QT syndrome.* N Engl J Med, 2010. **363**(15): p. 1397-409.
108. Nichols, J.E., et al., *Novel in vitro respiratory models to study lung development, physiology, pathology and toxicology.* Stem Cell Research & Therapy, 2013. **4**(1): p. S7.
109. Katt, M.E., et al., *In Vitro Tumor Models: Advantages, Disadvantages, Variables, and Selecting the Right Platform.* Frontiers in Bioengineering and Biotechnology, 2016. **4**: p. 12.
110. Kim, K., et al., *Epigenetic memory in induced pluripotent stem cells.* Nature, 2010. **467**(7313): p. 285-290.
111. Sommer, C.A., et al., *Excision of reprogramming transgenes improves the differentiation potential of iPS cells generated with a single excisable vector.* Stem Cells, 2010. **28**(1): p. 64-74.
112. Fainsod, A., H. Steinbeisser, and E.M. De Robertis, *On the function of BMP-4 in patterning the marginal zone of the Xenopus embryo.* The EMBO Journal, 1994. **13**(21): p. 5015-5025.
113. Marchant, L., et al., *The inductive properties of mesoderm suggest that the neural crest cells are specified by a BMP gradient.* Developmental Biology, 1998. **198**(2): p. 319-329.

114. Bond, A.M., O.G. Bhalala, and J.A. Kessler, *The Dynamic Role of Bone Morphogenetic Proteins in Neural Stem Cell Fate and Maturation.* Developmental neurobiology, 2012. **72**(7): p. 1068-1084.
115. Monsoro-Burq, A.H., R.B. Fletcher, and R.M. Harland, *Neural crest induction by paraxial mesoderm in Xenopus embryos requires FGF signals.* Development, 2003. **130**(14): p. 3111-24.
116. Mayor, R., R. Morgan, and M.G. Sargent, *Induction of the prospective neural crest of Xenopus.* Development, 1995. **121**(3): p. 767-77.
117. LaBonne, C. and M. Bronner-Fraser, *Neural crest induction in Xenopus: evidence for a two-signal model.* Development, 1998. **125**(13): p. 2403-14.
118. van Straaten, H.W., et al., *Effect of the notochord on the differentiation of a floor plate area in the neural tube of the chick embryo.* Anat Embryol (Berl), 1988. **177**(4): p. 317-24.
119. Haigo, S.L., et al., *Shroom Induces Apical Constriction and Is Required for Hingepoint Formation during Neural Tube Closure.* Current Biology, 2003. **13**(24): p. 2125-2137.
120. Kulesa, P.M. and S.E. Fraser, *Neural Crest Cell Dynamics Revealed by Time-Lapse Video Microscopy of Whole Embryo Chick Explant Cultures.* Developmental Biology, 1998. **204**(2): p. 327-344.
121. Kulesa, P.M. and S.E. Fraser, *In ovo time-lapse analysis of chick hindbrain neural crest cell migration shows cell interactions during migration to the branchial arches.* Development, 2000. **127**(6): p. 1161-1172.
122. Le Douarin, G.H., *The Neural Crest*. 1982, New York, NY: Cambridge University Press. 272.
123. Thiery, J.P., J.L. Duband, and A. Delouvée, *Pathways and mechanisms of avian trunk neural crest cell migration and localization.* Developmental Biology, 1982. **93**(2): p. 324-343.
124. Bernd, P., *Appearance of nerve growth factor receptors on cultured neural crest cells.* Dev Biol, 1985. **112**(1): p. 145-56.
125. Anderson, R.B., D.F. Newgreen, and H.M. Young, *Neural crest and the development of the enteric nervous system.* Adv Exp Med Biol, 2006. **589**: p. 181-96.
126. Estus, S., et al., *Altered gene expression in neurons during programmed cell death: identification of c-jun as necessary for neuronal apoptosis.* J Cell Biol, 1994. **127**(6 Pt 1): p. 1717-27.
127. Long, P.M., et al., *Differential Aminoacylase Expression in Neuroblastoma.* International journal of cancer. Journal international du cancer, 2011. **129**(6): p. 1322-1330.
128. Iwakura, H., et al., *Establishment of a novel neuroblastoma mouse model.* Int J Oncol, 2008. **33**(6): p. 1195-9.
129. Knoepfler, P.S., P.F. Cheng, and R.N. Eisenman, *N-myc is essential during neurogenesis for the rapid expansion of progenitor cell populations and the inhibition of neuronal differentiation.* Genes Dev, 2002. **16**(20): p. 2699-712.
130. Pattyn, A., et al., *The homeobox gene Phox2b is essential for the development of autonomic neural crest derivatives.* Nature, 1999. **399**(6734): p. 366-370.
131. Jiang, M., J. Stanke, and J.M. Lahti, *The Connections Between Neural Crest Development and Neuroblastoma.* Current topics in developmental biology, 2011. **94**: p. 77-127.
132. Garcia-Barceló, M., et al., *Association study of PHOX2B as a candidate gene for Hirschsprung's disease.* Gut, 2003. **52**(4): p. 563-567.
133. Amiel, J., et al., *Polyalanine expansion and frameshift mutations of the paired-like homeobox gene PHOX2B in congenital central hypoventilation syndrome.* Nat Genet, 2003. **33**(4): p. 459-61.
134. Weiss, W.A., et al., *Targeted expression of MYCN causes neuroblastoma in transgenic mice.* The EMBO Journal, 1997. **16**(11): p. 2985-2995.
135. Reiff, T., et al., *Neuroblastoma Phox2b Variants Stimulate Proliferation and Dedifferentiation of Immature Sympathetic Neurons.* The Journal of Neuroscience, 2010. **30**(3): p. 905-915.

136. Pei, D., et al., *Distinct Neuroblastoma-associated Alterations of PHOX2B Impair Sympathetic Neuronal Differentiation in Zebrafish Models.* PLoS Genet, 2013. **9**(6): p. e1003533.
137. Mosse, Y.P., et al., *Identification of ALK as a major familial neuroblastoma predisposition gene.* Nature, 2008. **455**(7215): p. 930-935.
138. Sauka-Spengler, T. and M. Bronner-Fraser, *A gene regulatory network orchestrates neural crest formation.* Nat Rev Mol Cell Biol, 2008. **9**(7): p. 557-568.
139. Wartiovaara, K., et al., *N-myc promotes survival and induces S-phase entry of postmitotic sympathetic neurons.* J Neurosci, 2002. **22**(3): p. 815-24.
140. Bowden, E.T., G.E. Stoica, and A. Wellstein, *Anti-apoptotic Signaling of Pleiotrophin through Its Receptor, Anaplastic Lymphoma Kinase.* Journal of Biological Chemistry, 2002. **277**(39): p. 35862-35868.
141. Hansford, L.M., et al., *Mechanisms of embryonal tumor initiation: Distinct roles for MycN expression and MYCN amplification.* Proceedings of the National Academy of Sciences of the United States of America, 2004. **101**(34): p. 12664-12669.
142. Chen, Y., et al., *Oncogenic mutations of ALK kinase in neuroblastoma.* Nature, 2008. **455**(7215): p. 971-974.
143. Castle, V.P., et al., *Expression of the apoptosis-suppressing protein bcl-2, in neuroblastoma is associated with unfavorable histology and N-myc amplification.* The American Journal of Pathology, 1993. **143**(6): p. 1543-1550.
144. Pang, Z.P., et al., *Induction of human neuronal cells by defined transcription factors.* Nature, 2011. **476**(7359): p. 220-223.
145. Pfisterer, U., et al., *Direct conversion of human fibroblasts to dopaminergic neurons.* Proc Natl Acad Sci U S A, 2011. **108**(25): p. 10343-8.
146. Taylor, S.M. and P.A. Jones, *Multiple new phenotypes induced in 10T 1 2 and 3T3 cells treated with 5-azacytidine.* Cell, 1979. **17**(4): p. 771-779.
147. Si, J., et al., *Chromatin remodeling is required for gene reactivation after Decitabine-mediated DNA hypomethylation.* Cancer research, 2010. **70**(17): p. 6968-6977.
148. Konieczny, S.F. and C.P. Emerson, Jr., *5-Azacytidine induction of stable mesodermal stem cell lineages from 10T1/2 cells: evidence for regulatory genes controlling determination.* Cell, 1984. **38**(3): p. 791-800.
149. Lassar, A.B., B.M. Paterson, and H. Weintraub, *Transfection of a DNA locus that mediates the conversion of 10T1/2 fibroblasts to myoblasts.* Cell, 1986. **47**(5): p. 649-56.
150. Davis, R.L., H. Weintraub, and A.B. Lassar, *Expression of a single transfected cDNA converts fibroblasts to myoblasts.* Cell, 1987. **51**(6): p. 987-1000.
151. Liu, Z., et al., *Experimental Studies on the Differentiation of Fibroblasts into Myoblasts induced by MyoD Genes in vitro.* International Journal of Biomedical Science : IJBS, 2008. **4**(1): p. 14-19.
152. Choi, J., et al., *MyoD converts primary dermal fibroblasts, chondroblasts, smooth muscle, and retinal pigmented epithelial cells into striated mononucleated myoblasts and multinucleated myotubes.* Proc Natl Acad Sci U S A, 1990. **87**(20): p. 7988-92.
153. Hausburg, F., et al., *Defining Optimized Properties of Modified mRNA to Enhance Virus- and DNA- Independent Protein Expression in Adult Stem Cells and Fibroblasts.* Cell Physiol Biochem, 2015. **35**(4): p. 1360-71.
154. Szabo, E., et al., *Direct conversion of human fibroblasts to multilineage blood progenitors.* Nature, 2010. **468**(7323): p. 521-6.
155. Kim, Y.J., et al., *Generation of multipotent induced neural crest by direct reprogramming of human postnatal fibroblasts with a single transcription factor.* Cell Stem Cell, 2014. **15**(4): p. 497-506.
156. Office, H. *The Humane Killing of Animals under Schedule 1 to the Animals (Scientific Procedures) Act 1986*. 1986.

157. Biedler, J.L., L. Helson, and B.A. Spengler, *Morphology and growth, tumorigenicity, and cytogenetics of human neuroblastoma cells in continuous culture.* Cancer Res, 1973. **33**(11): p. 2643-52.
158. Andrews, P.W., et al., *Pluripotent embryonal carcinoma clones derived from the human teratocarcinoma cell line Tera-2. Differentiation in vivo and in vitro.* Lab Invest, 1984. **50**(2): p. 147-62.
159. Kohler, G. and C. Milstein, *Continuous cultures of fused cells secreting antibody of predefined specificity.* Nature, 1975. **256**(5517): p. 495-7.
160. Williams, B.P., et al., *Biochemical and genetic analysis of the OKa blood group antigen.* Immunogenetics, 1988. **27**(5): p. 322-9.
161. Andrews, P.W., et al., *Three monoclonal antibodies defining distinct differentiation antigens associated with different high molecular weight polypeptides on the surface of human embryonal carcinoma cells.* Hybridoma, 1984. **3**(4): p. 347-61.
162. Berkes, C.A., et al., *Pbx marks genes for activation by MyoD indicating a role for a homeodomain protein in establishing myogenic potential.* Mol Cell, 2004. **14**(4): p. 465-77.
163. Melton, D.A., et al., *Efficient in vitro synthesis of biologically active RNA and RNA hybridization probes from plasmids containing a bacteriophage SP6 promoter.* Nucleic Acids Research, 1984. **12**(18): p. 7035-7056.
164. Ai, H.-w., et al., *Hue-shifted monomeric variants of Clavularia cyan fluorescent protein: identification of the molecular determinants of color and applications in fluorescence imaging.* BMC Biology, 2008. **6**: p. 13-13.
165. Neely, M.D., et al., *DMH1, a Highly Selective Small Molecule BMP Inhibitor Promotes Neurogenesis of hiPSCs: Comparison of PAX6 and SOX1 Expression during Neural Induction.* ACS Chemical Neuroscience, 2012. **3**(6): p. 482-491.
166. Richter, A., et al., *BMP4 promotes EMT and mesodermal commitment in human embryonic stem cells via SLUG and MSX2.* Stem Cells, 2014. **32**(3): p. 636-48.
167. Watanabe, K., et al., *A ROCK inhibitor permits survival of dissociated human embryonic stem cells.* Nat Biotech, 2007. **25**(6): p. 681-686.
168. Mandal, P.K. and D.J. Rossi, *Reprogramming human fibroblasts to pluripotency using modified mRNA.* Nat. Protocols, 2013. **8**(3): p. 568-582.
169. Hocine, S., R.H. Singer, and D. Grünwald, *RNA Processing and Export.* Cold Spring Harbor Perspectives in Biology, 2010. **2**(12): p. a000752.
170. Sia, J., et al., *Dynamic culture improves cell reprogramming efficiency.* Biomaterials, 2016. **92**: p. 36-45.
171. Weintraub, H., et al., *Activation of muscle-specific genes in pigment, nerve, fat, liver, and fibroblast cell lines by forced expression of MyoD.* Proc Natl Acad Sci U S A, 1989. **86**(14): p. 5434-8.
172. Yang, C.-S., Z. Li, and T.M. Rana, *microRNAs modulate iPS cell generation.* RNA, 2011. **17**(8): p. 1451-1460.
173. Pahlman, S., et al., *Retinoic acid-induced differentiation of cultured human neuroblastoma cells: a comparison with phorbolester-induced differentiation.* Cell Differ, 1984. **14**(2): p. 135-44.
174. Preis, P.N., et al., *Neuronal cell differentiation of human neuroblastoma cells by retinoic acid plus herbimycin A.* Cancer Res, 1988. **48**(22): p. 6530-4.
175. Vaskova, E.A., et al., *"Epigenetic Memory" Phenomenon in Induced Pluripotent Stem Cells.* Acta Naturae, 2013. **5**(4): p. 15-21.
176. George, R.E., et al., *Genome-Wide Analysis of Neuroblastomas using High-Density Single Nucleotide Polymorphism Arrays.* PLoS ONE, 2007. **2**(2): p. e255.
177. Stallings, R.L., et al., *Are gains of chromosomal regions 7q and 11p important abnormalities in neuroblastoma?* Cancer Genet Cytogenet, 2003. **140**(2): p. 133-7.

178. Gunaseeli, I., et al., *Induced Pluripotent Stem Cells as a Model for Accelerated Patient- and Disease-specific Drug Discovery.* Current medicinal chemistry, 2010. **17**(8): p. 759-766.
179. Chan, E.M., et al., *Live cell imaging distinguishes bona fide human iPS cells from partially reprogrammed cells.* Nat Biotechnol, 2009. **27**(11): p. 1033-7.
180. Braam, S.R., et al., *Improved genetic manipulation of human embryonic stem cells.* Nat Meth, 2008. **5**(5): p. 389-392.
181. Zha, Y., et al., *Functional Dissection of HOXD Cluster Genes in Regulation of Neuroblastoma Cell Proliferation and Differentiation.* PLoS ONE, 2012. **7**(8): p. e40728.
182. Gerber, A.N., et al., *Two domains of MyoD mediate transcriptional activation of genes in repressive chromatin: a mechanism for lineage determination in myogenesis.* Genes Dev, 1997. **11**(4): p. 436-50.
183. Blum, R., et al., *Genome-wide identification of enhancers in skeletal muscle: the role of MyoD1.* Genes & Development, 2012. **26**(24): p. 2763-2779.
184. de la Serna, I.L., K.A. Carlson, and A.N. Imbalzano, *Mammalian SWI/SNF complexes promote MyoD-mediated muscle differentiation.* Nat Genet, 2001. **27**(2): p. 187-90.
185. Garner, M.M. and A. Chrambach, *Resolution of circular, nicked circular and linear DNA, 4.4 kb in length, by electrophoresis in polyacrylamide solutions.* Electrophoresis, 1992. **13**(3): p. 176-8.
186. Mamchaoui, K., et al., *Immortalized pathological human myoblasts: towards a universal tool for the study of neuromuscular disorders.* Skelet Muscle, 2011. **1**: p. 34.
187. Thayer, M.J., et al., *Positive autoregulation of the myogenic determination gene MyoD1.* Cell, 1989. **58**(2): p. 241-8.
188. Guo, K., et al., *MyoD-induced expression of p21 inhibits cyclin-dependent kinase activity upon myocyte terminal differentiation.* Molecular and Cellular Biology, 1995. **15**(7): p. 3823-3829.
189. Edmondson, D.G., T.J. Brennan, and E.N. Olson, *Mitogenic repression of myogenin autoregulation.* J Biol Chem, 1991. **266**(32): p. 21343-6.
190. Agley, C.C., et al., *Human skeletal muscle fibroblasts, but not myogenic cells, readily undergo adipogenic differentiation.* Journal of Cell Science, 2013. **126**(24): p. 5610-5625.
191. Bock, C., et al., *Reference Maps of Human ES and iPS Cell Variation Enable High-Throughput Characterization of Pluripotent Cell Lines.* Cell, 2011. **144**(3): p. 439-452.
192. Li, C., et al., *Genetic Heterogeneity of Induced Pluripotent Stem Cells: Results from 24 Clones Derived from a Single C57BL/6 Mouse.* PLoS ONE, 2015. **10**(3): p. e0120585.
193. Islam, S.M.R., et al., *Sendai virus-mediated expression of reprogramming factors promotes plasticity of human neuroblastoma cells.* Cancer Science, 2015. **106**(10): p. 1351-1361.
194. Kabadi, A.M., et al., *Enhanced MyoD-Induced Transdifferentiation to a Myogenic Lineage by Fusion to a Potent Transactivation Domain.* ACS Synthetic Biology, 2015. **4**(6): p. 689-699.
195. Kim, K.-Y., E. Hysolli, and I.-H. Park, *Reprogramming Human Somatic Cells into Induced Pluripotent Stem Cells (iPSCs) Using Retroviral Vector with GFP.* Journal of Visualized Experiments : JoVE, 2012(62): p. 3804.
196. Gadue, P. and G. Cotsarelis, *Epidermal cells rev up reprogramming.* Nature biotechnology, 2008. **26**(11): p. 1243-1244.
197. Kim, J.B., et al., *Pluripotent stem cells induced from adult neural stem cells by reprogramming with two factors.* Nature, 2008. **454**(7204): p. 646-50.
198. Eminli, S., et al., *Reprogramming of neural progenitor cells into induced pluripotent stem cells in the absence of exogenous Sox2 expression.* Stem Cells, 2008. **26**(10): p. 2467-74.
199. Westermann, F., et al., *Distinct transcriptional MYCN/c-MYC activities are associated with spontaneous regression or malignant progression in neuroblastomas.* Genome Biology, 2008. **9**(10): p. R150-R150.
200. Lin, C.Y., et al., *Transcriptional Amplification in Tumor Cells with Elevated c-Myc.* Cell, 2012. **151**(1): p. 56-67.

201. Liu, J., et al., *The oncogene c-Jun impedes somatic cell reprogramming.* Nat Cell Biol, 2015. **17**(7): p. 856-67.
202. Wernig, M., et al., *c-Myc is dispensable for direct reprogramming of mouse fibroblasts.* Cell Stem Cell, 2008. **2**(1): p. 10-2.
203. Macarthur, C.C., et al., *Generation of human-induced pluripotent stem cells by a nonintegrating RNA Sendai virus vector in feeder-free or xeno-free conditions.* Stem Cells Int, 2012. **2012**: p. 564612.
204. Mintz, B. and W.W. Baker, *Normal mammalian muscle differentiation and gene control of isocitrate dehydrogenase synthesis.* Proc Natl Acad Sci U S A, 1967. **58**(2): p. 592-8.
205. Hausburg, F., et al., *Defining Optimized Properties of Modified mRNA to Enhance Virus- and DNA- Independent Protein Expression in Adult Stem Cells and Fibroblasts.* Cellular Physiology and Biochemistry, 2015. **35**(4): p. 1360-1371.
206. Malik, N. and M.S. Rao, *A Review of the Methods for Human iPSC Derivation.* Methods in molecular biology (Clifton, N.J.), 2013. **997**: p. 23-33.
207. Guo, X., et al., *In vitro Differentiation of Functional Human Skeletal Myotubes in a Defined System.* Biomaterials science, 2014. **2**(1): p. 131-138.
208. Das, M., et al., *Differentiation of skeletal muscle and integration of myotubes with silicon microstructures using serum-free medium and a synthetic silane substrate.* Nat Protoc, 2007. **2**(7): p. 1795-801.